REMARKS/ARGUMENTS

I. STATUS OF THE CLAIMS

With entry of this amendment, claims 1-5, 7-8, and 10-13 are pending. Claims 1-5 and 7 are amended, and claims 10-13 are new. Claims 2 and 3 are currently amended merely to include reference to newly added claim 10. Support for the amendments can be found the specification as filed.

Independent claim 1 is amended to recite that nucleic acid (3) has 95% identity to nucleic acid sequence as shown in SEQ ID NO 2. Support for this amendment can be found for example, at page 6, line 35 to page 7, line 3. Claim 1 is also amended to recite that the amino acid sequence encoded by nucleic acid (3) binds PSD-95. Support for this amendment can be found, for example at page 27, line 5 and at page 29, lines 4-5 of the specification. Claim 1 is also amended to recite hybridization conditions for nucleic acid (4). Support for the stringent hybridization conditions of 2x SSC, 0.1% SDS, 50°C or 1x SSC, 0.1% SDS, 37°C can be found for example, at page 6, lines 11-12 of the specification.

Claims 2 and 3 are amended to include reference to newly added claim 10.

Claim 4 is currently amended to add the step of culturing the host cell comprising the polynucleotide of claim 1, and recovering the expressed protein. Support for the amendment to claim 4 can be found, for example, at page 16, lines 15-18 and at page 17, lines 22-25 of the specification.

Claim 5 is amended to recite a "purified" fragment. Support for this amendment can be found, for example, at page 17, lines 25-26 of the specification. Claim 5 is also amended for presentation in independent form by incorporating the elements presently recited in independent claim 1. Support for this amendment is the same as discussed above with regard to claim 1.

Claim 7 is also amended for presentation in independent form. Support for this amendment can also be found in the passages discussed above with regard to independent claim 1. Claim 7 is further amended to recite that the fragment comprises at least eight amino acids

residues and a PET domain. Support for this limitation can be found at page 14, line 35 to page 15, line 10 of the specification.

Support for new claims 10-13 can be found throughout the specification as filed. In particular, support for new claim 10, directed to an isolated polynucleotide complementary to the polynucleotide of claim 1 can be found, for example, at page 3, lines 27-29 of the specification. Support for new claim 11, directed to a polynucleotide of claim 1 having 99% identity with a nucleic acid sequence as shown in SEQ ID NO:2, can be found at page 6, line 35 to page 7, line 3. Support for new claim 12, directed to a polynucleotide of claim 1, encoding a PET domain and a LIM domain can be found for example, at page 22, lines 18-20 of the specification. Support for new claim 13 directed to the polynucleotide of claim 12, wherein the PET and LIM domains correspond to the stated amino acid positions of SEQ ID NO:1, can be found in Figure 2. No new matter is added with entry of this amendment.

II. SPECIFICATION

A. Sequence Compliance

The Examiner alleges that the application fails to comply with the sequence requirements as set forth in 37 C.F.R. §1.821-§1.825. Specifically, the Examiner alleges that no sequence identification has been provided for the sequences presented in Figures 2 and 3. In order to comply with the requirements of 37 C.F.R. §1.821 through §1.825, the specification is currently amended to add sequence identifiers to the brief description for Figure 2 in the paragraph beginning at page 23, line 5 and to Figure 3 in the paragraph beginning at page 23, line 7 of the specification. Applicants submit that the specification as presently amended addresses the Examiner's concerns and is in compliance with 37 C.F.R. §1.821-§1.825.

B. Specification Informalities

The Examiner has objected to the specification for the informality of containing embedded hypertext in the specification. Applicants have amended the paragraphs beginning at page 6, line 31, and at page 22, line 7, to remove the "http" portion of the internet addresses from the specification.

Applicants believe that the specification as presently amended addresses all of the Examiner's concerns, and request that the Examiner withdraw the objection.

III. CLAIM OBJECTIONS

Claims 5 and 7 stand objected to as allegedly being of improper dependent form for failing to further limit the subject matter of a previous claim.

Applicants have amended claims 5 and 7 so as to be presented in independent form.

In view of claims 5 and 7 as presently amended, Applicants request that the Examiner withdraw the objection.

IV. REJECTION UNDER 35 U.S.C. §101

A. Non-Statutory Subject Matter

Claims 1, 3, 5 and 7 stand rejected under 35 U.S.C. §101, as allegedly being directed to non-statutory subject matter. Specifically, the Examiner alleges that the claims as previously recited failed to include any limitations that would distinguish the claimed polynucleotides and polypeptides from those which occur in nature.

Applicants note that the claims as presently amended recite limitations that distinguish the polynucleotides and the polypeptides from those that occur naturally. In particular, claims 1, 7 and 10 recite an "isolated" polynucleotide, and claim 5 recites a "purified" fragment of a polypeptide.

In light of the claims as presently amended, Applicants request that the Examiner withdraw the rejection.

B. Utility Rejection

Claims 1-5 and 7-8 stand rejected under 35 U.S.C. §101 as allegedly not being supported by either a specific and substantial credible asserted utility or a well established utility. Specifically, the Examiner alleges that the instant application does not disclose a specific biological role for the m-Prickle protein or its significance to a particular disease, disorder, or

physiological process, which a skilled artisan would wish to manipulate for a desired clinical effect. To the extent that the rejection applies to the claims as presently presented, Applicants disagree.

The m-Prickle protein possesses three LIM domains and one PET domain, as shown in Figure 4, and discussed in Example 4 of the specification. At the time of filing the application, a skilled artisan would recognize that each of the LIM domains can function as a protein interaction module (*see*, e.g., abstract of Dawid I.B., *et al.* (1998) *Trends in Genet.* 14:156-162; and abstract of Bach, I. (2000) *Mech. Dev.* 91:5-17, copies of which are enclosed as Exhibits 1 and 2, respectively). Similarly, the skilled artisan would also understand that the PET domain is likely involved in interactions with other proteins, such as actin cytoskeletal components (*see, e.g.*, page 2325, left col. lines 1-7 of Gubb, D., *et al.* (1999) *Genes Dev.* 13:2315-2327, a copy of which is enclosed as Exhibit 3). The presence of the highly conserved LIM and PET domains in the m-Prickle protein, would lead the skilled artisan to reasonably understand that the m-Prickle protein acts either as a scaffold protein, or as an integral part of a scaffold complex.

Furthermore, the present Inventors have shown that the m-Prickle protein is concentrated in a post-synaptic density (PSD) fraction (*see*, Example 6 and Figure 5). The PSD is known as a region having a pivotal role in the physiological processes underlying learning and memory (*see, e.g.*, page 627, left col. line 16 to page 630 right col line 54 of Wheal, H.V. *et al.* (1998) *Prog. Neurobiol.* 55:611-640, a copy of which is enclosed as Exhibit 4). As discussed above, the m-Prickle protein is reasonably expected to interact with numerous other proteins through the highly conserved LIM and PET domains, the skilled artisan would also reasonably expect that the m-Prickle protein is involved in the structural organization of the PSD. Therefore, the skilled artisan would reasonably expect the m-Prickle proteins and nucleic acids of the invention to be a potential target for affecting the physiological processes underlying learning and memory.

Even more specifically, the present inventors have shown that the m-Prickle protein binds to the PSD-95 scaffold complex in the PSD (*see*, page 2, lines 20-21 and page 3, lines 20-22 of the specification). It was well known in the art at the time of filing the instant

application that PSD-95, a protein within the PSD, forms a complex with the NMDA receptors (NMDA-R) and is considered a model for synapse maturation, learning and memory at the cellular level and is known to play an important role in the expression of long term potentiation (LTP) (*see, e.g.* page 2, lines 21-26 of the specification; and Migaud, M. *et al. Nature* 396:433-439 (1998), abstract and figure 6, page 438, a copy of which is attached as Exhibit 5). Indeed, the interaction of m-Prickle with the NMDA-R is evidenced by the present inventor's demonstration of the co-precipitation of m-Prickle with the NMDA-R using an anti-m-Prickle antibody.

Because m-Prickle is known to bind PSD-95, which is known to associate with NMDA-Rs in the PSD, and m-prickle can be co-precipitated with NMDA-Rs, the skilled artisan would understand that manipulation of m-Prickle can be used to modulate the processes underlying learning and memory at the cellular level.

This use of the m-Prickle proteins and nucleic acids disclosed in the present invention as potential targets for effecting learning and memory is particularly evident in view of Kemp *et al*, which discloses that NMDA-receptor pathways are promising drug targets (*see, e.g.*, abstract of Kemp, J.A., *et al.* (2002) *Nat. Neurosci 5 Suppl*:1039-1042, a copy of which is enclosed as Exhibit 6). Specifically, Kemp et al. teaches that:

> The balance of evidence indicates that potentiating NMDA receptors should be beneficial for treating cognitive disorders and schizophrenia....Reduction of NMDA receptor function with drugs or genetic manipulation clearly disrupts learning and memory in animals. Similarly, overexpression of the NR2B subunit improves learning and memory in mice. Perhaps it will be possible to find small molecules that potentiate NMDA receptors in the way that benzodiazepines (such as Valium) enhance activation of $GABA_A$ receptors. *See*, Kemp *et al.* page 1041, "NMDA receptor enhancers."

A skilled artisan reading the present application would readily understand that the m-Prickle proteins and nucleic acids of the present invention have a specific and substantial credible utility in screening for compounds that modulate NMDA-R function. In particular, the proteins and nucleic acids of the present invention are useful in the identification of compounds that modulate the binding between m-Prickle, PSD-95, and/or the NMDA-R, thereby effecting

the clustering of NMDA-Rs in the PSD. A compound capable of regulating the cluster formation of NMDA-Rs is useful in developing unique drugs that would enable a subtle regulation of NMDA-R function, possibly overcoming the undesirable side-effects associated with typical agonists and antagonists. *See*, Kemp *et al.*

A skilled artisan reading the instant specification would recognize that the proteins and nucleic acids of the present invention are useful in designing experimental systems for screening compounds that affect the clustering of NMDA-Rs. For example, as shown in Example 9 of the instant specification, antibodies recognizing R-Prickle can be used to localize R-Prickle (and thus PSD-95 and NMDA-Rs) in primary cultures of rat embryo hippocampal neurons. By monitoring a change in the clustering pattern of R-Prickle following addition of various test compounds, potential drug candidates that effect the clustering of NMDA-Rs in the PSD can be identified.

In light of the Exhibits and discussion above, and the asserted specific and substantial credible utility for the proteins and nucleic acids of the invention, Applicants submit that the claimed invention meets the requirements of 35 U.S.C. §101 and request that the Examiner withdraw the rejection.

V. REJECTIONS UNDER 35 U.S.C. §112

Claims 1-5 and 7-8 stand rejected under 35 U.S.C. §112, first paragraph, because the claimed invention is not supported by either a specific and substantial credible asserted utility or a well-established utility and one skilled in the art would not know how to use the claimed invention.

In light of the arguments and exhibits presented above, Applicants request reconsideration by the Examiner.

A. Enablement

Claims 1-5 and 7-8 stand rejected under 35 U.S.C. §112, first paragraph for allegedly lacking enablement. Specifically, the Examiner alleges that the specification is enabling for a polynucleotide encoding mammalian Prickle protein, wherein the polynucleotide comprises sense sequences associated with the Prickle protein, the specification does not

reasonably provide enablement for making antisense polynucleotide encoding a Prickle protein. To the extent that the rejection applies to the claims as presently amended, Applicants disagree.

Independent claim 1 as presently amended does not recite a "complementary sequence." This limitation has been moved to dependent claim 10, which recites an isolated polynucleotide comprising a complementary sequence to the polynucleotide of claim 1.

In light of the claims as presently amended, and the arguments presented above, Applicants request that the Examiner withdraw the rejection.

B. Written Description

Claims 1-5 and 7-8 stand rejected under 35 U.S.C. §112, first paragraph as allegedly failing to satisfy the written description requirement. Specifically, the Examiner alleges that the instant specification fails to describe the entire genus of nucleic acids and proteins encompassed by the claims. To the extent that the rejection applies to the claims as presently amended, Applicants disagree.

As an initial matter, Applicants direct the Examiner's attention to nucleic acid (3) of independent claims 1, 5 and 7 as presently amended. Specifically, the claim as amended encompasses nucleic acid sequence variants having at least 95% identity to the nucleic acid sequence as shown in SEQ ID NO:2, and wherein the encoded polypeptide binds PSD-95.

With the above limitations in mind, Applicants now direct the Examiner's attention to the Synopsis of Application of Written Description Guidelines, Example 14. This particular example analyzes a claim directed to a protein with an amino acid sequence at least 95% identical to SEQ ID NO:3 and that has catalytic activity. In Example 14, the specification provided one example of a protein that was a member of the claimed genus. The Patent Office concluded that the claim of 95% identity to a reference sequence with a specified catalytic activity was adequately described within the meaning of 35 U.S.C. §112, first paragraph.

The Synopsis reasons that the genus of proteins that must be variants of the claimed SEQ ID NO:3 does **not** have substantial variation since all of the members must have 95% identity to the reference sequence and must have the specified catalytic activity. Therefore, according to the Synopsis, the "single species disclosed is representative of the genus because all

members have at least 95% structural identity with the reference compound and because of the presence of an assay..." that could be used to identify members of the claimed genus. The instant specification discloses the that mammalian prickle binds to PSD-95 and methods for determining this binding are also disclosed in the application, as well as known in the art. Thus, at a minimum, on the basis of the Synopsis of Application of Written Description Guidelines issued by the USPTO, the present claims that recite 95% identity to SEQ ID NO:2 meet the written description requirement as set forth in 35 U.S.C. §112, first paragraph..

Dependent claims 2-4 and new claims 10-13 depend either directly or indirectly from independent claim 1, and therefore include all of the limitations of independent claim 1. The arguments as presented above with regard to the independent claims is also applicable to the dependent claims.

In view of the claims as presently amended, and the arguments presented above, Applicants request that the Examiner withdraw the rejection.

C. Indefiniteness

Claims 1-5 and 7-8 stand rejected under 35 U.S.C. §112, second paragraph as allegedly being indefinite. Specifically, The Examiner alleges that recitation of hybridization "under stringent conditions" is vague and indefinite. Further, the Examiner alleges that claim 4 is indefinite for omitting essential steps. To the extent that the rejection applies to the claims as presently amended, Applicants disagree.

Claim 1 as presently amended recites specific hybridization conditions of "2x SSC, 0.1% SDS, 50°C or 1x SSC, 0.1% SDS, 37°C." Support for this amendment can be found at page 6, lines 11-14 of the specification.

Claim 4 as presently amended recites the specific steps of culturing the host cell comprising the polynucleotide and recovering the expressed polypeptide from the host cell or culture supernatant. Support for this amendment can be found, for example, at page 16, lines 16-18 of the specification.

VI. REJECTION UNDER 35 U.S.C. §102(b)

Claims 5 and 7 stand rejected under 35 U.S.C. §102(b) as allegedly being anticipated by Drmanac *et al.* (WO 01/75067 A2). Specifically, the Examiner alleges that Drmanac *et al.* discloses a polypeptide sequence that has 80.5% sequence similarity to the instantly claimed molecules, and thus anticipates the claimed invention.

To anticipate a claim, the reference must teach each and every element of the claim. "A claim is anticipated only if each and every element as set forth in the claim is found...in a single prior art reference." *Verdegaal Bros. v. Union Oil of California*, 814 F.2d 628, 631, 2 USPQ2d 1051, 1053 (Fed. Cir. 1987). Thus, in order to anticipate, the cited reference must contain every element of the claims as at issue. The cited reference, Drmanac *et al.*, does not.

Claims 5 and 7 as presently amended recite that the polypeptide fragment comprises at least eight amino acid residues and a PET domain. Drmanac *et al.* does not teach nor suggest a polypeptide fragment having at least eight amino acid residues and a PET domain as presently claimed. Rather, Drmanac *et al.* teaches a plurality of nucleic acids obtained from cDNA and genomic libraries. As noted by the Examiner, SEQ ID NO:37384 of Drmanac *et al.* shows some similarity to the claimed polypeptide fragments and nucleotide chains. SEQ ID NO:37384 of Drmanac *et al.*, however, does not contain a PET domain.

Because Drmanac *et al.* does not disclose all of the elements of claims 5 or 7 as presently amended, Drmanac *et al.* does not anticipate the claims.

In light of the claims as presently amended, and the arguments as presented above, Applicants request that the Examiner withdraw the rejection.

CONCLUSION

In view of the foregoing, Applicants believe all claims now pending in this Application are in condition for allowance. The issuance of a formal Notice of Allowance at an early date is respectfully requested.

If the Examiner believes a telephone conference would expedite prosecution of this application, please telephone the undersigned at 415-576-0200.

Respectfully submitted,

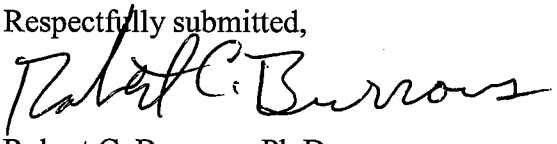

Robert C. Burrows, Ph.D.
Reg. No. 61,039

TOWNSEND and TOWNSEND and CREW LLP
Two Embarcadero Center, Eighth Floor
San Francisco, California 94111-3834
Tel: 415-576-0200
Fax: 415-576-0300
Attachments: Exhibits 1-6
RCB:rcb
61259576 v1

LIM domains: multiple roles as adapters and functional modifiers in protein interactions

IGOR B. DAWID (idawid@nih.gov)
JOSEPH J. BREEN (breenj@nih.gov)
REIKO TOYAMA (reiko@nih.gov)

The LIM domain is a specialized double-zinc finger motif found in a variety of proteins, in association with domains of divergent functions or forming proteins composed primarily of LIM domains. LIM domains interact specifically with other LIM domains and with many different protein domains. LIM domains are thought to function as protein interaction modules, mediating specific contacts between members of functional complexes and modulating the activity of some of the constituent proteins. Nucleic acid binding by LIM domains, while suggested by structural considerations, remains an unproven possibility. LIM-domain proteins can be nuclear, cytoplasmic, or can shuttle between compartments. Several important LIM proteins are associated with the cytoskeleton, having a role in adhesion-plaque and actin-microfilament organization. Among nuclear LIM proteins, the LIM homeodomain proteins form a major subfamily with important functions in cell lineage determination and pattern formation during animal development.

The LIM domain was recognized as a distinct protein motif within LIM homeodomain (LHX; Box 1) proteins by genetic and biochemical methods[1–3]. Quite rapidly, the family expanded by the discovery of LIM proteins that lack homeodomains, either by being composed almost entirely of LIM domains or containing additional functional domains of various types (reviewed in Refs 4–7). Thus, LIM-domain proteins do not form a functional family like, for example, metalloproteases or helix–loop–helix transcription factors; rather, a variety of quite dissimilar proteins share domains that can be classified as similar by sequence comparison. As we discuss in this article, the common thread of LIM-domain function is the mediation of protein–protein interactions.

LIM-domain structure

The solution structure of the C-terminal LIM domain of CRP1, a protein that contains two LIM domains and no other discernible structural motif, was solved by NMR in 1994 (Ref. 8). The solution structure of the related protein CRIP (Ref. 9) and of the C-terminal LIM domain of CRP2 (Ref. 10) have been solved to yield rather similar structures. The two zinc fingers that constitute a LIM domain represent separate structural entities that are held together in a particular configuration by hydrophobic interactions (Fig. 1). The similarity of the C-terminal finger segment in CRP1 and CRP2 to the zinc finger in the DNA-binding domain of GATA1 emphasizes the structural implication that this LIM domain might be capable of specific binding to DNA; however, experimental evidence to support this possibility is lacking.

Recently, the solution structure of the entire CRP1 molecule has been solved (X. Yao and M.F. Summers, pers. commun.). The structure of the N-terminal LIM domain within the whole protein is very similar to that of the previously described, isolated C-terminal segment. The two LIM domains form independent structural units that are held together by the linker region, which is disordered in solution, and there are no apparent interactions between the LIM1 and LIM2 domains. These important results raise certain questions in the context of interactions of LIM domains with other proteins that will be discussed below.

Classification of LIM proteins

The classification we proposed previously[11] is reproduced in Fig. 1 with minor changes, because this scheme continues to accommodate most of the recently discovered LIM-domain proteins. This classification is based on sequence relationships among LIM domains and on the overall structure of the proteins. Using the GCG PILEUP program, LIM domains were grouped by sequence similarity into four classes, with some outliers[5]. A re-analysis, which included recently published LIM-domain sequences, yielded a similar pattern (not shown). A and B class LIM domains always occur in tandem in LHX proteins, and in LMOs and LIM kinases (LIMKs); these proteins are classified as Group 1. Class C LIM domains are well-defined by sequence similarity and are found in proteins composed largely of LIM domains; these proteins are classified as Group 2. Group 3 is more heterogeneous with most, but not all, of the LIM domains of proteins included in this group belonging to sequence class D. Group 3 proteins contain different numbers of LIM domains located at the C-terminus. Certain distantly related LIM proteins in yeast and a few other examples remain ungrouped in this scheme. Recently discovered LIM proteins[12–19] largely fit into this scheme. While most studies on LIM proteins deal with animal material, such proteins also occur in plants, where they appear to have a role in pollen development[20].

A second classification principle fits quite well with the scheme in Fig. 1: Group 1 proteins are primarily nuclear while Group 2 and 3 proteins are cytoplasmic. This distinction is not rigid, however. For example, CRPs are distributed in the nucleus and the cytoplasm[21], the LHX protein XLIM1/LHX1 is mostly nuclear but can be found in the cytoplasm, for example, in differentiating embryonal carcinoma cells (A. Karavanov and I.B. Dawid, unpublished), and zyxin, which is mostly found in adhesion plaques, shuttles in and out of the nucleus by virtue of its nuclear export signal[17,22]. Nevertheless, localization and known functions broadly distinguish Group 1 from Group 2 and 3 proteins. In Group 1, the LHX proteins are transcription factors that bind DNA through their homeodomain and are important developmental regulators; LMO proteins appear to be transcriptional cofactors that are components of regulatory complexes[23,24]. The LIMKs do not fall as neatly into the pattern, being found in the nucleus and the cytoplasm[25].

PII: S0168-9525(98)01424-3

Group 2 and 3 proteins are primarily cytoplasmic, and many are associated with the cytoskeleton, for example, zyxin, CRP and paxillin. Enigma binds to a set of cytoplasmic proteins with tyrosine tight-turn motifs and appears to be involved in protein trafficking[26]. The ability to undergo multiple protein–protein interactions is the common denominator in considering these LIM proteins.

Protein–protein interactions

During the past few years it has become increasingly clear that LIM domains are multiple binding and adapter modules, and that many LIM-domain proteins contain additional motifs that can mediate interactions with a variety of proteins. Some LIM proteins appear to function solely as adapters to bring other components together in a complex; this might be the role of proteins containing only short regions beyond their LIM domains, such as LMO and CRP. Presenting a more complex pattern, zyxin binds to CRP1 through its first LIM domain, and to α-actinin, VAV and ENA/VASP through its proline-rich N-terminal domain, although not necessarily at the same site[17,27]. While the function of some LIM proteins might be entirely to act as binding partners and adapters, others clearly have separate functional domains, for example, the DNA-binding homeodomain in LHX proteins and the kinase domain in LIMKs. In these cases, the LIM domains might connect the parent protein to other partners through their interactive abilities, or could modulate the activity of other domains within the LIM protein; we discuss evidence supporting both of these types of function.

The known binding partners of LIM domains are quite varied (Table 1). Certain LIM domains form dimers with other LIM domains, and it appears that all LIM domains can bind various structurally distinct protein motifs. For example, the amino-proximal LIM domain of zyxin can bind CRP1 (Ref. 27), and CRP1 and CRP3/MLP have been reported to form homodimers[21,28]. While A/B class LIM domains can interact with other A/B LIM proteins *in vivo*[21], it is possible that this interaction is mediated by LDB/NLI (see below) or similar proteins. While homo- and heterodimer formation of LIM

Box 1. Abbreviations, nomenclature, definitions

Nomenclature and the use of abbreviations in the LIM protein field is unfortunately complex. We use the term LHX for LIM homeodomain proteins; this is simply an abbreviation used in this article. In contrast, *Lhx1, -2* and so on are accepted names for individual LIM homeobox genes in the mouse and human. Orthologs of several of these genes in non-mammalian vertebrates are named *Lim1, -2* and so on; thus, *Xlim-3* and *Lhx3* are orthologous genes in *Xenopus* and mouse, respectively. In these cases, an effort is being made to assign the same numerals to orthologous genes. Not all LHX genes in vertebrates are named '*Lim*' or '*Lhx*', with *Isl* and *Lmx* identifying additional genes in this class. LHX genes in invertebrates all have distinct names (e.g. *mec-3, lin-11, apterous*).

LMO is the name given to certain proteins composed of only LIM domains, previously known as Rhombotin or Ttg; while the term 'LMO' was generated from 'LIM only', LMO is not an abbreviation, it is a name, and should never be expanded to 'LIM only'. Other proteins, such as CRP, CRIP and PINCH, are also composed of LIM domains with few additional sequences, but are not closely related to the LMOs. When the term LMO is recognized as a name rather than as an abbreviation, confusion about relationships between these groups is avoided.

LIMK stands for LIM kinase, a name given to proteins that contain two LIM domains and a kinase domain.

A number of proteins mentioned in this article have multiple names, so to facilitate cross-referencing the alternative names are divided by a forward slash, for example, ENA/VASP.

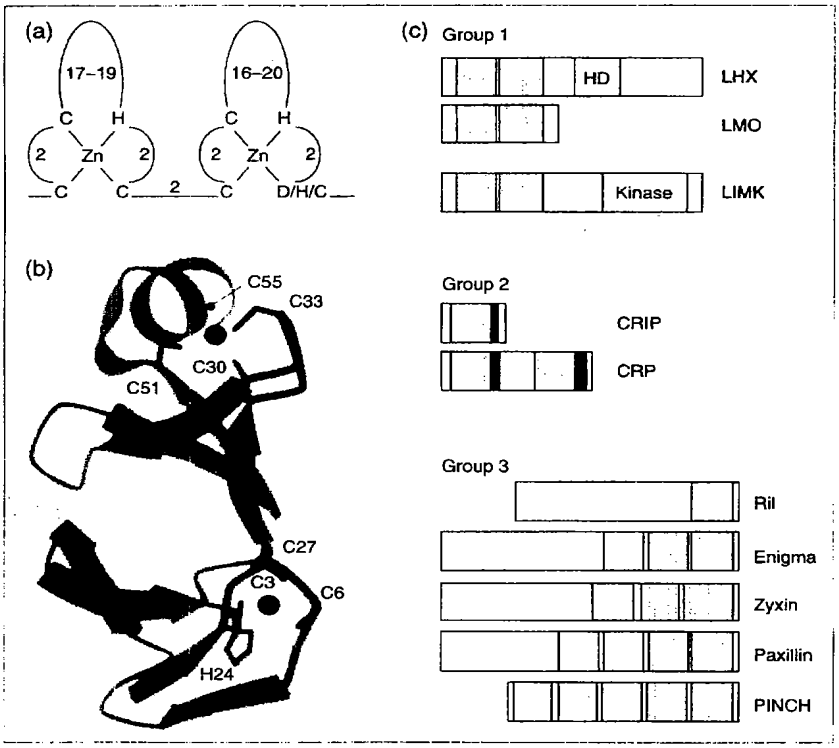

FIGURE 1. LIM protein structure and classification. The double-zinc finger protein motif of the LIM domain is shown in (a). The structure of CRIP is shown in (b) (reproduced by permission from Ref. 9). Both finger domains are constituted by two antiparallel β-sheets; in the N-terminal module, these are followed by a tight turn that forms the linker to the following module. At the C-terminus of the second module, the β-sheets are followed by a short α-helix. Classification of LIM-domain proteins is presented in (c) (modified from Ref. 11). LIM domains in LHX (LIM homeodomain) proteins, and in LMO and LIMK, are related by sequence, forming Group 1; sequence similarity between LIMK and other Group 1 proteins is lower than similarity between LHX and LMO proteins. Group 2 proteins have related LIM domains and contain only a short additional conserved motif (dark gray). Although Group 3 is quite heterogeneous, LIM domains in this group are more closely related to each other than to those in Groups 1 and 2. LIM domains are shown in pale gray.

domains is intriguing but of uncertain general significance, LIM domain interactions with other proteins are clearly functional. At least one LHX protein, LMX1, the LMOs and CRP3/MLP interact physically and functionally with helix–loop–helix transcription factors (Table 1), as shown by functional synergy in *in vivo* transcription assays and the presence of complexes containing these components in the cell[23,24,29,30]. A particularly interesting partner protein, LDB/NLI, is discussed below.

Interactions with a variety of partners have been described for different Group 3 proteins. Several of these proteins are localized primarily in adhesion plaques, also named focal adhesions, through which cells adhere to the extracellular matrix. The adhesion plaque constitutes a marcromolecular complex that mediates the contact between matrix receptors and the cytoskeleton. Zyxin, an important component of adhesion plaques, has recently been reviewed in detail[17]. Paxillin is likewise found in adhesion plaques, where it is localized through the action of its third LIM domain[31]. In contrast, the interactions of paxillin with vinculin and the focal adhesion kinase are mediated by non-LIM regions of the molecule[31].

Enigma binds to the tyrosine-containing tight turn in the insulin receptor[26], and was shown also to bind the receptor tyrosine kinase RET in a LIM-domain-dependent manner[32]. In addition, the LIM domains of enigma and its relative ENH bind some, but not all, isoforms of protein kinase C (PKC); it is particularly intriguing that the specificity of enigma and ENH for different PKCs is partly overlapping and partly different, allowing for potentially subtle regulatory interactions[33]. Certain PKC isoforms also interact with LIMK1, requiring the C-terminal LIM domain for binding[33]. Given the wide-ranging regulatory functions of PKC in cell metabolism, it will be interesting to explore the biological consequences of these interactions.

Table 1. Interactions of LIM domains with other proteins

LIM Protein	Partner	Refs
LHX proteins, LMOs	LDB/NLI/CLIM/CHIP	24, 36–41, 43
PLIM/LHX3/LIM3	PIT1	77
LMX1.1	E47/PAN1	29
LMO1,2	TAL1, LYL1	78
LMO2	GATA1, GATA2, RBP	79, 80
CRP1	CRP1[a], α-actinin	28, 81
Zyxin	CRP1, -2, -3, NOC2	27, 76, 82, 83
CRP3/MLP	CRP3/MLP, α-actinin, LMO1, Apterous, MyoD	21, 30, 82
Enigma	Insulin receptor, RET/PTC2, PKC-α,βI,ζ	26, 32, 33
Enigma homolog (ENH)	PKC-βI,γ,ϵ	33
LIMK1	LIMK1, 2, PKC-γ,ζ	33, 84

Note that only interactions in which LIM domains are involved are listed in this table. Interactions of other domains of some of these proteins are mentioned in the text.
[a]Homodimer formation of CRP has been shown by overlay and two-hybrid assays[28] but not in sedimentation studies[85].

LDB/NLI – an important mediator of protein interactions

The existence of LIM-domain-binding factors was suggested by several observations, for example, certain properties of LHX proteins. As homeodomain proteins, they could be expected to function as developmentally important transcription factors, and genetic evidence supports this view (see below). However, studies of DNA binding by the ISL1 protein *in vitro*[34] and functional studies of XLIM1 by overexpression in frog embryos[35] showed that the wild-type LHX protein is not effective in DNA binding and transcriptional regulation. Mutation or deletion of the LIM domains activated the XLIM1 protein, suggesting that the LIM domains exert a negative regulatory role in LHX proteins; a binding protein was postulated as a cofactor for LHX function *in vivo*[5,35].

Such a protein was indeed isolated independently by different laboratories and named LIM-domain-binding protein, LDB1 (Refs 24, 36), nuclear LIM interactor, NLI (Ref. 37) and, subsequently, CLIM2 (Ref. 38). LDB1 can functionally synergize with XLIM1 in the frog embryo in activating target genes[36]. A related protein, LDB2/CLIM1, has been seen in the mouse[38], and LDB1, LDB2 and an additional related protein, LDB3, have been found in zebrafish[39]. LDB proteins are highly conserved, in that mouse, frog and fish LDB1 are 95% identical for their entire length of 375 residues[36,39], and human and *Caenorhabditis elegans* relatives are found in the database; no similarity to other proteins has been seen.

LDB1/NLI binds LIM domains from LHX and LMO proteins effectively, but does not bind LIMK or Group 2 or 3 proteins[36,37,39]. Truncation and binding experiments using different methods show that LDB1/NLI can bind single LIM domains but binds a pair of A/B LIM domains with much higher affinity[40,41]. Furthermore, the LIM-binding domain has been assigned to the C-terminal half of LDB1/NLI and specifically localized between residues 300 and 338 (Ref. 40).

LIM-domain binding does not exhaust the interaction repertoire of LDB1/NLI. In addition, this protein can form homodimers that involve its N-terminal region[40,41], implying that LDB1 can act as a bridging factor in building up complexes of different LHX proteins (Fig. 2). Furthermore, the range of such partners is not limited to LIM proteins: CLIM1 interacts efficiently with the LIM domains of LHX3 (also named P-LIM) and of other LHX proteins, but also with the homeodomain protein P-OTX, which lacks LIM domains; functional synergy on a promoter construct was shown for LHX3+P-OTX+CLIM1 (Ref. 38). This observation opens a host of possibilities for complex formation between different proteins mediated by LDB/NLI/CLIM. In fact, a large complex has been isolated from erythroid cells that contains LDB1 and LMO2 as well as TAL1, GATA1 and E2A; this complex binds to a bipartite motif containing an E-box and GATA site[23]. Interaction of LMO2 and LDB1 within such a complex acts as a negative regulator of erythroid differentiation[24].

A major advance in studying the function of LDB1/NLI came with the discovery of a *Drosophila* homolog encoded by a gene named *Chip*; Chip is 58% identical to LDB1, and effectively binds LIM domains[42,43]. While *Chip* does interact genetically with the LIM homeobox gene *apterous*, the severe segmentation defects exhibited by the *Chip* null phenotype cannot be explained by interruption of the function of any known LIM protein[43]. This phenotype might result from the interaction of Chip with

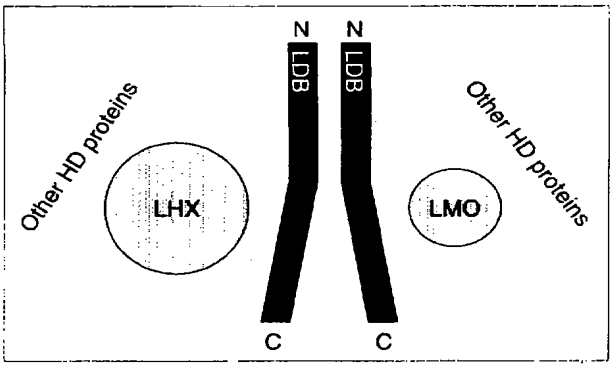

FIGURE 2. Some of the protein–protein interactions involving LDB/NLI. Dimer formation via its N-terminal region might allow LDB/NLI to mediate interactions between different LHX and LMO proteins that bind to the C-terminal region by way of their LIM domains. Other homeodomain proteins, as shown for P-OTX, might be recruited to such a complex. (Based on Refs 38, 40, 41.)

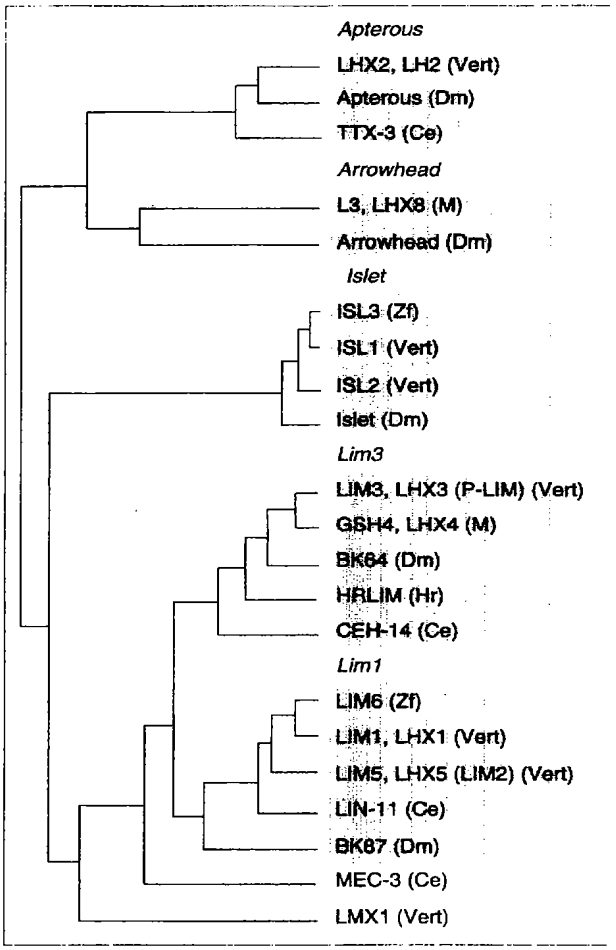

FIGURE 3. LHX protein family tree. Only one of each set of vertebrate orthologs is included for clarity, and the different synonymous names in use are shown. The tree is based on pile-up comparisons of homeodomains. (Vert) indicates that orthologs are known from two or more vertebrate species; otherwise, species are identified as M, mouse; Zf, zebrafish; Hr, *Halocynthia roretzi* (ascidian); Dm, *Drosophila melanogaster*; Ce, *Caenorhabditis elegans*.

transcription factors other than LIM proteins, as shown already for CLIM/P-OTX (Ref. 38); indeed, an interaction of Chip with Bicoid has been observed (D. Dorsett and E. Torigoi, pers. commun.). Nevertheless, additional studies in *Drosophila* support the LIM-domain-binding aspect of Chip function. Mutations reducing the level of the *Drosophila* LMO (DLMO) protein result in a wing phenotype that is modified in a quantitative manner by the dosage of Chip; it appears that the fly requires a precise ratio of DLMO and Chip/LDB proteins, with deviations in either direction leading to various phenotypes (D. Segal and M. Shoresh, pers. commun.). These interesting results offer the opportunity to study protein–protein interactions in the context of the whole organism.

Genetic and molecular studies on LIM homeodomain protein function

LIM domains were discovered within homeodomain proteins[1–3], and the LHX family continues as the largest group of LIM-domain proteins. LHX proteins can also be viewed as a subfamily of the very large family of homeodomain proteins[44]. LHX protein sequences have been conserved from nematodes to mammals and are particularly well conserved among vertebrates. As summarized in Fig. 3, nematode or fly genes mostly have two vertebrate homologs that are closely related to each other, but the matrix is not complete, suggesting that additional LHX genes will be found.

LHX proteins have a role in the determination of cell lineage and identity, as discovered initially for two of the founding members of the group, *mec-3* (Ref. 1) and *lin-11* (Ref. 2). Since then, genetic studies (Table 2), supplemented by inhibition and overexpression approaches, have expanded our knowledge of the role of these genes in development. As is common for regulatory molecules and particularly for homeodomain proteins, individual proteins can participate in multiple regulatory cascades in different cell types and tissues.

Considering the increase in complexity during the evolution from nematodes to vertebrates, we note that not only has the number of LHX genes increased and their function become more complex, but their role in development has become more varied. In *C. elegans*, three LHX genes have been studied in detail, although several more exist[45]. Two of these have a role in the specification and function of a narrowly limited set of neurons: *mec-3* for mechanosensory neurons[1] and *ttx-3* for certain interneurons in the thermoregulatory pathway[45]. *lin-11*, originally recognized as affecting the fate of cells in the vulva[2], also affects certain neurons engaged in thermoregulation[46]. Thus, mutations in these genes affect specific pathways, but most other aspects of development proceed normally.

The range of functions subsumed by LHX proteins appears to be substantially greater in *Drosophila*. *Apterous* has a role in neuronal specificity and guidance[47] but also has a critical role in the patterning of the wing[48] and is involved in muscle development[49]. The *Drosophila islet* (*isl*) gene likewise has a role in axonal identity and guidance[50]. *Arrowhead* (*Awh*) is required for the development of one type of imaginal (adult) cells but represses the development of another type[51]. Thus, deficiency or overexpression of *Awh* leads to severe developmental abnormalities on a broader scale than reported for any *C. elegans* LHX gene.

TABLE 2. Genetics of LIM gene function

Gene	Species	Loss-of-function phenotype	Refs
LIM homeobox genes			
mec-3	*C. elegans*	Failure of touch receptor neurons to differentiate	1
lin-11	*C. elegans*	Incorrect lineage in vulval cells; functional deficit in neurons controlling thermoregulation	2, 46
Lhx1 (Lim1)	Mouse	Lack head structures anterior of otic vesicles; about 5% develop partial secondary axis; lethal at day 9.5; the few escapers that were still-born lack a urogenital system	56
ttx-3	*C. elegans*	Functional deficit in thermoregulatory interneurons	45
Apterous	*Drosophila*	Required in wing patterning, axon guidance, muscle formation	47–49
Lhx2	Mouse	Anophthalmia; malformation in cerebral cortex; cell non-autonomous deficit in definitive erythropoiesis; embryonic lethal	63
Lhx3	Mouse	Anterior and intermediate lobes of pituitary fail to form although Rathke's pouch develops; perinatal lethal	64, 70
Gsh4 (Lhx4)	Mouse	Perinatal lethal due to failure of lungs to inflate, but unknown primary defect; affects pituitary development	69, 70
Islet	*Drosophila*	Defects in axon pathfinding and neurotransmitter production in motor neurons	50
Isl1	Mouse	Lack of motor neurons, *en1*-expressing interneurons fail to differentiate as a secondary effect	62
Arrowhead	*Drosophila*	Cells forming certain adult structures fail to proliferate	51
Other LIM genes			
LMO2	Mouse	Early failure of erythropoiesis	72
CRP3/MLP	Mouse	Cardiomyopathy	73
LIMK1	Human	Is involved in Williams syndrome	74

Vertebrates contain a larger number of LHX genes than invertebrates. Usually, vertebrate LHX genes occur in closely related pairs (Fig. 3), except in zebrafish, which usually contain triplets. A clear example for a fundamental role of an LHX gene in vertebrate development is provided by the *XLIM1/Lhx1* gene (Fig. 4). *XLIM1* is expressed in the organizer of *Xenopus* embryos and the equivalent region in the gastrulae of other vertebrates[52–54]. When activated artificially or by synergy with LDB1, *XLIM1* can turn naive ectodermal cells into organizer-like cells that are capable of inducing anterior neural tissue[35,36,41,55], and disruption of *Lim1/Lhx1* in the mouse led to embryos missing head structures anterior of the otic vesicles[56]. These observations indicate that *Lim1* has an early and fundamental role in vertebrate embryogenesis. It is possible that the severe phenotype of $Lhx1^{-/-}$ mice arises because the closely similar *Lhx5* gene is expressed in a non-overlapping pattern at gastrulation[57], precluding functional redundancy. In addition, the *Lim1/Lhx1* gene is expressed later in the central nervous system, kidney and other organs[58–61], suggesting multiple functions of more restricted scope at later stages.

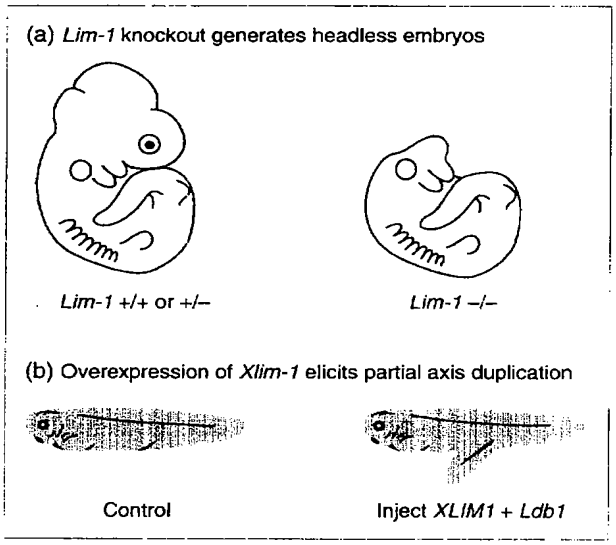

FIGURE 4. The biological role of *Lim-1* (*XLIM1/Lhx1*) in early embryogenesis. (a) *Lim-1*-deficient mouse embryos lack head structures anterior of the otic vesicle[56]. (b) Ventral injection of activated *XLIM1* RNA or of *XLIM1* plus *Ldb1* RNAs led to partial axis duplications[35,36].

Different LHX genes exhibit varied specific functions in multiple tissues as seen from studies of mutations (Table 2) and other approaches. Although *Isl1* is widely expressed, disruption of the gene in the mouse results in the absence of a restricted set of neurons[62], a similar phenotype to *islet* mutations in *Drosophila*[50]. In contrast, $Lhx2^{-/-}$ mice show massive brain defects, including a complete lack of eyes, which agrees with the expression of the gene in the brain; in addition, a severe non-cell autonomous hematopoietic defect leads to early fetal death of mutant mice[63]. A highly specific ablation of the anterior and intermediate lobes of the pituitary is seen in $Lhx3^{-/-}$ mice[64]. This phenotype agrees with the expression of the gene in the pituitary, but because it is also expressed in the pineal and in motor neurons[65–68], the question arises why these structures are not affected as well. The answer probably can be found in the closely related *Gsh4/Lhx4* gene which is expressed in the same cell types and whose ablation also affects pituitary development[69,70].

LHX genes as a class have been implicated in the specification of neuronal identity and axon pathfinding, as already mentioned in the case of *C. elegans* and *Drosophila*. In vertebrates, the expression of different members of the LHX family has been correlated with neuronal classification and their organization into structural and functional columns[66], and LHX gene expression

was changed after experimental alteration of motor neuron fate[67]. These results suggest that LHX genes are involved in the specification of neuronal identity in the vertebrate CNS.

Apterous is a major regulator of wing patterning in *Drosophila*, but the apparent *apterous* homolog in vertebrates, *Lhx2/LH2*, has distinct multiple roles in eye, brain and erythroid development[63] but not in the developing limb. An important role in limb morphogenesis in vertebrates is carried out by the *lmx1* gene, which has no known fly homolog. *Lmx1* is induced by *Wnt7* in dorsal cells of the limb bud, and is believed to mediate dorsal development in this tissue (reviewed in Ref. 71). *Lmx1* might represent another example of the diversification and expansion of functions of LHX genes from invertebrate to vertebrate animals.

A fundamental role in different developmental processes has also been demonstrated for several non-homeodomain LIM proteins (Table 2). LMO2 is required in erythropoiesis[72] at an early stage, such that LMO2-deficient mice die by day 10.5. MLP/CPR3 has been implicated in muscle development, and mutant mice suffer severe cardiomyopathy[73]. LIMK1 is involved in Williams syndrome[74], a complex human inherited disorder involving congenital heart disease, defects in visuospatial cognition, and several other defects whose developmental relationships are not obvious. This fascinating observation will have to be correlated with the recently discovered major role of LIMK in the regulation of actin polymerization (S. Arber, O. Bernard and P. Caroni, pers. commun.). Furthermore, LIMK might be involved in the ras signaling pathway[75], pointing to the possibility of multiple functions in cell regulation.

Conclusions and outlook

The biological roles of LIM proteins are highly varied. The theme of LIM domain involvement in protein–protein interactions is certain to be continued as more partner proteins are discovered and structure–function relationships in such interactions, already analyzed to some extent[21,40,41,76], are explored further. Many processes in the cell proceed in large complexes involving many different molecules. Cytoskeletal switching stations like adhesion plaques are examples of such complexes in which several LIM-domain proteins have an important role. Likewise, it is rapidly becoming clear that transcription and its regulation require the orderly assembly of numerous proteins on the DNA, involving protein–DNA and protein–protein interactions. LIM domains, with their ability to mediate varied interactions, play an important part in these cellular processes.

Acknowledgements

We apologize to authors whose work could not be cited for space reasons. We thank O. Hobert, P. Caroni, D. Dorsett, D. Segal and M. Summers for providing unpublished information. J.J.B. was supported by a Research Associateship from the National Research Council.

References

1 Way, J.C. and Chalfie, M. (1988) *Cell* 54, 5–16
2 Freyd, G., Kim, S.K. and Horvitz, H.R. (1990) *Nature* 344, 876–879
3 Karlsson, O. *et al.* (1990) *Nature* 344, 879–882
4 Sánchez-García, I. and Rabbitts, T.H. (1994) *Trends Genet.* 10, 315–320
5 Dawid, I.B., Toyama, R. and Taira, M. (1995) *C. R. Acad. Sci. Ser. III, Sciences de la Vie/Life Sciences* 318, 295–306
6 Jurata, L.W. and Gill, G.N. (1998) *Curr. Top. Microbiol. Immunol.* 228, 75–118
7 Curtiss, J. and Heilig, J.S. *BioEssays* (in press)
8 Perez-Alvarado, G.C. *et al.* (1994) *Nat. Struct. Biol.* 1, 388–398
9 Perez-Alvarado, G.C. *et al.* (1996) *J. Mol. Biol.* 257, 153–174
10 Konrat, R., Weiskirchen, R., Krautler, B. and Bister, K. (1997) *J. Biol. Chem.* 272, 12001–12007
11 Taira, M., Evrard, J-L., Steinmetz, A. and Dawid, I.B. (1995) *Trends Genet.* 11, 431–432
12 Jain, M.K. *et al.* (1996) *J. Biol. Chem.* 271, 10194–10199
13 Petit, M.M.R. *et al.* (1996) *Genomics* 36, 118–129
14 Morgan, M.J. and Madgwick, A.J. (1996) *Biochem. Biophys. Res. Commun.* 225, 632–638
15 Genini, M. *et al.* (1997) *DNA Cell Biol.* 16, 433–442
16 Taniguchi, Y. (1998) *Mol. Cell. Biol.* 18, 644–654
17 Beckerle, M.C. (1997) *BioEssays* 19, 949–957
18 Tomasetto, C. *et al.* (1995) *FEBS Lett.* 373, 245–249
19 Roof, D.J. *et al.* (1997) *J. Cell Biol.* 138, 575–588
20 Baltz, R., Evrard, J-L., Domon, C. and Steinmetz, A. (1992) *Plant Cell* 12, 1465–1466
21 Arber, S. and Caroni, P. (1996) *Genes Dev.* 10, 289–300
22 Nix, D.A. and Beckerle, M.C. (1997) *J. Cell Biol.* 138, 1139–1147
23 Wadman, I.A. *et al.* (1997) *EMBO J.* 16, 3145–3157
24 Visvader, J. *et al.* (1997) *Proc. Natl. Acad. Sci. U. S. A.* 94, 13707–13712
25 Smolich, B. *et al.* (1997) *J. Biochem. (Tokyo)* 121, 382–388
26 Wu, R.Y. and Gill, G.N. (1994) *J. Biol. Chem.* 269, 25085–25090
27 Schmeichel, K.L. and Beckerle, M.C. (1994) *Cell* 79, 211–219
28 Feuerstein, R. *et al.* (1994) *Proc. Natl. Acad. Sci. U. S. A.* 91, 10655–10659
29 Johnson, J.D. *et al.* (1997) *Mol. Cell. Biol.* 17, 3488–3496
30 Kong, Y., Flick, M.J., Kudla, A.J. and Konieczny, S.F. (1997) *Mol. Cell. Biol.* 17, 4750–4760
31 Brown, M.C., Perrotta, J.A. and Turner, C.E. (1996) *J. Cell Biol.* 135, 1109–1123
32 Wu, R. *et al.* (1996) *J. Biol. Chem.* 271, 15934–15941
33 Kuroda, S. *et al.* (1996) *J. Biol. Chem.* 271, 31029–31032
34 Sánchez-García, I., Osada, H., Forster, A. and Rabbitts, T.H. (1993) *EMBO J.* 12, 4243–4250
35 Taira, M., Otani, H., Saint-Jeannet, J-P and Dawid, I.B. (1994) *Nature* 372, 677–679
36 Agulnick, A.D. *et al.* (1996) *Nature* 384, 270–272
37 Jurata, L.W., Kenny, D.A. and Gill, G.N. (1996) *Proc. Natl. Acad. Sci. U. S. A.* 93, 11693–11698
38 Bach, I. *et al.* (1997) *Genes Dev.* 11, 1370–1380
39 Toyama, R., Kobayashi, M., Tomita, T. and Dawid, I.B. *Mech. Dev.* (in press)
40 Jurata, L.W. and Gill, G.N. (1997) *Mol. Cell Biol.* 17, 5688–5698
41 Breen, J.J., Agulnick, A.D., Westphal, H. and Dawid, I.B. *J. Biol. Chem.* (in press)
42 Morcillo, P., Rosen, C. and Dorsett, D (1996) *Genetics* 144, 1143–1154
43 Morcillo, P., Rosen, C., Baylies, M.K. and Dorsett, D. (1997) *Genes Dev* 11, 2729–2740
44 Duboule, D., ed. (1994) *Guidebook to the Homeobox Genes*, Oxford University Press
45 Hobert, O. *et al.* (1997) *Neuron* 19, 345–357
46 Hobert, O., D'Alberti, T., Liu, Y. and Ruvkun, G. *J. Neurosci.* (in press)
47 Lundgren, S.E., Callahan, C.A., Thor, S. and Thomas, J.B. (1995) *Development* 121, 1769–1773

48 Cohen, B. *et al.* (1992) *Genes Dev.* 6, 715–729
49 Bourgouin, C., Lundgren, S.E. and Thomas, J.B. (1992) *Neuron* 9, 549–561
50 Thor, S. and Thomas, J.B. (1997) *Neuron* 18, 397–409
51 Curtiss, J. and Heilig, J.S. (1997) *Dev. Biol.* 190, 129–141
52 Taira, M., Jamrich, M., Good, P.J. and Dawid, I.B. (1992) *Genes Dev.* 6, 356–366
53 Toyama, R. *et al.* (1995) *Development* 121, 383–391
54 Barnes, J.D. *et al.* (1994) *Dev. Biol.* 161, 168–178
55 Taira, M., Saint-Jeannet, J-P. and Dawid, I.B. (1997) *Proc. Natl. Acad. Sci. U. S. A.* 94, 895–900
56 Shawlot, W. and Behringer, R.R. (1995) *Nature* 374, 425–430
57 Toyama, R. *et al.* (1995) *Dev. Biol.* 170, 583–593
58 Taira, M., Otani, H., Jamrich, M. and Dawid, I.B. (1994) *Development* 120, 1525–1536
58 Fujii, T. *et al.* (1994) *Dev. Dyn.* 199, 73–83
60 Karavanov, A.A. *et al.* (1996) *Int. J. Dev. Biol.* 40, 453–461
61 Toyama, R. and Dawid, I.B. (1997) *Dev. Dyn.* 209, 406–417
62 Pfaff, S.L. *et al.* (1996) *Cell* 84, 309–320
63 Porter, F.D. *et al.* (1997) *Development* 124, 2935–2944
64 Sheng, H.Z. *et al.* (1996) *Science* 272, 1004–1007
65 Zhadanov, A.B. *et al.* (1995) *Dev. Dyn.* 202, 354–364
66 Tsuchida, T. *et al.* (1994) *Cell* 79, 957–970
67 Appel, B. *et al.* (1995) *Development* 121, 4117–4125
68 Glasgow, E., Karavanov, A.A. and Dawid, I.B. (1997) *Dev. Biol.* 192, 405–419
69 Li, H. *et al.* (1994) *EMBO J.* 13, 2876–2885
70 Sheng, H.Z. *et al.* (1997) *Science* 278, 1809–1812
71 Johnson, R.L. and Tabin, C.J. (1997) *Cell* 90, 979–990
72 Warren, A.J. *et al.* (1994) *Cell* 78, 45–57
73 Arber, S. *et al.* (1997) *Cell* 88, 393–403
74 Frangiskakis, J.M. *et al.* (1996) *Cell* 86, 59–69
75 Higuchi, O., Amano, T., Yang, N. and Mizuno, K. (1997) *Oncogene* 14, 1819–1825
76 Schmeichel, K.L. and Beckerle, M.C. (1997) *Mol. Biol. Cell* 8, 219–230
77 Bach, I. *et al.* (1995) *Proc. Natl. Acad. Sci. U. S. A.* 92, 2720–2724
78 Wadman, I. *et al.* (1994) *EMBO J.* 13, 4831–4839
79 Osada, H. *et al.* (1995) *Proc. Natl. Acad. Sci. U. S. A.* 92, 9585–9589
80 Mao, S., Neale, G.A. and Goorha, R.M. (1997) *Oncogene* 14, 1531–1539
81 Pomiès, P., Louis, H.A. and Beckerle, M.C. (1997) *J. Cell Biol.* 139, 157–168
82 Louis, H.A. *et al.* (1997) *J. Biol. Chem.* 272, 27484–27491
83 Kotake, K. *et al.* (1997) *J. Biol. Chem.* 272, 29407–29410
84 Hiraoka, J. *et al.* (1996) *FEBS Lett.* 399, 117–121
85 Crawford, A.W., Pino, J.D. and Beckerle, M.C. (1994) *J. Cell Biol.* 124, 117–127

***I.B. Dawid, J.J. Breen and R. Toyama** are in the Laboratory of Molecular Genetics, National Institute of Child Health and Human Development, National Institutes of Health, Bethesda, MD 20892, USA.*

GENETWORK

Genetwork

Exploring protein homology with the Blocks server

Proteins typically contain regions of conserved sequence and structure punctuated by regions showing little conservation. These more-conserved regions can be revealed as ungapped 'blocks' in alignments of related sequences. Blocks describe characteristic regions of protein families and the range of sequences they can adopt. Consequently, the identification and analysis of blocks can be valuable for understanding protein function, and computational tools based on them have been developed and refined as sequence databanks have grown.

The Blocks Database[1] was introduced in 1991 as a method for classifying newly determined sequences. A fully automated system finds and extends motif alignments for a collection of related proteins and chooses the highest-scoring set of blocks in which the blocks are in the same order along the sequences. When applied to the current collection of 932 unique protein families documented in Prosite[2] (v. 9.3), a total of 3417 blocks are produced. The median block is 34 amino acids wide and includes 11 sequences. The Blocks Database is searched with either a protein or (translated) DNA sequence query. In a search, the alignment information available in a block is extracted by using recently improved methodology to convert the block to a position-specific scoring matrix (PSSM)[3]. High-scoring hits for single or multiple blocks representing a family are reported along with estimates that these hits occurred by chance, based on rank statistics. Searching can also be performed on the Prints Database[4], which currently represents 800 protein families. Prints are conceptually similar to Blocks, but they are constructed using a semi-manual alignment method. The current default for searching is a composite database consisting of

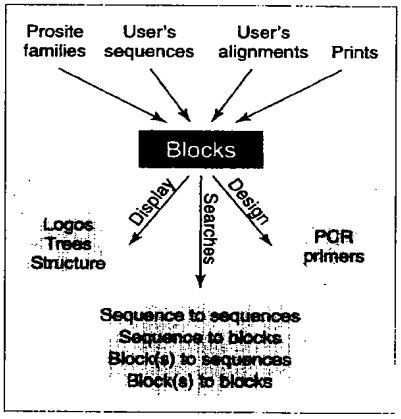

FIGURE 1. Overview of the Blocks WWW site.

Blocks supplemented with the 231 protein families in Prints that are not represented in Blocks. Both Prosite (on which Blocks is based) and Prints provide key documentation and references for each protein family. Search results can be conveniently explored via WWW links from Blocks output to Prosite, Prints, other sources of protein family documentation[5] and individual sequence entries via Entrez[6] and beyond.

PII: S0168-9525(98)01421-8

ELSEVIER

Mechanisms of Development 91 (2000) 5–17

www.elsevier.com/locate/modo

Review article

The LIM domain: regulation by association

Ingolf Bach*

Center for Molecular Neurobiology, University of Hamburg, Martinistrasse 85, 20246 Hamburg, Germany

Received 30 September 1999; received in revised form 22 November 1999; accepted 22 November 1999

Abstract

The LIM domain is a zinc finger structure that is present in several types of proteins, including homeodomain transcription factors, kinases and proteins that consist of several LIM domains. Proteins containing LIM domains have been discovered to play important roles in a variety of fundamental biological processes including cytoskeleton organization, cell lineage specification and organ development, but also for pathological functions such as oncogenesis, leading to human disease. The LIM domain has been demonstrated to be a protein–protein interaction motif that is critically involved in these processes. The recent isolation and analysis of more LIM domain-containing proteins from several species have confirmed and broadened our knowledge about LIM protein function. Furthermore, the identification and characterization of factors that interact with LIM domains illuminates mechanisms of combinatorial developmental regulation. © 2000 Elsevier Science Ireland Ltd. All rights reserved.

Keywords: LIM domain; Regulation; Protein–protein interaction

1. Introduction

Specific protein–protein interactions are of fundamental importance for many biological processes. These interactions are mediated by specific protein surfaces which, according to their biological significance, remain conserved during evolution. Proteins often contain more than one interaction domain, thereby allowing multiprotein complexes to form. Multiprotein complexes are thought to be responsible for many key processes in biology, their protein composition also being a determinant of specificity. The LIM domain, discovered 10 years ago as a conserved zinc finger motif, has been found in a variety of different proteins. LIM proteins that are nuclear, cytoplasmic or shuttled between both compartments have been identified in many different species. These proteins contain one, two or multiple LIM domains and can be categorized into different classes according to their amino acid sequence homologies. In recent years, accumulating results have continued to attribute essential functions to LIM proteins in a variety of different biological processes. Identified as a domain mediating protein–protein interactions, the LIM domain is a crucial protein structure for the biological functions of many LIM proteins, thus emphasizing their importance for the assembly of multiprotein complexes. This article reviews recent advances in the characterization of members of the LIM protein family, their biological roles, LIM domain binding proteins and regulation of activity.

2. A defining family feature: the LIM domain

Named by the initials of the three homeodomain proteins Lin11, Isl-1 and Mec-3 in which it was first discovered, the LIM domain has proved to be a conserved domain found in proteins from ascidians to man. Subsequently, a number of LIM homeodomain (LIM-hd) genes were identified that all shared two tandemly repeated LIM domains fused to a conserved homeodomain (Table 1). LIM motifs were also found in other classes of genes encoding nuclear and cytoplasmic LIM domain proteins (Table 2). Some proteins that are localized in the nucleus consist primarily of two LIM domains and were therefore named LIM only proteins (LMO). In Lmk1 and Lmk2, LIM domains are associated with kinases, and other LIM proteins with varying numbers of LIM domains have been identified that are localized mainly in the cytoplasm (Curtiss and Heilig, 1998; Dawid et al., 1998; Jurata and Gill, 1998).

The LIM domain is a cysteine-histidine rich, zinc-coordinating domain, consisting of two tandemly repeated zinc fingers (Dawid et al., 1998; Jurata and Gill, 1998). NMR studies of the cytoplasmic LIM proteins CRP1 and CRIP revealed that the LIM domain is structurally similar to GATA-type zinc fingers (Perez-Alvarado et al., 1994,

* Tel.: +49-40-42803-5668; fax: +49-40-42803-4774.
E-mail address: ingolf.bach@zmnh.uni-hamburg.de (I. Bach)

0925-4773/00/$ - see front matter
PII: S0925-4773(99)00314-7

Table 1
LIM homeodomain domain factors

Gene	Species[a]	Molecular disturbance	Phenotype/expression	Other	Refs.
Ceh-14	Ce			Lhx3/4 subclass	see Dawid et al., 1998
Lin11	Ce	Transposon insertion	Vulval cell types missing, thermoregulatory interneurons	Lhx1/5 subclass	Freyd et al., 1990; Hobert et al., 1998
Lim-4	Ce	Point mutations	Required for olfactory neurons, changes in movement and foraging behavior	Lhx6/7 subclass	Sagasti et al., 1999
Lim-6	Ce	Gene deletion	Affects differentiation of GABAergic neurons, uterine morphogenesis	Lmx subclass	Hobert et al., 1999b
Mec-3	Ce	Point mutation	Required for specific mechanosensory neurons	Lhx1/5 subclass	Way and Chalfie, 1988
Ttx-3	Ce	Point mutation	Required for specific thermoregulatory interneurons	Apterous subclass	Hobert et al., 1997
Apterous	Dm	Gene deletion, PZ insertion	Defective wing patterning, muscle formation, axon guidance	Apterous subclass	Bourgouin et al., 1992; Cohen et al., 1992; Lundgren et al., 1995
Arrowhead	Dm	Transposon insertion	Requirement for subset of imaginal disc tissues	Ectopic expression represses development of certain imaginal disc cell types, Lhx8 subclass	Curtiss and Heilig, 1997
BK64	Dm			Lhx3/4 subclass	see Dawid et al., 1998
BK87	Dm			Lhx1/5 subclass	see Dawid et al., 1998
Islet	Dm	Gene deletion	Required for motorneruon pathfinding and neurotransmitter production	Ectopic expression in Dm induces changes in pathfinding and neurotransmitter identity, Islet subclass	Thor and Thomas, 1997
HRLIM	Hr		Expressed transiently at 32 cell stage and in notochord precursor cells, later expressed in specific brain and spinal cord cell lineages	Lhx3/4 subclass	Wada et al., 1995
Isl-1	Vert	KO	Required for certain motor- and interneurons, pancreatic mesenchyme and islet cells, and pituitary cell differentiation	Islet subclass	Pfaff et al., 1996; Ahlgren et al., 1997; Takuma et al., 1998
Isl-2	Vert		Expressed in brain and spinal cord	Islet subclass	Tsuchida et al., 1994
Isl-3	Zf		Expressed in brain and spinal cord	Islet subclass	Gong et al., 1995
Lhx1	Vert	KO	Missing anterior head structures, embryonic lethal	LIM domain deleted Lhx1 induces secondary axis in early *Xenopus* embryos, Lhx 1/5 subclass	Taira et al., 1994; Shawlot and Behringer, 1995
Lhx2	Vert	KO	No eyes, forebrain defects, no definitive erythropoiesis, embryonic lethal	Expression in ES cells produces multipotent hematopoietic cells; Apterous subclass	Xu et al., 1993; Porter et al., 1997; Pinto do Ó et al., 1998

Table 1 (*continued*)

Gene	Species[a]	Molecular disturbance	Phenotype/expression	Other	Refs.
Lhx3/P-Lim	Vert	KO	4 of 5 anterior pituitary cell types missing, required for projections of specific motorneurons, perinatal lethal	Lhx3/4 subclass	Sheng et al., 1996; Sharma et al., 1998; Thor et al., 1999
Lhx4	Vert	KO	Hypoplastic anterior pituitary, required for projections of specific motorneurons, perinatal lethal	Lhx3/4 subclass	Li et al., 1994; Sheng et al., 1997
Lhx5	Vert	KO	Morphogenesis of hippocampus, postnatal lethal	Lhx1/5 subclass	Zhao et al., 1999
Lhx6	M		Expressed in first branchial arch and basal forebrain	Lhx6/7 subclass	Grigoriou et al., 1998
Lhx7	M		Expressed in first branchial arch and basal forebrain	Lhx6/7 subclass	Grigoriou et al., 1998
Lhx8	M		Expressed in ventral forebrain	Lhx8 subclass	Matsumoto et al., 1996
Lhx9	M		Expressed in pioneer neurons in the cortex, limbs	Apterous subclass	Rétaux et al., 1999; Bertuzzi et al., 1999
Lmx1a	Vert		Expressed in pancreas, brain and spinal cord	Specifies dorsal cell fate in chick limb development, Lmx subclass	Riddle et al., 1995; Vogel et al., 1995
Lmx1b	Vert	KO	Limb, kidney and calvarial defects	Mutations Lmx1b cause human nail patella syndrome; Lmx subclass	Chen et al., 1998; Dreyer et al., 1998

[a] Ce, *Caenorhabditis elegans*; Dm, *Drosophila melanogaster*; Hr, *Halocynthia roretzi*; M, mouse; Vert, two or more vertebrates; Zf, zebrafish.

1996). However, unlike GATA-type zinc fingers, the LIM domains of animal LIM proteins do not seem to bind DNA. Rather, the LIM domain has been implicated in conferring specific protein–protein interactions (Feuerstein et al., 1994; Schmeichel and Beckerle, 1994; Arber and Caroni, 1996). Sequence comparisons show that several classes of LIM domains can be distinguished (Dawid et al., 1995, 1998; Jurata and Gill, 1998). According to this classification, LIM-hd factors, LMOs and the LIM kinases contain LIM domains of classes A and B. Consequently, this protein group has been designated as group 1. The primarily cytoplasmic LIM proteins contain LIM domains of the C and D classes. Group 2 LIM factors are mainly composed of LIM domains of class C, whereas the heterogeneous group 3 LIM proteins contain primarily class D LIM domains (Fig. 1) (Dawid et al., 1998). In LIM-hd factors, positive and negative functions have been attributed to the LIM domain. It has been shown to be required for the synergistic activation of target genes together with other classes of transcription factors (German et al., 1992; Bach et al., 1995; Jurata and Gill, 1997), whereas LIM domain mutated or deleted versions of Lhx1, but not the full length protein, is capable of inducing a secondary axis, when injected ventrally in *Xenopus* embryos (Taira et al., 1994).

2.1. Setting cell fates: LIM-hd factors

In recent years the LIM protein family has grown considerably (see Tables 1 and 2) and has been attributed with essential roles in diverse biological processes. LIM-hd proteins have been shown in numerous examples to play important roles in cell fate decisions and organ development. These proteins contain two conserved N-terminal LIM domains and can be grouped pair-wise according to their overall sequence homologies (Dawid et al., 1998; Jurata and Gill, 1998).

The *C. elegans* LIM-hd factor, Mec-3, was shown to be involved in the specification of mechanosensory neurons (Way and Chalfie, 1988), whereas Lin11 specifies certain vulval cell lineages (Karlsson et al., 1990). In addition, Lin11 and ttx-3 factors have been connected with the development of specific thermoregulatory neurons (Hobert et al., 1997, 1998). Recently, the *C. elegans* lim-4 gene has been implicated in olfactory neuronal cell fates (Sagasti et al., 1999), whereas the lim-6 gene is involved in the function of specific GABAergic neurons (Hobert et al., 1999b). In *Drosophila*, the LIM-hd protein, Apterous, is required for dorsal cell identity during wing development (Cohen et al., 1992; Diaz-Benjumea and Cohen, 1993; Blair et al., 1994),

Table 2
Nuclear and cytoplasmic LIM proteins

Protein	No. of LIM domains	Localization	Tissue distribution	Function/KO phenotype	Other	Refs.
LMO-1	2	Nuclear	Brain, ventral spinal cord, trigeminal and facial neurons, retina		Causes T-cell leukemia when overexpressed in T-cells	Greenberg et al., 1990; Boehm et al., 1991; Fisch et al., 1992; McGuire et al., 1992
LMO-2	2	Nuclear	Widely expressed, brain, spleen, liver, kidney, eye, lung, limb buds	Lmo2$^{-/-}$ mice die at e10.5; no erythropoiesis	Causes T-cell leukemia when overexpressed in T-cells	Royer-Pokora et al., 1991; Fisch et al., 1992; Warren et al., 1994; Larson et al., 1995; Neale et al., 1995
LMO-3	2	Nuclear	Brain, ventral spinal cord, trigeminal and facial neurons, retina			Foroni et al., 1992; Hinks et al., 1997
LMO-4	2	Nuclear	Widely expressed, brain, thymus, eye, lung, pituitary			Grutz et al., 1998; Kenny et al., 1998; Sugihara et al., 1998
dLMO	2	Nuclear	Wing, leg and eye imaginal discs, brain	Encodes Beadex gene, loss of tissue at wing margin	D-V misexpression: loss of wing margin; A-P misexpression: ectopic margin formation	Zhu et al., 1995; Zeng et al., 1998; Milán and Cohen, 1999
LMK1	2	Cytoplasmic	Mainly CNS, skeletal muscle	Regulator of actin dynamics by cofilin phosphorylation, activates serum response factor (SRF)	Lmk1 is substrate for Rho-associated kinase ROCK	Arber et al., 1998; Yang et al., 1998; Maekawa et al., 1999; Sotiropoulos et al., 1999
LMK2	2	Cytoplasmic	Widely expressed, highest in placenta, liver			Okano et al., 1995
CRP1	2	Cytoplasmic	Lung, intestine, arteries, fibroblast, stomach			Louis et al., 1997
CRP2	2	Cytoplasmic	Arteries, fibroblast			Louis et al., 1997
CRP3/MLP	2	Cytoplasmic/ nuclear	Heart, skeletal muscle	MLP KO mice exhibit disruption of cardiac cytoarchitectural organization, dilated cardiomyopathy		Arber et al., 1997; Louis et al., 1997
CRIP	1	Cytoplasmic				Perez-Alvarado et al., 1996
Ril	1	Cytoplasmic				Kiess et al., 1995
Enigma	3	Cytoplasmic				Wu and Gill, 1994
Zyxin	3	Cytoplasmic/ nuclear	Lung, skeletal muscle, intestine, heart, arteries, stomach, fibroblast		Shuttles between cell adhesion sites and nucleus	Sadler et al., 1992; Nix and Beckerle, 1997
Prickle/Testin	3	Cytoplasmic	*Drosophila* pupal intervein cells, eye and wing imaginal discs, cells engaged in morphogenetic movements	Mutations or overexpression affects tissue polarity	Several splice variants	Dicheva and Charleston, 1995; Gubb et al., 1999
Ajuba	3	Cytoplasmic		Promotes meiotic maturation		Goyal et al., 1999
LPP	3		Widely expressed		Fusion partner gene of HMGIC in lipomas	Petit et al., 1996
Paxillin	4	Cytoplasmic			Localizes to focal adhesions sites	Turner et al., 1990

Table 2 (*continued*)

Protein	No. of LIM domains	Localization	Tissue distribution	Function/KO phenotype	Other	Refs.
SLIM1/KyoT	4 (2)	Cytoplasmic (nuclear)	Skeletal muscle, lung, skin, kidney		Alternative spliced form KyoT2 inhibits RBP-J mediated activation	Morgan and Madgwick, 1996; Taniguchi et al., 1998
ACT	4	Nuclear	Testis		Mediates CBP-independent activation of CREM and CREB	Fimia et al., 1999
PINCH/Unc-98	5	Cytoplasmic/ nuclear	Vulval and body wall muscles, mechanosensory neurons; colocalizes with β-integrin to focal adhesion sites	Affects specific muscle adherens junctions and mechanosensory functions of touch neurons		Rearden, 1994; Hobert et al., 1999a

and Arrowhead was shown to be essential for the development of one set of imaginal cells, but incompatible with the development of another (Curtiss and Heilig, 1997). Important developmental roles for cell type specification have also been attributed to LIM-hd factors in higher vertebrates. Mice lacking functional Lhx1 fail to develop anterior head structures (Shawlot and Behringer, 1995). Isl-1$^{-/-}$ mice do not develop certain motor- and interneurons, pituitary cell types are unable to differentiate (Pfaff et al., 1996; Takuma et al., 1998), and the formation of pancreatic mesenchyme and islet cells is impaired (Ahlgren et al., 1997). Lhx2 is implicated in the development of the eye, forebrain, erythrocytes and the chicken limbs (Porter et al., 1997; Rodriguez-Esteban et al., 1998). Lhx3/P-Lim and Lhx4/Gsh4 are implicated in the control of anterior pituitary development and specification of certain motorneurons (Sheng et al., 1996, 1997; Sharma et al., 1998; Thor et al., 1999), whereas Lhx5 controls the morphogenesis of hippocampal structures (Zhao et al., 1999). LMX1a controls the dorsoventral patterning of chick limbs (Riddle et al., 1995; Vogel et al., 1995) and mutations in the LMX1b gene cause human nail patella syndrome (Chen et al., 1998; Dreyer et al., 1998). Several other LIM homeobox factors are known to exist, including Ceh-14, BK64 and BK87 (see Dawid et al., 1998), or have been isolated, and the specific mRNA expression patterns of at least some of those proteins promise important functions for the development of further embryonic cell types and structures (see Fig. 1).

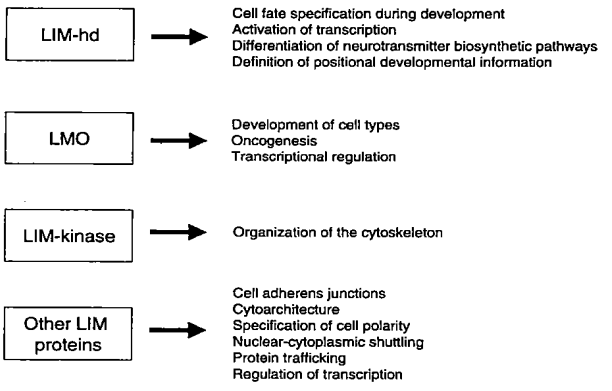

Fig. 1. Regulation of cellular processes regulated by proteins containing LIM domains.

There are many examples of developing organs in which specific LIM-hd genes are expressed in highly restricted but spatially and temporarily overlapping patterns. These tissue types include the developing pituitary, retina, limbs, thymus, pancreatic islet cells, spinal cord and brain. In the developing central nervous system, specific territories called neuromeres were identified on the basis of mitotic zones and fate maps and on the expression patterns of many developmental genes (Puelles and Rubenstein, 1993). LIM-hd expression patterns have been shown to respect the boundaries of neuromeres and the regions that express LIM-hd genes entirely cover the transverse and longitudinal neuromeres (Rétaux et al., 1999). Therefore, it is likely that the LIM-hd protein family is involved in fundamental events of anteroposterior and dorsoventral patterning of the central nervous system and it has been suggested that the combinatorial expression of LIM-hd genes may define distinct subclasses of neuronal cell types (e.g. Tsuchida et al., 1994). Indeed, in the developing spinal cord it has been demonstrated recently that the LIM-hd proteins Lhx3 and Lhx4 participate in a combinatorial code which defines the positional information required for the generation of distinct motorneuron subfamilies (Sharma et al., 1998; Thor et al., 1999).

Several papers have reported the induction of LIM-hd gene expression by various inducing signals for different organs. In the ventral neural tube, Isl-1 expression is induced by Sonic Hedgehog (Ericson et al., 1995), whereas WNT7a controls the expression of Lmx1 for the dorsoventral pattern formation of the chick limb (Riddle et al., 1995; Vogel et al., 1995). In *Xenopus*, dorsal mesoderm inducers of the TGF-β superfamily, including activin, nodal and act-Vg1, have been shown to activate the Xlim1 promoter (Rebbert and Dawid, 1997), whereas FGF8 has been identified as the likely candidate signaling molecule for the expression of Lhx6 and Lhx7, as well as for their cofactor CLIM2/NLI/LDB1 in branchial arch mesenchyme cells

(Tucker et al., 1999) and for Lhx3 and Lhx4 in the embryonic anterior pituitary (Ericson et al., 1998; Treier et al., 1998). Thus, the expression of different LIM-hd factors in various organ systems appears to be induced by multiple signals during embryogenesis. Interestingly, the *Drosophila* LIM-hd protein, Apterous, has been shown to activate the Notch signal transduction pathway during wing development (Diaz-Benjumea and Cohen, 1993).

2.2. Nuclear LIM-only (LMO) proteins in development and oncogenesis

Nuclear LIM-only proteins consist of two LIM domains and little else and are thought to act as molecular adapter molecules, linking proteins of various types together. As shown for the LIM-hd genes, the LIM-only genes occupy important biological roles in development. Additionally, this class of LIM proteins has also been shown to be involved in oncogenesis (Rabbitts, 1998). The LIM-only genes LMO-1 and LMO-2 were first discovered because of their localization at translocation breakpoints of T-cell leukemia patients. These translocations resulted in an abnormal expression of LMO-1 or LMO-2 in the thymus and in T-cells, tissues that normally express only low levels of both of these proteins. The overexpression of LMO-1 or LMO-2 in the thymus of transgenic animals was subsequently shown to be sufficient for the occurrences of T-cell transformations (Larson et al., 1995, 1996). The role of LMO-2 in erythropoiesis was further demonstrated by a gene deletion experiment: LMO-2 deleted mice die during embryogenesis due to a failure to develop mature erythrocytes (Warren et al., 1994). Subsequently, it was shown that LMO-2 is also required for the hematopoiesis in the adult animals (Yamada et al., 1998). These results place LMO-2 function at least prior to the bifurcation of myeloid and lymphoid lineages. The nuclear LMO family has been extended with the isolation of LMO-3 (Foroni et al., 1992) and recently, LMO-4 (Grutz et al., 1998; Kenny et al., 1998; Sugihara et al., 1998). Interestingly, unlike mRNA from the other LMO proteins, transcripts encoding LMO-4 can be detected at high levels in the thymus. Other LMO-4-expressing tissues include the brain, skin, and pituitary gland (Grutz et al., 1998; Kenny et al., 1998; Sugihara et al., 1998) (see Table 2). A *Drosophila* LMO protein, dLMO, that is expressed in developing wing imaginal discs has been discovered, and its misexpression in the anterior-posterior boundary of the wing imaginal disc leads to extra wing outgrowth, a phenotype that is similar to that observed for the inactivation of the LIM-hd protein Apterous. Overexpression along the dorsal-ventral boundary leads to a phenotype similar to *Beadex*, a dominant mutation that causes the loss of the wing margin. Indeed, it has been shown that *Beadex* disrupts dLMO transcripts in the 3′ untranslated region (Milán et al., 1998; Zeng et al., 1998).

2.3. LIM kinases: regulators of cytoskeleton dynamics

Two LIM kinases, Lmk1 (Kiz) and Lmk2, have been discovered thus far, and both proteins display two N-terminal LIM domains linked to a C-terminal kinase domain (Bernard et al., 1994; Mizuno et al., 1994; Okano et al., 1995; Stanyon and Bernard, 1999). Recent studies on Lmk1 have greatly advanced this field of research. Lmk1 was found to shuttle between the cytoplasm and the nucleus (Yang and Mizuno, 1999). Whereas a nuclear role for Lmks has not been reported, recent work demonstrated a central cytoplasmic role of Lmk1 in the organization of the actin cytoskeleton. This is achieved by its ability to phosphorylate cofilin, thereby reversing cofilin-induced actin depolymerization (Arber et al., 1998; Yang et al., 1998). The fact that Lmk1 has recently been shown to be itself phosphorylated by the small guanosine triphosphatase Rho-associated kinase ROCK places Lmk1 in the pathway of Rho-induced reorganization of the actin cytoskeleton (Maekawa et al., 1999). Furthermore, Lmk1 is able to activate the serum response factor (SRF), a transcription factor that regulates the expression of many serum-inducible and muscle-specific genes. Here, Lmk1-mediated SRF activation was not dependent on serum, but rather on signals that depend on alterations in actin dynamics (Sotiropoulos et al., 1999). These results demonstrate a major role of Lmk1 in the regulation of cell motility and morphogenesis.

2.4. Diverse functions for other classes of LIM proteins

The primarily cytoplasmic cysteine-rich protein (CRP) subfamily members, CRP1, CRP2, CRP3/MLP and CRIP, consist primarily of characteristic LIM domains that are each linked to a short additional conserved motif. CRIP contains only one, whereas the other three members, CRP1–3, each contain two of these characteristic LIM domains (Perez-Alvarado et al., 1996; Dawid et al., 1998). Mice which lack the CRP3/MLP gene show disturbances of the cytoarchitecture of both cardiac and skeletal muscle (Arber et al., 1997). The fact that all three CRP proteins are associated with actin filaments and with the Z lines of myofibers, display very similar biochemical properties, but show distinct protein expression profiles suggests that they perform similar functions which are executed in distinct locations during vertebrate development (Arber et al., 1997; Louis et al., 1997). In addition to the cytoplasmic localization of CRP3/MLP, nuclear localization has also been reported (Arber and Caroni, 1996), and a recent report links CRP3/MLP to an enhancement of the activity of the bHLH transcription factor MyoD (Kong et al., 1997). Furthermore, the *Drosophila* CRP gene, Mlp, might be the direct target of the myocyte enhancer-binding factor 2 (MEF2) (Stronach et al., 1999).

The divergent group 3 of LIM proteins is divided in two subgroups. One is comprised of members such as Ril, Enigma, Zyxin, Prickle and Paxillin. Ril contains one LIM

domain, whereas Enigma, Zyxin and Prickle contain three, and Paxillin four, conserved LIM domains at their C-terminal ends. Besides their LIM domains, these proteins carry additional functional protein domains at their N-termini (Beckerle, 1997; Dawid et al., 1998; Jurata and Gill, 1998). Sequences of several more putative group 3 members as yet unpublished are found in sequence databases (see Dawid et al., 1998; Gubb et al., 1999; Hobert et al., 1999a,b). Most of the proteins of this group have been shown to be associated with the cytoskeleton (Turner et al., 1990; Sadler et al., 1992; Guy et al., 1999). In addition, Enigma seems to be involved in protein trafficking (Wu and Gill, 1994). Several alternatively spliced mRNAs of the recently identified Prickle protein have been shown to be involved in the specification of planar polarity in *Drosophila* (Gubb et al., 1999).

The SLIM1/KyoT/ACT and PINCH subgroups consist primarily of four and five LIM domains, respectively. Unc-98, a recently identified *C. elegans* LIM protein of the PINCH subclass, affects the structural integrity of the integrin-containing muscle adherens junctions and is important for the mechanosensory functions of touch receptor neurons (Hobert et al., 1999a). SLIM1/KyoT1 has been shown to be localized in the cytoplasm, but KyoT2, an alternative spliced form of the same gene that contains only the N-terminal two LIM domains, is localized in the nucleus (Taniguchi et al., 1998). Recently, the LIM protein ACT has been identified that consists of four LIM domains. ACT protein is highly and specifically expressed in the nuclei of mouse testis cells (Fimia et al., 1999).

2.5. LIM domains are versatile protein–protein interaction domains

Because protein–protein interactions have been discovered to be of fundamental functional and regulatory importance for many biological processes, and because of the essential biological roles documented for LIM proteins, the finding that the LIM domain serves as a protein–protein interaction interface has been of great interest (Feuerstein et al., 1994; Schmeichel and Beckerle, 1994; Arber and Caroni, 1996). Indeed, many different types of proteins capable of interacting with LIM domains have been identified, including structural proteins, kinases, LIM domain proteins, several classes of transcription factors and cofactors.

CRP proteins have been shown to dimerize and to bind specifically to the adhesion plaque LIM protein Zyxin (Feuerstein et al., 1994; Schmeichel and Beckerle, 1994, 1997; Louis et al., 1997). The other known cytoskeletal interaction partner is the actin-crosslinking protein α-actinin (Pomiès et al., 1997). CRP3/MLP has been shown to bind to the nuclear LIM proteins Lmo1 and Apterous (Arber and Caroni, 1996) and to the muscle bHLH factor MyoD. This last interaction promotes the myogenic activity of MyoD (Kong et al., 1997).

The interaction of Zyxin with CRP1 has been shown to be mediated by LIM domain 1, whereas the binding of Zyxin to α-actinin, which links this protein to the cytoskeleton, is not mediated through the LIM domain, but with an N-terminal proline-rich region (Schmeichel and Beckerle, 1994; Louis et al., 1997). The LIM protein Paxillin has been shown to interact via its N-terminal protein region with the cytoskeleton protein Vinculin and the focal adhesion kinase (FAK) (Turner et al., 1990). A possible link to apoptosis may be indicated by the interaction reported between Paxillin and bcl-2, an inhibitor of apoptosis (Sorenson and Sheibani, 1999), however, the involvement of the LIM domains in this interaction remains unclear (C. Sorenson, pers. commun.). Protein interactions that are mediated via the LIM domains of Enigma and the Enigma homologue (ENH) include the insulin receptor, receptor tyrosine kinases and protein kinase C (PKC) (Wu and Gill, 1994; Kuroda et al., 1996; Wu et al., 1996). Moreover, an interaction of Enigma's PDZ domain with β-tropomyosin has been published recently (Guy et al., 1999). The LIM domains of Lmk1 can interact with themselves, and with PKC (Kuroda et al., 1996). For the LIM protein PINCH, an interaction with integrin-linked kinase (ILK) has been demonstrated (Tu et al., 1999). The SLIM/KyoT alternatively spliced nuclear variant KyoT2 binds to and represses the transcriptional activity of the transcription factor RBP-J, an effector protein of the Notch signal transduction pathway. However, this interaction is not mediated via its LIM domain but with its specific C-terminus (Taniguchi et al., 1998). The nuclear LIM protein ACT has been shown to interact with the effector proteins of the cAMP signaling pathway, CREM and CREB, that were previously shown to be active via their interaction with the coactivator CREB-binding protein (CBP). ACT stimulates the transcriptional activity mediated by CREM and CREB in a CBP-independent manner (Fimia et al., 1999).

The LIM domains of the nuclear LIM-only protein LMO-2 interact with at least two classes of DNA binding proteins: the zinc finger transcription factors GATA-1 and GATA-2, and Tal1/Scl protein, which belongs to the bHLH class of transcription factors (Table 3). These interactions are believed to be of physiological relevance, since knock-out mice of any one of these three genes result in the similar phenotype of inhibition of erythropoiesis (Rabbitts, 1998). Furthermore, the efficiency of T-cell transformations was greatly increased in double transgenic animals in which Tal1 was overexpressed together with LMO-2, demonstrating a synergistic oncogenic potential of both proteins (Larson et al., 1996). LMO-4 has been shown to be able to interact in vivo with mDEAF (Table 3) (Sugihara et al., 1998), the mouse homologue of the *Drosophila* DNA-binding protein, deformed epidermal autoregulatory factor 1 (DEAF1). These studies show that nuclear LIM proteins participate in the formation of larger multiprotein complexes that form on DNA and that influence transcription.

The LIM domain of LIM-hd factors has also been reported to interact with several classes of other transcription factors (Table 3). The LIM domain of Lmx1 has been shown to interact with the bHLH factor E47 on the insulin gene minienhancer. This interaction is specific, since E47 does not bind to Isl-1, and results in a synergistic gene activation (German et al., 1992; Johnson et al., 1997; Jurata and Gill, 1997). In the anterior pituitary, the LIM domain of

Table 3
Proteins interacting with LIM domains

Interacting LIM protein	Partner protein	Class	Functional significance	Refs.
Enigma	InsR	Insulin receptor		Wu and Gill, 1994
	RET/PTC2	Receptor tyrosine kinase		Wu et al., 1996
	PKC-α, βI, ζ	Protein kinase C		Kuroda et al., 1996
ENH	PKC-βI, γ, ϵ	Protein kinase C		Kuroda et al., 1996
Zyxin	CRP1–3	LIM proteins		Schmeichel and Beckerle, 1994
	NOC2	Zinc finger protein		Kotake et al., 1997
ACT	CREM	Transcription factor	Interaction mediates CBP-independent gene activation	Fimia et al., 1999
	CREB	Transcription factor		
PINCH	ILK	Integrin-linked kinase	Might be the substrate of ILK	Tu et al., 1999
CRP1, 2	CRP1	LIM protein		Feuerstein et al., 1994
	Zyxin	LIM protein		Louis et al., 1997
CRP3/MLP	Zyxin	LIM protein		Schmeichel and Beckerle, 1994; Louis et al., 1997
	MyoD	bHLH transcription factor	Enhances activity of MyoD	Kong et al., 1997
	Lmo1	LIM-only protein		Arber and Caroni, 1996
	Apterous	LIM-homeodomain transcription factor		
LMK1	Lmk1, 2	LIM kinase 1, 2		Kuroda et al., 1996
	PKC-γ, ζ	Protein kinase C		
LMO-1, 2	Tal1	bHLH transcription factor	Synergistic induction of T-ALL, functional roles in erythropoiesis	Wadman et al., 1994
	Lyl1	bHLH transcription factor		Wadman et al., 1997
	E47	bHLH transcription factor		
LMO-2	GATA-1	Zinc finger transcription factor	Functional roles in erythropoiesis	Osada et al., 1995
	GATA-2	Zinc finger transcription factor		Wadman et al., 1997
	RBP	Retinoblastoma-binding protein		Mao et al., 1997
LMO-4	DEAF1	Transcription factor		Sugihara et al., 1998
LMX1	E47	bHLH transcription factor	Interaction required for synergistic gene activation	German et al., 1992; Jurata and Gill, 1997
LHX3	Pit-1	POU-homeodomain transcription factor	Interaction required for synergistic gene activation	Bach et al., 1995; Meier et al., 1999
	Isl-1,2	LIM homeodomain transcription factors		Jurata et al., 1998
LHX and LMO	CLIM/NLI/ Ldb/Chip	Cofactor	Required for biological activity of LIM homeodomain factors	Agulnick et al., 1996; Morcillo et al., 1997; Bach et al., 1999; Milán and Cohen, 1999; van Meyel et al., 1999
LHX, LMO and LMK1	RLIM	RING zinc finger cofactor	Overexpression inhibits functional activity of LIM homeodomain factors	Bach et al., 1999

Lhx3/P-Lim can interact with the POU domain transcription factor Pit-1. This interaction also promotes synergistic gene activation events from the promoters/enhancers of several pituitary genes (Bach et al., 1995; Meier et al., 1999). Furthermore, the LIM domain of Lhx3/P-Lim has also been reported to interact with the homeodomain of Isl-1 (Jurata et al., 1998).

LIM domains of nuclear LIM proteins have been shown not only to interact with transcription factors, but also with cofactors that do not bind to DNA. Several laboratories reported the cloning of a conserved family of cofactors that bind to LIM domains of nuclear LIM proteins, consisting of CLIM1/Ldb2 and CLIM2/Ldb1/NLI/Chip (Agulnick et al., 1996; Jurata et al., 1996; Bach et al., 1997; Morcillo et al., 1997; Visvader et al., 1997). Highest CLIM1 and -2 mRNA levels can be detected in regions of specific LIM-hd gene expression (Jurata et al., 1996; Bach et al., 1997; Visvader et al., 1997; Toyama et al., 1998). The CLIM cofactors can homodimerize and form multiprotein complexes consisting of LIM homeodomain, LMO, Pitx, bHLH and GATA transcription factors (Agulnick et al., 1996; Jurata et al., 1996, 1998; Bach et al., 1997; Jurata and Gill, 1997; Morcillo et al., 1997; Visvader et al., 1997; Wadman et al., 1997; Breen et al., 1998), suggesting that the formations of protein complexes is an important feature for CLIM function.

Recently, another cofactor named RLIM, which is a RING H2 zinc finger protein, has been isolated that also associates with LIM domains of nuclear LIM proteins. Interestingly, the expression pattern of RLIM-encoding mRNA strongly resembles the pattern of CLIM2/Ldb1/NLI in mouse and chicken as determined by in situ hybridization. RLIM can interact not only with nuclear LIM domain containing proteins, but also with the CLIM cofactors and with members of the histone deacetylase corepressor complex (Bach et al., 1999).

These results show that LIM proteins interact with a variety of proteins in different cellular compartments via their LIM domains, and that these interactions are important for the biological function of LIM proteins. Thus, LIM domains seem to be adapter molecules promoting the formation of protein complexes. Since so many different LIM proteins are implicated in various cellular processes, it is plausible that still more proteins exist that are recruited into these complexes via binding to LIM domains.

2.6. Regulation of nuclear LIM proteins by associated cofactors

Tissue-specific combinations of transcription factors regulate distinct target genes required for the development of different tissues. This regulation is thought to rely in part on the recruitment of additional proteins into specific multiprotein complexes that direct transcription from distinct promoter elements. Since many members of the nuclear LIM protein families are expressed in an overlapping fashion, one would imagine that they must rely on strict control mechanisms to ensure proper development. However, little is known about these mechanisms underlying the regulation of activity of nuclear LIM proteins. The isolation of factors that bind to LIM domains has started to illuminate this issue.

The CLIM cofactors are important for the activity of LIM-hd proteins (Agulnick et al., 1996; Morcillo et al., 1997; Breen et al., 1998) and have been implicated in the synergistic activation or in an inhibition of target genes, depending on the promoter context (Bach et al., 1997; Jurata and Gill, 1997). In *Drosophila*, it has been demonstrated that the relative amount of Apterous and CLIM/Chip expression is critical for proper wing development (Fernandez-Funez et al., 1998; Milán et al., 1998; Milán and Cohen, 1999; van Meyel et al., 1999). The developmental requirement of CLIM molecules in conjunction with LIM-hd factors has recently been demonstrated by using dominant-negative approaches in chick and *Drosophila* (Bach et al., 1999; Milán and Cohen, 1999; van Meyel et al., 1999). Furthermore, the requirement of CLIM/Chip for Apterous activity has been demonstrated in an elegant experiment in which the LIM domain of Apterous is replaced by the dimerization domain of Chip. This fusion protein proved to be equally active as wild-type Apterous protein for *Drosophila* wing development (Milán and Cohen, 1999; van Meyel et al., 1999). However, exactly how the CLIM molecules exert their functions that lead to LIM-hd protein activity is not clear. Several lines of evidence suggest that the CLIM cofactor family is also important for the functioning of proteins other than LIM-hd transcription factors. The CLIM protein family members bind to Pitx1/POTX, a transcription factor of the bicoid class (Bach et al., 1997) and mutations in Chip, the *Drosophila* CLIM homologue, display severe segmentation disorders well before the expression of any known LIM-hd factor (Morcillo et al., 1997).

The involvement of CLIM cofactors in the pathogenesis of acute T-cell leukemia is suggested by the observation that CLIM proteins are associated with LMO-1 in patients with T-ALL (Valge-Archer et al., 1998). It has been shown that forced overexpression of CLIM2 in the G1ER proerythroblast cell line keeps these cells in an undifferentiated state, preventing their differentiation into erythrocytes (Visvader et al., 1997). Furthermore, it has been proposed that the abnormally high levels of LMO-1 or -2 in T-cell leukemia patients displaces LMO-4 from its complex with CLIM cofactors and that this displacement influences T-cell differentiation prior to T-cell tumor occurrence (Grutz et al., 1998).

The RING zinc finger protein, RLIM, is another cofactor that has been identified by its ability to interact with nuclear LIM domains. RLIM inhibits not only the transcriptional activity of P-Lim/Lhx3 in transient cotransfections, but all of the previously observed synergistic activations of Lhx3/P-Lim with other transcription factor families. This transcriptional inhibition seems to be mediated by the recruit-

ment of the Sin3A/histone deacetylase repressor complex. The overexpression of RLIM in chicken wings results in phenotypes that resemble specific inhibition of LIM-hd proteins during development. Combined, these data show that RLIM inhibits functional activity of LIM-hd factors. However, because of an CLIM–RLIM interaction independent of the involvement of LIM domains, it is unclear whether RLIM inhibits LIM-hd factors directly or indirectly via the CLIM cofactors, or both (Bach et al., 1999).

The CLIM cofactors, as well as RLIM, also interact with nuclear LMO proteins in vivo. An interesting model has been presented of how the activity of LIM-hd factors can be inhibited by the overexpression of LMO proteins. This is done by competing the CLIM cofactors away from their LIM-hd protein partners. In this context, it has been shown that a tetramer consisting of two Apterous and Chip molecules can be regulated by dLMO proteins (Milán et al., 1998; Zeng et al., 1998; Milán and Cohen, 1999; van Meyel et al., 1999). This scenario requires the CLIM–LIM-hd factor interaction for proper developmental activity with CLIM molecules being present in limiting amounts. These and previous results suggest that the RLIM and CLIM cofactors as well as LMO proteins should be able to strongly contribute to the duration, intensity and specificity of the LIM-hd factor-conferred activation of the genes which in fine will determine the growth and differentiation properties of cell types.

Taken together, biochemical and genetic data place the CLIM cofactor family in a central position for the exertion of the developmental program mediated by LIM-hd transcription factors. Further evidence suggests that the CLIM cofactors play important roles not only in the LMO class of nuclear LIM proteins, but also in the activity of other transcription factors. Thus, the identification of CLIM and RLIM cofactors and LMO proteins demonstrates that in vertebrates, where LIM-hd factors are often expressed in a temporally and spatially overlapping fashion, regulation of LIM homeobox factor activity underlies a complex regulatory mode.

3. Conclusions

It seems clear that the protein–protein interactions mediated by the LIM domain are crucial components for the execution and combinatorial regulation of at least some of the cellular processes controlled by LIM proteins. Thus, LIM domains can be regarded as scaffolds for the formation of higher order complexes. This basic theme of forming multiprotein complexes held together by LIM domains seems to be applied in nature for a variety of functional contexts and is crucial for the proper function of several independent regulatory pathways. Undoubtedly, the identification/characterization of more LIM domain proteins and the further deciphering of the regulatory pathways in which these proteins are involved will continue to illuminate new and exciting basic biological mechanisms.

Acknowledgements

I wish to thank H. Ostendorff for helpful comments on the manuscript. This work was supported by the Deutsche Forschungsgemeinschaft.

References

Agulnick, A.D., Taira, M., Breen, J.J., Tanaka, T., Dawid, I.B., Westphal, H., 1996. Interactions of the LIM-domain-binding factor Ldb1 with LIM homeodomain proteins. Nature 384, 270–272.

Ahlgren, U., Pfaff, S.L., Jessell, T.M., Edlund, T., Edlund, H., 1997. Independent requirement for ISL1 in formation of pancreatic mesenchyme and islet cells. Nature 385, 257–260.

Arber, S., Caroni, P., 1996. Specificity of single LIM motifs in targeting and LIM/LIM interactions in situ. Genes Dev. 10, 289–300.

Arber, S., Hunter, J.J., Ross, J., Hongo, M., Sansig, G., Borg, J., Perriard, J.C., Chien, K.R., Caroni, P., 1997. MLP-deficient mice exhibit a disruption of cardiac cytoarchitectural organization, dilated cardiomyopathy, and heart failure. Cell 88, 393–403.

Arber, S., Barbayannis, F.A., Hanser, H., Schneider, C., Stanyon, C.A., Bernard, O., Caroni, P., 1998. Regulation of actin dynamics through phosphorylation of cofilin by LIM-kinase. Nature 393, 805–809.

Bach, I., Rhodes, S.J., Pearse II, R.V., Heinzel, T., Gloss, B., Scully, K.M., Sawchenko, P.E., Rosenfeld, M.G., 1995. P-Lim, a LIM homeodomain factor, is expressed during pituitary organ and cell commitment and synergizes with Pit-1. Proc. Natl. Acad. Sci. USA 92, 2720–2724.

Bach, I., Carrière, C., Ostendorff, H.P., Andersen, B., Rosenfeld, M.G., 1997. A family of LIM domain interacting cofactors confer transcriptional synergism between LIM and Otx homeoproteins. Genes Dev. 11, 1370–1380.

Bach, I., Rodriguez-Esteban, C., Carrière, C., Bhushan, A., Krones, A., Glass, C.K., Andersen, B., Izpisúa Belmonte, J.C., Rosenfeld, M.G., 1999. R-LIM inhibits functional activity of LIM homeodomain transcription factors via recruitment of the histone deacetylase complex. Nat. Genet. 22, 394–399.

Beckerle, M.C., 1997. Zyxin: zinc fingers at sites of cell adhesion. BioEssays 19, 949–957.

Bernard, O., Ganiatsas, S., Kannourakis, G., Dringen, R., 1994. Kiz-1, a protein with LIM zinc finger and kinase domains, is expressed mainly in neurons. Cell Growth Diff. 5, 1159–1171.

Bertuzzi, S., Porter, F.D., Pitts, A., Kumar, M., Agulnick, A., Wassif, C., Westphal, H., 1999. Characterization of Lhx9, a novel LIM/homeobox gene expressed by the pioneer neurons in the mouse cerebral cortex. Mech. Dev. 81, 193–198.

Blair, S.S., Brower, D.L., Thomas, J.B., Zavortink, M., 1994. The role of apterous in the control of dorso-ventral compartmentalization and PS integrin gene expression in the developing wing of Drosophila. Development 120, 1805–1815.

Boehm, T., Foroni, L., Kaneko, Y., Perutz, M.P., Rabbitts, T.H., 1991. The rhombotin family of cysteine-rich LIM-domain oncogenes: distinct members are involved in T-cell translocations to human chromosomes 11p15 and 11p13. Proc. Natl. Acad. Sci. USA 88, 4367–4371.

Bourgouin, C., Lundgren, S.E., Thomas, J.B., 1992. Apterous is a Drosophila LIM domain gene required for the development of a subset of embryonic muscles. Neuron 9, 549–561.

Breen, J.J., Agulnick, A.D., Westphal, H., Dawid, I., 1998. Interactions between LIM domains and the LIM domain-binding protein Ldb1. J. Biol. Chem. 273, 4712–4717.

Chen, H., Lun, Y., Ovchinnikov, D., Kokubo, H., Oberg, K.C., Pepicelli, C.V., Gan, L., Lee, B., Johnson, R.L., 1998. Limb and kidney defects in Lmx1b mutant mice suggest an involvement of LMX1B in human nail patella syndrome. Nat. Genet. 19, 51–55.

Cohen, B., McGuffin, M.E., Pfeifle, C., Segal, D., Cohen, S.M., 1992. Apterous: a gene required for imaginal disc development in Drosophila

encodes a member of the LIM family of developmental regulatory proteins. Genes Dev. 6, 715–729.

Curtiss, J., Heilig, J.S., 1997. Arrowhead encodes a LIM homeodomain protein that distinguishes subsets of Drosophila imaginal cells. Dev. Biol. 190, 129–141.

Curtiss, J., Heilig, J.S., 1998. DeLIMiting development. BioEssays 20, 58–69.

Dawid, I.B., Toyama, R., Taira, M., 1995. LIM domain proteins. C. R. Acad. Sci. III 318, 295–306.

Dawid, I.B., Breen, J.J., Toyama, R., 1998. LIM domains: multiple roles as adaptors and functional modifiers in protein interactions. Trends Genet. 14, 156–162.

Diaz-Benjumea, F.J., Cohen, S.M., 1993. Interaction between dorsal and ventral cells in the imaginal discs directs wing development in Drosophila. Cell 75, 741–752.

Dicheva, N., Charleston, B., 1995. Cloning and characterization of two new cDNAs encoding murine triple LIM domains. Gene 156, 283–286.

Dreyer, S.D., Zhou, G., Baldini, A., Winterpacht, A., Zabel, B., Cole, W., Johnson, R.L., Lee, B., 1998. Mutations in LMX1B cause abnormal skeletal patterning and renal dysplasia in nail patella syndrome. Nat. Genet. 19, 47–50.

Ericson, J., Muhr, J., Paczek, M., Lints, T., Jessell, T.M., Edlund, T., 1995. Sonic hedgehog induces the differentiation of ventral forebrain neurons: a common signal for ventral patterning within the neural tube. Cell 81, 747–756.

Ericson, J., Norlin, S., Jessell, T.M., Edlund, T., 1998. Integrated FGF and BMP signaling controls the progression of progenitor cell differentiation and the emergence of pattern in the embryonic anterior pituitary. Development 125, 1005–1015.

Fernandez-Funez, P., Lu, C.H., Rincon-Limas, D.E., Garcia-Bellido, A., Botas, J., 1998. The relative expression amounts of apterous and its co-factor dLdb/Chip are critical for dorso-ventral compartmentalization in the Drosophila wing. EMBO J. 17, 6846–6853.

Feuerstein, R., Wang, X., Song, D., Cooke, N.E., Liebhaber, S.A., 1994. The LIM/double zinc-finger motif functions as a protein dimerization domain. Proc. Natl. Acad. Sci. USA 91, 10655–10659.

Fimia, G.M., De Ceasare, D., Sassone-Corsi, P., 1999. CBP-independent activation of CREM and CREB by the LIM-only protein ACT. Nature 398, 165–169.

Fisch, P., Boehm, T., Lavenir, I., Larson, T., Arno, J., Forster, A., Rabbitts, T.H., 1992. T-Cell acute lymphoblastic lymphoma induced in transgenic mice by the RBTN1 and RBTN2 LIM domain genes. Oncogene 7, 2389–2397.

Foroni, L., Boehm, T., White, L., Forster, A., Sherrington, P., Liao, X.B., Brannan, C.I., Jenkins, N.A., Copeland, N.G., Rabbitts, T.H., 1992. The rhombotin gene family encode related LIM-domain proteins whose differing expression suggests multiple roles in mouse development. J. Mol. Biol. 226, 747–761.

Freyd, G., Kim, S.K., Horvitz, H.R., 1990. Novel cysteine-rich motif and homeodomain in the product of the Caenorhabditis elegans cell lineage gene lin-11. Nature 344, 876–879.

German, M.S., Wang, J., Chadwick, R.B., Rutter, W.J., 1992. Synergistic activation of the insulin gene by a LIM-homeo domain protein and a basic helix-loop-helix protein, building a functional insulin minienhancer complex. Genes Dev. 6, 2165–2176.

Gong, Z., Hui, C., Hew, C.L., 1995. Presence of isl-1-related LIM domain homeobox genes in teleost and their similar patterns of expression in brain and spinal cord. J. Biol. Chem. 270, 3335–3345.

Goyal, R.K., Lin, P., Kanungo, J., Payne, A.S., Muslin, A.J., Longmore, G.D., 1999. Ajuba, a novel LIM protein, interacts with Grb2, augments mitogen-activated protein kinase activity in fibroblasts, and promotes meiotic maturation of Xenopus oocytes in a Grb2 and Ras-dependent manner. Mol. Chem. Biol. 19, 4379–4389.

Greenberg, J.M., Boehm, T., Sofroniew, M.W., Keynes, R.J., Barton, S.C., Norris, M.L., Surani, M.A., Spillantini, M.-G., Rabbitts, T.H., 1990. Segmental and developmental regulation of a presumptive T-cell oncogene in the central nervous system. Nature 344, 158–160.

Grigoriou, M., Tucker, A.S., Sharpe, P.T., Pachnis, V., 1998. Expression and regulation of Lhx6 and Lhx7, a novel subfamily of LIM homeodomain encoding genes, suggests a role in mammalian head development. Development 125, 2063–2074.

Grutz, G., Forster, A., Rabbitts, T.H., 1998. Identification of the LMO4 gene encoding an interaction partner of the LIM-binding protein LDB1/NLI: a candidate for displacement by LMO proteins in T cell acute leukaemia. Oncogene 17, 2799–2803.

Gubb, D., Green, C., Huen, D., Coulson, D., Johnson, G., Tree, D., Collier, S., Roote, J., 1999. The balance between isoforms of the prickle LIM domain protein is critical for planar polarity in Drosophila imaginal discs. Genes Dev. 13, 2315–2327.

Guy, P.M., Kenny, D.A., Gill, G.N., 1999. The PDZ domain of the LIM protein enigma binds to beta-tropomyosin. Mol. Biol. Cell 10, 1973–1984.

Hinks, G.L., Shah, B., French, S.J., Campos, L.S., Staley, K., Hughes, J., Sofroniew, M.V., 1997. Expression of LIM protein genes Lmo1, Lmo2 and Lmo3 in adult mouse hippocampus and other forebrain regions: differential regulation by seizure activity. J. Neurosci. 17, 5549–5559.

Hobert, O., Mori, I., Yamashita, Y., Honda, H., Oshima, Y., Liu, Y., Ruvkun, G., 1997. Regulation of interneuron function in the C. elegans thermoregulatory pathway by the ttc-3 LIM homeobox gene. Neuron 19, 345–357.

Hobert, O., D'Alberti, T., Liu, Y., Ruvkun, G., 1998. Control of neural development and function in a thermoregulatory network by the LIM homeobox gene lin-11. J. Neurosci. 18, 2084–2096.

Hobert, O., Moerman, D.G., Clark, K.A., Beckerle, M.C., Ruvkun, G., 1999a. A conserved LIM protein that affects muscular adherens junction integrity and mechanosensory function in Caenorhabditis elegans. J. Cell Biol. 144, 45–57.

Hobert, O., Tessmar, K., Ruvkun, G., 1999b. The Caenorhabditis elegans lim-6 LIM homeobox gene regulates neurite outgrowth and function of particular GABAergic neurons. Development 126, 1547–1562.

Johnson, J.D., Zhang, W., Rudnick, A., Rutter, W.J., German, M.S., 1997. Transcriptional synergy between LIM-homeodomain proteins and basic helix-loop-helix proteins: the LIM2 domain determines specificity. Mol. Cell. Biol. 17, 3488–3496.

Jurata, L.W., Gill, G.N., 1997. Functional analysis of the nuclear LIM domain interactor NLI. Mol. Cell. Biol. 17, 5688–5698.

Jurata, L.W., Gill, G.N., 1998. Structure and function of LIM domains. Curr. Top. Microbiol. Immunol. 228, 75–118.

Jurata, L.W., Kenny, D.A., Gill, G.N., 1996. Nuclear LIM interactor, a rhombotin and LIM homeodomain interacting protein, is expressed early in neuronal development. Proc. Natl. Acad. Sci. USA 93, 11693–11698.

Jurata, L.W., Pfaff, S.L., Gill, G.N., 1998. The nuclear LIM domain interactor NLI mediates homo- and heterodimerization of LIM domain transcription factors. J. Biol. Chem. 273, 3152–3157.

Karlsson, O., Thor, S., Norberg, T., Ohlsson, H., Edlund, T., 1990. Insulin gene enhancer binding protein Isl-1 is a member of a novel class of proteins containing both a homeo- and a Cys-His domain. Nature 344, 879–882.

Kenny, D.A., Jurata, L.W., Saga, Y., Gill, G.N., 1998. Identification and characterization of LMO4, an LMO gene with a novel pattern of expression during embryogenesis. Proc. Natl. Acad. Sci. USA 95, 11257–11262.

Kiess, M., Scharm, B., Aguzzi, A., Hajnal, A., Klemenz, R., Schwarte-Waldhoff, I., Schafer, R., 1995. Expression of ril, a novel LIM domain gene, is down-regulated in Hras-transformed cells and restored in phenotypic revertants. Oncogene 10, 61–68.

Kong, Y., Flick, M.J., Kudla, A.J., Konieczny, S.F., 1997. Muscle LIM protein promotes myogenesis by enhancing the activity of MyoD. Mol. Cell. Biol. 17, 4750–4760.

Kotake, K., Ozaki, N., Mizuta, M., Sekiya, S., Inagaki, N., Seino, S.J., 1997. Noc2, a putative zinc finger protein involved in exocytosis in endocrine cells. J. Biol. Chem. 272, 29407–29410.

Kuroda, S., Tokunaga, C., Kiyohara, Y., Higuchi, O., Konishi, H., Mizuno, K., Gill, G.N., Kikkawa, U., 1996. Protein-protein interaction of zinc finger domains with protein kinase C. J. Biol. Chem. 271, 31029–31032.

Larson, R.C., Osada, H., Larson, T.A., Lavenir, I., Rabbitts, T.H., 1995. The oncogenic LIM protein Rbtn2 causes thymic developmental aberrations that precede malignancy in transgenic mice. Oncogene 11, 853–862.

Larson, R.C., Lavenir, I., Larson, T.A., Baer, R., Warren, A.J., Wadman, I., Nottage, K., Rabbitts, T.H., 1996. Protein dimerization between Lmo2 (RBTN2) and Tal1 alters thymocyte development and potentiates T cell tumorigenesis in transgenic mice. EMBO J. 15, 1021–1027.

Li, H., Witte, D.P., Branford, W.W., Aronow, B.J., Weinstein, M., Kaur, S., Wert, S., Singh, G., Schreiner, C.M., Whitsett, J.A., Scott, W.A., Potter, S.S., 1994. Gsh-4 encodes a LIM-type homeodomain, is expressed in the developing central nervous system and is required for early postnatal survival. EMBO J. 13, 2876–2885.

Louis, H.A., Pino, J.D., Schmeichel, K.L., Pomies, P., Beckerle, M.C., 1997. Comparison of three members of the cysteine-rich protein family reveals functional conservation and divergent patterns of gene expression. J. Biol. Chem. 272, 27484–27491.

Lundgren, S.E., Callahan, C.A., Thor, S., Thomas, J.B., 1995. Control of neuronal pathway selection the Drosophila LIM homeodomain gene apterous. Development 121, 1769–1773.

Maekawa, M., Ishizaki, T., Boku, S., Watanabe, N., Fujita, A., Iwamatsu, A., Obinata, T., Ohashi, K., Mizuno, K., Narumiya, S., 1999. Signaling from Rho to the actin cytoskeleton through protein kinases ROCK and LIM-kinase. Science 285, 895–898.

Mao, S., Neale, G.A., Goorha, R.M., 1997. T-Cell oncogene rhombotin-2 interacts with retinoblastoma-binding protein 2. Oncogene 14, 1531–1539.

Matsumoto, K., Tanaka, T., Furuyama, T., Kashihara, Y., Ishii, N., Tohyama, M., Kitanaka, J., Takemura, M., Mori, T., Wanaka, A., 1996. Differential expression of LIM-homeodomain genes in the embryonic brain. Neurosci. Lett. 211, 147–150.

McGuire, E.A., Rintoul, C.E., Sclar, G.M., Korsmeyer, S.J., 1992. Thymic overexpression of Ttg-1 in transgenic mice results in T-cell acute lymphoblastic leukaemia/lymphoma. Mol. Cell. Biol. 12, 4186–4196.

Meier, B.C., Price, J.R., Parker, G.E., Bridwell, J.L., Rhodes, S.J., 1999. Characterization of the porcine Lhx3/LIM-3/P-Lim LIM homeodomain transcription factor. Mol. Cell. Endocrinol. 147, 65–74.

Milán, M., Cohen, S.M., 1999. Regulation of LIM homeodomain activity in vivo: a tetramer of dLDB and Apterous confers activity and capacity for regulation by dLMO. Mol. Cell 4, 267–273.

Milán, M., Diaz-Benjumea, F.J., Cohen, S.M., 1998. Beadex encodes an LMO protein that regulates Apterous LIM-homeodomain activity in Drosophila wing development: a model for LMO oncogene function. Genes Dev. 12, 2912–2920.

Mizuno, K., Okano, I., Ohashi, K., Nunoue, K., Kuma, K., Miyata, T., Nakamura, T., 1994. Identification of a human cDNA encoding a novel protein kinase with two repeats of the LIM/double zinc finger motif. Oncogene 9, 1605–1612.

Morcillo, P., Rosen, C., Baylies, M.K., Dorsett, D., 1997. Chip, a widely expressed chromosomal protein required for segmentation and activity of a remote wing margin enhancer in Drosophila. Genes Dev. 11, 2729–2740.

Morgan, M.J., Madgwick, A.J., 1996. Slim defines a novel family of LIM-proteins expressed in the skeletal muscle. Biochem. Biophys. Res. Commun. 225, 632–638.

Neale, G.A., Rehg, J.E., Goorha, R.M., 1995. Ectopic expression of rhombotin-2 causes selective expansion of the thymus and T-cell tumors in transgenic mice. Blood 86, 3060–3071.

Nix, D.A., Beckerle, M.C., 1997. Nuclear-cytoplasmic shuttling of the focal contact protein, zyxin: a potential mechanism for communication between sites of cell adhesion and the nucleus. J. Cell Biol. 138, 1139–1147.

Okano, I., Hiraoka, J., Otera, H., Nunoue, K., Ohashi, K., Iwashita, S., Hirai, M., Mizuno, K., 1995. Identification and characterization of a novel family of serine/threonine kinases containing two N-terminal LIM-motifs. J. Biol. Chem. 270, 31321–31330.

Osada, H., Grutz, G., Axelson, H., Forster, A., Rabbitts, T.H., 1995. Association of erythroid transcription factors: complexes involving the LIM protein RBTN2 and the zinc-finger protein GATA1. Proc. Natl. Acad. Sci. USA 92, 9585–9589.

Perez-Alvarado, G.C., Miles, C., Michelson, J.W., Louis, H.A., Winge, D.R., Beckerle, M.C., Summers, M.F., 1994. Structure of the carboxy-terminal LIM domain from the cysteine rich protein CRP. Nat. Struct. Biol. 1, 388–398.

Perez-Alvarado, G.C., Kosa, J.L., Louis, H.A., Beckerle, M.C., Winge, D.R., Summers, M.F., 1996. Structure of the cystein-rich intestinal protein, CRIP. J. Mol. Biol. 257, 153–174.

Petit, M.M.R., Mols, R., Schoemakers, E.F.P.M., Mandahl, N., Van den Ven, W.J.M., 1996. LLP, the preferred fusion partner gene of HMGIC in Lipomas, is a novel member of the LIM protein gene family. Genomics 36, 118–129.

Pfaff, S.L., Mendelsohn, M., Stewart, C.L., Edlund, T., Jessell, T.M., 1996. Requirement for LIM homeobox gene Isl1 in motor neuron generation reveals a motor neuron-dependant step in interneuron differentiation. Cell 84, 309–320.

Pinto do Ó, Kolterud, A., Carlsson, L., 1998. Expression of the LIM-homeobox gene LH2 generates immortalized Steel factor-dependent multipotent hematopoietic precursors. EMBO J. 17, 5744–5756.

Pomiès, P., Louis, H.A., Beckerle, M.C., 1997. CRP1, a LIM domain protein implicated in muscle differentiation, interacts with alpha-actinin. J. Cell Biol. 139, 157–168.

Porter, F.D., Drago, J., Xu, Y., Cheema, S.S., Wassif, C., Huang, S.-P., Lee, E., Grinberg, A., Massalas, J.S., Bodine, E., Alt, F., Westphal, H., 1997. Lhx2, a LIM homeodomain gene, is required for eye, forebrain, and definitive erythrocyte development. Development 124, 2935–2944.

Puelles, L., Rubenstein, J.L.R., 1993. Trends Neurosci. 11, 472–479.

Rabbitts, T.H., 1998. LMO T-cell translocation oncogenes typify genes activated by chromosomal translocations that alter transcription and developmental processes. Genes Dev. 12, 2651–2657.

Rearden, A., 1994. A new LIM protein containing an autoepitope homologous to "senescent cell antigen". Biochem. Biophys. Res. Commun. 1201, 1124–1131.

Rebbert, M.L., Dawid, I.B., 1997. Transcriptional regulation of the Xlim-1 gene by activin is mediated by an element in intron I. Proc. Natl. Acad. Sci. USA 94, 9717–9722.

Rétaux, S., Rogard, M., Bach, I., Failli, V., Besson, M.-J., 1999. Lhx9: a novel LIM homeodomain gene expressed in the developing forebrain. J. Neurosci. 19, 783–793.

Riddle, R.D., Ensini, M., Nelson, C., Tsuchida, T., Jessell, T.M., Tabin, C., 1995. Induction of the LIM homeobox gene Lmx1 by Wnt7a establishes dorsoventral pattern in the vertebrate limb. Cell 83, 631–640.

Rodriguez-Esteban, C., Schwabe, J.W., Pena, J.D., Rincon-Limas, D.E., Magallon, J., Botas, J., Izpisúa Belmonte, J.C., 1998. Lhx2, a vertebrate homologue of apterous, regulates vertebrate limb outgrowth. Development 125, 3925–3934.

Royer-Pokora, B., Loos, U., Ludwig, W.-D., 1991. TTG-2, a new gene encoding a cysteine-rich protein with the LIM motif, is overexpressed in acute T-cell leukemia with the t(11;14)(p13;q11). Oncogene 6, 1887–1893.

Sadler, I., Crawford, A.W., Michelsen, J.W., Beckerle, M.C., 1992. Zyxin and cCRP: two interactive LIM domain proteins associated with the cytoskeleton. J. Cell Biol. 119, 1573–1587.

Sagasti, A., Hobert, O., Troemel, E.R., Ruvkun, G., Bargmann, C.I., 1999. Alternative olfactory neuron fates are specified by the LIM homeobox gene lim-4. Genes Dev. 13, 1794–1806.

Schmeichel, K.L., Beckerle, M.C., 1994. The LIM domain is a modular protein-binding interface. Cell 79, 211–219.

Schmeichel, K.L., Beckerle, M.C., 1997. Molecular dissection of a LIM domain. Mol. Biol. Cell 8, 219–230.

Sharma, K., Sheng, H.S., Lettieri, K., Li, H., Karavanov, A., Potter, S.,

Westphal, H., Pfaff, S.L., 1998. LIM homeodomain factors Lhx3 and Lhx4 assign subtype identities for motor neurons. Cell 95, 817–828.
Shawlot, W., Behringer, R.R., 1995. Requirement for Lim1 in head-organizer function. Nature 374, 425–430.
Sheng, H.Z., Zhadanov, A.B., Mosinger, B., Fujii, T., Bertuzzi, S., Grinberg, A., Lee, E.J., Huang, S.-P., Mahon, K.A., Westphal, H., 1996. The LIM homeobox gene Lhx-3 is essential for the specification and proliferation of pituitary cell lineages. Science 256, 1555–1560.
Sheng, H.Z., Moriyama, K., Yamashita, T., Li, H., Potter, S.S., Mahon, K.A., Westphal, H., 1997. Multistep control of pituitary organogenesis. Science 278, 1809–1812.
Sorenson, C.M., Sheibani, N., 1999. Focal adhesion kinase, paxillin, and bcl-2: analysis of expression, phosphorylation, and association during morphogenesis. Dev. Dyn. 215, 371–382.
Sotiropoulos, A., Gineitis, D., Copeland, J., Treisman, R., 1999. Signal-induced activation of serum response factor is mediated by changes in actin dynamics. Cell 98, 159–169.
Stanyon, C.A., Bernard, O., 1999. LIM-kinase1. Int. J. Biochem. Cell Biol. 31, 389–394.
Stronach, B.E., Renfranz, P.J., Lilly, B., Beckerle, M.C., 1999. Muscle LIM proteins are associated with muscle sarcomeres and require dMEF2 for their expression during Drosophila myogenesis. Mol. Biol. Cell 10, 2329–2342.
Sugihara, T.M., Bach, I., Kioussi, C., Rosenfeld, M.G., Andersen, B., 1998. Mouse DEAF-1 recruits a novel LIM domain factor, LMO-4, and CLIM co-regulators. Proc. Natl. Acad. Sci. USA 95, 15418–15423.
Taira, M., Otani, H., Saint-Jeannet, J.-P., Dawid, I.B., 1994. Role of the LIM class homeodomain protein Xlim-1 in neural and muscle induction by the Spemann organizer in *Xenopus*. Nature 372, 677–679.
Takuma, N., Sheng, H.Z., Furuta, Y., Ward, J.M., Sharma, K., Hogan, B.L., Pfaff, S.L., Westphal, H., Kimura, S., Mahon, K.A., 1998. Formation of Rathke's pouch requires dual induction from the diencephalon. Development 125, 4835–4840.
Taniguchi, Y., Furukawa, T., Tun, T., Han, H., Honjo, T., 1998. LIM protein KyoT2 negatively regulates transcription by association with the RBP-J DNA-binding protein. Mol. Cell. Biol. 18, 644–654.
Thor, S., Thomas, J.B., 1997. The Drosophila islet gene governs axon pathfinding and neurotransmitter identity. Neuron 18, 397–409.
Thor, S., Andersson, S.G.E., Tomlinson, A., Thomas, J.B., 1999. A LIM-homeodomain combinatorial code for motor-neuron pathway selection. Nature 397, 76–80.
Toyama, R., Kobayashi, M., Tomita, T., Dawid, I.B., 1998. Expression of LIM-domain binding protein (ldb) genes during zebrafish embryogenesis. Mech. Dev. 71, 197–200.
Treier, M., Gleiberman, A.S., O'Connell, S.M., Szeto, D.P., McMahon, J.A., McMahon, A.P., Rosenfeld, M.G., 1998. Multistep signaling requirements for pituitary organogenesis in vivo. Genes Dev. 12, 1691–1704.
Tsuchida, T., Ensini, M., Morton, S.B., Baldassare, M., Edlund, T., Jessell, T.M., Pfaff, S.L., 1994. Topographic organization of embryonic motor neurons defined by expression of LIM homeobox genes. Cell 79, 957–970.
Tu, Y., Li, F., Goicoechea, S., Wu, C., 1999. The LIM-only protein PINCH directly interacts with integrin-linked kinase and is recruited to integrin-rich sites in spreading cells. Mol. Cell. Biol. 19, 2425–2434.
Tucker, A.S., Al Khamis, A., Ferguson, C.A., Bach, I., Rosenfeld, M.G., Sharpe, P.T., 1999. Conserved regulation of mesenchymal gene expression by Fgf-8 in face and limb development. Development 126, 221–228.
Turner, C.E., Glenney, J.R., Burridge, K., 1990. Paxillin: a new vinculin-binding protein present in focal adhesions. J. Cell Biol. 111, 1059–1068.
Valge-Archer, V., Forster, A., Rabbitts, T.H., 1998. The LMO1 and LDB2 proteins interact in human T cell acute leukaemia with the chromosomal translocation t(11;14)(p15;q11). Oncogene 17, 3199–3202.
van Meyel, D.J., O'Keefe, D.D., Jurata, L.W., Thor, S., Gill, G.N., Thomas, J.B., 1999. Chip and Apterous physically interact to form a functional complex during Drosophila development. Mol. Cell 4, 259–265.
Visvader, J.E., Mao, X., Fujiwara, Y., Hahm, K., Orkin, S.H., 1997. The LIM-domain binding protein Ldb1 and its partner LMO2 act as negative regulators of erythroid differentiation. Proc. Natl. Acad. Sci. USA 94, 13707–13712.
Vogel, A., Rodriguez, C., Warnken, W., Izpisúa Belmonte, J.C., 1995. Dorsal cell fate specified by chick Lmx1 during vertebrate limb development. Nature 378, 716–720.
Wada, S., Katsuyama, Y., Yasugi, S., Saiga, H., 1995. Spatially and temporally regulated expression of the LIM class homeobox gene Hrlim suggests multiple distinct functions in development of the ascidian, Halocynthia roretzi. Mech. Dev. 51, 115–126.
Wadman, I., Li, J., Bash, R.O., Forster, A., Osada, H., Rabbitts, T.H., Baer, R., 1994. Specific in vivo association between the bHLH and LIM proteins implicated in human T cell leukemia. EMBO J. 13, 4831–4839.
Wadman, I.A., Osada, H., Grütz, G.G., Agulnick, A.D., Westphal, H., Forster, A., Rabbitts, T.H., 1997. The LIM-only protein Lmo2 is a bridging molecule assembling an erythroid DNA-binding complex which includes TAL1, E47, GATA-1 and Ldb1/NLI proteins. EMBO J. 16, 3145–3157.
Warren, A.J., Colledge, W.H., Carlton, M.B., Evans, M.J., Smith, A.J., Rabbitts, T.H., 1994. The oncogenic cysteine-rich LIM domain protein rbtn2 is essential for erythroid development. Cell 78, 45–57.
Way, J.C., Chalfie, M., 1988. mec-3, a homeobox containing gene that specifies differentiation of the touch receptor neurons in C. elegans. Cell 54, 5–16.
Wu, R.Y., Gill, G.N., 1994. LIM domain recognition of a tyrosine-containing tight turn. J. Biol. Chem. 269, 25085–25090.
Wu, R.Y., Durick, K., Songyang, Z., Cantley, L.C., Taylor, S.S., Gill, G.N., 1996. Specificity of LIM domain interaction with receptor tyrosine kinases. J. Biol. Chem. 271, 15934–15941.
Xu, Y., Baldassare, M., Fisher, P., Rathbun, G., Oltz, E.M., Yancopoulos, G.D., Jessell, T.M., Alt, F.W., 1993. LH-2: a LIM/homeodomain gene expressed in developing lymphocytes and neural cells. Proc. Natl. Acad. Sci. USA 90, 227–231.
Yamada, Y., Warren, A.W., Dobson, C., Forster, A., Pannell, R., Rabbitts, T.H., 1998. The T cell leukemia LIM protein Lmo2 is necessary for adult mouse hematopoiesis. Proc. Natl. Acad. Sci. USA 95, 3890–3895.
Yang, N., Mizuno, K., 1999. Nuclear export of LIM-kinase1, mediated by two leucine-rich nuclear-export signals within the PDZ domain. Biochem. J. 338, 793–798.
Yang, N., Higuchi, O., Ohashi, K., Nagata, K., Wada, A., Kangawa, K., Nishida, E., Mizuno, K., 1998. Cofilin phosphorylation by LIM-kinase 1 and its role in Rac-mediated actin reorganization. Nature 393, 809–812.
Zeng, C., Justice, N.J., Abdelilah, S., Chan, Y.N., Jan, L.Y., Jan, Y.N., 1998. The Drosophila LIM-only gene, dLMO, is mutated in Beadex alleles and might represent an evolutionarily conserved function in appendage development. Proc. Natl. Acad. Sci. USA 95, 10637–10642.
Zhao, Y., Sheng, H.Z., Amini, R., Grinberg, A., Lee, E., Huang, S., Taira, M., Westphal, H., 1999. Control of hippocampal morphogenesis and neuronal differentiation by the LIM homeobox gene Lhx5. Science 284, 1155–1158.
Zhu, T., Bodem, J., Keppel, E., Paro, R., Royer-Pokora, B., 1995. A single ancestral gene of the human LIM domain oncogene family LMO in Drosophila: characterization of the Drosophila Dlmo gene. Oncogene 11, 1283–1290.

The balance between isoforms of the Prickle LIM domain protein is critical for planar polarity in Drosophila imaginal discs

David Gubb, Clare Green, David Huen, Darin Coulson, Glynnis Johnson, David Tree, Simon Collier and John Roote

Genes & Dev. 1999 13: 2315-2327
Access the most recent version at doi:10.1101/gad.13.17.2315

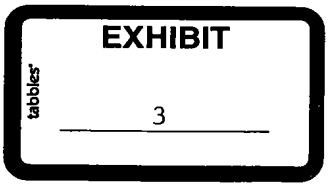

The balance between isoforms of the Prickle LIM domain protein is critical for planar polarity in *Drosophila* imaginal discs

David Gubb,[1] Clare Green, David Huen, Darin Coulson, Glynnis Johnson, David Tree, Simon Collier, and John Roote

Department of Genetics, University of Cambridge, Cambridge CB2 3EH, UK

The tissue polarity mutants in *Drosophila* include a set of conserved gene products that appear to be involved in the control of cytoskeletal architecture. Here we show that the tissue polarity gene *prickle* (*pk*) encodes a protein with a triple LIM domain and a novel domain that is present in human, murine, and *Caenorhabditis elegans* homologs which we designate PET. Three transcripts have been identified, *pk*, *pkM*, and *sple*, encoding 93-, 100-, and 129-kD conceptual proteins, respectively. The three transcripts span 70 kb and share 6 exons that contain the conserved domains. The *pk* and *sple* transcripts are expressed with similar tissue-specific patterns but have qualitatively different activities. The phenotypes of *pk* mutants, and transgenic flies in which the different isoforms are overexpressed show that the balance between Pk and Sple is critical for the specification of planar polarity. In addition, these phenotypes suggest a tessellation model in which the alignment of wing hairs is dependent on cell shape and need not reflect fine-grained positional information. Lack of both *pk* and *sple* transcripts gives a phenotype affecting the whole body surface that is similar to those of *dishevelled* and *frizzled* (*fz*) suggesting a functional relationship between *pk* and *fz* signaling.

[*Key Words*: *Drosophila*; *prickle*; *spiny-legs*; polarity; LIM domain]

Received March 22, 1999; revised version accepted July 16, 1999.

The *Drosophila* "tissue polarity" genes control the orientation of bristles and hairs in the adult cuticle (Gubb and Garcia-Bellido 1982; Adler et al. 1990; Adler 1992). Mutant flies have the polarity of cells altered in the plane of the epithelium without gross changes in the overall shape of imaginal structures or the distribution of differentiated cell types within them. Other tissue polarity defects include mirror-image duplications of the tarsal joints (Held et al. 1986), rotations of bristle sockets in the leg (Gubb and Garcia-Bellido 1982), and changes in ommatidial polarity (Gubb 1993, 1998; Theisen et al. 1994; Zheng et al. 1995).

There is evidence that these planar polarity phenotypes involve the organisation of the cytoskeleton. For example, localization of the actin fibers that form the prehair is the first observable manifestation of polarity in the pupal wing. Multiple wing hairs are seen in many of the tissue polarity mutants (Gubb and Garcia-Bellido 1982; Wong and Adler 1993) and result from formation of more than one prehair per cell (Wong and Adler 1993). Furthermore, genes identified in other organisms as having major roles in cytoskeletal reorganization, for example, *Rac*, *RhoA*, and *Cdc42*, have been shown to have a role in *Drosophila* planar polarity (Harden et al. 1995; Eaton et al. 1996; Strutt et al. 1997).

The tissue polarity genes have been divided into three groups (Wong and Adler 1993). Type 1 genes [*dishevelled* (*dsh*), *frizzled* (*fz*), and *prickle* (*pk*)], affect the whole body surface and are therefore believed to directly establish tissue polarity (Shulman et al. 1998). In contrast, the type 2 [*inturned* (*in*) and *fuzzy* (*fy*) and type 3 [*multiple wing hairs* (*mwh*)] genes affect distinct subsets of body areas and are thought to interpret the polarity established by the type 1 genes. A number of tissue polarity genes have been cloned [*fz* (Vinson et al. 1989); *in* (Park et al. 1996); *fy* (Collier and Gubb 1998), and *strabismus* (*stbm*; Wolff and Rubin 1998)] and some of these have been shown to have important roles in signal transduction at many points in development. The family of *fz* homologs are thought to be involved in reception of the Wingless (Wg) signal (Bhanot et al. 1996; Orsulic and Peifer 1996; Cadigan et al. 1997); whereas Dsh acts as an intracellular protein affecting both the Wg and Notch (N)

[1]Corresponding author.
E-MAIL dg27@mole.bio.cam.ac.uk; FAX 44-1223-333992.

pathways (Klingensmith et al. 1994; Thiesen et al. 1994; Axelrod et al. 1996, 1998)

In this paper we describe the molecular organization of the tissue polarity gene *pk*. Loss-of-function lesions in alternatively spliced transcripts of this one locus result in two genetically distinct phenotypes, Pk and Spinylegs (Sple). The *pk* and *sple* transcripts encode proteins that contain three LIM motifs and a novel conserved domain that we have called PET (Prickle Espinas Testin). Surprisingly, deletion of the entire gene gives a phenotype that is much weaker than that of either the *pk* or *sple* single mutants. This unusual result can be explained by the *pk* and *sple* gene products acting in concert. The single-mutant phenotypes result from misactivation, rather than simply blocking, of a pathway of polarity formation. We propose that the correct balance of the Pk and Sple variants is required for normal planar polarity signaling in *Drosophila* imaginal discs.

Results

Phenotypic analysis of pk *and* sple

To undertake a thorough analysis of the *pk* locus we used a variety of genetic strategies to isolate new alleles. These alleles can be divided into three phenotypic classes, Pk, Pk–Sple, and Sple (Table 1; Figs. 1 and 2). None of these classes show any embryonic phenotype (even when homozygous mutant embryos develop from homozygous mutant mothers). Consistent with this lack of either a zygotic or maternal requirement, deletions of the *pk* gene are fully viable and fertile. The defects of double mutant, $pk^{pk-sple}$, alleles are the same as those seen with overlapping deletions that remove the entire gene and eliminate all *pk* functions. Paradoxically, these $pk^{pk-sple}$ alleles do not produce the most severe phenotypes. Instead the single mutant alleles pk^{pk} and pk^{sple} give more extreme phenotypes, but in reciprocal regions of the body; pk^{pk} in the wing and notum and pk^{sple} in the legs, abdomen, and eyes. Complementation between these classes of allele indicates two subtly different functions at the *pk* locus.

The duplicated wing hair phenotype typical of most type 1 tissue polarity mutants (Gubb and Garcia-Bellido 1982; Wong and Adler 1993) also affects pk^{pk} alleles, but only 2%–3% of cells show doubled hairs. Where the polarity vectors are changing sharply, however, cells frequently show doubled hairs (Figs. 2E and 3G). After the last cell division in the pupal wing, the cytoskeleton is reorganized. Cells become hexagonal, and prehairs grow out from the distal vertex of each cell (for review, see Eaton 1997). It is not possible, however, to fill an irregular shape such as the wing blade with a perfect hexagonal array of cells, and occasional defects, such as a distorted four-pentagon array, are seen (Fig. 3C). The relationship between hair orientation and the cell shape, implied by the localization of prehair initiation sites, is confirmed by the doubled hairs near stacking flaws (Figs. 2E and 3G) and the lack of regular hexagonal packing in the vicinity of the anterior whorl (Fig. 3B).

Molecular organization of the pk *locus*

The breakpoints of *pk*-associated mutations map across 70 kb (Fig. 4; Table 1). Single-mutant pk^{pk} alleles carry lesions within the proximal 30 kb, whereas $pk^{pk-sple}$ double-mutant alleles map between 42 and 69 kb and none of the pk^{sple} single mutations have been localized. Two putative *pk* transcripts were detected as weak bands of ~4.2 and 5.1 kb in embryos and 2-day pupae on developmental Northern blots (Fig. 5). The shorter transcript corresponds to *pk* and the larger to *sple* (Fig. 5). The 5′ end of *pk* hybridizes to the region of the pk^{pk} breakpoints and is separated by a large intron from the remaining 6 exons (Fig. 4). The 5′ end of *sple* is within the large *pk* intron. An additional medial transcript, *pkM*, is only detected in embryonic stages (Fig. 5B). The identity of the *pk* and *sple* transcripts was confirmed by rescue experiments (Figs. 7 and 8, below).

The molecular analysis therefore identifies three different transcripts from the *pk* locus. The relationship between these transcripts and the different classes of lesion associated with mutant alleles explains the three classes of mutant alleles at the *pk* locus. Breakpoints that interrupt the common exons cause $pk^{pk-sple}$ mutations equivalent to deletions of the entire locus. pk^{pk} mutations map to the proximal region and interrupt the 5′ region of the *pk* transcript. The *pkM* transcript appears to have no adult function, as the $In(2LR)pk^{pk20}$ breakpoint is 3′ to the *pkM* 5′ exon (Table 1) but gives a similar phenotype to other pk^{pk} alleles.

pk *encodes a LIM domain protein*

The second to seventh exons of *pk* are common to the three transcripts (Fig. 4). These common exons encode a peptide sequence containing three LIM domains, but no recognized DNA binding, membrane spanning, or signal peptide motifs (Table 2). LIM domains are cysteine-rich sequences with a double zinc finger motif (for review, see Sanchez-Garcia and Rabbitts 1994; Dawid et al. 1998). Four closely related LIM domain sequences were found by database searches; one murine (*Testin*, Divecha and Charleston 1995), one human (*LMO6*, Fisher et al. 1997), and two *Caenorhabditis elegans*. An additional *pk* cognate gene in *Drosophila*, *espinas* (*esn*), maps just proximal to the 43A1.2 Serpin cluster (C. Green and D. Gubb, unpubl.). Comparison of these sequences (Table 3) identifies a novel conserved PET domain, 5′ to the LIM domains. Two further incomplete sequences with PET domain homology were identified by database searches, a human EST and a *C. elegans* ORF. The PET domain is unrelated to other sequence motifs in the protein database and encodes a neutral stretch of amino acids with no obvious distinguishing features. Database searches failed to identify any sequences with significant homology to peptides encoded by the unique 5′ *pk*, *pkM*, or *sple* exons (Table 2).

Expression patterns of pk *transcripts*

The expression patterns of the *pk* transcripts were inves-

Table 1. *Molecular and cytological breakpoints of* pk *mutations and deficiencies*

Mutant class	Allele: associated aberration	Molecular breakpoint	Mutagen	Cytology
pk^{pk}	*1*	0 E; 2.2 X	*S*	+
	2	14.7 E; 15.5 S	*X*	+
	15, 16, 17	0 E; 2.2 X	*P*	+
	19 In(2R)pk^{19}	16.8 S; 20.3 E	*X*	*43A1-3;57C13.14*
	20 In(2LR)pk^{20}	27.5 E; 28.7 X	*X*	*36C9-11;43A1.2*
	21 In(2LR)pk^{21}	14.0 X; 14.7 E	*X*	*40;43A3*
	28 In(2LR)TE35B-4	16.8 S; 20.3 E	*S*	*35B1.2;43A1.2*
	29 T(2;3)pk^{78t}	14.0 X; 15.5 S	*X*	*42F1.2-43A1;68F-69A*
	30 Df(2R)pk-30	0 E; 4.8 E	*X*	+
pk^{sple}	*1*		*S*	+
	3	33.6 B; 36.1 E	*EMS*	+
	4, 27, 36, 42		*X*	+
	5		*EMS*	+
pk$^{pk\text{-}sple}$	*6, 7, 8, 9, 25*		*EMS*	+
	10, 11, 12, 18, 32, 34, 38,		*X*	+
	39, 41, 43,		*X*	+
	13	40.2 E; 66.2 E	*X*	+
	14	41.3 H; 48.6 E	*X*	+
	23	53.8 H; 54.1 B	*X*	+
	26 Tp(2;2)pk-sple^{26}	50.3 X; 53.5 H	*X*	*CyO + 29F;58E-58B;42A-42F;45A-42F;29F*
	33		*P*	+
	35	58.4 X; 61.8 E	*X*	+
	37 T(2;3)pk-sple^{37}	58.4 X; 62.2 X	*X*	*CyO + 43A2-3;73C3-5*
	40 In(2R)pk-sple^{40}	62.2 X; 66.2 E	*X*	*43A1.2; 57E7-11*
	46	62.7 X; 66.2 E	*X*	*CyO*
	47 In(2LR)pk-sple^{47}	58.4 X; 61.8 E	*X*	*CyO + 25F3.6; 43A1.2*
	48	65.7 X; 69.3 E	*X*	*CyO*
	49 Tp(2;2)pk-sple^{49}	50.3 X; 58.4 X	*X*	*CyO + 42A1; 46B; 30B*
nec pk	*3 In(2R)nec^{3} pk^{3}*		*EMS*	*h38R-h46; 43A1.2*
	5 In(2R)nec^{5} pk^{5}		*X*	*h38R-h46; 43A1.2*
	22 Tp(2;2)pk-sple^{22}	61.9 E; 66.2 X	*X*	*41E-F;42F3;43A1*
	24 Tp(2;3)pk-sple^{24}		*X*	*41;43A1.2;81*
	31 T(2;3)pk-sple^{31}+ In(3L)		*X*	*43A1.2;h47;87*
	44 In(2LR)pk^{44}	66.2 E; 70.9 X	*X*	*h35-h38L;43A2-3*
	45 T(Y;2)pk-sple^{45}		*X*	*Y;43A1.2*
	50 Df(2R)pk-sple-50		*X*	*CyO + 43A1;43A2*
	51 Df(2R)pk-sple-51		*X*	*43A1;43A2*
Deletions (with one breakpoint in 43A1-3)	*Df(2R)Drl-rv30*	86.2 E; 87.0 H	*X*	*43B1.2;43E5-7*
	Df(2R)CA58	97.0 E; 100.2 E	*X*	*43A3;43F6*
	Df(2R)sple-D1	Prox. to - 8.1 X	*X*	*43A1.2;43B2*
	Df(2R)sple-D2	0 E; 2.2 X	*P*	*43A2;43C2*
	Df(2R)sple-J1	0 E; 2.2 X	*P*	*43A1;43C3-7*
	Df(2R)sple-J2	0 E; 2.2 X	*P*	*43A2;43B3*
	Df(2R)pk-N5	90.4 E; 92.2 S	*X*	*41B-C;43A*
	Df(2R)nap-2	16.8 S; 20.3 E	*X*	*41F4-9;43A1.2*
	Df(2R)cn-76k3	31.1 H; 33.6 B	*γ*	*43A1.2;44B7-C1*
	Df(2R)cn-88e43 + T(2;3)	14.0 X; 14.7 E	*γ*	*43A1.2;44B3-5;93B11-C1*

The molecular breakpoints are given with respect to the E, S, B, X, and H (*Eco*RI, *Sal*I, *Sal*I, *Bam*HI, *Xho*I, and *Hin*dIII) sites within the phage walk, e.g., 14.7 E, 66.2 X being the *Eco*RI and *Xho*I sites that are 14.7 and 66.2 kb distal to the origin (Fig. 3). Mutagens were EMS, X-rays (X), P-element (P), γ-rays (γ), or spontaneous (S). Allele numbers in boldface type were isolated in this study. Four of the six X-ray-induced *pk^{pk}* alleles and 11 of the 21 *pk$^{pk-sple}$* alleles are associated with a cytologically visible chromosomal breakpoint affect the 43A1.2 doublet band, all of the *pk^{sple}* alleles are cytologically wild type. The *pk^{sple3}* chromosome carries a small insertion between 34 and 36 kb not present in other chromosomes analyzed, but the progenitor chromosome of *pk^{sple3}* was not available so the relationship between this insertion and the mutant phenotype remains equivocal. Nine of the mutant chromosomes carry an associated mutation in the *necrotic* (*nec*) gene.

tigated on developmental Northern blots and by tissue in situs using probes to the common exons and the unique 5′ exons. Both the temporal and spatial patterns of expression of the three transcripts were indistinguishable, with the exception that the *pkM* transcript was only detected during the embryonic stages. In 28- to 34-hr pupal

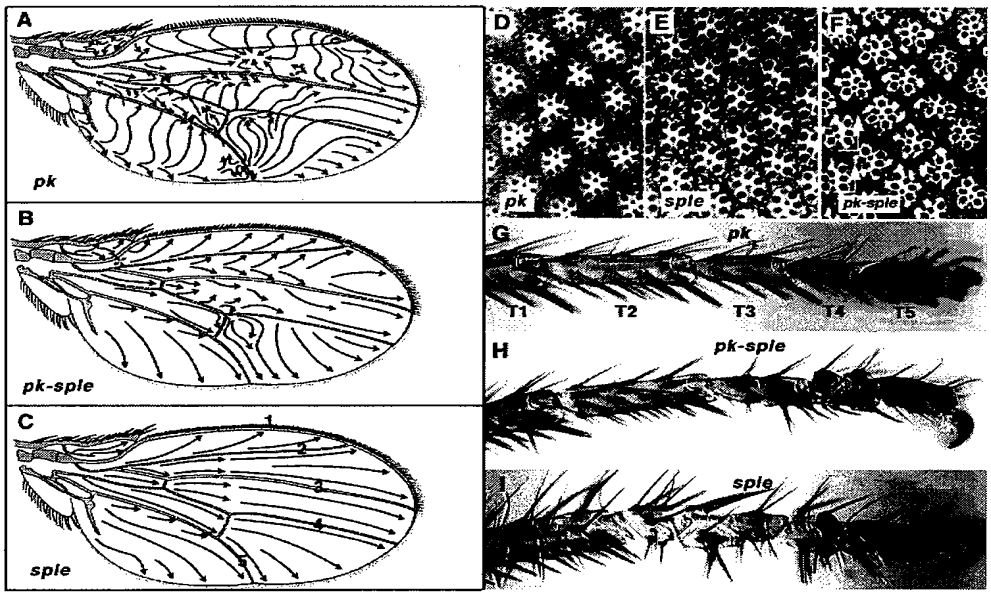

Figure 1. Pk mutant phenotypes. Complete lack of Pk function, in $pk^{pk-sple}$ alleles, gives a weak polarity phenotype in the wing, notum, abdomen, eye, and legs. pk^{pk} alleles cause an extreme polarity phenotype in the wing and notum; pk^{sple} alleles affect eye, abdomen, and leg. The pk^{pk} wing phenotype shows a characteristic reversal in the triple-row bristles along the anterior margin, a whorl in the wing hairs near the tip of vein 2, and abrupt discontinuities in hair polarity, e.g., pk^{pk1} (*A*). The weak $Pk^{pk-sple}$ phenotype shows a slight effect on triple-row bristle orientation and gives gently curved hair polarity vectors, e.g., $pk^{pk-sple13}$ (*B*); *sple* alleles are completely wild type, e.g., pk^{sple1} (*C*). Arrows indicate the direction along which hairs are aligned; wing veins are designated 1–5 (*C*). The eye phenotype is wild-type in pk^{pk1} (*D*), showing a line of mirror symmetry along the equator (line). On both sides of the equator the R3 photoreceptor cell is aligned towards the pole, in the direction of the arrowhead. In addition to being rotated through 180° ommatidia show reversed chirality around the equator, so that both a rotation and a reflection in the plane of the epithelium is required to superimpose the ommatidial patterns. (*E*) pk^{sple1} eyes contain a mixture of ommatidia with reversed polarity and chirality in both hemispheres of the eye. These ommatidia remain aligned along the polar axis, but with their R3 photoreceptors directed toward the equator rather than the pole giving rise to D/V mirror-image reversals of the normal rhabdomere pattern. In addition, all the pk^{sple} alleles show out ~1% anteroposterior (A/P) reversed ommatidia (not shown). (*F*) $pk^{pk-sple13}$ eyes contain a mixture of chiral forms of ommatidia. Some ommatidia fail to rotate properly, and the resulting imperfections in the hexagonal stacking give a slightly rough eye phenotype. Some ommatidia are aligned at 60° to the equator (black arrows) and some show A/P reversals (white arrows), with the R3 rhabdomere anterior to R4. (*G*) The tarsi of pk^{pk1} are wild type; tarsal segments are numbered T1–T5. (*H*) In $pk^{pk-sple13}$, the T3 and T4 segments carry medial duplications of the proximal and distal joint structures, with the middle of each segment deleted. This results in alternating reversed-proximal and reversed-distal tarsal joint structures with half the length of a normal segment. (*I*) In pk^{sple1} the tarsal duplications affect T2, T3, and T4 segments, with an occasional incipient ectopic joint in the distal T1. The distal T5 segment remains unaffected in all mutant alleles.

wings, *pk* and *sple* transcripts are expressed uniformly in intervein cells but leave the presumptive vein regions unstained (Fig. 6A,B). At the same stage in the pupal legs *pk* and *sple* transcripts are expressed in a similar pattern, uniform in most cells, but excluded from the segmental boundaries (Fig. 6C,D). In third larval instar imaginal discs, a low level of pk transcripts can be detected in restricted domains that correlate with the places where *pk* is required. In the eye disc, maximal expression is detected in a stripe of cells behind the morphogenetic furrow (in the region where ommatidial organization and polarity is being specified) (Fig. 6G). In wing discs, *pk* transcripts are expressed at higher levels along the dorsoventral (D/V) compartment boundary, where the bristles of the wing margin will form (Fig. 6F). In the embryo, *pk* probes show a dynamic expression pattern in cells engaged in morphogenetic movements, such as invaginating mid-line cells, in the cephalic fold, and at parasegmental boundaries (Fig. 6H,I).

Functional relationships between Pk and Sple proteins

To investigate the functional relationship between the Pk and Sple protein variants, mutant combinations that alter the ratio of the *pk* and *sple* transcripts were generated. The strongest phenotypes result from lack of either one of these two transcripts in homozygous mutants. When the single mutant alleles are combined with $pk^{pk-sple}$ alleles or deficiencies, the resulting phenotypes are weaker than the corresponding homozygous single mutant phenotypes. Thus, flies that carry only a single functional copy of the *sple* transcript [*Df(2R)pk-30/*

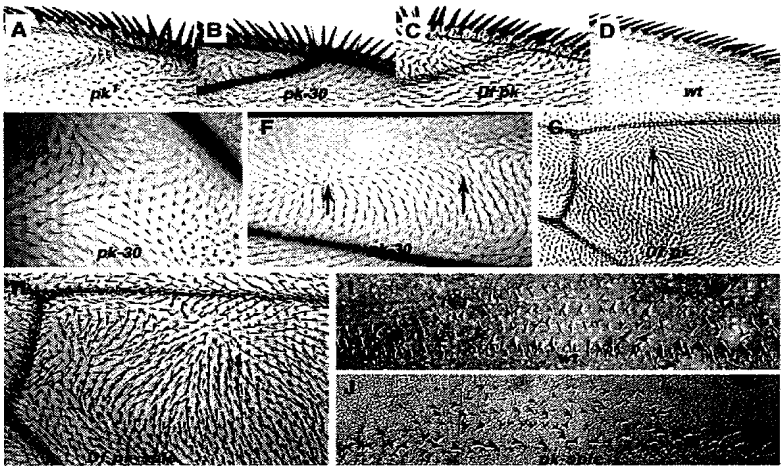

Figure 2. Comparison of wing polarity patterns between different alleles of pk^{pk}. Junction of vein 1 and 2 at anterior margin in pk^{pk1} (*A*), *Df(2R)pk-30* (*B*), *Df(2R)nap-2/Df(2R)sple-J2* (*C*), and wild type (*D*). In pk^{pk} mutant wings, the whorl close to the junction of vein 2 with the wing margin marks a discontinuity in polarity, or stacking flaw. Stacking flaws with different topologies are found in different regions of the wing. (*E*) *Df(2R)pk-30*, a cruciform discontinuity posterior to vein 5; note doubled hairs. (*F*) *Df(2R)pk-30*, radial and cruciform discontinuities (arrows) between veins 2 and 3. (*G*) Overlapping pk^{pk} deletions, *Df(2R)nap-2/Df(2R)sple-J2*. Note triangular dislocation in polarity (arrow) distal to the posterior cross vein as in pk^{pk1} (Fig. 1A). (*H*) Overlapping $pk^{pk-sple}$ deletions removing the entire gene *Df(2R)pk-N5/Df(2R)sple-J2* (cf. the $pk^{pk-sple13}$ pattern; Fig. 1B). Embryonic denticle belt in wild type (*I*) and $pk^{pk-sple13}$ (*J*). There is no detectable embryonic phenotype with alleles of pk^{pk}, pk^{sple}, or $pk^{pk-sple}$; in particular, the denticle belt morphology and denticle orientation remains normal.

$pk^{pk-sple13}$] or the *pk* transcript ($pk^{sple1}/pk^{pk-sple13}$), show an intermediate phenotype more similar to $pk^{pk-sple13}$ than the single mutant (Fig. 7). These results imply that the presence of one transcript without the other (as in pk^{pk} or pk^{sple} single mutants) creates an extreme phenotype that is corrected when the dose of the remaining transcript is reduced. The implication is that both the relative and absolute levels of the Pk and Sple proteins are important for the function of putative Pk–Sple homomeric or heteromeric protein complexes.

The importance of the levels of Pk and Sple expression and the balance between them was investigated further with overexpression constructs. When driven by the expression of the uniform drivers *gal4–da* (*daughterless*) or *gal4–C765*, P[*UAS:pk*$^+$] gives an extreme tarsal duplication phenotype, including a duplicated socket structure

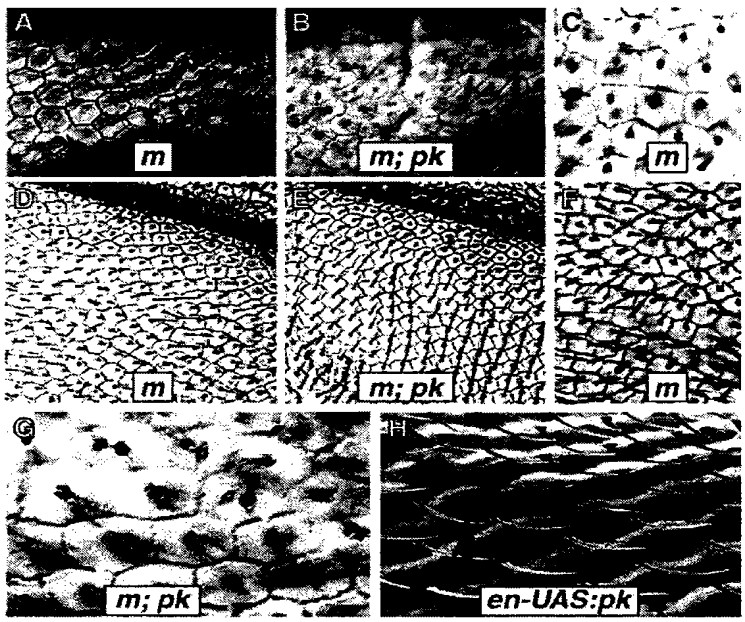

Figure 3. Cell shapes and polarity. The m^{38c} mutation was used to visualize cell boundaries in both wild-type and *Df(2R)pk-30* backgrounds. In m^{38c} wings the majority of cells are hexagonal, although occasional pentagonal cells are seen. (*A*) Distal vein 2 region in m^{38c} wings. (*B*) The same region in m^{38c}; *Df(2R)pk-30* wings, with more irregular cell shapes. (*C*) A common packing defect consisting of a group of four irregular pentagons with one 90° corner fitted within the surrounding hexagonal array. (*D*) The region posterior to vein 5 in m^{38c} shows a regular hexagonal array, although cells close to the vein tend to be trapezoidal or square. Wing hairs are aligned along the proximodistal axis. (*E*) The same region in m^{38c}; *Df(2R)pk-30* wings shows parallel rows of hexagons with hairs oriented anteriorly. (*F*) A small region between veins 3 and 4 in m^{38c} wings shows cuboidal cells, with local polarity disruptions near the transition between cuboidal and hexagonal packing. (*G*) Cells near the anterior whorl in m^{38c}; *Df(2R)pk-30* wings tend to be roughly cuboidal and associated with duplicated hairs. (*H*) Hairs fail to migrate from the distal vertex of pupal wing cells in *en–UAS:pk flies* (*gal4–en*; P[*UAS:pk*$^+$]). This S.E.M. micrograph of adult wings shows hairs remaining at the distal vertex; the pedicel in the middle of the mature cell (arrow) marks the position that the adult hair would normally occupy.

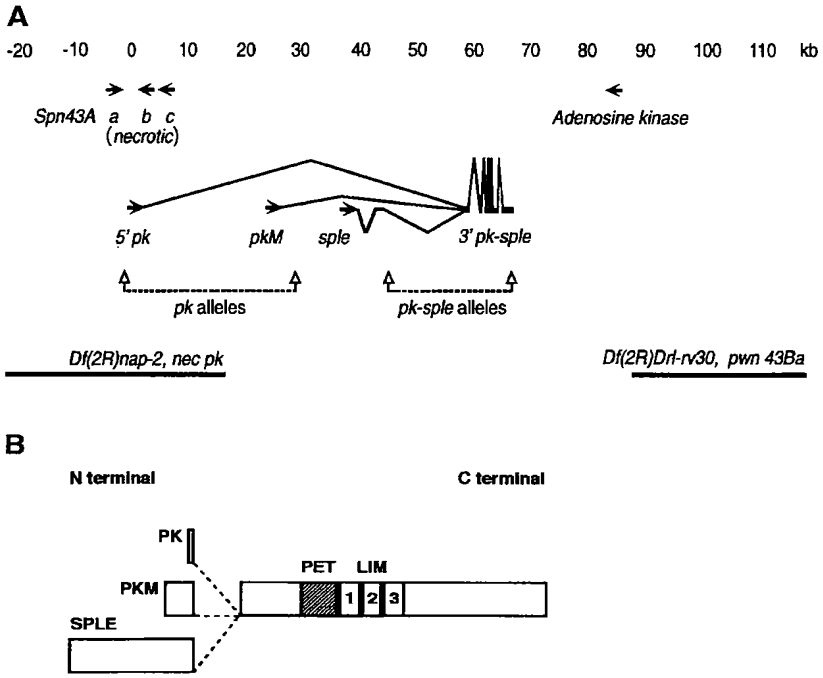

Figure 4. (*A*) Map showing the location of pk mutant breakpoints with respect to transcripts in the region. The zero coordinate is the *Eco*RI site 973 bp proximal to the *pk* transcription start site. Transcripts are indicated below the molecular coordinates. The 5′ start of the *pk* transcript lies within a cluster of three serpins (serine Proteinase inhibitors) (*Spn43Aa*, *Spn43Ab*, and *Spn43Ac*), one of which corresponds to the *necrotic* gene, and a transcript with homology to Adenosine kinases maps just distal to *pk*. Aberrations that break between coordinates 0 and 30 kb cause *pk* mutations, similar to the homozygous deletion *Df(2R)pk-30*, which deletes the *pk* 5′ start and the 3′ end of the medial serpin transcript *Spn43Ab*. Aberrations between coordinates 40 and 70 kb, which interrupt the common exons, give the weaker $Pk^{Pk\text{–}Sple}$ phenotype typical of $pk^{pk\text{–}sple13}$. Overlapping deletions give an additional necrotic phenotype when the serpin cluster is removed, but deletion of the *adenosine kinase* transcript [Df(2R)sple–J2/Df(2R)pk-N5] gives no further phenotype. (*B*) The Pk protein isoforms encode putative 870 (*pk*), 936 (*pkM*), and 1206 (*sple*) amino acid peptides with the conserved PET and LIM domains mapping entirely within the common exons. The first *pk* exon contains an untranslated leader sequence of 0.8 kb, with the putative translation start site (Cavener and Ray 1991) being 39 bp 5′ to the large intron. The putative translation start sites of the *pkM* and *sple* transcripts are within their first and second introns, respectively.

in the proximal T1 segment. Overexpression of $UAS{:}sple^{+}$ with these drivers gives a Pk phenotype in the wing triple row bristles; the tarsi, however, remain completely wild type (Fig. 8). These results confirm that overexpression of *pk* gives a phenotype analogous to lack of the *sple* transcript, whereas overexpression of *sple* gives a phenotype similar to lack of *pk*. The $da\text{–}UAS{:}pk^{+}$ and $da\text{–}UAS{:}sple^{+}$ wing phenotypes show an unexpected feature that is not seen in mutant alleles. Instead of uniform polarity patterns, swirls are seen in the wing hair

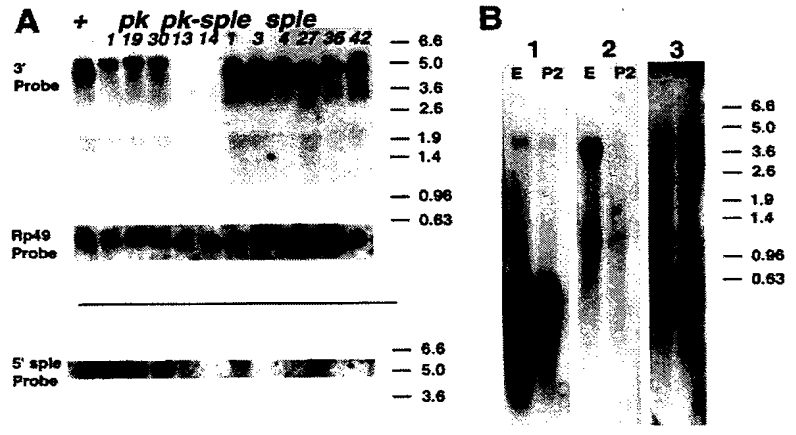

Figure 5. Northern analysis. A probe homologous to *sple* 5′ sequences detects a 5.1-kb mRNA, but this band is no longer detected, or has an altered length, in the *sple* mutants. A shorter, 4.2-kb transcript is missing in pk^{pk} mutants. Both 5.1- and 4.2-kb transcripts are detected by a common exon probe in wild-type RNA, and neither are detected in $pk^{pk\text{–}sple}$ mutant strains. (*A*) Total 2-day pupal RNA from homozygous wild-type (+) and mutant flies (pk^{pk1}, pk^{pk19}, *Df(2R)pk-30*, $pk^{pk\text{–}sple13}$, $pk^{pk\text{–}sple14}$, pk^{sple1}, pk^{sple3}, pk^{sple4}, pk^{sple27}, pk^{sple36}, pk^{sple42}) hybridized with a 3′ common exon probe (3′), an *Rp49* loading control (Rp49) and a unique sple exon probe (5′). The 4.2-kb transcript is missing in pk^{pk} and $pk^{pk\text{–}sple}$ alleles but retained in pk^{sple} alleles. The 5.1-kb transcript is present in pk^{pk1}, pk^{pk19} and *Df(2R)pk-30*; missing in $pk^{pk\text{–}sple13}$, $pk^{pk\text{–}sple14}$ and lost, or reduced in length, in pk^{sple3}, pk^{sple4}, pk^{sple27}, and pk^{sple36}. (*B*) Three strips cut from a filter carrying wild-type embryonic (E) and 2-day pupal (P2) poly(A)$^{+}$ RNA at the same sample loading. Individual strips were hybridized with *pk* 5′ + *Rp49* (*1*), *pkM* 5′ (*2*), and *sple* 5′ (*3*) probes. The *pk* and *sple* transcripts are expressed in embryo and 2-day pupae. The *pkM* transcript was only detected during the embryonic stage.

Table 2. *The translated amino acid sequence of the alternative 5′ and common exons*

pk 5′
MDTPNQMPVELER

pkM 5′
MNDSTDNLHADCDGRVSNNNNGNSNTNDGPNNDGD
SDEEVIEGMALLEGNYQVLRQWVPPAPNYWDAPPKAII
KSAEVR

sple 5′
MSSLSTGGGAGGSSGGPGGADAAAAPAAGQATVTATG
NMEPAMVPRTANLLACKQWWRVCFLYGDQQKYYRQ
LYSKAAAQRLADANQEPDNARDREYDTVDCDLIAGQ
LDAVEDADDGIDLGDHSSTPKGGATTAGRPLFPHSSSP
RRSKKLLRSLRAHVRGEKLPKNDTTTANVSNEVTQRN
ARVTALDDPFLFGIDADHLGDLVVRGKRYSTLDATEN
MARFYAEQEATAQVLEIIEQEEESPEQEAPKPALPPKQKQ
QRPVPPLPPPPANRVTQDPGTQPAAPQVPLQPLTAGDL
QFLNLSLRQRSLPRSMKPFKDAHDISFTFNELDTSAEPEV
ATGAAQQESNE

Common exons
PISRTPLTQISYLQKIPTLPRHFSPSGQGLATPPALGSGGMG
LPSSSSASALYAAQAAAGILPTSPLPLQRHQQYLPPHHQ
QHPGAGMGPGPGSGAAAGPPLGPQYSPGCSANPKYS
NAQLPPPPHHHHQLSPALSTPSPPSLLHHPAGGTSSASA
HAPFLGGPHMDMQRQSHSDDDSGCALEEYTWVPPGL
RPDQVRLYFSQIPDDKVPYVNSPGEQYRVRQLLHQLPP
HDNEVRYCHSLTDEERKELRLFSTQRKRDALGRGNVR
QLMS ARPCDGCDDLISTGDIAVFATRLGPNASWHPAC
FACSVCRELLVDLIYFHRDGRMYCGRHHAETLKPRCSA
CDEIILADECTEAEGRAWHMNHFGCHECDKQLGGQR
YIMREGKPYCLHCFDAMFGEYCDYCGEGIGVDQGQM
SHDGQHWHATDECFS CNTCRCSLLGRAFLPRRGGIYC
SIACSKGEPPTPSDSSGTGMYTTPTPPTQGVRPHPQAPL
PARIPSSHASSSPPMSPQQQQQHQATFNQAMYQMQSQ
QMEAAGGLVDQSKSYAASDSDAGVVKDLEHGGHMG
GGDLTDFSGGRASSTSQNLSPLNSPGDFQPHFLPKPME
LQRQLLENPHTASMPELAGKLVAPPAHMQHLSQLHAV
SSHQFQQHEYADIVHPPPPPPGEIPELPTPNLSVASTALP
PELMGSPTHSAGDRSLNTPMS TQSASHAPPHPVSILSG
ASSSSPMSGEPAKKKGVRFEGIPDTLPDHAATPVTERER
VVAARGSGIGTRETRREEVAMVTVTPREGEDVASPPPA
RRTIAAAAVIAPTRPLERTPMHLRNPILVLPGSTFGSAG
CQPGPRVTQPTAEGTGARAGTQGVRGV

orientation with different patterns from wing to wing (Fig. 8).

In addition to phenotypes resembling loss of function, misexpression of *pk* in *engrailed (en)–UAS:pk*$^+$ flies blocks the migration of wing hairs from the distal vertex of wing cells to the central position (Fig. 3H).

The relationship of pk *to* dsh

Deletion of the entire *pk* gene gives a phenotype over the whole body surface that is similar to *dsh* and *fz*. To test whether these mutants affect the same signaling pathway, double mutant combinations were made. Double mutants of pk^{pk} and *dsh* in the triple row give a Dsh phenotype, suggesting that *dsh* is epistatic to pk^{pk} (Fig. 9). The situation within the wing blade is less clear, as the double mutants give an intermediate phenotype. The *dsh*; pk^{sple} double mutant retains a Dsh phenotype in the triple row, but the wing hair pattern is altered (Fig. 9), despite the fact that pk^{sple} alleles have no wing phenotype. In the leg the Dsh tarsal phenotype is not modified by pk^{pk}. There is a synergistic interaction between *dsh* and pk^{sple}, with the double mutant giving a more extreme mirror-image transformation of the T1 segment than either of the single mutants. This extreme transformation is also seen with *UAS:pk*$^+$ overexpression and in *fz* (Figs. 8 and 9).

Clones of *fz* show a directional nonautonomy that has been interpreted to mean that *fz* mediates the intercellular communication of a polarity signal (Vinson and Adler 1987). On the other hand, *dsh* is strictly cell autonomous in clones (Theisen et al. 1994), implying that it is involved in signal reception. To investigate whether *pk* participates in both reception and transmission of a polarity signal we studied pk^{pk} clones in the wing. Large clones in the wing express the mutant polarity typical of that region of the wing in homozygous flies. There is an occasional nonautonomous disruption of polarity in wild-type cells adjacent to the proximal or lateral margins of a pk^{pk} clone (12 cases in 150 clones induced at 48–72 hr after egg laying). In these cases, a short range perturbation aligns wild-type cells with the mutant polarity pattern (Fig. 9). There is no clear pattern to the position of such clones, but small peninsulas of *pwn*$^+$ tissue surrounded by pk^{pk} *pwn* tissue tend to adopt the mutant polarity pattern. Smaller clones, induced later than 72–96 hr, did not alter the polarity of adjacent *pawn* (*pwn*$^+$) tissue.

In contrast to the autonomous behavior of *pk*, clones of *fz tricornered* (*trc*) cause long-range domineering nonautonomy both distal (as reported by Vinson and Adler 1987) and lateral to the clone. Wild-type hairs are oriented toward the clone as though it is acting as a polarity 'sink' (Fig. 9). Proximal cells are also directed toward the *fz trc* clone, but as this is the normal orientation for wing cells no polarity changes would be expected.

Discussion

Genetic structure of pk *and activity of the different transcripts*

The *pk* gene encodes three transcripts (*pk*, *sple*, and *pkM*) that differ in their 5′ exons (Figs. 4 and 6). That these transcripts have qualitatively different activities in transgenic constructs, together with the intermediate phenotypes of mutant combinations that titrate the number of doses of *pk* and *sple*, suggests that the Pk and Sple products are required in stoichiometric ratios. Although pk^{pk} and pk^{sple} mutants affect reciprocal regions of the body, their transcripts are expressed with a similar distribution in wing, leg, and eye discs. This implies a function for both transcripts in all tissues that is not obvious from the mutant phenotypes. In overexpression constructs [*pk*$^+$] gives a Sple phenotype in the tarsi,

Table 3. *Alignment of amino acid sequence of PET and LIM domains within the* pk *family*

pk	DmQRqShSDDDSGCALEEYtWVPPGLrPdQVRlYfSQiPdDKVPYVNSPGEqYRvrQLLHQLPPHDNE	PET Domain
esn	DfQRnSqSDDDSGCALEEYtWVPPGLrPdQVRlYfSQLPdDKVPYVNSPGEKYRvKQLLHQLPPqDNE	
Human LMO6	DfQRhSiSDDDSGCAsEEYaWVPPGLkPeQVyQffScLPEDKVPYVNSPGEKYRiKQLLHQLPPHDsE	
Mouse Testin	iltnpvaakknvsintvtYeWaPPvQnqalarQYMqmLPkeKqPvagSeGaqYRkKQLakQLPaHDqd	
C. el bo496.8	ssdseSerggsnnkenvqYaWa*PlpdknlVsrYMkalPEDerPlVgSkGeqnRksrLqfQLPlyDcn	
C. el zk381.7	DahRhStSDDDSGCALDEYaWVPsGLkPnmVhaYMacLPEnKVPfigSaGEKwRqrQsryQLPRqDsd	
Human h90439	**********glsngqviymlsvlQVhQYyScLPEeKVPYVNSPGEKlRiKQLLHQLPPHDNE	
C. el f25h5.1	enmRgdplmirfmhkageffrktknnwlidVeeYMSQLPnnvVPrtNSnGEKlReKQLLlQLPrqDls	
pk	VRYCHSLt*dEERKELRlFStQRKRdALGRGnVRqlmsa***************************	
esn	VRYCHSLs*dEERKELRiFSaQRKREALGRGaVRllsde***************************	
Human LMO6	aqYCtaLe*eEEkKELRaFSqQRKREnLGRGiVRiFpvtitg***************************	
Mouse Testin	pskCHeLs*pkEvKEmeqFvkkyKsEALGvGdVk*Fpsemnaqgdkvhncgnrhapaavaskdksaes	
C. el bo496.8	Vedarf*veekdvKtLqnFvenvrnnviGvGrVveigkdsdnygdnentnefeksmtaalkglkiget	
C. el zk381.7	VRYCedLn*aEEadtLRmFertRKtEcLGsGvVqyapfdtkcekvsifhq	
Human h90439	VRYCnSLd*eEEkrELklFSsqRKREnLGRGnVRpFpvtmtgaqsa	
C. el f25h5.1	VaYCrhLtSqtERKvyeeFvnaRneiALdiGyVssninka***************************	
pk	****rpCdgCddlistGDIAVFAtRLGpnasWHPACFaCSVCrELLVDLIYFhrDGrmYCGRHHAE	LIM 1
esn	****rpCkgCeeplsgGDIVVFAqRLGaqlcWHPgCFvCSVCkELLVDLIYFqrDGnlYCGRHHAE	Domain
Human LMO6	****asCeeCgkqiggGDIAVFAsRaGlgacWHPqCFvCtVCqELLVDLIYFyhvGKvYCGRHHAE	
Mouse Testin	kktqysCycCkhttneGepAiyAeRaGydklWHPACFiCStCgELLVDmIYFwknGKlYCGRHycd	
C. el bo496.8	kigetdCkdCnemmetGdigvechhhsttdtyHPnCFrCetCrqlLVDnIYFfyknKyYCGRHyAd	
C. el f25h5.1	****meChkCsgiletnemAViApkLGdstgWHPACFtCqaCeqLLVDLtYcvkDnqiYCeRHyAE	
pk	tlKPRCSACDEIIladECTEAEGRaWHMnHFgChECDKqLGGQRYIMRegKPYCLhCfdam	LIM 2
esn	tqKPRCSACDEIIFSdECTEAEGRtWHMkHFgChECDKqLGGQRYIMRegKPYCLaCfdtm	Domain
Human LMO6	clrPRCqACDEIIFSpECTEAEGRhWHMdHFCCfECeasLGGQRYvMRqsrPhCcaCYear	
Mouse Testin	seKPRCagCDElIFSnEyTqAEnqnWHlkHFCCfdCDhiLaGkiYvMvtdKPVCkpCYvkn	
C. el bo496.8	qlyPRCagCDElIFanEyTfAEeksWHfdHFaCykCDfklGGsRYmtRdenPfCLdCylkh	
C. el f25h5.1	lhKPRCSACDElIFagEyTkAmnkdWHsdHFCCwqCDqtLtGQRYIMRdeqPYCikCYedv	
pk	FgEYCDyCGEGIGvDQGQMShdGQHWHATDeCFsCntCrcSLLGraFLPRRGgIyCSiACSkGe	LIM 3
esn	FAEYCDyCGEvIGvDQGQMShdGQHWHATDqCFsCctCrcSLLGrpFLPRRGtIyCSiACSkGe	Domain
Human LMO6	hAEYCDgCGEhIGlDQGQMaYeGQHWHASDrCFcCSrCgraLLGprFLPRRGlIFCSrACSlGr	
Mouse Testin	hAvvCqgChnaIdpevqrvtYnnfsWHASteCFlCScCskcLiGqkFmPveGmvFCSvECkrmm	
C. el bo496.8	*FAktCDtCqskIgpDekrlnYnetHWHAeerCFqCvqCkmnLiGkkFmlknhkllCSsqCkany	
C. el f25h5.1	FAnqCDeCakpIGiDskdlsYkdkHWH**ehCFlCSmCkiSLvdmpFgskndrIFCSn*Cydqa	

Conserved amino acids are shown in uppercase and putative zinc binding ligands in bold. Sequence accession nos., LMO6 (EMBL AJ011654), Testin (SwissProt P47226), *C. elegans* (bo496.8, EMBL U58748; zk381.7, EMBL U52003; f25h5.1, EMBL z81068) and the human EST (GenBank h90439). The novel PET domain is 101 amino acids in length in *pk, esn, LMO6* and *f25h5.1* but is 5′ truncated in the other four family members. The length of the individual LIM domains and the unusual spacing of the putative zinc binding ligands in the third LIM motif are conserved features of the *pk* family. The amino acid sequence homology for both the PET and LIM domains ranges between 40% identity (52% similarity) for bo496.8 compared to *pk* and 87% identity (92% similarity) for *esn* compared to *pk* [percentages calculated using Best Fit (GCG)].

whereas [*sple*$^+$] gives a Pk phenotype in the wing (Fig. 8). This antagonism between the *pk* and *sple* transcripts implies either that both proteins compete for a target that is present in limiting amounts, or that they form protein complexes with distinct activities. In pk^{pk} and pk^{sple} mutants excess homodimers would misactivate polarity signaling. Stoichiometric ratios of the LIM domain proteins Apterous and Chip have been shown to be critical in their developmental function (Fernandez-Funez et al. 1998).

Both the human and mouse homologs, LMO6 and Testin (Divecha and Charleston 1995; Fisher et al. 1997), encode alternative 5′ transcripts that may be a general feature of the *pk* family.

Sequence analysis and homologies

The LIM domain motif is a zinc binding finger that was originally described in homeodomain proteins but has since been found in combination with kinase or GAP domains (Dawid et al. 1995) and in proteins with no other identified domains. Many nonhomeodomain LIM proteins are associated with the cytoskeleton, several of them being localized primarily in adhesion plaques (Dawid et al. 1998) and having multiple LIM domains. The LIM domain appears to be involved in protein–protein interactions, with the highly charged zinc finger domains binding to target proteins. Homotypic interactions between two LIM domain partner proteins are also thought to occur (Dawid et al. 1998), although it is unclear how two zinc fingers might interdigitate.

There are a number of conserved features within the LIM domains of the *pk* family proteins. In the first LIM domain, there is a proline residue between the third (H) and fourth (C) zinc binding residues. This internal proline residue might introduce a kink within the zinc binding site. Similar LIMP domains with an internal P at this site are found in the human SLIM 2, SLIM 3, PINCH,

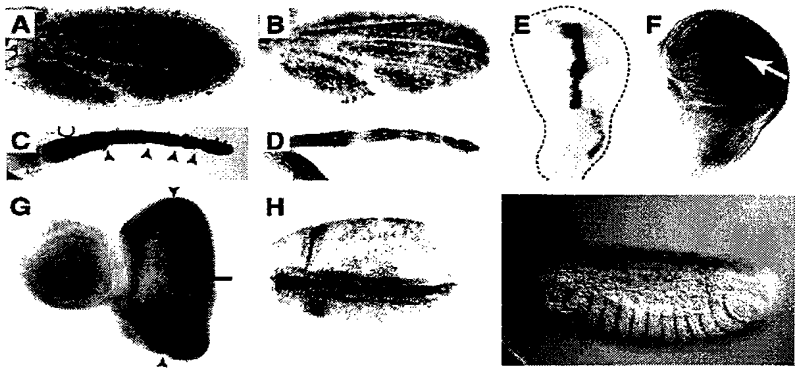

Figure 6. Tissue in situs. Wild-type pupal leg and wing discs (28–32 hr) probed with *pk*-specific (*A*,*C*) or *sple*-specific (*B*,*D*) 5′ probes. Hybridization is uniform with both probes, with the exception of the wing veins and the tarsal segment boundaries (arrowheads in *C*). The expression in larval imaginal discs is much weaker; no endogenous signal is detected with a common exon probe at a level at which *dpp–UAS:pk* (*gal4–dpp P*[*UAS:pk*$^+$]) wing discs show strong hybridization within the *dpp* domain (*E*) (the dotted line indicates disc boundary). With increasing development times a signal is seen along both sides of the D/V compartment boundary (arrow) in the wing (*F*) and as a discrete band (arrow) behind the morphogenetic furrow (arrowheads) in the eye disc (*G*). These preparations show a high background of nonspecific signal (retained in $pk^{pk-sple13}$ discs and with antisense probes; data not shown). In the embryo, *pkM*, *sple*, and common exon probes give similar patterns of expression. Stage 8 embryos (*H*) show a strong signal in the cephalic furrow and dorsal fold, *pkM* probe. (*I*) Stage 14 embryos show signal in the parasegmental folds, common exon probe.

Zyxin, and Paxillin proteins and LIM domain kinase 2 (LIK2) from chicken, mouse, rat, and human.

In addition, the length of the consecutive LIM domains is constant in the *pk* family, with LIM1 containing 57, LIM2 containing 52, and LIM3 containing 56 amino acids. The implication is that the conservation of the triple LIM domain itself is important, rather than the individual LIM domains. In the case of the triple LIM domain protein Zyxin, the individual LIM domains may bind different target proteins and act as a template for the assembly of a number of structural components (Beckerle 1997).

A similar scaffold function for the Pk protein would be consistent with the cell autonomy of *pk* in clones and the expression of *pk* transcripts in cells that are changing shape. The blocking of the normal migration of the actin-rich prehair structure to the center of wing cells by overexpression of *pk* also implies a role in cytoskeletal remodelling. The lack of embryonic phenotype, despite the dynamic expression pattern, implies that *pk* function is redundant during embryonic development. A putative embryonic *pk* function could, in principle, be maternally supplied, but *pk* mutant strains of all three classes are fully fertile and homozygous *pk* embryos from homozygous mothers remain wild type. Similarly, *gal4–da*; P[*UAS:pk*$^+$], and *gal4–da*; P[*UAS:sple*$^+$] flies are com-

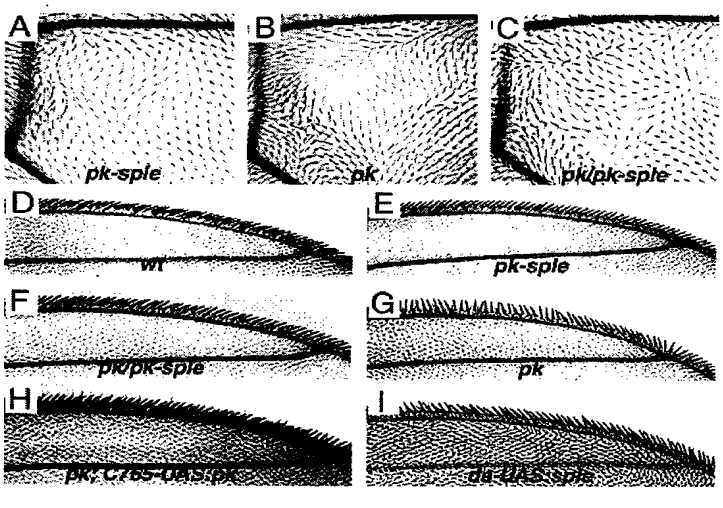

Figure 7. The wing phenotypes associated with titrating the number of intact copies of *pk* and *sple*. (*A*) *pk–sple*, moderate phenotype resulting from homozygous deletion of the common exons, $pk^{pk-sple13}/pk^{pk-sple13}$. (*B*) *pk*, extreme phenotype resulting from deletion of the *pk* transcript, *Df(2R)pk-30/Df(2R)pk-30*. (*C*) *pk/pk–sple*, moderate phenotype resulting from deleting *pk* and halving the number of *sple* copies in *Df(2R)pk-30*/$pk^{pk-sple13}$ flies. The polarity pattern shown here, distal to the posterior cross vein, is stronger than in the remainder of the wing blade, which is closer to $pk^{pk-sple13}$. (*D*) polarity of the marginal triple row bristles in wild type. (*E*) *pk–sple* triple row ($pk^{pk-sple13}/pk^{pk-sple13}$). (*F*) *pk/pk–sple* triple row [*Df(2R)pk-30*/$pk^{pk-sple13}$]; (*G*) *pk* triple row [*Df(2R)pk-30* /*Df(2R)pk-30*]. The *pk* wing phenotype was rescued by driving *UAS:pk*$^+$ expression with the *gal4–C765* driver, which is expressed in the wing and leg disks. (*H*) The pk^{pk} triple row bristle phenotype is completely rescued and the wing hair polarity is close to wild type in *pk*; *C765–UAS:pk* wings [*Df(2R)pk-30*; *gal4–C765*/P[*UAS:pk*$^+$]]. Small regions of abnormal polarity remain within the wing blade (both in *pk*; *C765–UAS:pk* and *C765–UAS:pk* in a wild-type background). *sple* overexpression also gives a wing phenotype in *da–UAS:sple*$^+$ wings (*I*); the wing shown is *EP(2)2557/+*; *gal4–da/+* (*EP(2)2557* inserts a UAS driver 80 bp 5′ to the *sple* first intron), but the same phenotype is shown with a P[*UAS:sple*$^+$] transformant line, in P[*UAS:sple*$^+$]/+; *gal4–da*/+ wings.

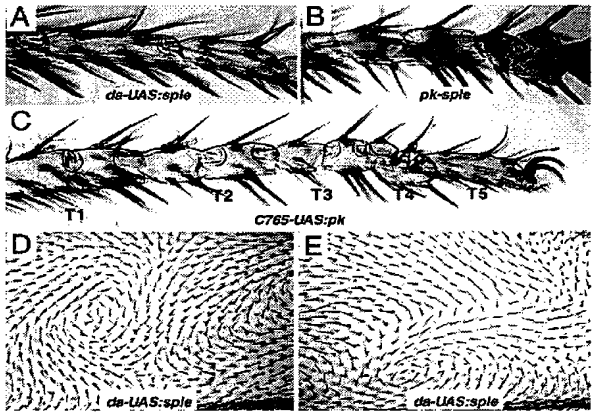

Figure 8. Overexpression phenotypes in leg and wing blade. Overexpression of *sple* in *da–UAS:sple*$^{+}$ [*EP(2)2557/+; gal4–da/+*] legs gives no mutant phenotype; the wild-type morphology of T3 and T4 tarsal segments is shown in *A*. For comparison, the duplicated proximal (ball) and distal (socket) joint structures of the T3 and T4 segments resulting from lack of function in $pk^{pk-sple-3}$ legs is shown in *B*; the T1, T2, and T5 segments (not shown) remain normal. A more extreme tarsal duplication phenotype affecting T1–T4 segments is given by Pk overexpression in *765–UAS:pk*$^{+}$ (P[*UAS:pk*]$^{+}$/*gal4–C765*) flies (*C*). (*D,E*) The same region anterior to vein 4 in two different *da–UAS:sple* [EP(2)2557/+; *gal4–da*/+] wings. The polarity in any given region is unpredictable from wing to wing, but hair orientation changes gradually across large fields of cells. Whorls, cruciform, and radial stacking flaws are seen as in pk^{pk} wings, but at variable positions within the wing blade.

pletely viable and show no embryonic phenotype, despite the embryonic expression of the *gal4–da* driver.

Tessellation models and fine-grained positional information during planar polarity formation

Perhaps the most surprising feature of the tissue polarity mutants is the precise polarity patterns seen in the wing hairs (Gubb and Garcia-Bellido 1982). Rather than reflecting fine-grained positional information, however, the precision of the final pattern might be dependent on a tessellation mechanism. The orientation of the first cell would determine the alignment of subsequent cells, like sticking tiles on a bathroom wall. In pk^{pk} mutants, the alignment of wing hairs deviates progressively with occasional abrupt changes. In the adult mutant wing, hair polarity alters gradually with sudden topological discontinuities (Fig. 2E–G) that resemble the stacking flaws in liquid crystals (Frank 1958). In *Df(2R)pk-30* wings, regions where the wing hairs are uniformly oriented retain a predominantly hexagonal array. Regions surrounding topological discontinuities, such as the anterior whorl, show irregular cell shapes frequently associated with duplicated wing hairs.

Strong support for a tessellation mechanism is given by the overexpression phenotype of Pk and Sple when driven by a ubiquitous promotor (e.g., Fig. 8D,E). Although polarity patterns are variable, hair orientation alters smoothly from cell to cell across the wing surface, indicating that the polarity of cytoskeletal structures is aligned within large fields of cells. It is as if cell packing had nucleated randomly and then spread to neighboring cells until meeting an adjacent domain. The short-range perturbation in polarity that is occasionally seen proximal and lateral to a pk^{pk} clone is consistent with mechanical adjustment of cells to fit against their immediate neighbors, unlike the long-range domineering nonautonomy lateral and distal to *fz* clones. With both classes of clones, a tessellation mechanism might impose a threshold. Below this threshold, disruptions in polarity signaling would fail to affect the orientation of neighboring cells.

Tarsal duplications and polarity signaling pathways

The tarsal phenotype of *dsh* is very similar to $pk^{pksple13}$ causing duplications of the T3 and T4 segments. A more extreme phenotype including complete duplications of T2 to T4 together with a well-developed ectopic T1 joint are seen in *dsh; pk*^{sple}, overexpression *UAS:pk*$^{+}$ and *fz* mutant strains, implying that a similar polarity signaling pathway is affected. It has been suggested that *pk* and *fz* are upstream in a signaling pathway leading to *dsh* (Wong and Adler 1993; Shulman et al 1998). There are several problems with a simple linear pathway, however, and the relationship between *pk* and *fz* is unclear. First, neither *fz* nor *pk* is clearly epistatic to the other; rather, the double mutant (*pk*^{pk}; *fz*) phenotype is intermediate between pk^{pk} and *fz* (Gubb and Garcia-Bellido 1982; Wong and Adler 1993). Second, whereas *fz* clones cause a long-range nonautonomous disruption in surrounding tissue (Gubb and Garcia-Bellido 1982; Vinson and Adler 1987) we show here that pk^{pk} clones resemble *dsh* clones (Theisen et al. 1994) in being almost completely cell autonomous. (Both pk^{sple1} and $pk^{pk-sple13}$ clones are cell autonomous in the eye (Zheng et al. 1995; Gubb 1998).) On the other hand, the pk^{pk} triple row bristle phenotype (that results from Sple expression in the absence of Pk) is suppressed in *dsh; pk*^{pk} wings and the *dsh* polarity pattern is modified in *dsh; pk*^{sple} wings (despite pk^{sple} on its own not having a wing phenotype). Finally, complete lack of *pk* transcripts produces a phenotype very similar to *dsh*. Taken together, these results indicate that PK is not downstream of Fz but may represent an alternative input into Dsh-mediated planar polarity signaling.

Conclusions

We show that the two genetically distinct phenotypes Pk and Sple arise from discrete lesions in a single gene and suggest that the relative and absolute levels of the two gene products are critical to wild-type activity. The developmental expression of a third transcript, *pkM*, suggests an embryonic function. We have not recovered mutant alleles of *pkM*, however, and the lack of embryonic phenotype with deletions of the entire *pk* gene implies that any embryonic function must be redundant.

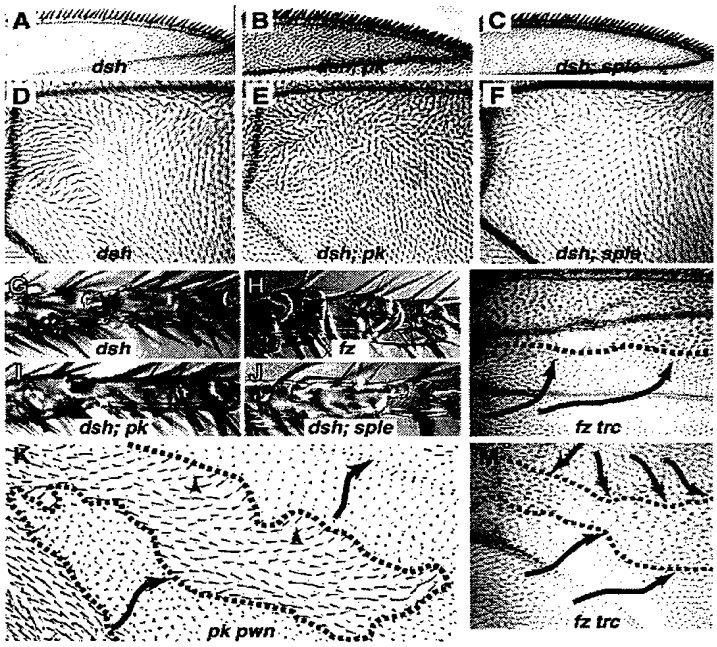

Figure 9. Comparison of different planar polarity phenotypes in wing and tarsi. The triple row bristle phenotype and wing blade polarity patterns of *dsh* are similar to $pk^{pk-sple13}$ (*A,D*). The extreme triple row phenotype of *Df(2R)pk-30* is suppressed in *dsh; Df(2R)pk-30* flies and becomes phenotypically Dsh in both *dsh; Df(2R)pk-30* and *dsh;* pks^{ple1} double mutants (*B,C*). In *dsh; Df(2R)pk-30* double mutants, the wing blade phenotype is intermediate between the respective single mutants (*E*). A slight, but consistent modification in the Dsh polarity is also seen in *dsh;* pk^{sple1} wings, despite the fact that pk^{sple} alleles show no wing phenotype (*F*). The Dsh tarsal phenotype is similar to $pk^{pk-sple13}$ in giving complete duplications of the T3 and T4 segments; an incipient joint is present in T1 and T2 (arrows), but the external morphology of these segments remains normal (*G*). This phenotype is unaffected in *dsh; Df(2R)pk-30* (*I*). The most extreme tarsal phenotypes, with complete duplications in T2–T4 and an ectopic joint structure in T1, are seen in *fz* (*H*), P[*UAS:pk*$^+$] overexpression (Fig. 8C) and *dsh;* pk^{sple} (*J*) mutant strains. In somatic mosaics, the effects of *pk* and *fz* are distinct. Within pk^{pk} *pwn* clones, the polarity pattern is autonomous. A pk^{pk} *pwn* clone in cell E of the wing is shown in *K* which expresses pk^{pk} polarity (black arrows) (cf. Fig. 1A); a short range alteration in polarity (gray arrowheads) is seen close to the clone boundary (broken line). This effect is clearest when a small peninsula of pk^{pk} *pwn* tissue is surrounded by *pwn*$^+$ tissue. In contrast, *frz trc* clones cause a long-range nonautonomous alteration in the polarity of surrounding cells, which tend to point toward the mutant clone (*L,M*).

We have also identified the PET domain, a novel protein motif that is highly conserved in metazoan evolution. We speculate that the PET domain is involved in interactions with as yet unidentified proteins to form a planar polarity signaling complex. Potential partners could include the currently known tissue polarity genes and actin cytoskeletal components. Overexpression of Pk transcripts produces mutant phenotypes similar to recessive lack of function. This unusual property is also shown with overexpression of Fz (Krasnow and Adler 1994) and Dsh (Axelrod et al. 1998). If Dsh is acting as a scaffolding or adapter protein (Axelrod et al. 1998) then it would be required in stoichiometric ratios to its target proteins, and overexpression would prevent assembly of functional complexes. It may be that the Pk protein isoforms are components of this protein complex that are expressed in cells remodeling their cytoskeletal architecture.

Materials and methods

Drosophila *stocks*

The original alleles of pk^{pk} and pk^{sple} are spontaneous. Subsequent alleles were induced in this study (see below and http://www.gen.cam.ac.uk/dept/gubb.html) or described in FlyBase (http://flybase.bio.indiana.edu). The *EP* line (Rorth 1996), *EP*(2)2557 maps in the *pk* region and gives a recessive polarity phenotype in notum and tarsus (B. Reed, pers. comm.). *Gal4* driver strains were *gal4–pannier* (/) $pnrM^{D237}$; *gal4–C765; gal4–dpp* (*decapentaplegic*), *gal4–en*, and *gal4–da*^{G32} (FlyBase 1999). The boundaries of adult wing cells were visualized using the *miniature* (*m*) mutant strain $In(1)m^{38c}$ (Newby et al. 1991).

To extend the analysis of *pk*, new alleles were recovered in a variety of screens. Four pk^{pk} (*19, 20, 21, 30*) and four $pk^{pk-sple}$ (*11, 12, 13, 31*) alleles were isolated among 4207 X-irradiated chromosomes, heterozygous with either *Df(2R)pk78k* or *pr pk cn sp*. Twenty further alleles of $pk^{pk-sple}$ (*22, 24, 26, 28, 32, 34, 35, 37, 38, 39, 40, 41, 43–51*) and two of pk^{sple} (*36, 42*) were recovered among 34, 491 X-irradiated chromosomes heterozygous with pk^{sple1}. Together with preexisting alleles, this gave a collection of eleven pk^{pk} alleles, 28 $pk^{pk-sple}$ alleles, and seven pk^{sple} alleles (Table 1).

Mutagenesis

New X-ray-induced alleles of pk^{pk} and $pk^{pk-sple}$ were recovered heterozygous with *Df(2R)pk78k*, or *pr pk cn sp* following the methods of Heitzler et al. (1993). Additional X-ray-induced $pk^{pk-sple}$ and pk^{sple} alleles were screened for the pk^{sple} phenotype heterozygous with pk^{sple1}.

Molecular techniques

A chromosome walk of 150 kb was isolated using the phage genomic insert library of John Tamkun (University fo California, Santa Cruz). The walk was extended from a 3-kb genomic fragment with weak homology to *raf* (Mark et al. 1987) proxi-

mally to FP11/3 and distally to FP0/4, until the *Df(2R)sple-J2* and *Df(2R)Drl-rv30* breakpoints defining the region had been uncovered. The complete restriction maps of these phage for *Eco*RI, *Sal*I, *Bam*HI, *Xho*I, and *Hin*dIII and other details are available at the http://www.gen.cam.ac.uk/dept/gubb.html web site.

Chromosome breakpoints were mapped relative to the genomic phage inserts by in situ hybridization with biotin-labeled probes and genomic Southern blots (as described in Gubb et al. 1997). Tissue in situs used riboprobes to the unique exons and the 3′ common exons, made with the Boehringer DIG RNA labeling kit (SP6/T7).

Identification of transcripts and recovery of cDNAs

As the walk progressed, gel-purified genomic fragments were used to probe developmental Northern blots and cDNA library filters. Although three Serpin transcripts and a putative adenosine kinase were identified on Northern blots using random primed genomic insert probes, the much less abundant *pk* transcripts were not detected. A single putative full-length *pk* cDNA, *Pk4a3*, was finally recovered from 5×10^5 clones of an embryonic library (Brown and Kafatos 1988). Additional *pk* transcripts were identified from embryonic cDNA using nested oligonucleotides from the second exon of *Pk4a3* with the Marathon (Clontech)-modified RACE protocol. Products were cloned into the pCR2.1 vector with a TA cloning kit (Invitrogen). This generated three fragments of 1.8, 0.88, and 0.65-kb, which were hybridized to the genomic walk. The 0.88-kb product is equivalent to the 5′ end of *Pk4a3*; whereas the other two products represent alternative 5′ exons. The 1.8-kb product corresponds to the 5′ *sple* transcript, whereas the 0.65-kb fragment identifies a third, medial transcript, which we have designated *pkM*.

Northern analysis

Total RNA was isolated from staged wild-type (Canton-S) flies (Ashburner 1989). Poly $(A)^+$ RNA was prepared using the PolyAT tract mRNA isolation kit (Promega). Developmental Northern blots used ~0.5 μg of Poly$(A)^+$ RNA from each stage. For *pk* mutants, 25 μg per lane of total RNA from 2-day pupae was used. Gels were blotted on nylon membrane and hybridized with random-primed ^{32}P-radiolabeled *pk* common exon probe (the *Pk4a3 Pst*I–*Xho*I 617-bp plus *Xho*I–*Not*I 737-bp fragments) and a *Rp49* probe following standard procedures. Single-stranded antisense RNA probes for the alternative 5′ exons were synthesized from the pCR2.1 vector.

Nucleotide sequence analysis of cDNA, genomic clones, and exonic boundaries

Genomic fragments and cDNAs were subcloned into pBluescript SK+ (Stratagene Ltd.). *Sau*IIIA and *Taq*I restriction fragments of the *Pk4a3* cDNA and six-cutter fragments of the *sple* 5′ cDNA were sequenced from vector primers using the Prism Ready Reaction DyeDeoxy Terminator Cycle Sequencing Kit (Perkin-Elmer Corporation). Sequence gaps were filled using specific oligonucleotide primers.

The exon structure of a full-length 4.2-kb cDNA, *Pk4a3*, was mapped to the genomic walk by Southern blot and sequence analysis. Similarly, the 1.8-, 0.88-, and 0.65-kb 5′ RACE products were mapped against the genomic walk before being subcloned and sequenced. The precise boundaries of the *pk* 5′ exon were deduced by comparison to sequence from subcloned genomic fragments from our walk, whereas the 5′ exonic structure of *pkM* and *sple* was obtained by comparison of the cDNA sequence of the 1.8- and 0.65-kb RACE products to genomic sequence from the Berkeley *Drosophila* Genome project (P1 clone DS08462; AC005198).

Transformation constructs

Transformation constructs were cDNA sequences subcloned in the pUAST vector to utilize the *gal4* expression system (Brand and Perrimon 1993). The *UAS* [pk^+] transgenic construct was made from the *Pk4a3* cDNA, whereas *UAS* [$sple^+$] was synthesised from *Pk4a3* by replacing the 5′ *Hin*dIII–*Sma*I fragment with the *sple* 5′ *Hin*dIII–*Sma*I fragment from a pBluescript subclone of the 1.8-kb RACE product.

Analysis of somatic clones

Somatic mosaics of pk^{pk1} marked with the cell autonomous mutation *pwn* were generated using a P[*FRT*]*42D* pk^{pk1} *pwn* chromosome following the method of Xu and Rubin (1994) and *fz trc* as in Gubb and Garcia-Bellido (1982).

Acknowledgements

We thank Jose-Felix de Celis for advice and help with tissue in situs, Michael Ashburner for the cytological analysis of *In(2LR)CyO Tp(2;2)pk–sple*^{26}, and Carol McKimmie for injection of the P-element transformation constructs. Sarah Bray, Adelaide Carpenter, Jose-Felix de Celis, Miriam Hirshberg, Jean-Marc Reichhart, Steven Russell, and Josh Shulman are acknowledged for discussion and critical reading of the manuscript; Bruce Reed for sharing unpublished results; and John Tamkun and Nick Brown for phage and plasmid libraries. We thank the FlyBase consortium, particularly Rachel Drysdale, for rulings on the *pk–sple* nomenclature. This work was funded by Medical Research Council programme grants to Michael Ashburner, David Gubb, and Steven Russell.

The publication costs of this article were defrayed in part by payment of page charges. This article must therefore be hereby marked 'advertisement' in accordance with 18 USC section 1734 solely to indicate this fact.

Note

The EMBL accession numbers for the cDNA and genomic clone sequences in this paper are adenosine kinase (AJ236864), *pk* isoform (AJ243708), *pkM* isoform (AJ243709), and *sple* isoform (AJ243710).

References

Adler, P.N. 1992. The genetic control of tissue polarity in *Drosophila*. *BioEssays* **14:** 735–741.

Adler, P.N., C. Vinson, W.J. Park, S. Conover, and L. Klein. 1990. Molecular structure of *frizzled*, a *Drosophila* tissue polarity gene. *Genetics* **126:** 401–416.

Ashburner, M. 1989. Drosophila, *a laboratory manual*. Cold Spring Harbor Laboratory Press, Cold Spring Harbor, NY.

Axelrod, J.D., K. Matsuno, and S. Artavanis-Tsakonas. 1996. Interaction between Wingless and Notch signaling pathways mediated by Dishevelled. *Science* **271:** 1826–1832.

Axelrod, J.D., J.R. Miller, J.M. Shulman, R.T. Moon, and N. Perrimon. 1998. Differential recruitment of Dishevelled provides signaling specificity in the planar cell polarity and Wingless signaling pathways. *Genes & Dev.* **12:** 2610–2622.

Beckerle, M.C. 1997. Zyxin: Zinc fingers at sites of cell adhesion. *BioEssays* **19:** 949–956.

Bhanot, P., M Brink, C.H. Samos, J.C. Hsieh, Y. Wang, J.P. Macke, D. Andrew, J. Nathans, and R.A. Nusse. 1996. A new member of the *frizzled* family from *Drosophila* functions as a *wingless* receptor. *Nature* **382:** 225–230.

Brown, N.H and F.C. Kafatos. 1988. Functional cDNA libraries from *Drosophila* embryos. *J. Mol. Biol.* **203:** 425–437.

Brand, A.H. and N. Perrimon. 1993. Targeted gene expression as a means of altering cell fates and generating dominant phenotypes. *Development* **118:** 401–415.

Cadigan, K.M., M.P. Fish, E.J. Rulifson, and R. Nusse. 1997. Wingless repression of *Drosophila frizzled* 2 expression shapes the Wingless morphogen gradient in the wing. *Cell* **93:** 767–777.

Cavener, D.R. and S.C. Ray. 1991. Eukaryotic start and stop translation sites. *Nucleic Acids Res.* **19:** 3185–3192.

Collier, S. and D. Gubb. 1998. *Drosophila* tissue polarity requires the cell-autonomous activity of the *fuzzy* gene, which encodes a novel transmembrane protein. *Development* **124:** 4029–4037.

Dawid, I.B., R. Toyama, and M. Taira. 1995. LIM domain proteins. *C.R. Acad. Sci. Paris Ser. III* **318:** 295–306.

Dawid, I.B., J.J. Breen, and R. Toyama. 1998. LIM domains: Multiple roles as adapters and functional modifiers in protein interactions. *Trends Genet.* **14:** 156–162.

Divecha, N. and B. Charleston. 1995. Cloning and characterisation of two new cDNAs encoding murine triple LIM domains. *Gene* **156:** 283–286.

Eaton, S. 1997. Planar polarization of *Drosophila* and vertebrate epithelia. *Curr. Opin. Cell Biol.* **6:** 860–866.

Eaton, S., R. Wepf, and K. Simons. 1996. Roles for *Rac1* and *Cdc42* in planar polarization and hair outgrowth in the wing of *Drosophila*. *J. Cell Biol.* **135:** 1277–1289.

Fernandez-Funez, P., C.H. Lu, D.E. Rincon-Limas, A. Garcia-Bellido, and J. Botas. 1998. The relative expression amounts of apterous and its co-factor *dLdb/Chip* are critical for dorsoventral compartmentalization in the Drosophila wing. *EMBO J.* **17:** 6846–6853.

FlyBase. 1999. The FlyBase database of the Drosophila Genome projects and community literature. *Nucleic Acids Res.* **27:** 85–88. http://flybase.bio.indiana.edu

Fisher, S.E., A. Ciccodicola, K. Tanaka, A. Curci, S. Desicato, M. D'Urso, and, I.W. Craig. 1997. Sequence-based exon prediction around the Synaptophysin locus reveals a gene-rich area containing novel genes in human proximal Xp. *Genomics* **45:** 340–347.

Frank, F.C. 1958. On the theory of liquid crystals. *Discussions Faraday Soc.* **25:** 19–28.

Gubb, D. 1993. Genes controlling cellular polarity in *Drosophila*. *Dev. (Suppl.)* 269–277.

Gubb, D. 1998. Cellular polarity, mitotic synchrony and axes of symmetry during growth. Where does the information come from? *Int. J. Dev. Biol.* **42:** 369–377.

Gubb, D. and A. Garcia-Bellido. 1982. A genetic analysis of the determination of cuticular polarity during development in *Drosophila melanogaster*. *J. Embryol. Exp. Morphol.* **68:** 37–57.

Gubb, D., J. Roote, J. Trenear, D. Coulson, and M. Ashburner. 1997. Topological constraints on transvection between *white* genes within the transposing element *TE35B* in *Drosophila melanogaster*. *Genetics* **146:** 919–937.

Harden, N., H.Y. Loh, W. Chia, and L. Lim. 1995. A dominant inhibitory version of the small GTP-binding protein Rac disrupts cytoskeletal structures and inhibits developmental cell shape changes in *Drosophila*. *Development* **121:** 903–914.

Held, L.I., C.M. Duarte, and K. Derakhshanian. 1986. Extra tarsal joints and abnormal cuticular polarities in various mutants of *Drosophila melanogaster*. *Wilhelm Roux Arch. Dev. Biol.* **195:** 145–157.

Heitzler, P., D. Coulson, M.-T. Saenz-Robles, M. Ashburner, P. Simpson, J. Roote, and D. Gubb. 1993. Genetic and cytogenetic analysis of the 43A-E region containing the segment polarity gene costa and the cellular polarity genes *prickle* and *spiny-legs* in *Drosophila melanogaster*. *Genetics* **135:** 105–115.

Krasnow, R.E. and P. Adler. 1994. A single Frizzled protein has a dual function in tissue polarity. *Development* **120:** 1883–1893.

Klingensmith, J., R. Nusse, and N. Perrimon. 1994. The *Drosophila* segment polarity gene *dishevelled* encodes a novel protein required for response to the wingless signal. *Genes & Dev.* **8:** 118–130.

Mark, G.E., R. J. MacIntyre, M.E. Digan, L Ambrosio, and N. Perrimon.1987. *Drosophila melanogaster* homologs of the *raf* oncogene. *Mol. Cell. Biol.* **7:** 2134–2140.

Newby, L.M., L. White, S.M. DiBartolomeis, B.J. Walker, H.B. Dowse, J.M. Ringo, N. Khuda, and F.R. Jackson. 1991. Mutational analysis of the Drosophila *miniature-dusky* (*m-dy*) locus: Effects on cell size and circadian rhythms. *Genetics* **128:** 571–582.

Orsulic, S. and M. Peifer. 1996. An *in vivo* structure-function study of *armadillo*, the beta-catenin homologue, reveals both separate and overlapping regions of the protein required for cell adhesion and for *wingless* signaling. *J. Cell Biol.* **134:** 1283–1300.

Park, W.J., J. Liu, E.J. Sharp, and P.N. Adler. 1996. The *Drosophila* tissue polarity gene *inturned* acts cell autonomously and encodes a novel protein. *Development* **122:** 961–969.

Rorth, P. 1996. A modular misexpression screen in detecting tissue-specific phenotypes. *Proc. Natl. Acad. Sci.* **93:** 12418–12422.

Sanchez-Garcia, I. and T.H. Rabbitts. 1994. The LIM domain: A new structural motif found in zinc-finger-like proteins. *Trends Genet.* **10:** 315–320.

Shulman, J.M., N. Perrimon, and J.D. Axelrod. 1998. Frizzled signaling and the developmental control of cell polarity. *Trends Genet.* **14:** 452–458.

Strutt, D.I., U. Weber, and M. Mlodzik. 1997. The role of RhoA in tissue polarity and Frizzled signalling. *Nature* **387:** 292–295.

Theisen, H., J. Purcell, M. Bennett, D. Kansagara, A. Syed, and J.L. Marsh. 1994. *dishevelled* is required during wingless signaling to establish both cell polarity and cell identity. *Development* **120:** 347–360.

Vinson, C.R. and P.N. Adler 1987. Directional non-cell autonomy and the transmission of polarity information by the *frizzled* gene of *Drosophila*. *Nature* **329:** 549–551.

Vinson, C.R., S. Conover, and P.N. Adler. 1989. A *Drosophila* tissue polarity locus encodes a protein containing seven potential transmembrane domains. *Nature* **338:** 263–264.

Wolff, T. and G.M. Rubin. 1998. *strabismus*, a novel gene that regulates tissue polarity and cell fate decisions in *Drosophila*. *Development* **125:** 1149–1159.

Wong, L.L. and P.N. Adler. 1993. Tissue polarity genes of *Drosophila* regulate the subcellular location for prehair initiation in pupal wing cells. *J. Cell Biol.* **123:** 209–221.

Xu, T. and G.M. Rubin. 1994. Analysis of genetic mosaics in developing and adult *Drosophila* tissues. *Development* **117:** 1223–1237.

Zheng, L., J Zhang, and R.W. Carthew. 1995. *frizzled* regulates mirror-symmetric pattern formation in the *Drosophila* eye. *Development* **121:** 3045–3055.

Pergamon

Progress in Neurobiology Vol. 55, pp. 611 to 640, 1998

Printed in Great Britain
0301-0082/98/$19.00

PII: S0301-0082(98)00026-4

MOLECULAR MECHANISMS THAT UNDERLIE STRUCTURAL AND FUNCTIONAL CHANGES AT THE POSTSYNAPTIC MEMBRANE DURING SYNAPTIC PLASTICITY

HOWARD V. WHEAL*‖, YING CHEN*, JOHN MITCHELL*, MELITTA SCHACHNER†, WINFRIED MAERZ‡, HEINRICH WIELAND‡, DENISE VAN ROSSUM§ and JOACHIM KIRSCH§

**Neuroscience Research Group, School of Biological Sciences, University of Southampton, Bassett Crescent East, Southampton, SO16 6PX, U.K., †Zentrum für Molekulare Neurobiologie, Universität Hamburg, Martinistraße 52, 20246 Hamburg, Germany, ‡Division of Clinical Chemistry, Department of Medicine, Albert Ludwigs-University, Hugstetter Straße 55, 70106 Freiburg, Germany and §Department of Neurochemistry, Max-Planck-Institute for Brain Research, Deutschordenstraße 46, 60528 Frankfurt/Main, Germany*

Abstract—The synaptic plasticity that is addressed in this review follows neurodegeneration in the brain and thus has both structural as well as functional components. The model of neurodegeneration that has been selected is the kainic acid lesioned hippocampus. Degeneration of the CA3 pyramidal cells results in a loss of the Schaffer collateral afferents innervating the CA1 pyramidal cells. This is followed by a period of structural plasticity where new synapses are formed. These are associated with changes in the numbers and shapes of spines as well as changes in the morphometry of the dendrites. It is suggested that this synaptogenesis is responsible for an increase in the ratio of NMDA to AMPA receptors mediating excitatory synaptic transmission at these synapses. Changes in the temporal and spatial properties of these synapses resulted in an altered balance between LTP and LTD. These properties together with a reduction in the inhibitory drive increased the excitability of the surviving CA1 pyramidal cells which in turn triggered epileptiform bursting activity. In this review we discuss the insights that may be gained from studies of the underlying molecular machinery.

Developments in one of the collections of the cogs in this machinery has been summarized through recent studies characterizing the roles of neural recognition molecules in synaptic plasticity in the adult nervous systems of vertebrates and invertebrates. Such investigations of neural cell adhesion molecules, cadherins and amyloid precursor protein have shown the involvement of these molecules on the morphogenetic level of synaptic changes, on the one hand, and signal transduction effects, on the other. Further complex cogs are found in the forms of the low-density lipoprotein receptor (LDL-R) family of genes and their ligands play pivotal roles in the brain development and in regulating the growth and remodelling of neurones. Evidence is discussed for their role in the maintenance of cognitive function as well as Alzheimer's. The molecular mechanisms responsible for the clustering and maintenance of transmitter receptors at postsynaptic sites are the final cogs in the machinery that we have reviewed.

Postsynaptic densities (PSD) from excitatory synapses have yielded many cytoskeletal proteins including actin, spectrin, tubulin, microtubule-associated proteins and calcium/calmodulin-dependent protein kinase II. Isolated PSDs have also been shown to be enriched in AMPA, kainate and NMDA receptors. However, recently, a new family of proteins, the MAGUKs (for membrane-associated guanylate kinase) has emerged. The role of these proteins in clustering different NMDA receptor subunits is discussed. The MAGUK proteins are also thought to play a role in synaptic plasticity mediated by nitric oxide (NO). Both NMDA and non-NMDA receptors are highly clustered at excitatory postsynaptic sites in cortical and hippocampal neurones but have revealed differences in their choice of molecular components. Both $GABA_A$ and glycine (Gly) receptors mediate synaptic inhibition in the brain and spinal cord. Whilst little is known about how $GABA_A$ receptors are localized in the postsynaptic membrane, considerable progress has been made towards the elucidation of the molecular mechanisms underlying the formation of Gly receptors. It has been shown that the peripheral membrane protein gephyrin plays a pivotal role in the formation of Gly receptor clusters most likely by anchoring the receptor to the subsynaptic cytoskeleton. Evidence for the distribution as well as function of gephyrin and Gly receptors is discussed. Postsynaptic membrane specializations are complex molecular machinery subserving a multitude of functions in the proper communication between neurones. Despite the fact that only a few key players have been identified it will be a fascinating to watch the story as to how they contribute to structural and functional plasticity unfold.

‖Corresponding author. Tel.: +44 1703 594 319; Fax.: +44 1703 594 319; e-mail: wheal@soton.ac.uk.

CONTENTS

ABBREVIATIONS

AD	Alzheimer's disease
AMPA	α-Amino-3-hydroxy-5-methyl-4-isoxazoleproprionate
AMPA-EPSCs	α-Amino-3-hydroxy-5-methyl-4-isoxazoleproprionate mediated excitatory postsynaptic currents
ApCAM	*Alysia californica* cell adhesion molecule
APP	Amyloid precursor protein
EGF	Epidermal growth factor
EPSC	Excitatory postsynaptic current
EPSP	Excitatory postsynaptic potential
GABA	γ-Amino-butyric acid
GKAP	Guanine kinase-associated protein
Gly	Glycine
GlyR	Glycine receptor
HDL	High-density lipoprotein
KA	Kainic acid
LDL-R	Low-density lipoprotein receptor
LTD	Long term depression
LTP	Long term potentiation
MAGUK	Membrane-associated guanylate kinase
MAP	Mitogenic-activated protein
NCAM	Neural cell adhesion molecule
NMDA	*N*-Methyl-D-aspartate
NMDAR	*N*-Methyl-D-aspartate receptor
NMDA-EPSCs	*N*-Methyl-D-aspartate mediated post synaptic currents
NO	Nitric oxide
NOS	Nitric oxide synthase
PSD	Post synaptic density
VLDL-R	Very low-density lipoprotein receptor

1. INTRODUCTION

Focal degeneration of neurones in the brain has been found to trigger a cascade of structural and functional changes in the synapses as well as in the postsynaptic cell. The model that we will describe is the kainic acid lesioned hippocampus (Ben-Ari *et al.*, 1980; Nadler *et al.*, 1980b; Lancaster and Wheal, 1982; Ben-Ari, 1985; Phelps *et al.*, 1991; Mitchell *et al.*, 1993). Following the degeneration of the CA3 neurones and Schaffer collaterals there is a period of reactive growth when there are changes in the numbers and properties of the spines, postsynaptic receptors and dendritic architecture as well as changes in the functional properties of the synapses. Thus the term synaptic plasticity is used to embrace structural and/or functional changes at synapses. In this review we will discuss the insights into the structural and functional changes at synapses that may be gained from studies on the underlying molecular machinery, including the role of adhesion molecules and the mechanisms controlling the localization and accumulation of neurotransmitter receptors.

The plethora of recognition molecule functions during ontogenetic formation of the nervous system has received considerable attention, being spurred by the generation and thoughtful interpretation of transgenic null mutants in worms, flies and mice. However, relatively little attention has been paid to the function of recognition molecules in the adult nervous system, which is also capable to form new contacts between cells and to rearrange existing ones that determine regeneration after trauma and synaptic plasticity. Part of the aim of this review is to

summarize recent developments in studies characterizing the roles of neural recognition molecules in synaptic plasticity in the adult nervous system of vertebrates and invertebrates. Such investigations have shown an involvement of these molecules on the morphogenetic level of synaptic changes, on the one hand, and signal transducing effects, on the other. These studies have aimed at a deeper understanding of the similarities and differences in recognition molecule function during ontogenetic development and in the adult, and suggest highly conserved functions of recognition molecules in vertebrates and invertebrates. The view emerges that plastic changes in the functions of synapses recapitulate, at least to some extent, the molecular mechanisms underlying the formation of neuronal networks during development.

The presence of many members of the low-density lipoprotein receptor (LDL-R) family along with their ligands in the brain suggests that they may have important active roles in maintaining lipid transport and homeostasis. Recent evidence suggests that members of the LDL-R family of genes and their ligands play by themselves pivotal roles in the development of the brain and in regulating the growth and remodelling of neurones. Evidence is also reviewed for the role of LDL-R in Alzheimer's. High levels of this protein and apolipoprotein (apo) E-R2 have been found in the hippocampus and disruption of the apo E gene leads to synaptic loss and cognitive impairment.

The clustering of the transmitter receptors at postsynaptic sites is another fundamental mechanism that may contribute to changes in synaptic strength. Thus, understanding the mechanisms responsible for the localization and accumulation of receptors in nerve cells is anticipated to provide insights into the molecular basis of synaptic plasticity. The mechanisms which ensure the correct formation and maintenance of such specialized membrane domains upon differentiation and their contribution to plastic changes of synaptic efficacy are just about to emerge. Present evidence suggests that distinct polypeptides co-operating in these processes are employed by excitatory and inhibitory synapses, respectively.

Understanding these molecular mechanisms may in turn shed light on the molecular mechanisms that underlie functional and structural changes that occur during synaptic plasticity and reactive synaptogenesis induced by focal lesions of the hippocampus. Knowledge of the mechanisms underlying temporal lobe epilepsy may also provide novel approaches to the treatment of this debilitating and universal condition.

2. STRUCTURAL AND FUNCTIONAL CHANGES AT SYNAPSES IN THE KAINIC ACID LESIONED HIPPOCAMPUS

2.1. Reactive Synaptogenesis Following Neurodegeneration in the Hippocampus

The kainic acid lesioned hippocampus has proved to be a fascinating and fruitful experimental model in which to investigate the structural and functional changes in synaptic function. When the kainic acid

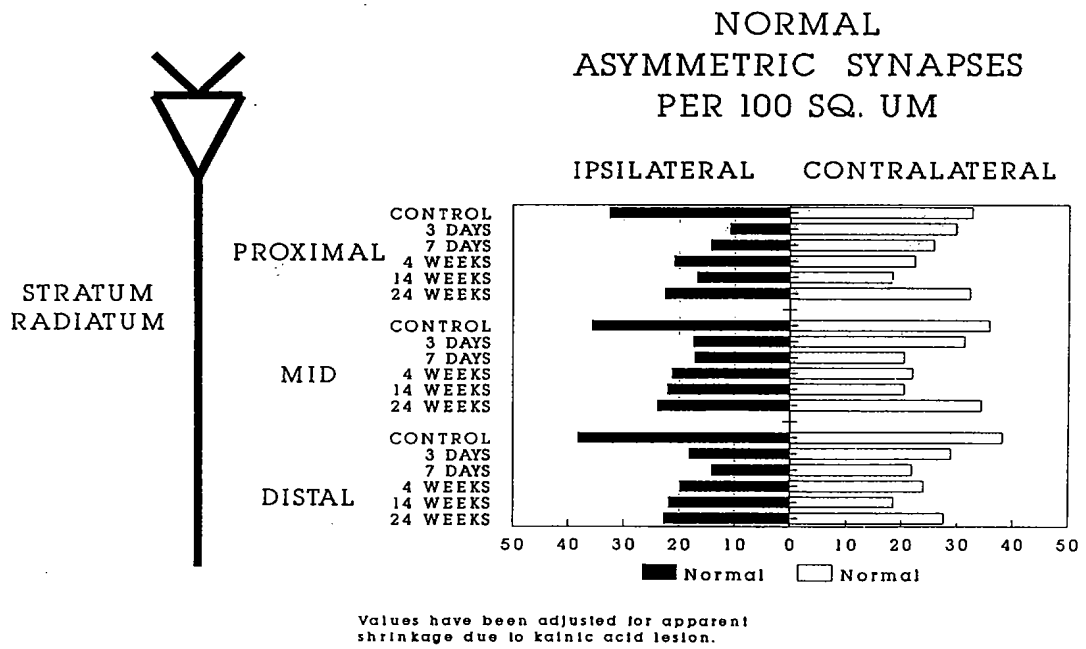

Fig. 1. Horizontal bar graphs to show the total normal asymmetric synapses per 100 μm^2 of tissue at proximal, mid and distal stratum radiatum of CA1, sampled at different intervals post lesion. Note the rapid reduction of normal excitatory synapses ipsilateral to the lesion over the first 3 days followed by some recovery over the next four weeks. Values have been adjusted for apparent shrinkage due to the loss of cells in the CA3 region of the ipsilateral hippocampus [from Phelps (1991)].

was applied unilaterally and intracerebroventricularly (i.c.v.) neurodegeneration and gliosis occurred in the CA3/CA4 regions of the hippocampus (Nadler *et al.*, 1980b; Lancaster and Wheal, 1982; Phelps *et al.*, 1991; Mitchell *et al.*, 1993). Similar patterns of loss were observed in tissue from patients with intractable temporal lobe epilepsy (Ben-Ari, 1985; Babb and Brown, 1987).

Following destruction of neurones in the hippocampus there is a surprising degree of reactive synaptic plasticity in which the surviving ipsilateral and contralateral afferents sprout to reinnervate deafferentated dendritic sites (Steward, 1986). Ultrastructural studies of the stratum radiatum in the surviving CA1 region in the kainic acid lesioned hippocampus showed a rapid fall in the number of Schaffer collateral boutons as the CA3 pyramidal cells degenerate. This was followed by recovery to 72% of control within 6–8 weeks (Nadler *et al.*, 1980a,b). In a more recent study, the peak of the loss ipsilaterally was at 3 days, followed by a 74% recovery at 4 weeks, reaching 80% after 24 weeks (Phelps *et al.*, 1991). When counts were compared from three arbitrarily defined regions of the stratum radiatum, whilst all the regions showed similar reductions, it was the proximal region, close to the pyramidal cell layer that exhibited the largest recovery [see Figure 3 in Phelps (1991)]. These measurements were made by counting the number of asymmetric synapses per 100 μm^2 and the actual values found in the stratum radiatum of CA1 in control and lesioned tissue compared very favourably with those previously reported following bilateral lesions (Nadler *et al.*, 1980a).

Preliminary quantitative results shown in Table 1 of Phelps *et al.* (1991) suggest that between 3 days and 4 weeks, reactive synaptogenesis occurs more quickly than the degenerating pre-terminal elements are cleared. This suggests that, in addition to the replacement of degenerating postsynaptic densities (PSD), new sites of contact are also formed. However, there appeared to be a permanent reduction in the number of asymmetric sites in the stratum radiatum (Fig. 1).

2.2. Changes in the Morphology of Spines

The morphology of spines in the CA1 region of the hippocampus has been well described by Harris and colleagues (Harris and Stevens, 1989; Harris and Kater, 1994). Various changes in the morphology of spines following reactive synaptogenesis have been described including increases in the numbers of, multi-synaptic boutons (Raisman, 1969), double-headed spines (Chen and Hillman, 1982), complex synapses (Goldowitz *et al.*, 1979). Phelps (1991) also found qualitative increases in the proportion of multi-synaptic boutons in the mid and distal layers of the stratum radiatum of CA1 ipsilateral to the lesion. The lack of any change in the proximal region was probably due to the high ratio of multi-synaptic boutons that was normally found in this layer. This "normal" sharing may explain why the fall in healthy synaptic contacts was so dramatic at 3 days, each degenerating multi-synaptic bouton contributing two degenerating synapses. In contrast, double-headed spines were rarely encountered (Phelps, 1991).

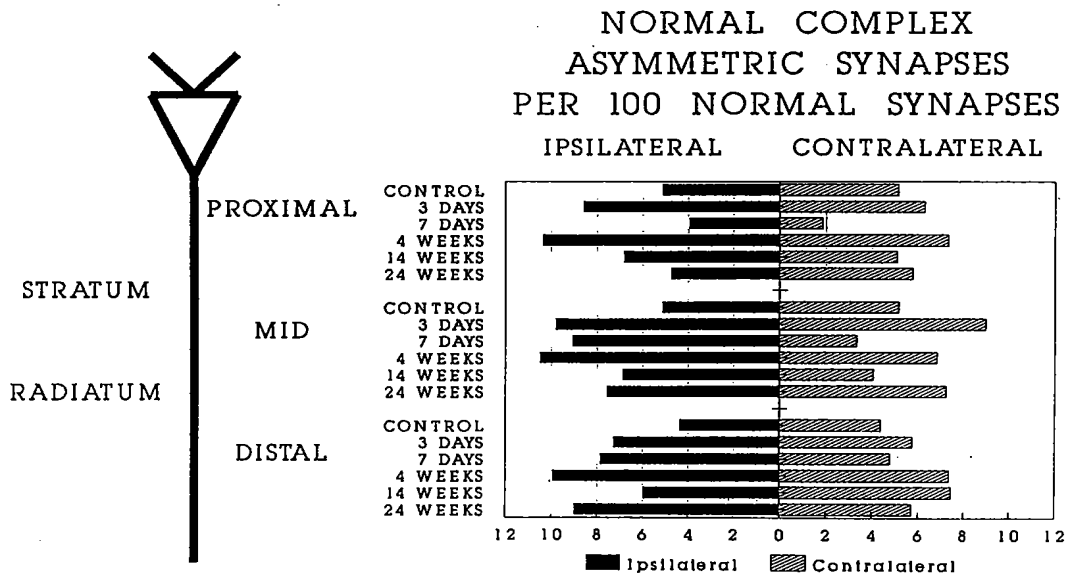

Fig. 2. Horizontal bar graphs to show the number of complex or perforated synapses per 100 μm^2 of tissue at proximal, mid and distal stratum radiatum of CA1, sampled at different intervals post lesion. Note the increase in all levels of the stratum radiatum by four weeks in the CA1 region ipsilateral to the lesion. Values have been adjusted for apparent shrinkage due to the loss of cells in the CA3 region of the ipsilateral hippocampus [from Phelps (1991)].

Complex synapses were identified in micrographs from the discontinuity of their PSD, often with a W-shaped synaptic contact. Figure 2 shows the increases in the number of complex synapses were found in all areas of the stratum radiatum of the surviving CA1 region at 4 weeks post lesion (Phelps, 1991). Increases were also found in the number of asymmetric synapses onto dendritic shafts proximal to the cell body layer at 7 days post lesion, which were coincident with increases in spine neck width (data not shown).

The numbers, the location and the properties of the asymmetric synapses are an important determinant of the excitatory drive onto the surviving CA1 pyramidal cells in this model. However, it is difficult to know whether any changes that have been observed are due to activity dependent plasticity or merely a product of ongoing degeneration (Phelps *et al.*, 1991; Phelps, 1991; Harris and Kater, 1994). One of the options is that, following neurodegeneration of the CA3 pyramidal cells and their Schaffer collateral's, there is straightforward *de novo* formation of additional synapses on the dendritic shaft. In normal tissue, the majority of synapses on dendritic shafts appear to occur on the aspinous dendrites of non-pyramidal cells. However, studies of LTP in the CA1 area (Lee *et al.*, 1980; Chang and Greenough, 1984) have detected an increase in asymmetric shaft synapses. Chang and Greenough also proposed that where these additional synapses occurred on a pyramidal neurone, they subsequently developed into sessile and then into mature spines with a head and neck. The abnormally thick necks measured at 1 week ipsilaterally lend further support to the notion of spines emerging from the dendrite. The same sequence has been noted in developmental studies of the dentate gyrus (Cotman *et al.*, 1973) in which spines are seen to increase in number and size after the full complement of synapses have been achieved. It is reasonable to propose that the degeneration of Schaffer collateral's in the kainic acid lesion serves to reawaken such developmental mechanisms, which in any case may play a part in the natural turnover of mature tissue (Sotelo and Palay, 1971).

Whilst one shouldn't forget that some of the increase in the number of shaft synapses may be on non-pyramidal cells, such *de novo* synthesis would presumably favour the proximal apical dendritic region which showed the most striking loss of asymmetric synapses following degeneration of the Schaffer collateral's (Phelps *et al.*, 1991). Interestingly, as illustrated in Fig. 3, the largest increase in the numbers of dendritic shaft synapses were found in this area (Phelps, 1991). It is also important to note that the increase was only temporary, providing further support that these shaft synapses are precursors of new spine contacts.

2.3. Reorganization of the Mossy Fibres

Several groups have been interested in the synaptic reorganization of mossy fibres (Babb *et al.*, 1991; Houser *et al.*, 1990; Represa *et al.*, 1989; Sutula *et al.*, 1989) and presumed inhibitory interneurones (DeLanerolle *et al.*, 1989) in tissue resected from patients with intractable epilepsy. Following the unilateral kainic acid lesion, Sundstrom *et al.* (1993) have observed bilateral reorganization of mossy fibres. One month post lesion they observed a prominent band of zinc-containing Timm's-stained terminals present in the inner molecular layer of the ipsilateral dentate gyrus. At 3 months, mossy fibre reorganization is also seen in the contralateral inner molecular layer of the dentate gyrus and in the

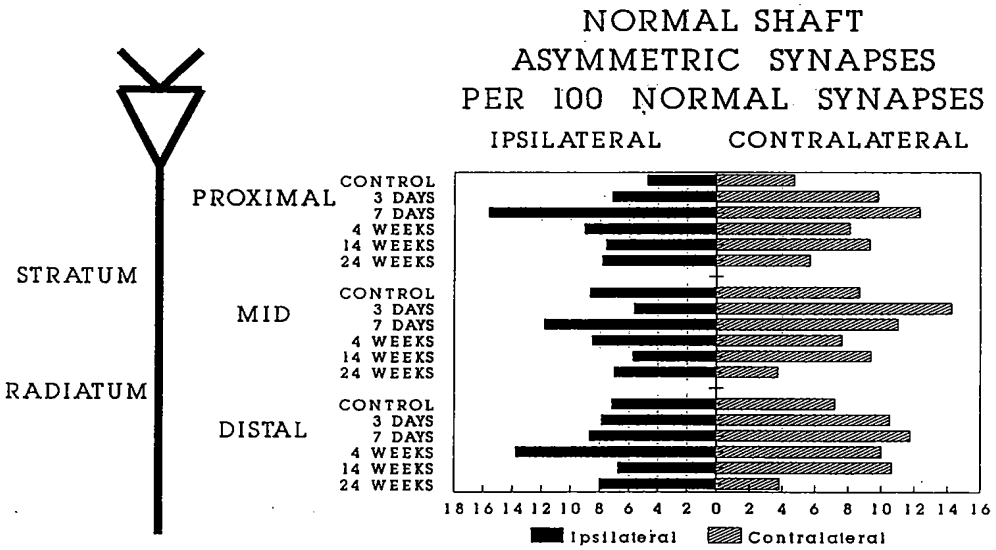

Fig. 3. Increases were also found in the number of asymmetric synapses onto dendritic shafts proximal to the cell body layer at 7 days post lesion, which were coincident with increases in spine neck width (data not shown). Values have been adjusted for apparent shrinkage due to the loss of cells in the CA3 region of the ipsilateral hippocampus [from Phelps (1991)].

infrapyramidal band in the contralateral CA3 (Sundstrom *et al.*, 1993). The time course of the appearance of supragranular labelling after unilateral i.c.v kainic acid, was slower that reported following intravenous, intrahippocampal kainic acid or kindling (Davenport *et al.*, 1990; Nadler *et al.*, 1983; Tauck and Nadler, 1985; Cavazos *et al.*, 1991; Represa *et al.*, 1989). The reason for this delay was unclear. However, the appearance of a suprapyramidal band in the contralateral hippocampus reported by Sundstrom *et al.* (1993), provides further evidence to suggest that the sprouting is linked to the spread of epileptiform activity (Ben-Ari and Represa, 1990) rather than to the CA3/CA4 lesion itself since contralateral sprouting occurred in the absence of any contralateral CA3/CA4 damage. Sutula *et al.* (1988) have also reported sprouting of mossy fibres in the dentate molecular layer in the absence of overt morphological damage, in the kindling model of epilepsy. Furthermore, the bilateral reorganization observed after kindling the amygdala, and the progressive relationship between the extent of sprouting and the stage of kindling indicates that epileptiform activity might be sufficient to induce sprouting (Cavazos *et al.*, 1991; Sutula *et al.*, 1988).

2.4. Increases in Dendritic Branches

A considerable amount of data has been presented in this review on the changes in the numbers and properties of pre-synaptic terminals and post-synaptic spines both before and after synaptogenesis. It would be interesting to know whether these changes are reflected in the three dimensional organization and structure of the dendrites of the pyramidal cells. The combination of intracellular electrophysiological recording and dye injection together with anatomical reconstruction of the labelled cells considerably facilitates this type of analysis (Pyapali and Turner, 1994; Stockley *et al.*, 1993; Turner *et al.*, 1991). Pyapali and Turner (1994) performed just this sort of analysis on the CA1 pyramidal cells following a unilateral kainic acid lesion. The primary differences in the morphometry were an increase in the number of branches in the apical dendrite, from 145 to 231, resulting in a significant increase in the total number of branches and terminals in these cells. The regions of growth reported by Pyapali and Turner (1994) started in the proximal third and peaked in the mid third of the apical dendrites, overlapping the peak areas of neurodegeneration recorded by Phelps (1991). Whilst these electrotonically distant regions may not facilitate the postsynaptic response, the shear numbers of new synapses, particularly if combined with a different array of ligand-gated channels, may have a contributing effect to both the reinnervation as well as the epileptiform activity (Fig. 4).

2.5. Functional Consequences of Synaptogenesis

A particularly challenging question that has been raised by those laboratories working on synaptogenesis is what is the origin of these new afferents? The commissural fibres, Schaffer collateral's and ipsilateral association fibres have a common source, the

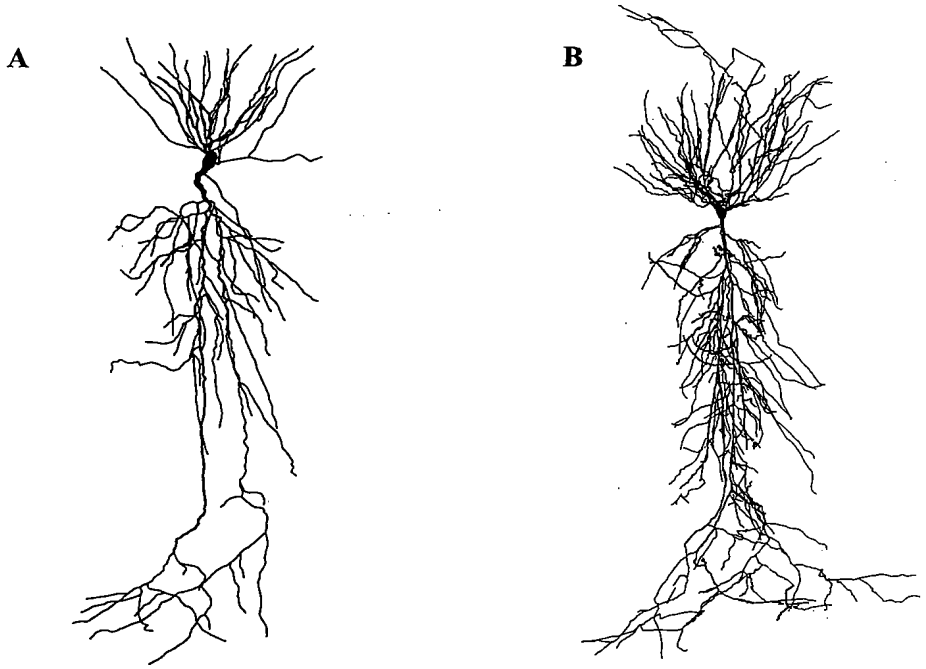

Fig. 4. Reconstructions of neurobiotin-injected CA1 pyramidal cells (A) from a control animal and (B) from a unilateral kainic acid lesioned host, 5 days post lesion. There was a significant increase in the number of branches in the apical dendrite in the mid stratum radiatum [from Pyapali and Turner (1994)]. Scale bars = 200 μm.

pyraidal cells of CA3. Within CA1, the terminals of these fibres are spread throughout stratum oriens and stratum radiatum from the septal to the temporal pole of the hippocampus, the commissural fibres follow a route parallel to the Schaffer collateral's (Gottlieb and Cowan, 1973; Ishizuka *et al.*, 1990; Bernard and Wheal, 1994; Bernard *et al.*, 1997). The homologous nature of these fibres, and the presumed proximity of their terminals undoubtedly makes commissural fibres, and spared ipsilateral association fibres favourites to replace the afflicted Schaffer collateral's ipsilaterally, whilst the contralateral CA1 pyramidal cells have their Schaffer collateral's and association fibres to compensate for commissural loss (Goldowitz *et al.*, 1979; Nadler *et al.*, 1980a). The CA1 pyramidal cells themselves also have collateral branches that could replace asymmetric contacts on neighbouring CA1 pyramids. These collateral's most notably innervate inhibitory non-pyramidal cells to generate inhibitory feedback. However, some CA1–CA1 connections have been detected (Christian and Dudek, 1988; Radpour and Thomson, 1990). Any abnormal rise in their usually low probability connections would seriously increase the excitability of the CA1 pyramidal cells, and possibly initiate reverberating excitatory activity. The terminals of these afferents have recently been traced to the basal dendrites of the CA1 pyramidal cell (Deuchars and Thomson, 1996) and following a bi-lateral kainic acid lesion sprouting has been reported in the stratum oriens of CA1 (Perez *et al.*, 1996). Recent unpublished data (C. Bernard, personal communication) from the unilaterally lesioned hippocampus has shown sprouting extends not only into the stratum oriens, but also into the pyramidal cell layer and the stratum radiatum of CA1. It is important to note that these data were obtained from animals that had had spontaneous seizures for 2 weeks, that is, about a month post i.c.v kainic acid injection. Suggesting that spontaneous seizures may be the product of the increased recurrent excitatory drive from the CA1–CA1 sprouting.

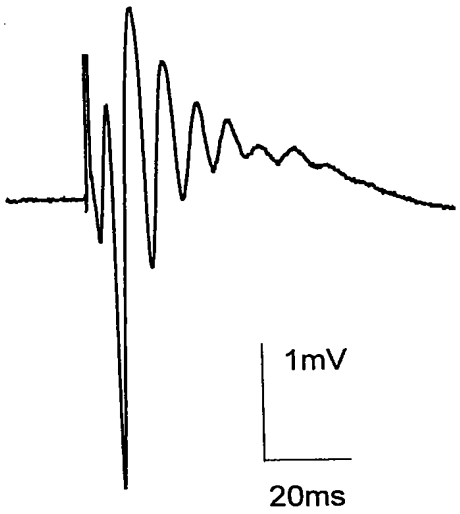

Fig. 5. Stimulus evoked synchronous epileptiform burst recorded from the CA1 pyramidal cell layer in the kainic acid lesioned hippocampal slice. The same stimulus applied to control slices resulted in only a single population spike.

Irrespective of the origin of the branching afferents, it was clear that there are long-term changes in the excitability of the surviving CA1 pyramidal neurones. Three different mechanisms were found to contribute to the expression of epileptiform bursting in this preparation (see Fig. 5). These included changes in the intrinsic excitability of the cells (Ashwood *et al.*, 1986), reduced inhibitory innervation from local interneurones radiatum (Ashwood *et al.*, 1986; Cornish and Wheal, 1989; Best *et al.*, 1993, 1994; Bernard and Wheal, 1995b) and an increased role for NMDARs in the excitatory synaptic drive (Ashwood and Wheal, 1987; Simpson *et al.*, 1991; Turner and Wheal, 1991). In this review we would like to focus on this latter mechanism and explore the possibility that the properties of the NMDARs may be due to the activity dependent expression of novel receptor protein.

We have previously reported the presence both AMPA receptor and NMDA receptor mediated graded epileptiform bursting activity in the kainic acid lesioned rat hippocampus. The prominent NMDA receptor mediated component contributing to the EPSPs and the epileptiform bursts that was found in the experiments was recorded in 1 mM $[Mg^{2+}]_o$ (Ashwood *et al.*, 1986; Ashwood and Wheal, 1987; Simpson *et al.*, 1991; Turner and Wheal, 1991; Williamson and Wheal, 1992). An NMDA component underlying epileptiform bursting was also found in the kindling model (Mody and Heinemann, 1987), or that induced by low extracellular Mg^{2+} concentrations (Thomson and West, 1986; Mody *et al.*, 1987; Traub *et al.*, 1994). NMDA receptors were also shown to be involved in bursting activity in human tissue (Avoli and Olivier, 1987).

2.6. Is a Novel Type of NMDA Receptor Expressed?

A number of surprising properties of these receptors have emerged. In response to suprathreshold stimuli, they contribute 24% of the excitatory synaptic drive (Bernard and Wheal, 1995b) when recorded as EPSPs. Under whole-cell patch configuration, EPSCs at resting membrane potential of −60 mV also exhibited larger than normal NMDA component [see Fig. 6(A)]. The AMPA–EPSCs was linear in relation to holding potentials, while the larger NMDA–EPSCs still showed the characteristic voltage dependence with a negative slope at negative holding potentials in 1 mM Mg^{2+}. However, the voltage dependence of the peak amplitude of NMDA–EPSCs is reduced in CA1 cells from lesioned rats compared with control experiments. As can be seen in Fig. 6(B), the negative slope of the *I–V* plot became sharper and shifted to the left. The relative conductance was calculated and the half-activation voltage for lesioned reduced to −45 mV from −20 mV for control. The voltage dependence was also found sensitive to Mg^{2+} concentrations in the ACSF. When increasing the $[Mg^{2+}]_o$ to 2.6 mM, the *I–V* plot was brought back in line with the control one. These suggested that in CA1 cells from lesioned rats, the NMDAR channel has a decreased affinity for Mg^{2+} and hence a

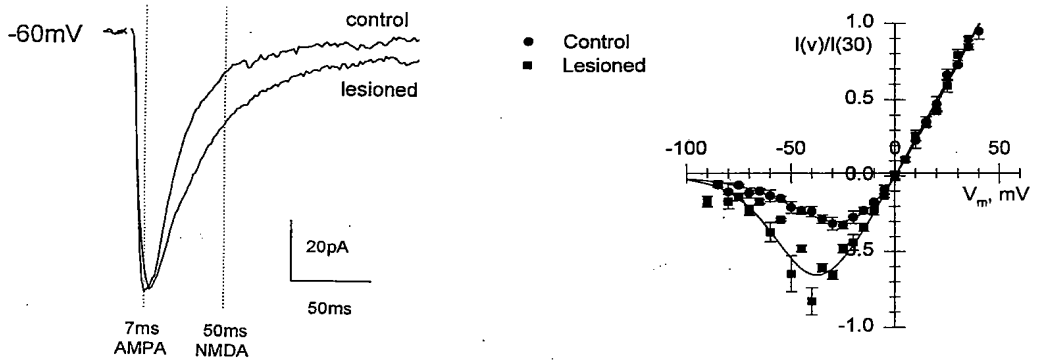

Fig. 6. (A) Measurements and the separation of AMPA and NMDA components of EPSCs from CA1 pyramidal cells in control and lesioned hippocampal slices. In lesioned slices there was clearly a larger NMDA component even at a holding potential of −60 mV. (B) An *I–V* curve illustrating the reduced voltage-dependence of the peak amplitudes of the NMDA EPSCs in 1 mM Mg^{2+} that was found in cells from lesioned slices. The values are normalized to that at +30 mV [from Chen *et al.* (1998)].

reduced voltage-dependent Mg^{2+} block (Chen *et al.*, 1998). These results also demonstrated a long-term (1–4 weeks) change in the functional state of the NMDAR channels. Similar functional change of the NMDAR channels was also found in the kindling model of epilepsy (Kohr *et al.*, 1993).

In light of the discovery of molecular and functional diversity of NMDA subunits (Monyer *et al.*, 1992), one possible explanation for the observed long-term functional change in NMDAR channels following kainic acid lesion is the formation of a new subunit composition. An increasing body of evidence indicates the activity dependent regulation of NMDA receptor subunit expression in brain tissue cultures (Audinat *et al.*, 1994; Resink *et al.*, 1995). Different subunit compositions generate different functional states of the NMDA channels, including changes in single channel conductance (Stern *et al.*, 1992; Farrant *et al.*, 1994), different Mg^{2+} sensitivity (Monyer *et al.*, 1992), diverse regulatory mechanisms (Kohr *et al.*, 1993) and a wide range of pharmacological profiles (Laurie and Seeburg, 1994).

On adult hippocampal CA1 cells, NR1–NR2A and NR1–NR2B are the dominant NMDA receptor subtypes, which are sensitive to Mg^{2+} ions. NR1–NR2C subtype is only expressed transiently in postnatal days 7–14 (Pollard *et al.*, 1993), and it is less sensitive to Mg^{2+} ions. Our electrophysiological results indicate the possible reversion switch of NMDAR channels to their neonatal form NR1–NR2C postlesion. The shift to the left would enable the less efficient synapses on the dendritic shaft [see Harris and Kater (1994)] to contribute to the excitatory drive.

2.7. Resultant Changes in Synaptic Plasticity and Cell Excitability

In a model such as the kainic acid lesion hippocampus where there is a failure of $GABA_A$ mediated synaptic inhibition (Ashwood *et al.*, 1986; Cornish and Wheal, 1989; Simpson *et al.*, 1991; Williamson and Wheal, 1992; Best *et al.*, 1993, 1994; Bernard and Wheal, 1995b) it is possible to focus on the relationship between the excitatory synaptic drive and cellular excitability. Over the past 10 years considerable attention has been given to resolving the role of synaptic plasticity in the form of LTP and LTD (Bliss and Collingridge, 1993; Bear and Malenka, 1994) in learning and memory mechanisms. However, few groups have thought about the implications of plasticity at these excitatory synapses on cell excitability.

Tetanic stimulation of the surviving afferents in the lesioned hippocampus produced overall LTP (Wheal *et al.*, 1983; Bliss *et al.*, 1983). However, this synaptic potentiation was made up of two components and whilst the AMPA receptor component showed LTP (Bernard and Wheal, 1995a), the NMDA mediated synaptic component produced LTD (Bernard and Wheal, 1995b). At the level of the synapse these two NMDA dependent processes were not only inducible but also seemed to be reversible and thus offered no clear explanation as to why learning and memory are impaired in some patients with epilepsy (Bernard and Wheal, 1996).

In parallel with the changes in synaptic plasticity there was a long-term increase in stimulus induced amplitude of the AMPA receptor mediated bursting activity and a long-term decrease of NMDA receptor mediated bursting activity (Bernard and Wheal, 1995b,c, 1996). NMDAR antagonists did not prevent these excitability changes. Of particular interest was the observation in the control hippocampus that use of low frequency stimulation resulted in LTD (Bear and Malenka, 1994) but with an increase in the excitability of the cells that was NMDAR independent (Bernard and Wheal, 1995d, 1996). We suggested that the synaptic-cell excitability coupling was caused by a modification of the firing threshold of the CA1 neurones. Furthermore, that the firing mechanisms controlling NMDA and AMPA receptor-mediated network bursting activity appeared to be different with epilepsy (Bernard and Wheal, 1996).

3. NEURAL ADHESION MOLECULES AND SYNAPTIC PLASTICITY

Recent studies on cell recognition molecules have revealed similarities between their functions during ontogenetic development and in neural plasticity in the adult. Observations both at the cellular level *in vitro* and the behavioural level *in vivo*, suggest that altered recognition molecule expression can lead to changes in synaptic efficacy and alterations in synaptic function in turn evoke changes in adhesion molecule expression. Thus, it appears that developmental cell recognition mechanisms can be, at least to some extent, recapitulated in the adult.

As for cells in other tissues, cells in the nervous system depend on temporally and spatially precise tuning of cellular interactions. Starting with neural induction, proliferation and migration of neural cells, these continue with determination of developmental fate and growth cone guidance during early embryogenesis, and ultimately ending with cell death incumbent with age or neurodegenerative disorders. Recognition molecules that interact with each other on neighbouring cells or with the extracellular matrix have been implicated in cellular interactions, traditionally thought of as developmentally regulated during critical stages of morphogenesis [for recent reviews, see Goodman (1996), Walsh and Dohert (1996) and Rutishauser (1996)]. Many recognition molecules that control such interactions have been identified and the number of such molecules still increases steadily. Functionally, these molecules make cells interact by different mechanisms, for example, by contact-mediated attraction and repulsion, or by chemo-attraction and chemo-repulsion, which accomplish signalling events over short and long distances, respectively. Several families of recognition molecules have been identified that are thought to associate with each other in lock-and-key-type interactions. Among these are molecules of the immunoglobulin superfamily, cadherins, integrins, netrins, semaphorins, laminins, collagens, tenascins, proteoglycans and the receptor tyrosine phosphatases and kinases (among them the eph-receptor family and their ligands, now known as ephrins). These molecules appear as transmembrane glycoproteins or extracellular matrix molecules, and many of them can exist in multiple forms, either as alternatively spliced variants or generated by proteolytic or phospholipase cleavage, thereby releasing them from their cell surface integrated forms. Whether these molecules are attractants or repellents depends on the environment that acts upon them and the signal transduction machinery triggered by different receptors in different cell types and at different developmental stages. Furthermore, the spatial distribution of a recognition molecule is a key factor in its attractant or repellent function. A recognition molecule can be inhibitory for neurite outgrowth when presented as an uphill gradient or a steep molecular barrier, but may be conductive to neurite outgrowth in a downhill gradient or as an uniformly distributed substrate. Adding even more complexity to the function of recognition molecules, they have been shown to act with each other in many ways. These include interactions within the membrane of one cell or in the extracellular matrix (*cis*-interactions), or between the cell surfaces of neighbouring cells and the cell surface and its surrounding extracellular matrix (*trans*-interactions). Such interactions can be either competitive, that is that they can block each other depending on the hierarchy of affinities, or they may enhance each other by conformational changes that can be triggered by the simultaneous occupancy of different sub-domains of a recognition molecule by its cognate ligands. Thus, a very complex network of functional associations and dependencies between recognition molecules needs to be accounted for in our understanding of neural cell interactions.

The plethora of recognition molecule functions during ontogenetic formation of the nervous system has received considerable attention, being particularly spurred by the generation and thoughtful interpretation of transgenic null mutants in worms, flies and mice. However, relatively little attention has been paid to the function of recognition molecules in the adult nervous system, which is also capable to form new contacts between cells and to rearrange existing ones that determine regeneration after trauma and synaptic plasticity. The aim of this review is to summarize recent developments in studies characterizing the roles of neural recognition molecules in synaptic plasticity in the adult nervous system of vertebrates and invertebrates. Such investigations have shown an involvement of these molecules on the morphogenetic level of synaptic changes, on the one hand, and signal transducing effects, on the other. These studies have aimed at a deeper understanding of the similarities and differences in recognition molecule function during ontogenetic development and in the adult, and suggest highly conserved functions of recognition molecules in vertebrates and invertebrates. The view emerges that plastic changes in the functions of synapses recapitulate, at least to some extent, the molecular mechanisms underlying the formation of neuronal networks during development.

3.1. Changes in the Expression of the Neural Cell Adhesion Molecule

Indications as to the involvement of neural recognition molecules in synaptic plasticity emerged when the major isoform of neural cell adhesion molecule (NCAM), comprising the longest cytoplasmic domain of the three major NCAM isoforms (NCAM 180) was found in some synapses but not in others (Persohn *et al.*, 1996). NCAM 180 interacts with the membrane-cytoskeleton linker protein spectrin which is highly enriched in PSDs and shows a highly reduced lateral mobility within the surface membrane, when compared to NCAM 140 (Pollerberg *et al.*, 1986). This observation led to the hypothesis that NCAM 180 may be crucial for the stabilization of cell contacts at synaptic sites. This idea was supported by the observation that the percentage of synapses expressing detectable levels of NCAM 180 postsynaptically increased by almost a factor of two 24 hr after long-term potentiation of the perforant path (T. Schuster, M. Krug, H. Hassan, M. Schachner, unpublished data). The cor-

relation with synaptic strengthening was underscored by the observation that shaft synapses or spine synapses in the inner part of the molecular layer, which are not triggered by the perforant path, did not change their expression of NCAM 180. Furthermore, a stimulation protocol that led to a less drastic increase in long-term potentiation was also less effective in raising the percentage of NCAM 180-positive synapses. The increase of NCAM 180 expression in the appropriate synapses and the appropriate part of the molecular layer could be inhibited by a non-competitive antagonist of the NMDA glutamate receptor subtype known to be involved in synaptic strengthening. In animals undergoing low frequency stimulation, the percentage of NCAM 180 positive synapses was decreased when compared to non-treated controls. Intriguingly, one trial training in an active avoidance task, evoked subtle changes in the distribution pattern but not in density of NCAM molecules in synaptic membranes 5–6 hr after training in a brain area involved in this particular learning task (Rusakov *et al.*, 1994). A significantly higher proportion of active zones were found to contain NCAM immunoreactivity after training, with the highest accumulation of NCAM at the edges of synaptic active zone profiles (Skibo *et al.*, in press). The polysialic acid-containing form of NCAM, known for its promotion of neurite outgrowth, redistributes to the edges only in the trained but not in control groups. Furthermore, the polysialylated form of NCAM 180 is increased in a passive avoidance learning paradigm (Doyle *et al.*, 1992). Waves of increased and decreased polysialic acid expression could also be found under multi-trial learning conditions (Murphy *et al.*, 1996). The combined observations indicate that a strengthening of synaptic efficacy leads to an increase in expression and change in distribution of NCAM isoforms, possibly as an early step in synaptic strengthening and/or remodelling.

The search for a causal relationship between adhesion molecule function and synaptic plasticity in vertebrates was initiated in experiments using antibodies and fragments of adhesion molecules as inhibitors, competitors or triggers of cell adhesion molecule function. Fragments of integrins and antibodies to NCAM and to L1, another adhesion molecule of the immunoglobin superfamily, were shown to interfere with long-term potentiation in vitro and with different learning paradigms *in vivo* (Arami *et al.*, 1996; Lüthi *et al.*, 1994; Ronn *et al.*, 1995; Scholey *et al.*, 1993, 1995; Doyle *et al.*, 1992; Staubli *et al.*, 1990; Bahr *et al.*, 1997). In addition, the polysialic acid of NCAM was found to be involved in long-term potentiation *in vitro* and learning *in vivo*: removal of this carbohydrate by the specific enzyme endoneuraminidase N decreased synaptic plasticity (Becker *et al.*, 1996; Müller *et al.*, 1996b). Similarly, NCAM null mutants have been shown to be impaired in learning and memory in a spatial learning test (Cremer *et al.*, 1994). Intriguingly, this impairment in spatial learning was seen in the context of increased anxiety and aggression probably mediated by the serotonin 1A receptor which is preferentially expressed in the limbic system (Stork *et al.*, 1997; Stork *et al.*, submitted—a). Dose–response curves using specific agonists of the serotonin 1A receptor, point to the sensitization of this receptor subtype as a direct or indirect consequence of the ablation of the NCAM molecule in this mutant. Reconstitution of NCAM 180 expression in an NCAM null mutant background obtained by cross-breeding NCAM null mutant mice with transgenic mice overexpressing NCAM 180 driven by the neuron specific neurofilament promoter largely reversed the receptor sensitization and the abnormal behaviour of NCAM null mutant mice to normal (Stork *et al.*, submitted—b). A relationship between NCAM function and the AMPA glutamate receptor subtype has also been seen, in that removal of polysialic acid of NCAM enhances the sensitivity of this receptor for glutamate (Hoffman *et al.*, 1996). Thus, NCAM may modulate neuronal excitability through different signal transduction pathways.

Another interesting mechanism highlighted by more systematic studies of a mutant deficient in Thy-1 (Nosten-Bertrand *et al.*, 1996; Errington *et al.*, 1997), another recognition molecule of the immunoglobulin superfamily, has emerged from investigations on the inhibitory mechanisms underlying long-term potentiation *in vitro* and *in vivo*. These studies point to a subtle deficit in the release mechanisms of the inhibitory, GABAergic interneurons in the hippocampus (I. Soltesz, personal communication), that was accompanied by impaired long-term potentiation *in vitro* and, to some extent, *in vivo*. However, the Thy-1 null mutant mice have so far not shown any impairment in spatial learning, underscoring previous findings that deficits in long-term potentiation do not always correlate with deficits in learning.

The combined observations point to exciting future venues of research in this area: the dissection of the relation between neurotransmitter receptors and adhesion molecules, possibly linked to ion channel function (Sontheimer *et al.*, 1990). Furthermore, these studies aim at resolving some of the problems inherent in antibody perturbation studies and work with null mutant animals: do the antibodies interfere with cell recognition or do they modify intercellular signalling cascades that result in modifications of almost any second messenger system that has been investigated so far [see Wong *et al.* (1996) also for references], including the pivotal second messenger Ca^{2+}. Some of the short-term effects that are seen within minutes after application of antibodies or fragments of adhesion molecules are most likely related to perturbation of intracellular signalling cascades. These could impinge on the ability to induce long-term potentiation by meddling with the pool of second messenger systems mediating synaptic changes. On the other hand, they may interfere with long-term morphogenetic events underlying changes in synaptic strength either by masking or simulating recognition at the cell surface.

3.2. NCAM in Aplysia

The importance of NCAM in synaptic plasticity is emphasized by a strict conservation of its impact in synaptic plasticity in phylogenetic evolution. A close homolog of NCAM in the marine mollusc *Aplysia californica*, called apCAM, was first discovered as a molecule that is down-regulated in expression during

long-term facilitation, a form of synaptic plasticity of sensory and motor neurons in the gill-withdrawal reflex of this animal (Mayford *et al.*, 1992). In addition to a reduction of newly synthesized apCAM, there was also a reduction in the expression of the transmembrane apCAM isoform at the cell surface of sensory, but not motor neurons, likely due to endocytotic internalization. This internalization process required new protein synthesis—a defining feature of long-term memory and growth of new synaptic connections. Antibodies recognizing the extracellular domain of NCAM cause defasciculation of sensory neurons (Keller and Schachner, 1990), a trait proposed to be necessary for the formation of new synaptic connections. Long-term facilitation and decrease of apCAM expression at the cell surface of sensory neurons could also be achieved through application of serotonin that modulates synaptic efficacy through elevation of cyclic AMP and protein kinase A in the sensory neuron (Bailey *et al.*, 1992). During this process, the mitogen-activated protein (MAP) kinase may phosphorylate the cytoplasmatic domain of apCAM (Bailey *et al.*, 1997) and translocate into the nucleus of the sensory neuron (Martin *et al.*, 1997). Training for long-term memory thus leads to reduction of apCAM expression at the cell surface, correlating with increases in synaptic strength.

3.3. The Genetics of NCAM in Drosophila

A major step forward in dissecting the different aspects of synaptic plasticity has come from work in Drosophila, an organism that allows the use of genetic manipulations to control the sites and levels of NCAM expression (Schuster *et al.*, 1996a,b; Davis *et al.*, 1996). The nerve-muscle synapse, in which individual motor cells and their target muscles can be identified, was studied at both structural and physiological levels. As many other types of synapses, this synapse can undergo activity-dependent alterations. Fasciclin II, the molecule most homologous to NCAM in vertebrates and apCAM in Aplysia, is present both pre- and postsynaptically. It is not required for synapse formation during development, but is necessary for the stabilization of the synapse by trans-interacting. Hypomorphs expressing half the normal dose of fasciclin II have an increased number of synaptic boutons when compared to wild type animals, indicating that the concentration of fasciclin II regulates sprouting and the ability of neurons to form new synapses. Interestingly, a mutant in the ergShaker K^+ channel and a mutant in the cyclic AMP specific phosphodiesterase (dunce) showing elevated intracellular cyclic AMP concentrations display increased synaptic sprouting accompanied by a surprising down-regulation of fasciclin II expression by approximately one half. This increase in synaptic sprouting is suppressed in transgenic animals expressing wild type concentrations of fasciclin II, suggesting that the down-regulation of fasciclin II is not only sufficient, but also necessary for activity-dependent synaptic growth. Synaptic efficacy is, however, not increased in animals expressing only half the dose of fasciclin II. This may be related to the fact that wild type levels of the neurotransmitter release machinery is distributed throughout more presynaptic endings in the mutants. In fasciclin II hypomorphic animals the presynaptic release machinery is upregulated by a cyclic AMP response element binding protein (CREB)-mediated mechanism, involving cyclic AMP- and protein kinase A-mediated transcription. These experiments suggest, as previously indicated by the experiments in Aplysia, that fasciclin II down-regulation may not only relieve a restraint on growth of presynaptic membranes, but predisposes the synapse for structural and functional alterations. The experiments also raise the questions about a causal link between fasciclin II expression and functional consequences at the synapse: is fasciclin II exerting its effects via modulation of cell recognition, thus modulating long-term morphology of the presynaptic structural elements, or does fasciclin II influence signal transduction mechanisms which then alter second messenger cascades that will then influence presynaptic morphology and the presynaptic release machinery? The results in Drosophila are in agreement with findings in NCAM null mutant mice which show morphological abnormalities of the mossy fibre pathway in the hippocampus (Cremer *et al.*, 1997) and inspire a search for morphogenetic alterations in limbic system structures involved in aggression and anxiety. Whether the abnormal phenotypes observed in the NCAM and fasciclin II mutations are related to the dysregulated expression of other adhesion molecules will also need investigation. By studying both genetic and antibody-mediated perturbations of adhesion molecules a comprehensive picture of adhesion molecule function relating to morphogenesis and signal transduction will likely emerge.

3.4. Different Mechanisms in Different Species?

An interesting problem pertains to the observation that in vertebrates, an increase in NCAM expression relates to synaptic plasticity, while in invertebrates a reduction of NCAM at the cell surface has been correlated with synaptic strengthening. The evidence that different isoforms of NCAM inhibit or enhance axon growth in vertebrates is therefore an important consideration. For instance, enhanced expression of NCAM containing the VASE exon leads to decreased neurite outgrowth when compared to the NCAM isoform not expressing this exon (Doherty *et al.*, 1992). Furthermore, the presence of the polysialic acid on NCAM leads to increased neurite outgrowth when compared to NCAM isoforms which do not carry this carbohydrate. It is interesting in this respect that polysialic acid is upregulated in synapses expressing increased levels of NCAM 180. Thus, it is conceivable that in vertebrates different ways of regulating morphogenetic alterations and signalling cascades have been acquired during evolution by structural modifications of adhesion molecules, while in invertebrates the functional properties of adhesion molecules are changed by alterations in their quantities at the cell surface. These possibilities need to be investigated by paying attention to the expression of alternatively spliced forms and post-translational modifications of adhesion molecules.

3.5. Ectopic Expression of L1

Does perturbation of adhesion molecule function necessarily lead to a decrease in synaptic plasticity? A physiological perturbation of adhesion molecule function *in vivo* has been achieved by generating a transgenic mouse that expresses L1 ectopically in astrocytes, where it is normally not present *in vivo* either at early or later stages of development. In the Morris water maze, these mice learned the position of an invisible target platform more quickly than their normal wild type litter mates, searched more selectively in the target quadrant and relearned more quickly the position of the platform after relocation (Wolfer *et al.*, in press). The improved performance of these L1 overexpressing mice was even more pronounced in aged mice (almost 2 years old) than in young adult mice (*ca* 3 months old). It will be interesting to see by which mechanisms the ectopic expression of L1 by astrocytes enhances the learning capabilities.

3.6. Cadherins and Amyloid Precursor Protein in Synaptic Plasticity

Two other groups of adhesion molecules have led to exciting insights into recognition molecule-mediated signalling during development in the last year. One concerns the cadherins and their possible involvement in synaptic plasticity via intracellular signalling to the nucleus. The other relates to a connection between the amyloid precursor protein (APP) and the presenilins in conjunction with Alzheimer's disease [AD; Yankner (1996)].

Cadherins are likely to be involved in synapse formation (Fannon and Colman, 1996) during development and, since they remain expressed in synaptic membranes in the adult (Beesley *et al.*, 1995; Uchida *et al.*, 1996; Cifuentes-Diaz *et al.*, 1994, 1996), they may also contribute to synaptic modifications. Cadherins are homophilic adhesion molecules that convey signals from the cell surface to the cytoplasm via their association with catenins (Kypta *et al.*, 1996). The extracellular wingless/wnt protein that signals, at least in part, through a cell surface receptor encoded by the frizzle gene competes with the binding of cadherins to catenins [for a review, see Huber *et al.* (1996a,b), Orsulic and Peifer (1996) and Sanson *et al.* (1996)]. Wingless is an important regulator of cell fate in early embryogenesis, as an inductor of neurulation in the dorsalizing centre (Fagotto *et al.*, 1997; Molenaar *et al.*, 1996). Since catenins can migrate to the cell nucleus where they interact with the transcription factor LEF-1 (Behrens *et al.*, 1996; Huber *et al.*, 1996a,b), the intriguing possibility arises that catenins serve in the functional cross-talk between recognition molecules and determinants of cell fate by regulating transcription. It will be interesting to see the consequences of this cross-talk in synaptic plasticity.

Another intriguing crosstalk among recognition molecules, namely APP and notch [for a recent review, see Campos-Ortega (1996)], has become apparent in studies on the function of presenilins with regard to AD (Haass, 1997). Mutations in the two presenilins cause abnormal processing of APP and deposition of the Aβ fragment of APP leading to formation of amyloid plaques and neurodegenerative disorders. The functional and structural interplay between presenilins and APP are yet unknown. In the context of synaptic plasticity, it is noteworthy that APP is highly expressed in axons and at the synapse. As the presenilins have also been found to be expressed in neurons (Lee *et al.*, 1996), they may act in concert with APP at the synapse in the adult stage. Since APP is released under conditions of long-term potentiation (Fazeli *et al.*, 1994) and mice with mutant forms of APP show drastically abnormal behaviour in spatial learning tasks (Müller *et al.*, 1994), it will be interesting to see the impact of presenilins on synaptic plasticity. Presenilins also influence the functions of the cell adhesion molecule notch either directly or indirectly: notch, a neurite outgrowth promoting cell surface glycoprotein with EGF-like repeats—characteristic of many neural recognition molecules—may only reach the cell surface in the presence of normal presenilins. Mutated presenilins may thus not be able to chaperone the notch protein to the cell surface. Alternatively, presenilins may associate with notch at the cell surface to ensure proper signalling to the cell interior. Although presenilins and notch have yet to be localized to synaptic membranes, it remains an intriguing possibility that the two recognition molecules, APP and notch, depend in their normal function and processing on the activity of presenilins. With the availability of mutants and antibodies for the three proteins this interrelationship is amenable to further studies.

3.7. Tenascin-C and Synaptic Plasticity During Development and in the Adult

Finally, the question of how developmental mechanisms in synapse formation and plasticity may be related to functional changes of synaptic strength in the adult may be addressed by investigations on the extracellular matrix glycoprotein tenascin-C [for review, see Faissner and Schachner (1995)]. Tenascin-C regulates neurite outgrowth in rather unconventional ways. When present as a uniform substrate, it enhances neurite growth and curbs dendritic growth. When presented as a molecular barrier adjacent to a neurite outgrowth conducive molecule, it interferes with neurite outgrowth. Tenascin-C is highly expressed in early phases of neural development and becomes down-regulated in the adult. However, it remains detectable in brain areas known to be involved in synaptic plasticity, such as the hypothalamus, the hippocampus and the cerebellum. Expression of tenascin-C, for instance in the somatosensory cortex, is down-regulated concomitantly with the segregation of afferent synaptic inputs from the thalamus (Mitrovic *et al.*, 1996). When segregation of afferent inputs is inhibited by the NMDA glutamate receptor antagonist MK801, the developmental down-regulation of tenascin-C is prevented, suggesting that tenascin may be involved in synapse elimination. Thus, tenascin-C expression coincides with the maintenance of synaptic malleability during development. Whether it is causally linked to keeping synapses in a prestabilized state remains to be seen.

A correlation between tenascin expression and induction of changes in synaptic remodelling in the adult could be shown in an animal model of epilepsy (Nakic *et al.*, 1996a,b; Nakic *et al.*, in press). Within 4 hr after injection of the excitotoxin kainic acid, and the occurrence of seizures, tenascin-C was upregulated in areas of the hippocampus undergoing plastic changes coincident with activation of granule cell neurons and sprouting of axon terminals. This upregulation of tenascin mRNA was followed 24 hr later by an upregulation of tenascin-C protein. Thirty days afterwards tenascin-C was again downregulated in neurons. In another synaptic activation paradigm in the hippocampal dentate gyrus, tenascin-C mRNA levels were increased in the granule cell layer 4 hr after tetanization (Nakic *et al.*, 1996a,b; Nakic *et al.*, in press). This was again followed by a peak of tenascin-C protein expression in the areas of synaptic remodelling. Inhibitors of the NMDA and metabotropic glutamate receptor subtypes prevented these changes in tenascin expression. Thus, tenascin-C expression appears to be correlated with changes in synaptic efficacy and remodelling.

That tenascin-C is indeed necessary for synaptic remodelling has become apparent in a learning paradigm involving acoustic imprinting in newly hatched chicken (Metzger *et al.*, 1995; Metzger *et al.*, submitted). Application of the monoclonal anti-tenascin antibody Tn68 into the brain areas involved in this type of learning completely abolished imprinting. Since tenascin-C is an extracellular matrix molecule, these antibodies must mask a functionally relevant domain on the tenascin molecule, possibly interfering with the binding of this domain to a transmembrane receptor, which will need to be identified. As control, monoclonal antibody 578 reacting with another epitope on the tenascin-C molecule did not interfere with learning. The prediction from these experiments is that application of tenascin-C or fragments thereof to brain areas undergoing synaptic remodelling will enhance synaptic flexibility. Interestingly, mutant mice expressing decreased levels and abnormal forms of tenascin-C develop relatively normally, but show alterations in several neurotransmitter systems and behavioural deficits (Fukamauchi *et al.*, 1996). These observations suggest that alterations in synaptic strength and remodelling may be generated by similar molecular strategies during development and in the adult.

3.8. Questions Remaining

The last year has witnessed a tightening of the link between recognition molecule function and synaptic plasticity not only during development, but particularly in the adult. The involvement of recognition molecules in changing synaptic strength and in remodelling of synapses has become even more tangible. However, we need to know:

- Do different synapses use different recognition molecules and/or different glycans carried by recognition molecules?
- Are some recognition molecules necessary for ontogenetic development not involved in synaptic plasticity?
- Do the various molecules modify synaptic activity pre- or postsynaptically?
- Do recognition molecules promote morphological changes such as size and shape of synaptic contacts, elaboration of spines, dendritic or axonal branching patterns and cell-specific connectivity after functional modification of synaptic strength?
- Contributions of glial cells to interactions with synaptic membranes also need to be studied. Since recognition molecules are known to influence the intracellular signalling cascades of second messenger systems, pressing question is how adhesion molecules will intermingle with signal transduction pathways known to be crucial in regulating synaptic strength. Clearly, this will be an extremely difficult problem to solve, since any alteration in signalling pathways will entail a cascade of changes, the extent and ramifications of which will resist easy dissection.
- Finally, how can morphological changes and alteration in signalling mechanisms be translated into long-term modifications at the synapse, involving the stabilization or destabilization of network interplays?

4. ROLE OF LOW DENSITY LIPOPROTEIN RECEPTOR GENE FAMILY AND THEIR LIGANDS IN STRUCTURAL AND FUNCTIONAL PLASTICITY: REAL PLAYERS OF INNOCENT BYSTANDERS?

The presence of many members of the LDL-R family along with their ligands in the brain suggests that they may have important active roles in maintaining lipid transport and homeostasis. Recent evidence suggests that members of the LDL-R family of genes and their ligands play by themselves pivotal roles in the development of the brain and in regulating the growth and remodelling of neurones. Most members of the LDL-R superfamily identified so far recognize multiple apo and non-apo ligands. This pluripotency indicates that they have functions beyond the endocytosis of lipoproteins, at the same time challenging the conventional "one receptor–one ligand" concept of receptor biology.

The prototype member of the LDL-R family is the LDL-R (Brown and Goldstein, 1986). Its major function is to mediate the cellular uptake of LDL. The LDL-R has a key role in regulating cellular and systemic cholesterol homeostasis; inborn defects of the LDL-R represent the molecular cause of familial hypercholesterolemia. The LDL-R is a membrane-spanning glycoprotein consisting of five structural domains (cf Fig. 7). LDL-R are expressed at varying levels in almost every type of cell or tissue. In the central nervous system (CNS), oligodendrites express LDL-R.

The LDL-R has two major ligands, apo B-100 and apo E (Brown and Goldstein, 1986; Südhof *et al.*, 1985). Apo B-100 is not produced in the CNS (Osman *et al.*, 1995). Apo E is a 34 kDa glycoprotein. In human plasma, apo E is associated with triglyceride-rich lipoproteins and high-density lipoprotein (HDL) (Mahley, 1988). Apo E also serves as a ligand of other members of the LDL-R gene

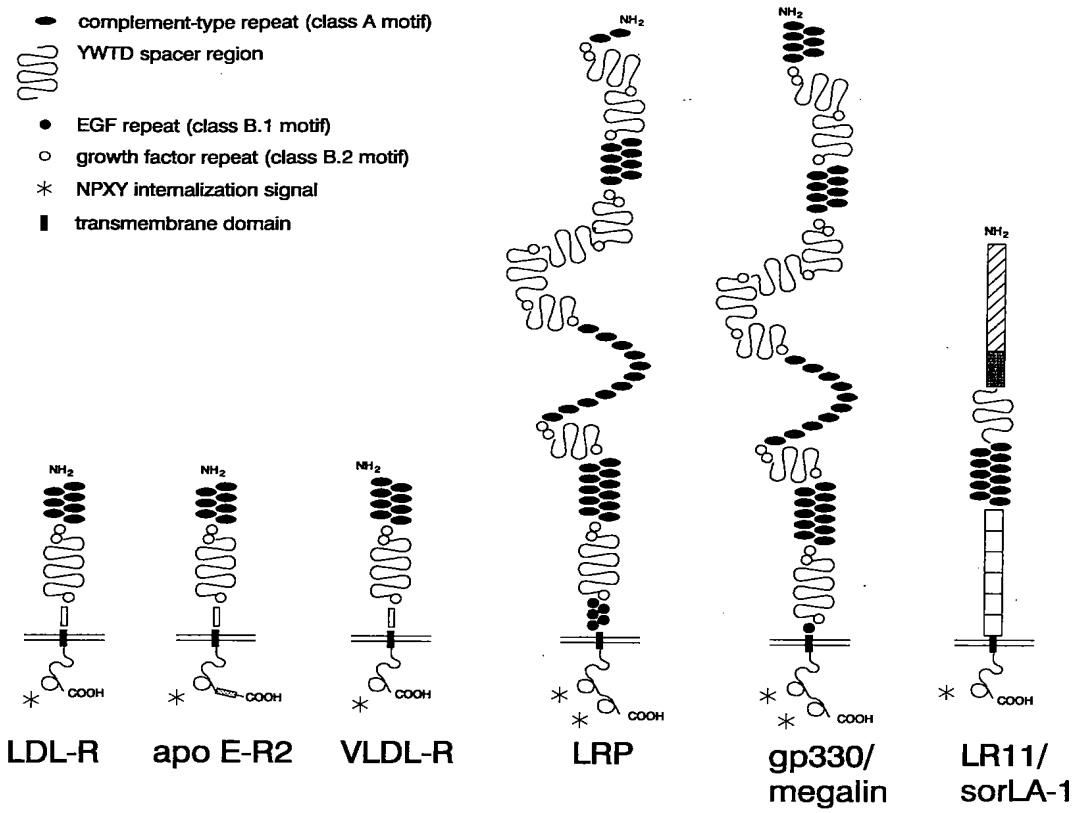

Fig. 7. Structure of the LDL receptor and the LDL receptor related protein. (A) The LDL-R contains five domains. The aminoterminal domain is responsible for the binding of ligands; it is rich in cyteine residues and consists of seven homologous complement-type repeats in which the positions of six cysteine residues are highly conserved. Each of these cysteine residues is involved in the formation of disulphide bonds. The binding of apo-B-100 and apo-E to the complements type repeats is mediated by clusters of negatively charged amino acid residues (glutamate and aspartate) between the fourth and the sixth cysteine residue. When these residues are protonized in the endosomes ligand molecules are released from its binding to the receptor. The second domain of the LDL-R shares a high degree of homology with the epidermal growth factor precursor. This domain consists of two cysteine-rich growth factor type repeats, a spacer region, and a third growth factor type repeat. The EGF precursor homologous region is required for the pH-dependent dissociation of the receptor from the ligand in the compartment of uncoupling receptor and ligand (CURL) (Davis *et al.*, 1987). The third domain contains 18 threonine or serine residues and O-linked carbohydrate residues. The transmembrane region consists of 22 hydrophobic amino acid. The cytoplasmic domain mediates the clustering of receptor molecules in coated-pits and the sorting of receptors to the basolateral cell surface in polarized cells (Yokode *et al.*, 1992; Matter *et al.*, 1992). (B) LRP contains 31 complement type repeats, arranged in four clusters of 2, 8, 10 and 11 repeats (Herz *et al.*, 1988). There are 22 growth factor repeats compared to three in the LDL-R. The growth factor repeats are constituents of four complete and four truncated EGF precursor homology regions (consisting of two EGF type cysteine repeats, a spacer region and a further EGF repeat). The cytoplasmic domain of LRP contains 100 amino acids, is thus twice as long as the cytoplasmic domain of the LDL-R. It contains two NPYX motif which serve as internalization signal. Mature LRP is a heterodimer of two non-covalently linked subunits with apparent molecular masses of 515 and 85 kDa, respectively. They arise from a monomeric 600 kDa precursor which is endoproteolytically cleaved by furin in the *trans*-Golgi complex (Willnow, 1996; Herz *et al.*, 1990a,b). The 515 kDa subunit lacks the membrane-spanning region, but it contains all of the ligand binding repeats present in LRP (Herz *et al.*, 1990a,b). The 85 kDa fragment encompasses the transmembrane region and the cytoplasmic tail.

family including LDL receptor related protein [LRP; Kowal *et al.* (1989) and Beisiegel *et al.* (1989)], the very low-density lipoprotein receptor [VLDL-R; Takahashi *et al.* (1992)], the apo E-R2 (Kim *et al.*, 1996a) and LR11 (Yamazaki *et al.*, 1996; Jacobsen *et al.*, 1996). Beyond this apo E is highly effective in promoting the efflux of non-esterified cholesterol from cells (Huang *et al.*, 1994; von Eckardstein *et al.*, 1995). Apo E is polymorphic in sequence.

Three common alleles designated $\epsilon 2$, $\epsilon 3$, $\epsilon 4$ at the apo E locus, give rise to six genotypes. Apo E3, the most frequent isoform, has arginine at position 112 and cysteine at position 158. Apo E4 has arginine, and apo E2 has cysteine at both positions (Mahley,

1988). Apo E2 is defective in binding to lipoprotein receptors (Schneider *et al.*, 1981; Lalazar *et al.*, 1988). Among the functional differences between apo E4 and apo E3 is that apo E4 preferentially associates with VLDL, whereas apo E3 associates with HDL (Dong *et al.*, 1994; Dong and Weisgraber, 1996).

In the CNS, apo E mRNA is found in astrocytes and glial cells; in the peripheral nervous system nonmyelinating glial cells express apo E (Boyles *et al.*, 1985; Lin *et al.*, 1986; Pitas *et al.*, 1987; Garcia *et al.*, 1996). Neurones produce virtually no apo E.

4.1. Apo E Responsible for Maintenance of Synaptic and Cognitive Function

In mice deficient in apo E, Masliah *et al.* (1995) observed losses of synaptophysin in nerve terminals and of microtubule-associated protein 2-immunoreactive dendrites in the neocortex and hippocampus, demonstrating that apo E is needed to maintain the integrity of the synapto-dendritic apparatus and Gordon *et al.* (1995) showed that the histomorphological alterations may translate in biochemical (low brain choline acetyltransferase activities in the hippocampus and frontal cortex) and cognitive impairment.

In recent years, a number of homologues of the LDL-R have been identified: the LRP (Herz *et al.*, 1988) the kidney membrane glycoprotein gp330 (Saito *et al.*, 1994); the VLDL receptor (Takahashi *et al.*, 1992); the apo E receptor 2 (Kim *et al.*, 1996a); the LR11 (Yamazaki *et al.*, 1996; Jacobsen *et al.*, 1996); and a VLDL receptor-like cell surface molecule present at high levels in the brain (Novak *et al.*, 1996).

Mature LRP consists of 4525 amino acids (Herz *et al.*, 1988). The extracellular domain of LRP contains multiple copies of motifs also found in the LDL-R, including the cysteine-rich ligand binding domain and the EGF precursor homology region including growth factor repeats. The O-linked sugar domain is missing in the LRP (for details cf Fig. 7).

LRP is an endocytotic receptor (Herz *et al.*, 1990a,b). The ligands of LRP can be divided into lipoprotein-related ligands, protease–antiprotease ligands, and miscellaneous. The lipoprotein-related ligands include apo E (Kowal *et al.*, 1989; Beisiegel *et al.*, 1989), apo B-100 (Wu and Pizzo, 1996), apo (a) (März *et al.*, 1993), lipases (Nielsen *et al.*, 1995; Argraves *et al.*, 1995; Chappell *et al.*, 1994; Kounnas *et al.*, 1995a,b). Other ligands are lactoferrin (Meilinger *et al.*, 1995), Pseudomonas aeruginosa exotoxin A (Willnow and Herz, 1994), thrombospondins (Chen *et al.*, 1996a,b; Godyna *et al.*, 1995), viruses (Hodits *et al.*, 1995; Marchetti *et al.*, 1996), the malaria circumsporozoite protein (Shakibaei and Frevert, 1996), activated α2-macroglobulin (α2M) (Nielsen *et al.*, 1996), tissue factor pathway inhibitor-1 (TFPI-1) (Narita *et al.*, 1995; Warshawsky *et al.*, 1996), the Kunitz domain containing isoform of the amyloid precursor protein (APPs-770) (Kounnas *et al.*, 1995a,b) and a wealth of complexes of other proteases and their endogenous antiproteases (Orth *et al.*, 1994; Noorman *et al.*, 1995; Horn *et al.*, 1995; Stefansson *et al.*, 1996; Kounnas *et al.*, 1996; Bonner *et al.*, 1995; Conese *et al.*, 1995).

When Strickland *et al.* (1991) prepared LRP from human placenta they co-purified a 39 Mr protein which they named receptor-associated protein (RAP). In the brain, RAP mRNA is *ca* 100-fold more abundant than in the liver (Bu *et al.*, 1994a,b). *In vitro* this protein inhibits the binding of many ligands to LRP (Kounnas *et al.*, 1992; Herz *et al.*, 1991; Orth *et al.*, 1992; Bu *et al.*, 1992; Moestrup and Gliemann, 1991). In the human glioblastoma cell line U87, LRP and RAP protein partially colocalized within the rough endoplasmic reticulum and the Golgi complex, suggesting intracellular interaction of the two proteins; in contrast, little RAP was found in the endosomes in which LRP occurred abundantly (Bu *et al.*, 1994a,b). RAP does not appear to be secreted from cells *in vivo*, but may serves as a chaperone (Willnow *et al.*, 1995, 1996a,b; Bu and Rennke, 1996) by inhibiting premature binding of ligands in the endoplasmic reticulum.

LRP is expressed in liver parenchymal cells (Herz *et al.*, 1988) and the syncytiothrophoblast of the placenta (Gafvels *et al.*, 1992; Jensen *et al.*, 1988). In the CNS, LRP is mainly found in neurones of the hippocampus and the entorhinal cortex and in glial cells (Bu *et al.*, 1994a,b; Moestrup *et al.*, 1992; Wolf *et al.*, 1992; Tooyama *et al.*, 1993; Lopes *et al.*, 1994). In rats, LRP mRNA emerges in the brain as early as in the 18 day old embryo and is continuously expressed thereafter, suggesting that it is involved in brain development (Ishiguro *et al.*, 1995).

The VLDL-R was cloned from a rabbit heart cDNA library (Takahashi *et al.*, 1992). The VLDL-R is highly homologous to the LDL-R, but contains eight complement type ligand binding repeats, in contrast to seven in the LDL-R. The VLDL-R is mainly found on the luminal surface of endothelial cells of the heart, the muscle, the adipose tissue and the brain (Gafvels *et al.*, 1994; Jokinen *et al.*, 1994; Wyne *et al.*, 1996; Webb *et al.*, 1994; Oka *et al.*, 1994). Apart from apo E (Takahashi *et al.*, 1996; Niemeier *et al.*, 1996) and RAP (Pfistermüller *et al.*, 1996), the VLDL-R has been shown to recognize LPL (Argraves *et al.*, 1995), uPA and complexes of uPA and PAI-1 (Heegard *et al.*, 1995). Unlike the LDL-R, the VLDL-R displays relaxed specificity towards mutant forms of apo E (Takahashi *et al.*, 1996).

The VLDL-R is believed to have a role in the delivery of triglyceride-rich lipoproteins to extrahepatic tissues, mainly adipose and muscle. In the brain, the VLDL-R is present on resting and activated microglia, particularly in senile plaques of patients with AD. VLDL-R immunoreactivity is also found in cortical neurons.

The apo E receptor 2 (apo E-R2) consists of five functional domains resembling the LDL-R and the VLDL-R. The apo E-R2 is able to bind and internalize apo E-enriched βVLDL. It is most highly expressed in human brain and placenta, but hardly in any other tissue. Within the brain, transcripts are found in the cerebellar cortex, choroid plexus, ependyma, hippocampus, olfactory bulb and, to a much lesser extent, in the cerebral cortex. In the cerebellar cortex, the receptor transcripts were densely deposited in Purkinje cell somata (Kim *et al.*, 1996a). The role of this receptor in CNS is not known.

Gp330/megalin is the autoantigen of Heymann's nephritis (Orlando *et al.*, 1992, 1995), an autoimmune glomerulonephritis in rats. The extracellular region of human gp330/megalin contains a total of 36 LDL-R ligand-binding repeats in four distinct clusters, 16 growth factor repeats and one epidermal growth factor-like repeat. There is a single transmembrane region and an intracellular C-terminus containing two copies of the internalization signal and, interestingly, several Src-homology 3 recognition motifs, one Src-homology 2 recognition motif for the p85 regulatory subunit of phosphatidylinositol 3-kinase, along with sites for protein kinase C, casein kinase II and cAMP-/cGMP-dependent protein kinase. Gp330/megalin is predominantly present in epithelial cells including the neuroepithelium, compared to LRP which is expressed mainly in cells of mesenchymal origin (Zheng *et al.*, 1994; Willnow *et al.*, 1996a,b). Gp330/megalin knockout mice die perinatally from respiratory insufficiency. In the brain of these mice, impaired proliferation of the neuroepithelium produces a holoprosencephalic syndrome (lack of olfactory bulbs, forebrain fusion and a common ventricular system) (Willnow *et al.*, 1996a,b).

LR11 is another member of LDL-R gene family described very recently (Yamazaki *et al.*, 1996; Jacobsen *et al.*, 1996). LR11 is a 250 kDa membrane protein. Its extracellular portion contains a cluster of 11 LDL-R ligand binding repeats, a group of five LDL-R YWTD repeats, six tandemly arranged fibronectin type III repeats reminiscent of neural adhesion molecules and a domain with similarity to a yeast receptor for vacuolar protein sorting. The cytoplasmic domain has features characteristic of endocytosis-competent receptors. LR11 is expressed abundantly in the spinal cord and in the brain, in particular in the hippocampus, dentate gyrus, and cerebral cortex, and is present at significant levels in liver, adrenal glands and testis as well. LR11 is able to bind apo E and RAP.

4.2. LDL-R and Alzheimer's Disease

Members of the LDL-R gene family and its ligands appear tightly related to the development of AD. Namba *et al.* (1991) first observed that apo E was deposited in AD brains. Strittmatter *et al.* (1993a,b) linked the apo E polymorphism to AD. Autopsy based studies showed that the load of β-amyloid peptide (βA4) was increased in brains from E4 carriers (Schmechel *et al.*, 1993; Rebeck *et al.*, 1993). Ohm *et al.* (1995) demonstrated a positive correlation between both βA4 deposition and the stage of intraneural neurofibrillary changes and the E4 gene dose.

LRP is also associated with senile plaques, tangles and dystrophic neurites in AD (Tooyama *et al.*, 1993). Ligands of LRP other than apo E including α2M, tPA and uPA, PAI-1, LPL, lactoferrin or TFPI (Schmechel *et al.*, 1993; Rebeck *et al.*, 1993; Kawamata *et al.*, 1993; Rebeck *et al.*, 1995; Hollister *et al.*, 1996) all accumulate in senile plaques. Interestingly, RAP was identified in the hippocampus of the normal brain, but not in senile plaques in the study by Rebeck *et al.* (1995). The mechanism linking the apo E polymorphism and AD has not been unravelled until now.

Strittmatter *et al.* (1993a,b) demonstrated that apo E and βA4 formed dodecyl sulphate-resistant complexes *in vitro*, apo E4 complexing more rapidly than apo E3. When βA4 and apo E were co-incubated, unique monofibrillar structures evolved, apo E4 yielding a denser matrix than apo E3 (Sanan *et al.*, 1994; Wisniewski *et al.*, 1994; Ma *et al.*, 1994). According to Castano and co-workers, apo E enhances both the rate and the amount at which fibrils are generated from soluble amyloid *in vitro*, apo E4 being more effective compared to apo E3 (Castano *et al.*, 1995).

When apo E3 plus a source of lipids was added to rabbit dorsal root ganglion or Neuro-2a cells, the extension of neurites was markedly enhanced. In contrast to apo E3, apo E4 plus a source of lipid reduced the branching and the outgrowth of neurites (Nathan *et al.*, 1994; Holtzmann *et al.*, 1995; Fagan *et al.*, 1996). Apo E thus appears to modify the outgrowth pattern in an isoform specific manner. At least some of the isoform specific effects of apo E are mediated by LRP (Nathan *et al.*, 1994) and that the VLDL-R is not required (Mahley, 1996).

It has been shown that apo E4 is less effective in protecting microtubuli from depolymerization than apo E3 (Nathan *et al.*, 1995; Mahley, 1996), suggesting that it has an intracellular role. Neurons, however, synthesize only small quantities, if any, of apo E. Thus, an effect of apo E on the organization of the cytoskeleton would require that apo E be taken up into neurons. It is reasonable to speculate that such uptake occurs by receptor-mediated endocytosis involving one or more members of the LDL-R family (Holtzmann *et al.*, 1995; Fagan *et al.*, 1996). However, receptor-mediated uptake of lipoproteins in non-neuronal cells results in their lysosomal degradation. If apo E had an intracellular role, then a possibility should exist by which apo E is protected from degradation in endosomes or lysosomes, at least in neurons. Support for that comes from a studies by Nathan *et al.* (1995) and by Lovestone *et al.* (1996). The latter authors showed in mammalian cells transiently expressing tau and the LDL-R that apo E is taken up from cerebrospinal fluid and that apo E3, but not apo E4, reaches the cytoplasm. The isoform difference in the intracellular distribution of apo E was dependent upon expression of tau, a finding which may explain the difference between the intracellular fate of apo E in neuronal and non-neuronal cells.

An alternative mode by which apo E and other ligands of LRP could affect cellular functions is that they generate biological signals themselves. There is in fact some evidence for this possibility. Misra *et al.* (1994) showed that binding of lactoferrin, Pseudomonas exotoxin A and LPL increases inositol 1,4,5-triphosphate (IP3) synthesis and cytosolic free calcium $[Ca^{2+}]_i$ by a pertussis toxin-sensitive G protein dependent mechanism. In addition, this group obtained evidence for a distinct signalling receptor that binds activated α_2M and activated alpha 1-inhibitor-3, a monomeric member of the α_2M/complement superfamily in the rat (Misra *et al.*, 1994, 1996; Howard *et al.*, 1996; Webb *et al.*, 1995) which

elicited IP3 and intracellular calcium responses through a pertussis toxin-insensitive G protein. We recently obtained evidence that complexes of βA4 and apo E produced ample increases in intracellular calcium levels in a mixed hippocampal primary cell culture model (Wüstenberg *et al.*, 1997).

In summary, current evidence shows that almost all members of the LDL-R family and many of their ligands are expressed in the brain. LRP, the apo E-R2 and LR11 are found at high levels in the hippocampus. Disruption of the apo E gene results in synaptic loss and cognitive impairment. These data indicate that members of the LDL-R gene family and their ligands may assume important functions in the CNS.

5. MOLECULAR ARCHITECTURE AT EXCITATORY AND INHIBITORY SYNAPSES

5.1. Postsynaptic Density at Excitatory Synapses

Over the past decades, many efforts were given to the purification and identification of the various proteins composing the specialized postsynaptic membrane of CNS synapses, namely the PSD [Banker *et al.* (1974) and Cohen *et al.* (1977); reviewed in Kennedy (1993, 1997)]. Two classes of PSD were described. Type 1 synapses contain a dense PSD and are excitatory whereas inhibitory or type 2 synapses contain a much less dense PSD which roughly corresponds to a thickening of the membrane bilayer. Much interest developed toward the characterization of the PSD as it was anticipated to contain molecules involved in receptor subcellular localization and clustering, modulating receptor functions as well as proteins that could provide a link to the presynaptic active zone. Despite the insolubility of the PSD proteins in traditional biochemical detergents, different groups have now succeeded in identifying several molecular constituents of the dense specialized structure. Cytoskeletal proteins including actin, spectrin, tubulin, microtubule-associated proteins and calcium/calmodulin-dependent protein kinase II are amongst the most abundant proteins of the PSD fractions. The glutamate receptors, AMPA, kainate and NMDA were also shown to be enriched in isolated PSDs. More recently, Cho *et al.* (1992) identified a new major protein (1–3% of total protein) from the PSD fraction that had an apparent molecular mass of 95 kDa and consequently was named PSD-95. PSD-95 is homologous to the Drosophila tumour suppressor protein, Dlg, in both sequence and structural organization. Both proteins are characterized by three 90 amino acid repeats in the amino-terminal region, a Src homology 3 (SH3) domain and a putative guanylate kinase (GK) in the carboxy-terminal region. The 90 residues repeat was later named PDZ, according to three proteins that contain such domain, PSD-95, the Drosophila discs—large tumour suppressor protein, DlgA and a tight junction protein, ZO-1. All these proteins are found in different cell junction structures and form an emerging new family of proteins, the MAGUKs (for membrane-associated GKs). In addition, close homologues to PSD-95 (SAP90) were recently described, namely SAP97 [hDlg; Müller *et al.* (1995)], SAP102 (Müller *et al.*, 1996a; Lau *et al.*, 1996) and chapsyn-110 [PSD-93; Kim *et al.* (1996b); Brenman *et al.* (1996)]. More distantly related PDZ-containing proteins include p55 (Hemming *et al.*, 1995; Marfatia *et al.*, 1995), CASK (Hata *et al.*, 1996), glutamate receptor interacting protein [GRIP; Dong *et al.* (1997)] and Homer (Brakeman *et al.*, 1997).

5.1.1. *NMDA Receptor Channel and MAGUK Proteins*

It was recently shown that PSD-95 interacts directly with the NMDA receptor channel complex (Kornau *et al.*, 1995; Niethammer *et al.*, 1996). The latter is composed of two different types of subunits, the NR1 and at least one of the NR2 (A–D). The last seven amino acid of both NR2A and NR2B could interact with the first two PDZ domains of the PSD-95. The sequence motif, X–T/S–X–V where X stands for any amino acid, revealed to be essential for PSD-95 binding (Kornau *et al.*, 1995). The analysis of the X-ray crystallographic structure of the third PDZ domain from either PSD-95 or DlgA shed light on the molecular players underlying this biochemical specificity (Doyle *et al.*, 1996; Cabral *et al.*, 1996). Indeed, a prominent conserved hydrophobic pocket, a Gly–Leu–Gly–Phe loop as well as a buried Arg are believed to play a key role in providing the binding specificity of the C-terminal peptides to the respective PDZ domains. It remains to be shown if the NR2C and NR2D as well as two of the splice variants of the NR1 subunit (NR1C-D) can also interact with PSD-95 or homologues, as potential C-terminal binding motif is present in these subunits. In support of a functional interaction between the PSD-95 and the NR2 subunits, mutation of the Dlg gene was shown to disrupt the synaptic morphology and particularly the subsynaptic reticulum of the Drosophila neuromuscular junction (Lahey *et al.*, 1994). These findings are thus in agreement with a key role for this family of proteins in the molecular organization of synapses.

The NR2A/B subunits of the NMDA receptor were reported to also interact directly with two other members of the MAGUK family, SAP102 and chapsyn-110 (Müller *et al.*, 1996a; Lau *et al.*, 1996; Kim *et al.*, 1996b). SAP102 is localized in dendritic shafts as well as spines of asymmetric type 1 synapses in various brain regions including cerebral cortex, hippocampus, olfactory bulb and cerebellum (Müller *et al.*, 1996a). Unlike PSD-95, all three of its PDZ domains could interact with the cytoplasmic tail sequence of the NR2B subunit with binding affinities ranging from 6 nM to 1 μM for the PDZ domains 2 and 3, respectively. Similarly high binding affinity was observed with the PDZ domain 2 of PSD-95 (Müller *et al.*, 1996a). According to its postsynaptic localization, tissue distribution and biochemical characteristics, SAP102 appears to be a good candidate to participate in the structural assembly of developing excitatory synapses.

5.1.2. *Clustering of NMDA Receptor Channel and K^+ Channel by MAGUK Proteins*

Similarly to PSD-95, chapsyn-110 (PSD-93) binds directly to the NR2A-B subunits as well as to the

shaker-subtype voltage-gated K^+ channel (Kim *et al.*, 1995; Kim *et al.*, 1996b). Interestingly, upon individual transfection of either PSD-95 or chapsyn-110 in heterologous cells, a diffuse distribution pattern in the cell was observed for the respective proteins. However, upon co-transfection of either chapsyn-110 or PSD-95 with the various channel subunits, clustering of both voltage-gated K^+ and NMDA receptor channels was reported (Kim *et al.*, 1996b). Co-transfected COS-7 cells with chapsyn-110 and PSD-95 again revealed a diffuse intracellular immunoreactivity for either proteins. Upon triple transfection, that is, NMDA or K^+ channel subunits together with both MAGUK proteins, surface clusters were formed and all the proteins were found to be colocalized. In conclusion, both the NR2A and NR2B subunits behaved like the shaker-subtype voltage-gated K^+ channel with respect to their ability to interact with both chapsyn-110 and PSD-95 within the same clusters. In contrast to the NR2 subunit, the NR1A polypeptide failed to bind the respective MAGUK proteins and remained diffusely distributed in the cell. However, upon co-transfection of the NR1 with the NR2 and either chapsyn-110 or PSD-95, NR1 immunoreactivity was also part of the clustered structure. Taken together, heteromeric NMDA receptors, the NR2 subunits alone and the shaker-type voltage-gated K^+ channel can form clusters upon co-transfection with either chapsyn-110 and/or PSD-95 in COS-7 cells. The formation of such channel clusters seems to involve disulphide links between the respective N-terminal domain of MAGUK proteins such as PSD-95 and chapsyn-110 (Hsueh *et al.*, 1997).

PSD-95 has been localized in the PSD at forebrain synapses where it colocalizes with the NMDA receptor (Hunt *et al.*, 1996). However, it was also reported to be located in presynaptic inhibitory synapses in the cerebellum (Kistner *et al.*, 1993). Data available regarding the cellular localization of chapsyn-110 is limited. Overall, it may be very similar to the distribution of PSD-95, especially in brain areas such as cerebral cortex and hippocampus (Kim *et al.*, 1996b). Shaker-subtype voltage-gated K^+ channels are located predominantly in presynaptic terminals and on axons in rat brain, whereas NMDA receptors are mostly found at postsynaptic sites. Although examples of colocalization of the respective proteins have been described in brain sections as well as in cultured neurons, the question remains which of these interactions are relevant *in vivo*. Furthermore, as the overall expression patterns of these proteins in brain do not overlap adequately, the existence of novel members of the MAGUK family and/or other functionally related proteins may be anticipated [e.g. GKAP, SAPAP (see below)].

5.1.3. *Cellular Signalling and MAGUK Proteins*

Several biological actions have been attributed to NO in both peripheral and central tissues [for review see Kerwin *et al.* (1995); Brenman and Bredt (1996)]. In brain, NO has been suggested to play a role in the molecular events underlying synaptic plasticity (Schuman and Madison, 1994). NO is derived from a complex enzymatic reaction catalysed by NO synthase (NOS). The N-terminal domain of the neuronal form of this enzyme contains a PDZ domain. PSD-95 as well as PSD-93 (chapsyn-110) were recently shown to interact with the PDZ domain of NOS (Brenman *et al.*, 1996). In particular, the second PDZ domain of PSD-95 is involved in the binding with the PDZ domain of the NOS enzyme. Moreover, the binding motif of the NR2A/B subunit could compete (although with low affinity, IC_{50} $\sim 10\ \mu M$) with the PDZ domain of the NOS for the second PDZ repeat of the PSD-95. Colocalization of the respective proteins were shown in several brain areas, in both developing and adult brain. NOS isoforms lacking the PDZ domain have altered subcellular distribution supporting a role for the PDZ domain in mediating the subsynaptic localization of NOS. The close proximity of the NOS and the NMDA receptor channel via their respective interaction with MAGUK protein(s) may thus facilitate rapid molecular responses during synaptic transmission and provide localized specificity [Fig. 8(A)].

PDZ–PDZ domain interaction also appear to be involved in other protein–protein associations. For example, the dystrophin glycoprotein complex and NOS are closely located at the neuromuscular junction via the respective PDZ domain of NOS and 1-syntrophin (Brenman *et al.*, 1996). Finally, PDZ domains of SAP97 (hDlg) revealed specific nucleotide-binding affinity for ATP (Marfatia *et al.*, 1996). This interaction could provide an additional regulating element to the neighbouring molecules. It thus appears the PDZ domains might play a basic role in organizing and modulating the molecular signalling complex at the synaptic subcellular domain. In agreement with such hypothesis, Tsunoda *et al.* (1997) most recently showed that InaD protein, which contains five PDZ domains, plays a crucial role in organizing the photoreceptor signalling complex *in vivo*.

5.1.4. *MAGUK Protein and Guanylate Kinase-Associated Protein*

Despite the description of a GK domain for the various MAGUK proteins, due to a significant identity (37%) with yeast GK, no GK activity have been described thus far for this emerging protein family. Furthermore, the ATP-binding site is not conserved in these GK domain and only low affinity of ATP (mM range) for PSD-95 (SAP90) was reported whereas GMP binds with micromolar affinity (Kistner *et al.*, 1995). The role of the GK domain is potentially very important as several modifications observed in the Dlg mutant Drosophila, such as changes in synaptic bouton morphology at the neuromuscular junction, can mostly be attributed to mutations in the GK domain. Most recently, a protein that binds specifically to the GK domain was described and named GKAP for guanine kinase-associated protein (Kim *et al.*, 1997). GKAP binds to PSD-95 and its close homologues. It also appears to be recruited in the cluster formed by either PSD-95/NR2B or PSD-95/shaker-subtype voltage-gated K^+ channel upon co-transfection of COS-7 cells. Although GKAP *per se* is not essential for the formation of these clusters, it might be involved in providing a link between the channel/PSD-95 clusters

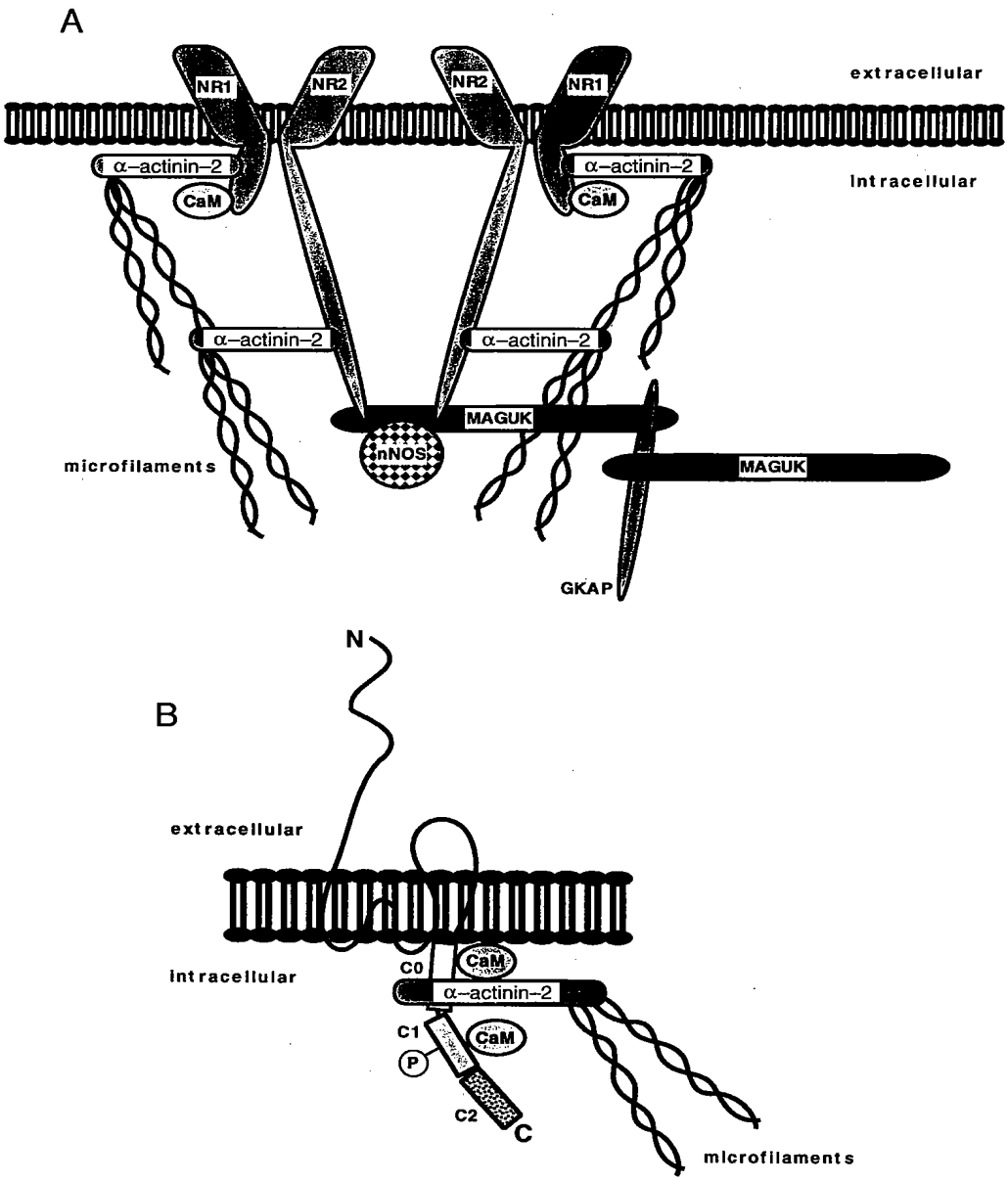

Fig. 8. (A) Simplified diagram of the subcellular architecture involved in the anchoring and clustering of the NMDA receptor channel complex. Both the N-terminal and the PDZ domains of the various MAGUK proteins as well as the 14 amino acid repeats of the GKAP (SAPAP) protein can potentially act as cross-linking agents in the subsynaptic domain. Alpha-actinin-2 might correspond to the link between the NMDA receptor complex and microfilaments. The latter interaction influencing the electrophysiological properties of the NMDA channel. Abbreviations: CaM, calmodulin; GKAP, guanylate kinase-associated protein; MAGUK, membrane-associated guanylate kinase; nNOS, neuronal nitric oxide synthase; SAPAP, SAP90/PSD-95-associated proteins. (B) Diagram of the NR1 subunit and proteins interacting with the cytoplasmic C-terminal domain. Upon calcium entry, CaM can displace alpha-actinin-2 from the NR1 cassette 0 domain which may contribute to the rundown of the NMDA channel. Abbreviations: CaM, calmodulin; C0, cassette 0; C1, cassette 1; C2, cassette 2; P, PKC phosphorylation site.

and the subcellular machinery. Indeed, the N-terminal region of GKAP is composed of five 14 amino acid repeats which seem to have the independent ability to bind to the GK domain of PSD-95. This finding therefore support that GKAP could act as a cross-linker between different PSD-95 or related proteins and contribute to the formation of heterogeneous clusters [summarized in Fig. 8(A)]. Homologues of GKAP have now also been described, namely SAPAP 1–4. In addition to interact with the GK domain of PSD-95, SAPAPs were shown to enrich the plasma membrane of PSD-95 upon co-transfection (Takeuchi *et al.*, 1997). Not only the PDZ domains of the various MAGUK family members thus appear to be involved in the multiple protein interactions but also, somehow unexpectedly, their GK domain.

Immunocytochemical studies of cultured cortical and hippocampal neurons show that NMDA as well as non-NMDA receptor channels are highly clustered at the excitatory postsynaptic membrane (Jones and Baughman, 1991; Benke *et al.*, 1993; Craig *et al.*, 1993). GRIP, a protein that contains seven PDZ but no putative GK domain, was reported to bind to AMPA receptors (Dong *et al.*, 1997). It likely provides a template which would allow the crosslinking of AMPA receptors as well as other proteins that are involved following excitatory synaptic transmission. The members of the PDZ-containing protein family might thus be elements that play a role in the complex events during synaptic specialization but they are poor candidates to provide the specificity required for the subcellular localization considering the diversity of proteins that can interact with them. Taken together, these proteins are thus more likely involved in the maintenance of the receptor cluster structure as well as of the subcellular machinery required at the synaptic domain (e.g. NOS) and to provide an anchoring domain for the underlying cytoskeleton.

5.1.5. *Clustering of Glutamate Receptors and Phosphorylation*

Spontaneous clustering of the NR1 receptor subunit of the NMDA receptor channel complex was reported upon transfection in fibroblasts (QT6) (Ehlers *et al.*, 1995). However, different splice variants of the NR1 subunit revealed different distribution pattern in those cells. Indeed, a stretch of 37 amino acid within the cytoplasmic C-terminal domain (also referred as cassette 1) present in some variants of the NR1 subunit was sufficient to cause the clustering into discrete domains. The phosphorylation of specific serines by protein kinase C within the cassette 1 domain could modulate the formation of these NR1 agglomerates (Ehlers *et al.*, 1995). In a similar way, the phosphorylation of a serine residue by protein kinase A could also modulate the interaction between the PSD-95 and an inward rectifier K^+ channel C-terminal domain (Cohen *et al.*, 1996). The cassette 1 domain of the NR1 subunit could also interact with high affinity with calmodulin, in a calcium-dependent manner. In addition, a second calmodulin binding domain, although of lower affinity, was located around 30 amino acid upstream of the cassette 1, that is, within cassette 0 [Fig. 8(B)]. Interestingly, the interaction of calmodulin with the NMDA receptor channel complex decreased the channel activity by modulating the opening rate as well as the mean opening time of the channel. The calmodulin binding to the NR1 subunit could thus act as a "calcium sensor" for the NMDA receptor channel complex and limit, to a certain extent, the calcium entry via these channels. Furthermore, earlier studies have shown the NMDA receptor channel activity is dependent on the integrity of the microfilaments (Legendre *et al.*, 1993; Rosenmund and Westbrook, 1993). In agreement with these reports, alpha-actinin-2, an actin-bundling protein, was recently shown to interact directly with residues within the cassette 0 of the NR1 C-terminal domain [Wyszynski *et al.* (1997); Fig. 8(A and B)]. The central rod domain of the alpha-actinin-2 is involved in this interaction. In contrast to the interactions with MAGUK proteins and calmodulin, both NR1 and NR2B subunits bound to alpha-actinin-2. Most interestingly though, only the binding of alpha-actinin-2 to the NR1 C-terminal domain could be competed by calmodulin, in a calcium-dependent fashion. These observations allow one to speculate that at resting *in vivo* intracellular Ca^{2+} levels, alpha-actinin-2 binds to the NMDA receptor channel complex but in response to Ca^{2+} entry, calmodulin could displace the alpha-actinin-2 from the NR1 subunit and consequently contributing to the Ca^{2+}-dependent inactivation and rundown of NMDA receptor channels. Future studies are required to confirm or not this scenario as well as to identify other putative molecules that might be involved as a tight modulation of the Ca^{2+} entry is highly desired.

Despite the explosion of most recent findings with respect to the characterization of the MAGUK and related proteins as well as their interaction with the respective receptor channels, as summarized in Fig. 8(A), limited knowledge is yet available regarding the sequence of events involved in the clustering, anchoring and subcellular targeting of proteins to the specialized subdomains of central synapses. The subcellular machinery involved at the neuromuscular junction is yet better defined and involves the interaction of >10 proteins such as rapsyn, utrophin and syntrophin, to name a few [reviewed in Froehner (1993) and Apel and Merlie (1995)]. The characterization of novel proteins such as GKAP and GRIP will allow to shed light on the molecular constituents involved in these complex interactions and ultimately lead to the basic understanding of the formation, structure and plasticity of neuronal synapses.

5.2. Role of Gephyrin at Inhibitory Synapses

Synaptic inhibition in the CNS is mediated by the amino acids γ-aminobutyric acid and glycine. The receptors for these neurotransmitters mediate inhibition of neuronal firing by ligand-induced gating of chloride ions leading to hyperpolarization of the cell membrane. Ionotropic receptors for γ-aminobutyric acid ($GABA_AR$) are predominant in cortex, hippocampus, basal ganglia and cerebellum (Wisden *et al.*, 1992; Laurie *et al.*, 1992) whereas glycine recep-

tors (GlyR) are mainly found in spinal cord and brain stem neurons but also in higher regions of the neuraxis like cerebellum, hippocampus and layer IV of the cortex (Malosio *et al.*, 1991). Due to significant structural and functional homologies, both $GABA_AR$ and GlyR are considered members of the same family of ligand gated ion channels which also includes nicotinic acetylcholine receptors, and serotonin type-3 receptors [reviewed in Kuhse *et al.* (1995)]. Whereas little is known how $GABA_AR$ are localized to postsynaptic membranes, significant progress has been made towards the elucidation of the molecular mechanisms underlying the formation of GlyR aggregates at postsynaptic membrane specializations. It could be shown that the peripheral membrane protein gephyrin plays a pivotal role in the formation of GlyR clusters most likely by anchoring the receptor to the subsynaptic cytoskeleton.

The GlyR is a pentameric ion channel complex composed of 3α and 2β subunits (Kuhse *et al.*, 1993). Four different α subunit isoforms ($\alpha1$–$\alpha4$; M_r 48–49 kDa), whose spatial and temporal expression is tightly regulated (Malosio *et al.*, 1991; Matzenbach *et al.*, 1994), confer distinct pharmacological properties to the heterooligomeric receptor (Schmieden *et al.*, 1992), whereas the β-polypeptide (58 kDa) can be considered a structural subunit (Kuhse *et al.*, 1995). Due to its high affinity for the alkaloid strychnine, GlyR can be affinity-purified from solubilized spinal cord membranes (Pfeiffer *et al.*, 1982; Schmitt *et al.*, 1987). In addition to the receptor subunits a third polypeptide with a relative molecular mass of 93 kDa is consistently copurified with the GlyR. This polypeptide was characterized as a peripheral membrane protein (Schmitt *et al.*, 1987) and lateron named gephyrin (from greek $\gamma\epsilon\varphi\upsilon\rho\alpha$: bridge).

Light and electron microscopic immunocytochemistry revealed that gephyrin decorates the cytoplasmic face of glycinergic and subset(s) of GABAergic postsynaptic membrane specializations in spinal cord, brain and retina (Triller *et al.*, 1985; Altschuler *et al.*, 1986; Sassoè-Pognetto *et al.*, 1995; Todd *et al.*, 1995). Surprisingly, gephyrin immunoreactivity is observed in most synaptically active regions of the brain and thus exceeds the distribution of the known GlyR α subunits (Kirsch and Betz, 1993). This observation indicates the presence of gephyrin at both glycinergic and GABAergic synapses, moreover, these data suggest that gephyrin can also be found at postsynaptic sites of yet unknown specificity.

The primary structure of gephyrin (Prior *et al.*, 1992) shows significant homology to polypeptides of bacteria (Prior *et al.*, 1992; Nohno *et al.*, 1988), plants (Stallmeyer *et al.*, 1995) and invertebrates (Kamdar *et al.*, 1994) involved in the biosynthesis of the molybdenum cofactor, however, the functional significance of this observation remains enigmatic. Transcription of the gephyrin gene is not restricted to the CNS, since gephyrin mRNA is also found in liver, kidney, heart and possibly lung (Prior *et al.*, 1992). Cloning of the gephyrin cDNA has identified several gephyrin transcripts in rat brain and spinal cord, which differ by the insertion of short nucleotide cassettes (C1–C4) in the 5′ half of the coding region (Prior *et al.*, 1992). This heterogeneity is most likely due to alternative splicing of the gephyrin pre-mRNA, The functional significance of multiple gephyrin transcripts has not been resolved. The distribution of gephyrin transcripts in the adult and developing brain (Kirsch *et al.*, 1993a) is consistent with immunohistochemical data (Kirsch and Betz, 1993). A detailed analysis revealed that gephyrin isoforms containing cassette C2 are the predominant variant which is expressed at high levels in most regions of the brain, whereas variants with cassettes C3 and/or C4 are detected only in hippocampus and cerebellum (Kirsch *et al.*, 1993a).

In cultured embryonic spinal neurons, the accumulation of gephyrin at developing postsynaptic sites precedes the synaptic clustering of the GlyR (Kirsch *et al.*, 1993b; Béchade *et al.*, 1996). Whereas focal accumulations of gephyrin immunoreactivity could be observed as early as 3 days *in vitro*, GlyR clusters are visualized only after *ca* 1 week in culture. The formation of postsynaptic GlyR clusters depends on the presence of gephyrin, since inhibition of gephyrin expression by antisense oligonucleotides prevents the formation of GlyR clusters in these cultures completely (Kirsch *et al.*, 1993b). Gephyrin expression is therefore considered essential for the formation of GlyR clusters an their synaptic localization (Kirsch *et al.*, 1993b).

Recently, overlay and coexpression studies identified the β subunit of the GlyR as binding partner for gephyrin (Meyer *et al.*, 1995; Kirsch *et al.*, 1995). The interface for gephyrin binding is confined to a continuous stretch of 18 amino acids located at the cytoplasmic pole of this subunit. Interestingly, insertion of the gephyrin binding motif in a $GABA_AR$ subunit (Meyer *et al.*, 1995) or the NR1 subunit of the NMDA receptor (S. Kins, J. Kuhse and J. Kirsch, unpublished observation) which are both not capable of interacting with gephyrin, conferred binding indistinguishable from that of the GlyR β subunit. In similar experiments it could be demonstrated that also the $\beta3$ subunit of GABAA receptors can interact with gephyrin (Meyer *et al.*, 1995) and this finding is consistent with immunohistochemical data demonstrating the presence of gephyrin underneath GABAergic synapses harbouring a $\beta3$ subunit (Todd *et al.*, 1996).

Overlay and copolymerization studies revealed a high-affinity interaction of gephyrin with polymerized tubulin *in vitro* (Kirsch *et al.*, 1991). Interestingly, the binding characteristics, in particular the stoichiometry and the positively co-operative nature of the interaction, are very similar to that of a classical microtubule-associated protein, namely MAP2. These findings from *in vitro* experiments were corroborated by the observation that postsynaptically localized gephyrin aggregates in cultured spinal neurons were sensitive to alkaloids affecting the integrity of the cytoskeleton (Kirsch and Betz, 1995). Therefore, gephyrin is thought to link postsynaptic inhibitory neurotransmitter receptors harbouring a gephyrin binding subunit to the cytoskeletal structures underlying postsynaptic membrane differentiations (Fig. 9). Specifically, depolymerization of microtubules led to a decreased packing density of gephyrin and GlyR in postsynaptic clusters, whereas receptor aggregates were con-

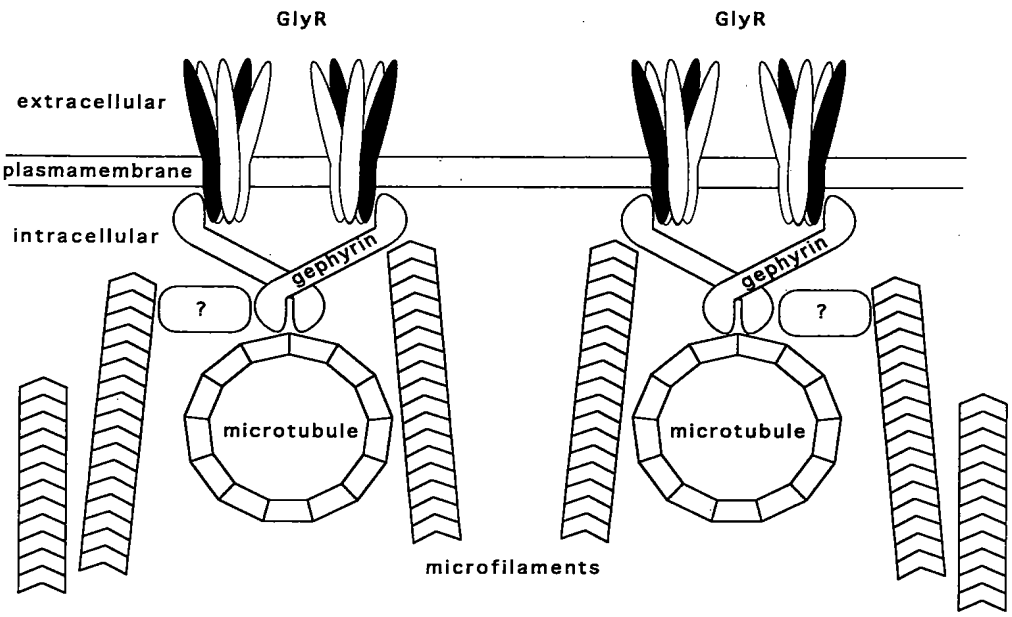

Fig. 9. Model of the interactions of gephyrin with the GlyR and the subsynaptic cytoskeleton. Gephyrin anchors the postsynaptic GlyR to microtubules forming a subsynaptic lattice. The interactions with microfilaments could either be direct (centre) or involve an additional regulatory actin-binding protein(s) (indicated by a question mark).

densed upon disruption of microfilaments. Thus, microtubules and microfilaments appear to act antagonistically on the packing density of gephyrin/GlyR clusters at postsynaptic sites. Since it could be shown that pharmacological characteristics of the GlyR depend on its packing density within the cell membrane (Taleb and Betz, 1994), it is tempting to speculate that the postsynaptic machinery of glycinergic membrane specializations could be involved in the tuning of synaptic efficacy.

Postsynaptic membrane specializations are complex molecular machineries subserving multiple functions important for the proper functioning of the nervous system. So far only a few key players in this concert of polypeptides have been identified. The investigation of the elements regulating their interaction and the identification and functional characterization of additional polypeptides should help to advance our understanding of the molecular mechanisms involved in the regulation of synaptic plasticity.

6. CONCLUSIONS

In pathological conditions, such as temporal lobe epilepsy, the plasticity at central synapses may be structural as well as functional. Important components of these changes are the types and properties of neurotransmitter receptors that are expressed. For example, the molecular and functional diversity of NMDA subunits (Monyer *et al.*, 1992), permits the suggestion that expression of new subunit composition may explain the long-term functional change in NMDAR channels found in several chronic experimental models of this condition (Chen *et al.*, 1998; Kohr *et al.*, 1993). However, in this review we have discussed possible roles for a broad spectrum of the molecular machinery that may be involved in the developmental as well as pathogenic mechanisms underlying these changes in synaptic function.

Another fundamental component of the postsynaptic membrane specialization is the complex molecular machinery's involved in the clustering and location of neurotransmitter receptors. So far only a few key players in this concert of polypeptides have been identified. The identification of additional components of the postsynaptic machinery and the investigation of the elements regulating their interactions should help to advance our understanding of the molecular mechanisms involved in the regulation of synaptic plasticity.

The last year has witnessed a tightening of the link between recognition molecule function and synaptic plasticity not only during development, but particularly in the adult. A role for recognition molecules in promoting morphological changes such as size and shape of synaptic contacts, elaboration of spines, dendritic or axonal branching patterns, and cell-specific connectivity after functional modification of synaptic strength has become more tangible. However, there are many questions that need to be addressed about the types, timing and location of expression molecules involved in these processes. Since recognition molecules are known to influence the intracellular signalling cascades of second messenger systems, a further pressing question is how adhesion molecules will interact with signal transduction pathways known to be crucial in regulating

synaptic strength. Clearly, this will be an extremely difficult problem to solve, since any alteration in signalling pathways will involve a cascade of changes, the extent and ramifications of which will resist easy analysis. Furthermore, how can morphological changes and alteration in signalling mechanisms be translated into long-term modifications at the synapse, involving the stabilization or destabilization of network interactions?

Understanding these molecular mechanisms may in turn shed light on the molecular mechanisms that underlie functional and structural changes that occur during synaptic plasticity and reactive synaptogenesis in temporal lobe epilepsy. Comparisons can also be made between the mechanisms underlying neurodegeneration in epilepsy and those found in dementias such as Alzheimer's and in turn provide novel approaches to the treatment of these debilitating and universal conditions..

Acknowledgements—H. V. W., Y. C. and J. M. were funded by grants from the Wellcome Trust, MRC and Action Research. J. K. was supported by the Heisenberg-Programm of the Deutsche Forschungsgemeinschaft and Grant No. Ki441/7-1. He presently holds an endowed Schilling Professorship of the Stifterverband für die Deutsche Wissenschaft. D.v.R. is supported by the Human Frontier Science Program Organization. The authors are also grateful to Professor Heinrich Betz, Ned Mantei, Thomas Schuster, Oliver Stork and Carsten Wotjak for their helpful comments on the manuscript.

REFERENCES

Altschuler, R. A., Betz, H., Parakkal, M., Reeks, K. and Wenthold, R. (1986) Identification of glycinergic synapses in the cochlear nucleus through immunocytochemical localization of the postsynaptic receptor. *Brain Res.* **369,** 316–320.

Apel, E. D. and Merlie, J. P. (1995) Assembly of the postsynaptic apparatus. *Curr. Opin. Neurobiol.* **5,** 62–67.

Arami, S., Jucker, M., Schachner, M. and Welzl, H. (1996) The effect of continuous intraventricular infusion of L1 and NCAM antibodies on spatial-learning in rats. *Behav. Brain Res.* **81,** 81–87.

Argraves, K. M., Battey, F. D., MacCalman, C. D., McCrae, K. R., Gafvels, M., Kozarsky, K. F., Chappel, D. A., Strauss, J. F. I. and Strickland, D. K. (1995) The very low density lipoprotein receptor mediates the cellular catabolism of lipoprotein lipase and urokinase-plamsinogen activator inhibitor type I complexes. *J. biol. Chem.* **270,** 26550–26557.

Ashwood, T. J. and Wheal, H. V. (1987) The expression of *N*-methyl-D-aspartate-receptor mediated component during epileptiform synaptic activity in the hippocampus. *Br. J. Pharm.* **91,** 815–822.

Ashwood, T. J., Lancaster, B. and Wheal, H. V. (1986) Intracellular electrophysiology of CA1 pyramidal neurones in slices of the kainic acid lesioned hippocampus. *Exp. Brain Res.* **62,** 189–198.

Audinat, E., Lambbolez, B., Rossier, J. and Crepel, F. (1994) Activity dependent regulation of NMDA subunit expression in rat cerebellar granule cells. *Eur. J. Neurosci.* **6,** 1792–1800.

Avoli, M. and Olivier, A. (1987) Bursting in human epileptogenic neocortex is depressed by an *N*-methyl-D-aspartate antagonist. *Neurosci. Lett.* **76,** 249–254.

Babb, T. L. and Brown, W. J. (1987) Pathological findings in epilepsy. In: *Surgical Treatment of the Epilepsies*, pp. 511–540. Ed. J. Engel Jr. Raven Press, New York.

Babb, T. L., Kupfer, W. R., Pretorius, J. K., Crandall, P. H. and Levesque, M. F. (1991) Synaptic reorganisation by mossy fibres in human epileptic fascia dentata. *Neuroscience* **42,** 351–363.

Bahr, B. A., Staubli, U., Xiao, P., Chun, D., Ji, Z-X., Esteban, E. T. and Lynch, G. (1997) Arg–Lly–Asp–Ser-selective adhesion and the stabilization of long-term potentiation: pharmacological studies and the characterization of a candidate matrix receptor. *J. Neurosci.* **17,** 1320–1329.

Bailey, C. H., Chen, M., Keller, F. and Kandel, E. R. (1992) Serotonin-mediated endocytosis of apCAM: an early step of learning-related growth in Aplysia. *Science* **256,** 645–649.

Bailey, C. H., Kaang, B. K., Chen, M., Martin, K. C., Lim, C.-S., Casadio, A. and Kandel, E. A. (1997) Mutation in the phosphorylation sites of MAP kinase blocks learning-related internalization of apCAM in Aplysia sensory neurons. *Neuron* **18,** 913–924.

Banker, G., Churchill, L. and Cotman, C. W. (1974) Proteins of the postsynaptic density. *J. Cell Biol.* **63,** 456–465.

Bear, M. and Malenka, R. (1994) Synaptic plasticity, LTP and LTD. *Curr. Opin. Neurobiol.* **4,** 389–399.

Béchade, C., Colin, I., Kirsch, J., Betz, H. and Triller, A. (1996) Glycine receptor a subunit and gephyrin expression in cultured spinal neurons: a quantitative analysis. *Eur. J. Neurosci.* **8,** 429–435.

Becker, C. G., Artola, A., Gerardy-Schahn, R., Becker, T., Welzl, H. and Schachner, M. (1996) The polysialic acid modification of the neural cell adhesion molecule is involved in spatial learning and hippocampal long-term potentiation. *J. Neurosci. Res.* **45,** 143–152.

Beesley, P. W., Mummery, R. and Tibaldi, J. (1995) *N*-Cadherin is a major glycoprotein component of isolated rat forebrain postsynaptic densities. *J. Neurochem.* **64,** 2288–2294.

Behrens, J., van Kries, J. P., Kuehl, M., Bruhn, L., Wedlich, D., Grosschedl, R. and Birchmeier, W. (1996) Functional interaction of beta-catenin with the transcription factor LEF-1. *Nature* **382,** 638–642.

Beisiegel, U., Weber, W., Ihrke, G., Herz, J. and Stanley, K. K. (1989) The LDL-Receptor-related-protein, LRP, is an apolipoprotein E binding protein. *Nature* **341,** 162–164.

Ben-Ari, Y. (1985) Limbic seizure and brain-damage produced by kainic acid-mechanisms and relevance to human temporal-lobe epilepsy. *Neuroscience* **14,** 375–403.

Ben-Ari, Y. and Represa, A. (1990) Brief seizure episodes induce long-term potentiation and mossy fibre sprouting in the hippocampus. *Trends Neurosci.* **13,** 312–318.

Ben-Ari, Y., Tremblay, E., Ottersen, O. P. and Meldrum, B. S. (1980) The role of epileptic activity in the hippocampus and "remote" cerebral lesions induced by kainic acid. *Brain Res.* **191,** 79–97.

Benke, T. A., Jones, O. T., Collingridge, G. L. and Angelides, K. J. (1993) *N*-Methyl-D-aspartate receptors are clustered and immobilized on dendrites of living cortical neurons. *Proc. natl Acad. Sci., U. S. A.* **90,** 7819–7823.

Bernard, C. and Wheal, H. V. (1994) Model of local connectivity patterns in CA3 and CA1 areas of the hippocampus. *Hippocampus* **4,** 497–529.

Bernard, C. and Wheal, H. V. (1995a) Simultaneous expression of long-term depression of NMDA and long-term potentiation of AMPA receptor-mediated synaptic responses in the CA1 area of the kainic acid lesioned hippocampus. *Eur. J. Neurosci.* **7,** 1651–1655.

Bernard, C. and Wheal, H. V. (1995b) Plasticity of AMPA and NMDA receptor-mediated epileptiform activity in a chronic model of temporal lobe epilepsy. *Epilepsy Res.* **21,** 95–107.

Bernard, C. and Wheal, H. V. (1995c) Simultaneous expression of EPSP/spike potentiation and EPSP/spike depression in the hippocampus. *Neuroscience* **67,** 73–82.

Bernard, C. and Wheal, H. V. (1995d) Expression of EPSP/spike potentiation following low frequency and tetanic stimulation in the CA1 area of the rat hippocampus. *J. Neurosci.* **15**(10), 6542–6551.

Bernard, C. and Wheal, H. V. (1996) A role for synaptic and network plasticity in controlling epileptiform activity in the CA1 in the kainic acid-lesioned rat hippocampus in vitro. *J. Physiol., Lond.* **495,** 127–142.

Bernard, C., Cannon, R. C., Ben-Ari, Y. and Wheal, H. V. (1997) A model of spatial-temporal propagation of action potentials in the Schaffer collateral pathway of the CA1 area of the rat hippocampus. *Hippocampus* **7,** 58–72.

Best, N., Mitchell, J., Baimbridge, K. G. and Wheal, H. V. (1993) Changes in the parvalbumin-immunoreactive neurons in the rat hippocampus following a kainic acid lesion. *Neurosci. Lett.* **15,** 1–6.

Best, N., Mitchell, J. and Wheal, H. V. (1994) Ultrastructure of parvalbumin-immunoreactivie neurons in the CA1 area of the rat hippocampus following kainic acid injection. *Acta Neuropath.* **87,** 187–195.

Bliss, T. V. P. and Collingridge, G. (1993) A synaptic model of memory: long-term potentiation in the hippocampus. *Nature* **361,** 31–39.

Bliss, T. V. P., Lancaster, B. and Wheal, H. V. (1983) Long-term potentiation in commissural and Schaffer projections to hippocampal CA1 cells: an in vivo study in the rat. *J. Physiol., Lond.* **341,** 617–626.

Bonner, J. C., Badgett, A., Hoffmann, M. and Lindroos, P. M. (1995) Inhibition of platelet-derived growth factor-BB-induced fibroblast proliferation by plasmin-activated alpha-2-macroglobulin is mediated via an alpha 2-macroglobulin receptor/low density lipoprotein receptor-related protein-dependent mechanism. *J. biol. Chem.* **270,** 6389–6395.

Boyles, J. K., Pitas, R. E., Wilson, E., Mahley, R. W. and Taylor, J. M. (1985) Apolipoprotein E associated with astrocytic glia of the central nervous system and with nonmyelinating glia of the peripheral nervous system. *J. clin. Invest.* **76,** 1501–1513.

Brakeman, P. R., Lanahan, A. A., O'Brien, R., Roche, K., Barnes, C. A., Huganir, R. L. and Worley, P. F. (1997) Homer: a protein that selectively binds metabotropic glutamate receptors. *Nature* **386,** 284–288.

Brenman, J. E. and Bredt, D. S. (1996) Nitric oxide signaling in the nervous system. *Meth. Enzymol.* **269,** 119–129.

Brenman, J. E., Chao, D. S., Gee, S. H., McGee, A. W., Craven, S. E., Santillano, D. R., Wu, Z., Huang, F., Xia, H., Peters, M. F., Froehner, S. C., Bredt, D. S. (1996) Interaction of nitric oxide synthase with the postsynaptic density protein PSD-95 and alpha1-syntrophin mediated by PDZ domains. *Cell* **84,** 757–767.

Brown, M. and Goldstein, J. L. (1986) A receptor mediated pathway for cholesterol homeostasis. *Science* **232,** 34–47.

Bu, G. and Rennke, S. (1996) Receptor asociated protein is a folding chaperone for low density lipoprotein receptor related protein. *J. biol. Chem.* **271,** 22218–22224.

Bu, G., Williams, S., Strickland, D. K. and Schwartz, A. L. (1992) Low density lipoprotein receptor-related/a2-macroglobulin receptor is an hepatic receptor for tissue-type plasminogen activator. *Proc. natl Acad. Sci. U. S. A.* **89,** 7426–7431.

Bu, G., Maksymovitch, E. A., Geuze, H. and Schwartz, A. L. (1994a) Subcellular localization and endocytotic function of low density lipoprotein receptor-related protein in human glioblastoma cells. *J. biol. Chem.* **269,** 29874–29882.

Bu, G., Maksymovitch, E. A., Nerbonne, J. M. and Schwartz, A. L. (1994b) Expression and function of the low density lipoprotein receptor-related protein (LRP) in mammalian central neurons. *J. biol. Chem.* **269,** 18521–18528.

Cabral, J. H., Petosa, C., Sutcliffe, M. J., Raza, S., Byron, O., Poy, F., Marfatia, S. M., Chishti, A. H. and Liddington, R. C. (1996) Crystal structure of a PDZ domain. *Nature* **382,** 649–652.

Campos-Ortega, J. A. (1996) Numb divers notch pathway off the tramtrack. *Neuron* **17,** 1–4.

Castano, E. M., Prelli, F., Wisniewski, T., Golabek, A., Kumar, R. A., Soto, C. and Frangione, B. (1995) Fibrillogenesis in Alzheimer's disease of amyloid beta peptides and apolipoprotein E. *Biochem. J.* **306,** 599–604.

Cavazos, J. E., Golarai, G. and Sutula, T. P. (1991) Mossy fibre synaptic reorganisation induced by kindling: tcme course of development, progression and permanence. *J. Neurosci.* **11,** 2795–2803.

Chang, F-L. F. and Greenough, W. T. (1984) Transient and enduring morphological correlates of synaptic activity and efficacy change in the rat hippocampal slice. *Brain Res.* **309,** 35–46.

Chappell, D. A., Inoue, I., Fry, G. L., Pladet, M. W., Bowen, S. L., Iverius, P. H., Lalouel, J. M. and Strickland, D. K. (1994) Cellular catabolism of normal very low density lipoproteins via the low density lipoprotein receptor-related protein/alpha 2-macroglobulin receptor is induced by the C-terminal domain of lipoprotein lipase. *J. biol. Chem.* **269,** 18001–18006.

Chen, S. and Hillman, D. E. (1982) Marked reorganisation of Purkinje cell dendrites and spines in adult rat following vacation of synapses due to deafferentation. *Brain Res.* **245,** 131–135.

Chen, H., Sottile, J., Strickland, D. K. and Mosher, D. F. (1996a) Binding and degradation of thrombospondin-1 mediated through heparan suphate proteoglycans and low density-lipoprotein receptor-related protein: localization of the functional activity to the trimeric N-terminal heparin-binding region of thrombospondin-1. *Biochem. J.* **318,** 959–963.

Chen, H., Strickland, D. K. and Mosher, D. F. (1996b) Metabolism of thrombospondin 2. Binding and degradation by 3T3 cells and glycosaminoglycan-variant Chinese hamster ovary cells. *J. biol. Chem.* **271,** 15993–15999.

Chen, Y., Chad, J. E., Cannon, R. C. and Wheal, H. V. (1998) Reduced Mg^{++} blockade of synaptically activated *N*-methyl-D-aspartate receptor channels in CA1 pyramidal neurones in kainic acid-lesioned rat hippocampus. *Neuroscience* in press.

Cho, K. O., Hunt, C. A. and Kennedy, M. B. (1992) The rat brain postsynaptic density fraction contains a homolog of the Drosophila discs–large tumor suppressor protein. *Neuron* **9,** 929–942.

Christian, E. P. and Dudek, F. E. (1988) Electrophysiological evidence from glutamate microapplications for local excitatory circuits in the CA1 area of rat hippocampal slices. *J. Neurophysiol.* **59,** 110–123.

Cifuentes-Diaz, C., Nicolet, M., Goudou, D., Rieger, F. and Mege, R. M. (1994) *N*-cadherin expression in developing, adult and denervated chicken neuromuscular system: accumulations at both the neuromuscular junction and the node of Ranvier. *Development* **120,** 1–11.

Cifuentes-Diaz, C., Padilla, F., Facchinetti, P., Nicolet, M., Mege, R. M. and Rieger, F. (1996) M-cadherin distribution in the mouse adult neuromuscular system suggest a role in muscle innervation. *Eur. J. Neurosci.* **8,** 1666–1676.

Cohen, N. A., Brenman, J. E., Snyder, S. H. and Bredt, D. S. (1996) Binding of the inward rectifier K^+ channel Kir 2.3 to PSD-95 is regulated by protein kinase A phosphorylation [see comments]. *Neuron* **17,** 759–767.

Cohen, R. S., Blomberg, F., Berzins, K. and Siekevitz, P. (1977) The structure of postsynaptic densities isolated from dog cerebral cortex. I. Overall morphology and protein composition. *J. Cell Biol.* **74,** 181–203.

Conese, M., Nykjaer, A., Petersen, C. M., Cremona, O., Pardi, R., Andreasen, P. A., Gliemann, J., Christensen, E. I. and Blasi, F. (1995) Alpha2-macroglobulin receptor/Ldl receptor related protein (Lrp)-dependent internalization of the urokinase receptor. *J. Cell Biol.* **131,** 1609–1622.

Cornish, S. and Wheal, H. V. (1989) Long-term loss of paired pulse inhibition in the kainic acid-lesioned hippocampus of the rat. *Neuroscience* **28,** 563–571.

Cotman, C. W., Taylor, D. and Lynch, G. (1973) Ultrastructural changes in synapses in the dentate gyrus of the rat during development. *Brain Res.* **63,** 205–215.

Craig, A. M., Blackstone, C. D., Huganir, R. L. and Banker, G. (1993) The distribution of glutamate receptors in cultured rat hippocampal neurons: postsynaptic clustering of AMPA-selective subunits. *Neuron* **10,** 1055–1068.

Cremer, H., Lange, R., Christoph, A., Plomann, M., Vopper, G., Roes, J., Brown, R., Baldwin, S., Kraemer, P., Scheff, S., Barthels, D., Rajewsky, K. and Wille, W. (1994) Inactivation of the NCAM gene in mice results in size-reduction of the olfactory bulb and deficits in spatial learning. *Nature* **367,** 455–459.

Cremer, H., Chazal, G., Goridis, C. and Represa, A. (1997) NCAM is essential for axonal growth and fasciculation in the hippocampus. *Mol. cell. Neurosci.* **8,** 323–335.

Davenport, C. J., Brown, W. J. and Babb, T. L. (1990) Sprouting of GABAergic and mossy fiber axons in dentate gyrus following intrahippocampal kainate in the rat. *Exp. Neurol.* **109,** 180–190.

Davis, C. G., Goldstein, J. L., Südhof, T. C., Anderson, R. G. W., Russel, D. W. and Brown, M. S. (1987) Acid-dependent ligand dissociation and recycling of LDL receptor mediated by growth factor homology region. *Nature* **326,** 760–765.

Davis, G. W., Schuster, C. M. and Goodman, C. S. (1996) Genetic dissection of structural and functional components of synaptic plasticity. III. CREB is necessary for presynaptic functional plasticity. *Neuron* **17,** 669–679.

DeLanerolle, N. C., Kim, J. H., Robbins, R. J. and Spencer, D. D. (1989) Hippocampal interneuron loss and plasticity in human temporal lobe epilepsy. *Brain Res.* **495,** 387–395.

Deuchars, J. and Thomson, A. M. (1996) CA1 pyramid-pyramid connections in rat hippocampus in-vitro dual intracellular-recordings with biocytin filling. *Neuroscience* **74,** 1009–1018.

Doherty, P., Moolenaar, C. E., Ashton, S. V., Michalides, R. J. and Walsh, F. S. (1992) The VASE exon down-regulates the neurite growth-promoting activity of NCAM 140. *Nature* **356,** 791–793.

Dong, H., O'Brien, R. J., Fung, E. T., Lanahan, A. A., Worley, P. F. and Huganir, R. L. (1997) GRIP: a synaptic PDZ domain-containing protein that interacts with AMPA receptors. *Nature* **386,** 279–284.

Dong, L. M. and Weisgraber, K. H. (1996) Human apolipoprotein E4 domain interaction. Arginine 61 and glutamic acid 255 interact to direct the preference for very low density lipoproteins. *J. biol. Chem.* **271,** 19053–19057.

Dong, L. M., Wilson, C., Wardell, M. R., Simmons, T., Mahley, R. W., Weisgraber, K. H. and Agard, D. A. (1994) Human apolipoprotein E. Role of arginine 61 in mediating the lipopro-

tein preferences of the E3 and E4 isoforms. *J. biol. Chem.* **269,** 22358–22365.

Doyle, E., Nolan, P. M., Bell, R. and Regan, C. M. (1992) Hippocampal NCAM 180 transiently increases sialylation during the acquisition and consolidation of a passive avoidance response in adult rat. *J. Neurosci. Res.* **31,** 513–523.

Doyle, D. A., Lee, A., Lewis, J., Kim, E., Sheng, M. and MacKinnon, R. (1996) Crystal structures of a complexed and peptide-free membrane protein-binding domain: molecular basis of peptide recognition by PDZ. *Cell* **85,** 1067–1076.

von Eckardstein, A., Huang, Y., Wu, S., Funke, H., Noseda, G. and Assmann, G. (1995) Reverse cholesterol transport in plasma of patients with different forms of familial HDL deficiency. *Arterioscler. Thromb. Vasc. Biol.* **15,** 691–703.

Ehlers, M. D., Tingley, W. G. and Huganir, R. L. (1995) Regulated subcellular distribution of the NR1 subunit of the NMDA receptor. *Science* **269,** 1734–1737.

Errington, M. L., Bliss, T. V. P., Morris, R. J., Laroche, S. and Davis, S. (1997) Long-term potentiation in awake mutant mice. *Nature* **387,** 666–667.

Fagan, A. M., Bu, G., Sun, Y., Daugherty, A. and Holtzman, D. M. (1996) Apolipoprotein E-containing high density lipoprotein promotes neurite outgrowth and is a ligand for the low density lipoprotein receptor-related protein. *J. biol. Chem.* **271,** 30121–30125.

Fagotto, F., Guger, K. and Gumbiner, B. M. (1997) Induction of the primary dorsalizing center in Xenopus by the Wnt/GSK/beta-catenin signaling pathway, but not by Vgl, activin or noggin. *Development* **124,** 453–460.

Faissner, A. and Schachner, M. (1995) Tenascin and Janusin: Glial recognition molecules involved in neural development and recognition. In: *Neuroglia*, pp. 422–426. Eds H. Kettenmann and B. R. Ransom. Oxford University Press, New York.

Fannon, A. M. and Colman, D. R. (1996) A model for central synaptic junctional complex formation based on the differential adhesive specificities of the cadherins. *Neuron* **17**(3), 423–434.

Farrant, M., Feldmeyer, D., Takahashi, T. and Cull-Candy, S. G. (1994) NMDA-receptor channel diversity in the developing cerebellum. *Nature* **368,** 335–339.

Fazeli, M. S., Breen, K. C., Errington, M. L. and Bliss, T. V. P. (1994) Increase in extracellular NCAM and amyloid precursor protein following induction of long-term potentiation in the dentate gyrus of anesthetized rats. *Neurosci. Lett.* **169,** 77–80.

Froehner, S. C. (1993) Regulation of ion channel distribution at synapses. *A. Rev. Neurosci.* **16,** 347–368.

Fukamauchi, F., Mataga, M., Wang, Y. J., Sato, S., Youshiki, A. and Kusakabe, M. (1996) Abnormal behavior and neurotransmissions of tenascin gene knockout mouse. *Biochem. biophys. Res. Commun.* **221,** 151–156.

Gafvels, M. E., Coukos, G., Sayegh, R., Coutifaris, C., Strickland, D. K. and Strauss, J. F. (1992) Regulated expression of the trophoblast a2-macroglobulin receptor/low-density lipoprotein receptor related protein. *J. biol. Chem.* **267,** 21230–21234.

Gafvels, M. E., Paavola, L. G., Boyd, C. O., Nolan, P. M., Wittmaack, F., Chawla, A., Lazar, M. A., Bucan, M., Angelin, B. and Strauss, J. F. I. (1994) Cloning of a complementary deoxyribonucleic acid encoding the murine homolog of the very low density lipoprotein/apolipoprotein-E receptor: expression pattern and assignment of the gene to mouse chromosome 19. *Endocrinology* **135,** 387–394.

Garcia, M. A., Vazquez, J., Gimenez, C., Valdivieso, F. and Zafra, F. (1996) Transcription factor AP-2 regulates human apolipoprotein E gene expression in astrocytoma cells. *J. Neurosci.* **16,** 750–756.

Godyna, S., Liau, G., Popa, I., Stefansson, S. and Argraves, W. S. (1995) Identification of the low density lipoprotein receptor related protein (LRP) as an endocytotic receptor for thrombospondin-1. *J. cell. Biol.* **129,** 1403–1410.

Goldowitz, D., Scheff, S. W. and Cotman, C. W. (1979) The specificity of reactive synaptogenesis: a comparative study in the adult rat hippocampal formation. *Brain Res.* **170,** 427–441.

Goodman, C. S. (1996) Mechanisms and molecules that control growth cone guidance. *A. Rev. Neurosci.* **19,** 341–377.

Gordon, I., Grauer, E., Genis, I., Sehayek, E. and Michaelson, D. M. (1995) Memory deficits and cholinergic impairments in apolipoprotein E-deficient mice. *Neurosci. Lett.* **199,** 1–4.

Gottlieb, D. I. and Cowan, W. M. (1973) Autoradiographic studies of the commissural and ispsilateral associational connections of the hippocampus and dentate gyrus of the rat. *J. comp. Neurol.* **149,** 393–422.

Haass, C. (1997) Presenilins: Genes for life and death. *Neuron* **18,** 687–690.

Harris, K. M. and Stevens, J. K. (1989) Dendritic spines of CA1 pyramidal cells in the rat hippocampus: serial electron microscopy with reference to their biophysical characteristics. *J. Neurosci.* **9,** 2982–2987.

Harris, K. M. and Kater, S. B. (1994) Dendritic spines, cellular specializations imparting both stability and flexibility to synaptic function. *A. Rev. Neurosci.* **17,** 342–371.

Hata, Y., Butz, S. and Sudhof, T. C. (1996) CASK: a novel dlg/PSD95 homolog with an N-terminal calmodulin-dependent protein kinase domain identified by interaction with neurexins. *J. Neurosci.* **16,** 2488–2494.

Heegard, C. W., Simonson, A. C., Oka, K., Kjoller, L., Christensen, A., Madsen, B., Ellgaard, L., Chan, L. and Andreasen, P. A. (1995) Very low density lipoprotein receptor binds and mediates endocytosis of urokinase-type plasminogen activator inhibitor complex. *J. biol. Chem.* **270,** 20855–20861.

Hemming, N. J., Anstee, D. J., Staricoff, M. A., Tanner, M. J. and Mohandas, N. (1995) Identification of the membrane attachment sites for protein 4.1 in the human erythrocyte. *J. biol. Chem.* **270,** 5360–5366.

Herz, J., Hamann, U., Rogne, S., Myklebost, O., Gausepohl, H. and Stanley, K. K. (1988) Surface location and high affinity for calcium of a 500 kD liver membrane protein closely related to the LDL-Receptor suggest a physiological role as lipoprotein receptor. *EMBO J.* **7,** 4119–4127.

Herz, J., Kowal, R. C., Ho, J. K., Brown, M. S. and Goldstein, Y. L. (1990a) Low density lipoprotein receptor-related protein mediates endocytosis of monoclonal antibodies in cultured cells and in rabbit liver. *J. biol. Chem.* **265,** 21355–21362.

Herz, J., Kowal, R. C., Goldstein, J. L. and Brown, M. S. (1990b) Proteolytic processing of the 600 kD low density lipoprotein receptor-related protein (LRP) occurs in a trans-Golgi compartment. *EMBO J.* **9,** 1769–1776.

Herz, J., Goldstein, J. L., Strickland, D. K., Ho, Y. K. and Brown, M. S. (1991) 39-kDa protein modulates binding of ligands to low density lipoprotein receptor-related protein/a2-macroglobulin receptor. *J. biol. Chem.* **266,** 21232–21238.

Hodits, R. A., Nimpf, J., Pfistermüller, D. M., Hiesberger, T., Schneider, W. J., Vaughan, T. J., Johnsoon, K. S., Haumer, M., Kuechler, E. and Winter, G. (1995) An antibody fragment from a phage display library competes for ligand binding to the low density lipoprotein receptor family and inhibits rhinovirus infection. *J. biol. Chem.* **270,** 24078–24085.

Hoffman, K. B., Kessler, M. and Lynch, G. (1996) Adhesion molecules and synaptic function; evidence that alterations in neural cell adhesion molecule (NCAM) affect the binding affinity of AMPA receptors. *Soc. Neurosci. Abstr.* **237,** 13.

Hollister, R. D., Kisiel, W. and Hyman, B. T. (1996) Immunohistochemical localization of tissue factor pathway inhibitor-1 (TFPI-1), a Kunitz proteinase inhibitor, in Alzheimer's disease. *Brain Res.* **728,** 13–19.

Holtzmann, D. M., Pitas, R. E., Kilbridge, J., Nathan, B., Mahley, R. W. and Bu, G. (1995) Low density lipoprotein receptor-related protein mediates apolipoprotein E-dependent neurite outgrowth in a central nervous system-derived neuronal cell line. *Proc. natl Acad. Sci. U. S.A.* **92,** 9480–9484.

Horn, I. R., Moestrup, S. K., van den Berg, B. M., Pannekoek, H., Nielsen, M. S. and Zonneveld, A. J. (1995) Analysis of the binding of pro-urokinase and urokinase-plasminogen activator inhibitor-1 complex to the low density lipoprotein receptor-related protein using Fab fragment selected from a phage-displayed Fab library. *J. biol. Chem.* **270,** 11770–11775.

Houser, C. R., Miyashiro, J. E., Swart, B. E., Walsh, G. O., Rich, J. R. and Delgado-Escueta, A. V. (1990) Altered patterns of dynorphin immunoreactivity suggest mossy fibre reorganisation in human hippocampal epilepsy. *J. Neurosci.* **10,** 257–282.

Howard, G. C., Yamaguchi, Y., Misra, U. K., Gawdi, G., Nelsen, A., DeCamp, D. L. and Pizzo, S. V. (1996) Selective mutations in cloned and expressed alpha-macroglobulin receptor binding fragment alter binding to either the alpha2-macroglobulin signaling receptor or the low density lipoprotein receptor-related protein/alpha2-macroglobulin receptor. *J. biol. Chem.* **271,** 14105–14111.

Hsueh, Y.-P., Kim, E. and Sheng, M. (1997) Disulfide-linked head-to-head multimerization in the mechanism of ion channel clustering by PSD-95. *Neuron* **18,** 803–814.

Huang, Y., von Eckardstein, A., Wu, S., Maeda, N. and Assmann, G. (1994) A plasma lipoprotein containing only apo E and with gamma-mobility on electrophoresis releases cholesterol from cells. *Proc. natl Acad. Sci. U. S.A.* **91,** 1834–1838.

Huber, O., Bierkamp, C. and Kemler, R. (1996a) Cadherins and catenins in development. *Curr. Opin. Cell Biol.* **8,** 685–691.

Huber, O., Korn, R., McLaughin, J., Ohsugi, M., Herrmann, B. G. and Kemler, R. (1996b) Nuclear localization of beta-catenin by interaction with transcription factor LEF-1. *Mechanisms Dev.* **59,** 3–10.

Hunt, C. A., Schenker, L. J. and Kennedy, M. B. (1996) PSD-95 is associated with the postsynaptic density and not with the presynaptic membrane at forebrain synapses. *J. Neurosci.* **16,** 1380–1388.

Ishiguro, M., Imai, Y. and Kohsaka, S. (1995) Expression and distribution of low density lipoprotein receptor-related protein mRNA in the rat central nervous system. *Mol. Brain Res.* **33,** 37–46.

Ishizuka, N., Webber, J. and Amaral, D. G. (1990) Organisation of intrahippocampal projections originating from CA3 pyramidal cells in the rat. *J. comp. Neurol.* **295,** 580–623.

Jacobsen, L., Madsen, P., Moestrup, S. K., Lund, A. H., Tommerup, N., Nykjaer, A., Sottrup-Jensen, L., Gliemann, J. and Petersen, C. M. (1996) Molecular characterization of a novel human hybrid-type receptor that binds the alpha2-macroglobulin receptor-associated protein. *J. biol. Chem.* **271,** 31379–31383.

Jensen, P. H., Moestrup, S. K., Sottrup-Jensen, L., Petersen, C. M. and Glieman, J. (1988) Receptors for alpha 2-macroglobulin- and pregnancy zone protein-proteinase complexes in the human placental syncytiotrophoblast. *Placenta* **9,** 463–477.

Jokinen, E. V., Landschulz, K. T., Wyne, K. L., Ho, Y. K., Frykman, P. K. and Hobbs, H. H. (1994) Regulation of the very low density lipoprotein receptor by thyroid hormone in rat skeletal muscle. *J. biol. Chem.* **269,** 26411–26418.

Jones, K. A. and Baughman, R. W. (1991) Both NMDA and non-NMDA subtypes of glutamate receptors are concentrated at synapses on cerebral cortical neurons in culture. *Neuron* **7,** 593–603.

Kamdar, K. P., Shelton, M. E. and Finnerty, V. (1994) The Drosophila molybdenum cofactor gene cinnamon is homologous to three *Escherichia coli* cofactor proteins and to the rat protein gephyrin. *Genetics* **137,** 791–801.

Kawamata, T., Tooyama, I., Yamada, T., Walker, D. G. and McGeer, P. L. (1993) Lactotransferrin immunocytochemistry in Alzheimer and normal human. *Am. J. Pathol.* **142,** 1574–1585.

Keller, F. and Schachner, S. (1990) Neuro-specific membrane glycoproteins promoting neurite fasciculation in *Aplysia california*. *J. cell. Biol.* **111,** 2637–2650.

Kennedy, M. B. (1993) The postsynaptic density. *Curr. opin. Neurobiol.* **3,** 732–737.

Kennedy, M. B. (1997) The postsynaptic density at glutamatergic synapses. *TINS* **20,** 264–268.

Kerwin, J. F., Jr, Lancaster, J. R., Jr and Feldman, P. L. (1995) Nitric oxide: a new paradigm for second messengers. *J. med. Chem.* **38,** 4343–4362.

Kim, E., Niethammer, M., Rothschild, A., Jan, Y. N. and Sheng, M. (1995) Clustering of Shaker-type K^+ channels by interaction with a family of membrane-associated guanylate kinases. *Nature* **378,** 85–88.

Kim, D. H., Iijma, H., Goto, K., Sakai, J., Ishii, H., Kim, H. J., Suzuki, H., Kondo, H., Saeki, S. and Yamamoto, T. (1996a) Human apolipoprotein E receptor 2. *J. biol. Chem.* **271,** 8373–8380.

Kim, E., Cho, K. O., Rothschild, A. and Sheng, M. (1996b) Heteromultimerization and NMDA receptor-clustering activity of Chapsyn-110, a member of the PSD-95 family of proteins. *Neuron* **17,** 103–113.

Kim, E., Naisbitt, S., Hsueh, Y.-P., Rao, A., Rothschild, A., Craig, A. M. and Sheng, M. (1997) GKAP, a novel synaptic protein that interacts with the guanylate kinase-like domain of the PSD-95/SAP90 family of channel clustering molecules. *J. Cell Biol.* **136,** 669–678.

Kirsch, J. and Betz, H. (1993) Widespread expression of gephyrin, a putative receptor-tubulin linker protein, in rat brain. *Brain Res.* **621,** 301–310.

Kirsch, J. and Betz, H. (1995) The postsynaptic localization of the glycine receptor-associated protein gephyrin is regulated by the cytoskeleton. *J. Neurosci.* **15,** 4148–4156.

Kirsch, J., Malosio, M.-L., Wolters, I. and Betz, H. (1993a) Distribution of gephyrin transcripts in the adult and developing rat brain. *Eur. J. Neurosci.* **5,** 1109–1117.

Kirsch, J., Wolters, I., Triller, A. and Betz, H. (1993b) Gephyrin antisense oligonucleotides prevent glycine receptor clustering in spinal neurons. *Nature* **366,** 745–748.

Kirsch, J., Kuhse, J. and Betz, H. (1995) Targeting of glycine receptor subunits to gephyrin-rich domains in transfected human embryonic kidney cells. *Mol. cell. Neurosci.* **6,** 450–461.

Kirsch, J., Langosch, D., Prior, P., Littauer, U. Z., Schmitt, B. and Betz, H. (1991) The 93-kDa glycine receptor-associated protein binds to tubulin. *J. biol. Chem.* **266,** 22242–22245.

Kistner, U., Wenzel, B. M., Veh, R. W., Cases-Langhoff, C., Garner, A. M., Appeltauer, U., Voss, B., Gundelfinger, E. D. and Garner, C. C. (1993) SAP90, a rat presynaptic protein related to the product of the Drosophila tumor suppressor gene dlg-A. *J. biol. Chem.* **268,** 4580–4583.

Kistner, U., Garner, C. C. and Linial, M. (1995) Nucleotide binding by the synapse associated protein SAP90. *FEBS Lett.* **359,** 159–163.

Kohr, G., De Konnick, Y. and Mody, I. (1993) Properties of NMDA receptor channels in neurons acutely isolated from epileptic (kindled) rats. *J. Neurosci.* **13,** 3615–3627.

Kornau, H. C., Schenker, L. T., Kennedy, M. B. and Seeburg, P. H. (1995) Domain interaction between NMDA receptor subunits and the postsynaptic density protein PSD-95. *Science* **269,** 1737–1740.

Kounnas, M. Z., Argraves, W. S. and Strickland, D. K. (1992) The 39-kDa receptor-associated protein interacts with two members of the low density lipoprotein receptor family, a2-macroglobulin receptor and glycoprotein 330. *J. biol. Chem.* **267,** 21162–21166.

Kounnas, M. Z., Cahppel, D. A., Wong, H., Argraves, W. S. and Strickland, D. K. (1995a) The cellular internalization and degradation of hepatic lipase is mediated by low density lipoprotein receptor-related protein and requires cell surface proteoglycans. *J. biol. Chem.* **270,** 9307–9312.

Kounnas, M. Z., Moir, R. D., Rebeck, G. W., Bush, A. I., Argraves, W. S., Tanzi, R. E., Hyman, B. T. and Strickland, D. K. (1995b) LDL receptor-related protein, a multifunctional apo E receptor, binds secreted beta-amyloid precursor protein and mediates its degradation. *Cell* **82,** 331–340.

Kounnas, M. Z., Church, F. C., Argraves, W. S. and Strickland, D. K. (1996) Cellular internalization and degradation of antithrombin III-thrombin, heparin cofactor II-thrombin, and alpha1-antitrypsin-trypsin complexes is mediated by the low density lipoprotein receptor-related protein. *J. biol. Chem.* **271,** 6523–6529.

Kowal, R. C., Herz, J., Goldstein, J. L., Esser, V. and Brown, M. S. (1989) Low density lipoprotein receptor-related protein mediates uptake of cholesteryl esters derived from apoprotein E-enriched lipoproteins. *Proc. natl Acad. Sci. U. S.A.* **86,** 5810–5814.

Kuhse, J., Laube, B., Magalei, D. and Betz, H. (1993) Assembly of the inhibitory glycine receptor: identification of amino acid sequence motifs governing subunit stoichiometry. *Neuron* **11,** 1049–1056.

Kuhse, J., Betz, H. and Kirsch, J. (1995) The inhibitory glycine receptor: architecture, synaptic localization and molecular pathology of a postsynaptic ion-channel complex. *Curr. Opin. Neurobiol.* **5,** 318–323.

Kypta, R. M., Su, H. and Reichardt, L. F. (1996) Association between a transmembrane protein tyrosine phosphatase and the cadherin–catenin complex. *J. Cell Biol.* **134,** 1519–1529.

Lahey, T., Gorczyca, M., Jia, X. X. and Budnik, V. (1994) The Drosophila tumor suppressor gene dlg is required for normal synaptic bouton structure. *Neuron* **13,** 823–835.

Lalazar, A., Weisgraber, K. H., Rall, S. C., Giladi, H., Innerarity, T. L., Levanon, A. Z., Boyles, J. K., Amit, B., Gorecki, M., Mahley, R. W. and Vogel, T. (1988) Site-specific mutagenesis of human apolipoprotein E. Receptor binding activity of variants with single amino acid substitutions. *J. biol. Chem.* **263,** 3542–3545.

Lancaster, B. and Wheal, H. V. (1982) A comparative histological and electrophysiological study of some neurotoxins in the rat hippocampus. *J. comp. Neurol.* **211,** 105–114.

Lau, L. F., Mammen, A., Ehlers, M. D., Kindler, S., Chung, W. J., Garner, C. C. and Huganir, R. L. (1996) Interaction of the *N*-methyl-D-aspartate receptor complex with a novel synapse-associated protein, SAP102. *J. biol. Chem.* **271,** 21622–21628.

Laurie, D. J. and Seeburg, P. H. (1994) Ligand affinities at recombinant NMDA receptors depend on subunit composition. *Eur. J. Pharmac. (Molec. Pharmac.)* **268,** 335–345.

Laurie, D. J., Seeburg, P. H. and Wisden, W. (1992) The distribution of 13 GABAA receptor subunit mRNAs in the rat brain. II. Olfactory bulb and cerebellum. *J. Neurosci.* **12,** 1063–1076.

Lee, K. S., Schottler, F., Oliver, M. and Lynch, G. (1980) Brief bursts of high frequency stimulation produce two types of structural change in rat hippocampus. *J. Neurophys.* **44,** 247–258.

Lee, M. K., Slunt, H. H., Martin, L. J., Thinakaran, G., Kim, G., Gandy, S. E., Seeger, M., Koo, E., Price, D. L. and Sisodia, S. S. (1996) Expression of presenilin 1 and 2 (PS1 and PS2) in human and murine tissues. *J. Neurosci.* **16,** 7513–7525.

Legendre, P., Rosenmund, C. and Westbrook, G. L. (1993) Inactivation of NMDA channels in cultured hippocampal neurons by intracellular calcium. *J. Neurosci.* **13,** 674–684.

Lin, C. T., Xu, Y., Wu, J. Y. and Chan, L. (1986) Immunoreactive apolipoprotein E is a widely distributed cellular protein. Immunohistochemical localization of apolipoprotein E in baboon tissues. *J. clin. Invest.* **78,** 947–958.

Lopes, M. B., Bogaev, C. A., Gonias, S. L. and Vanden Berg, S. R. (1994) Expression of alpha 2-macroglobulin receptor/low density lipoprotein receptor-related protein is increased in reactive and neoplastic glial cells. *FEBS Lett.* **338,** 301–305.

Lovestone, S., Anderton, B. H., Hartley, C., Jensen, T. G. and Jorgensen, A. L. (1996) The intracellular fate of apolipoprotein E is tau dependent and apoe allele-specific. *Neuroreport* **7,** 1005–1008.

Lüthi, A., Laurent, J. P., Figurov, A., Müller, D. and Schachner, M. (1994) Hippocampal long-term potentiation and neural cell adhesion molecules L1 and NCAM. *Nature* **372,** 777–779.

Ma, J., Yee, A., Brewer, H.Bj., Das, S. and Potter, H. (1994) Amyloid-associated proteins alpha 1-antichymotrypsin and apolipoprotein E promote assembly of Alzheimer beta-protein into filaments. *Nature* **372,** 92–94.

Mahley, R. W. (1988) Apolipoprotein E: cholesterol transport protein with expanding role in cell biology. *Science* **240,** 622–630.

Mahley, R. W. (1996) Heparan sulfate proteoglycan/low density lipoprotein receptor-related protein pathway involved in type III hyperlipoproteinemia. *Isr. J. med. Sci.* **32,** 414–429.

Malosio, M.-L., Marqueze-Pouey, B., Kuhse, J. and Betz, H. (1991) Widespread expression of glycine receptor subunit mRNAs in the adult and developing brain. *EMBO J.* **10,** 2401–2409.

Marchetti, M., Longhi, C., Conte, M. P., Pisani, S., Valenti, P. and Seganti, L. (1996) Lactoferrin inhibits herpes simplex virus type 1 adsorption to Vero cells. *Antiviral Res.* **29,** 221–231.

Marfatia, S. M., Leu, R. A., Branton, D. and Chishti, A. H. (1995) Identification of the protein 4.1 binding interface on glycophorin C and p55, a homologue of the Drosophila discs-large tumor suppressor protein. *J. biol. Chem.* **270,** 715–719.

Marfatia, S. M., Cabral, J. H., Lin, L., Hough, C., Bryant, P. J., Stolz, L. and Chishti, A. H. (1996) Modular organization of the PDZ domains in the human discs-large protein suggests a mechanism for coupling PDZ domain-binding proteins to ATP and the membrane cytoskeleton. *J. Cell Biol.* **135,** 753–766.

Martin, K. C., Michael, D., Rose, J. C., Barad, M., Casadio, A., Zhu, H. and Kandel, E. R. (1997) MAP kinase translocates into the nucleus of the presynaptic cell and is required for long-term facilitation in Aplysia. *Neuron* **18,** 899–912.

März, W., Beckmann, A., Scharnagl, H., Siekmeier, R., Mondorf, U., Held, I., Schneider, W., Preissner, K. T., Curtiss, L. K., Groß, W. and Hüttinger, M. (1993) Heterogenous lipoprotein (a) size isoforms differ by their interaction with the low density lipoprotein receptor and the low density lipoprotein receptor-related protein/a2-macroglobulin. *FEBS Lett.* **325,** 271–275.

Masliah, E., Mallory, M., Ge, N., Alford, M., Veinbergs, I. and Roses, A. D. (1995) Neurodegeneration in the central nervous system of apoE-deficient mice. *Exp. Neurol.* **136,** 107–122.

Matter, K., Hunziker, W. and Mellmann, I. (1992) Basolateral sorting of LDL receptor in MDCK cells: the cytoplasmmic domain contains two tyrosine-dependent targeting determinants. *Cell* **71,** 741–753.

Matzenbach, B., Maulet, Y., Sefton, L., Courtier, B., Avner, P., Guénet, J.-L. and Betz, H. (1994) Structural analysis of mouse glycine receptor a subunit genes: identification and chromosomal localization of a novel variant, a4. *J. biol. Chem.* **269,** 2607–2612.

Mayford, M., Barzilai, A., Keller, F., Schachner, S. and Kandel, E. R. (1992) Modulation of an NCAM-related adhesion molecule with long-term synaptic plasticity in Aplysia. *Science* **256,** 638–644.

Meilinger, M., Haumer, M., Szakmary, K., Steinböck, F., Scheiber, B., Goldenberg, H. and Huettinger, M. (1995) Removal of lactoferrin by liver is mediated by binding to low density lipoprotein receptor-related protein/a2-macroglobulin receptor and transport to endosomes. *FEBS Lett.* **360,** 70–74.

Metzger, M., Wang, J., Braun, K. and Schachner, M. (1995) Influence of the extracellular matrix protein tenascin on auditory filial imprinting in the domestic chick. *Soc. Neurosci. Abstr.* **21,** 1451.

Meyer, G., Kirsch, J., Betz, H. and Langosch, D. (1995) Identification of a gephyrin binding motif on the glycine receptor b subunit. *Neuron* **15,** 563–572.

Misra, U. K., Chu, C. T., Gawdi, G. and Pizzo, S. V. (1994) The relationship between low density lipoprotein-related protein/alpha 2-macroglobulin (alpha 2M) receptors and the newly described alpha 2M signaling receptor. *J. biol. Chem.* **269,** 18303–18306.

Misra, U. K., Gawdi, G. and Pizzo, S. V. (1996) Binding of rat alpha 1-inhibitor-3-methylamine to the alpha 2-macroglobulin signaling receptor induces second messengers. *J. Cell Biochem.* **61,** 61–71.

Mitchell, J., Sundstrom, L. E. and Wheal, H. V. (1993) Microglial and astrocytic cell responses in the rat hippocampus after an intracerebroventricular kainic acid injection. *Exp. Neurol.* **121,** 224–230.

Mitrovic, N., Mohajeri, H. and Schachner, M. (1996) Effects of NMDA receptor blockade in the developing rat somatosensory cortex on the expression of the glia-derived extracellular matrix glycoprotein tenascin-C. *Eur. J. Neurosci.* **8,** 1793–1802.

Mody, I. and Heinemann, U. (1987) NMDA receptors of dentate granule cells participate in synaptic transmission following kindling. *Nature* **326,** 701–704.

Mody, I., Lambert, J. D. C. and Heinemann, U. (1987) Low extracellular magnesium induces epileptiform activity and spreading depression in rat hippocampal slices. *J. Neurophys.* **57,** 869–888.

Moestrup, S. K. and Gliemann, J. (1991) Analysis of ligand recognition by the purified a2-macroglobulin receptor (low density lipoprotein receptor-related protein. *J. Biol. Chem.* **266,** 14011–14017.

Moestrup, S. K., Gliemann, J. and Pallesen, G. (1992) Distribution of the a2-macroglobulin receptor/low density lipoprotein receptor-related protein in human tissues. *Cell Tissue Res.* **269,** 375–382.

Molenaar, M., Vandewetering, M., Oosterwegel, M., Petersonmaduro, J., Godsave, S., Korinek, V., Roose, J., Destree, O. and Clevers, H. (1996) Xtcf-3 transcription factor mediates beta-catenin-induced axis formation in Xenopus embryos. *Cell* **86,** 391–399.

Monyer, H., Sprengel, R., Schoepfer, R., Herb, A., Higuchi, M., Lomeli, H., Burnashev, N., Sakmann, B. and Seeburg, P. H. (1992) Heteromeric NMDA receptors: molecular and functional distinction of subtypes. *Science* **256,** 1217–1221.

Müller, U., Cristina, N., Li, Z. W., Wolfer, D. P., Lipp, H. P., Rulicke, T., Brandner, S., Aguzzi, A. and Weissmann, C. (1994) Behavioral and anatomical deficits in mice homozygous for a modified beta-amyloid precursor protein gene. *Cell* **79,** 755–765.

Müller, B. M., Kistner, U., Veh, R. W., Cases-Langhoff, C., Becker, B., Gundelfinger, E. D. and Garner, C. C. (1995) Molecular characterization and spatial distribution of SAP97, a novel presynaptic protein homologous to SAP90 and the Drosophila discs-large tumor suppressor protein. *J. Neurosci.* **15,** 2354–2366.

Müller, B. M., Kistner, U., Kindler, S., Chung, W. J., Kuhlendahl, S., Fenster, S. D., Lau, L. F., Veh, R. W., Huganir, R. L., Gundelfinger, E. D. and Garner, C. C. (1996a) SAP102, a novel postsynaptic protein that interacts with NMDA receptor complexes in vivo. *Neuron* **17,** 255–265.

Müller, G., Wang, C., Skibo, G., Toni, N., Cremer, H., Calaora, V., Rougon, G. and Schachner, M. (1996b) PSA–NCAM is required for activity-induced synaptic plasticity. *Neuron* **17,** 413–422.

Murphy, K. J., O'Connell, A. W. and Regan, C. M. (1996) Repetitive and transient increases in hippocampal neural cell adhesion molecule polysialylation state following multitrial spatial training. *J. Neurochem.* **67,** 1268–1274.

Nadler, J. V., Perry, B. W., Gentry, C. and Cotman, C. W. (1980a) Loss and reacquisition of hippocampal synapses after selective destruction of CA3–CA4 efferents with kainic acid. *Brain Res.* **191,** 387–403.

Nadler, J., Perry, B. and Cotman, C. (1980b) Selective reinnervation of hippocampal area CA1 and fascia dentata after destruction of CA3–CA4 afferents with kainic acid. *Brain Res.* **182,** 1–9.

Nadler, J. V., Tauck, D. L., Evenson, D. A. and Davis, J. (1983) Synaptic rearrangements in the kainic acid model of Ammon's horn sclerosis. In: *Excitotoxins as Tools as Neuroscience*, pp. 256–270. Eds. K. Fuxe, E. Roberts and R. Schwartz. Macmillan, London.

Nakic, M., Mitrovic, N., Sperk, G. and Schachner, M. (1996a) Kainic acid activates transient expression of tenascin-C in the adult rat hippocampus. *J. Neurosci. Res.* **44,** 355–362.

Nakic, M., Mitrovic, N., Manahan-Vaughan, D., Butler, L., McNamara, J., Sperk, G., Reymann, K. and Schachner, M. (1996b) Kainic acid induced limbic seizures, electrical kindling and LTP in vivo increase expression of tenascin-C in rat hippocampal neurons. *Soc. Neuroci. Abstr.* **22,** 1397.

Nakic, M., Manhan-Vaughan, D., Reymann, K. G. and Schachner, M. (in press) Long-term potentiation in vivo increases rat hippocampal tenascin-C expression. *Beh. Neurosci.* in press.

Namba, Y., Tomonaga, M., Kawasaki, H. and Otomo, E. K. (1991) I. Apolipoprotein E immunoreactivity in cerebral amyloid deposits and neurofibrillary tangles in Alzheimer's disease and kuru plaque amyloid in Creutzfeld–Jakob disease. *Brain Res.* **541,** 163–166.

Narita, M., Bu, G., Olins, G. M., Higuchi, D. A., Herz, J., Broze, G. J. J. and Schwartz, A. L. (1995) Two receptor systems are involved in the plasma clearance of tissue factor pathway inhibitor in vivo. *J. biol. Chem.* **270,** 24800–24804.

Nathan, B. P., Bellosta, S., Sanan, D. A., Weisgraber, K. H., Mahley, R. W. and Pitas, R. E. (1994) Differential effects of apolipoproteins E3 and E4 on neuronal growth in vitro. *Science* **264,** 850–852.

Nathan, B. P., Chang, K. C., Bellosta, S., Brisch, E., Ge, N., Mahley, R. W. and Pitas, R. E. (1995) The inhibitory effect of apolipoprotein E4 on neurite outgrowth is associated with microtubule depolymerization. *J. biol. Chem.* **270,** 19790–19791.

Nielsen, K. L., Holtet, T. L., Etzerodt, M., Moestrup, S. K., Glieman, J., Sottrup-Jensen, L. and Thogersen, H. C. (1996) Identification of residues in alpha-macroglobulins important for binding to the alpha2-macroglobulin receptor/low density lipoprotein receptor-related protein. *J. biol. Chem.* **271,** 12909–12912.

Nielsen, M. S., Nykjaer, A., Warshawsky, I., Schwartz, A. L. and Gliemann, J. (1995) Analysis of ligand binding to the alpha 2-macroglobulin receptor/low density lipoprotein receptor-related protein. Evidence that lipoprotein lipase and the carboxylterminal domain of the receptor-associated protein bind to the same site. *J. biol. Chem.* **270,** 23713–23719.

Niemeier, A., Gafvels, M., Heeren, J., Meyer, N., Angelin, B. and Beisiegel, U. (1996) VLDL receptor mediates the uptake of human chylomicron remnants in vitro. *J. Lipid Res.* **37,** 1733–1742.

Niethammer, M., Kim, E. and Sheng, M. (1996) Interaction between the C terminus of NMDA receptor subunits and multiple members of the PSD-95 family of membrane-associated guanylate kinases. *J. Neurosci.* **16,** 2157–2163.

Nohno, T., Kasai, Y. and Saito, T. (1988) Cloning and sequencing of the Escherichia coli chlEN operon involved in molybdopterin biosynthesis. *J. Bact.* **170,** 4097–4102.

Noorman, F., Braat, E. A. and Rijken, D. C. (1995) Degradation of tissue plasminogen activator by human monocyte-derived macrophages is mediated by the mannose receptor and by the low density lipoprotein receptor-related protein. *Blood* **86,** 3421–3427.

Nosten-Bertrand, M., Errington, M. L., Murphy, K. P., Tokugawa, Y., Barboni, E., Kozlova, E., Michalovich, D., Morris, R. G., Silver, J., Stewart, C. L., Bliss, T. V. P. and Morris, R. J. (1996) Normal spatial learing despite regional inhibition of LTP in mice lacking Thy-1. *Nature* **379,** 826–829.

Novak, S., Hiesberger, T., Schneider, W. J. and Nimpf, J. (1996) A new low density lipoprotein receptor homologue with 8 ligand binding repeats in brain of chicken and mouse. *J. biol. Chem.* **271,** 11732–11736.

Ohm, T. G., Kirca, M., Bohl, J., Scharnagl, H., Groá, W. and März, W. (1995) Apo E influences not only cerebral senile plaque load, but also Alzheimer-type neurofibrillary tangles. *Neuroscience* **66,** 583–587.

Oka, K., Ishimura-Oka, K., Chu, M. J., Sullivan, M., Krushkal, J., Li, W. H. and Chan, L. (1994) Mouse very-low-density-lipoprotein receptor (VLDLR) cDNA cloning, tissue-specific expression and evolutionary relationship with the low-density-lipoprotein receptor. *Eur. J. Biochem.* **224,** 975–982.

Orlando, R. A., Kerjaschki, D., Kurihura, H. and Biemesderfer, D. (1992) Farquhar MG. gp330 associates with 44-kDa protein in the rat kidney to form the Heymann nephritis antigenic complex. *Proc. natl Acad. Sci. U. S. A.* **89,** 6698–6702.

Orlando, R. A., Kerjaschki, D. and Farquhar, M. G. (1995) Megalin (gp330) possesses an antigenic epitope capable of inducing passive Heymann nephritis independent of the nephritogenic epitope in receptor-associated protein. *J. Am. Soc. Nephrol.* **6,** 61–67.

Orsulic, S. and Peifer, M. (1996) An in vivo structure–function study of armadillo, the beta-catenin homologue, reveals both separate and overlapping regions of the protein required for cell adhesion and for wingless signaling. *J. Cell Biol.* **134,** 1283–1300.

Orth, K., Madison, E. L., Gething, M-J., Sambrook, J. F. and Herz, J. (1992) Complexes of tissue-type plasminogen activator and its serpin inhibitor plasminogen-activator inhibitor type 1 are internalized by means of the low density lipoprotein receptor-related protein/a2-macroglobulin receptor. *Proc. natl Acad. Sci. U. S. A.* **89,** 7422–7426.

Orth, K., Willnow, T., Herz, J., Gething, M. J. and Sambrook, J. (1994) Low density lipoprotein receptor-related protein is necessary for the internalization of both tissue-type plasminogen activator complexes and free tissue-type plasminogen activator. *J. biol. Chem.* **269,** 21117–21122.

Osman, I., Gaillard, O., Meillet, D., Bordas-Fonfred, M., Gervais, A., Schuller, E., Delattre, J. and Legrand, A. (1995) A sensitive time-resolved immunofluorometric assay for the measurement of apolipoprotein B in cerebrospinal fluid. *Eur. J. Clin. Chem. Clin. Biochem.* **33,** 53–58.

Perez, Y., Morin, F., Beaulieu, C. and Lacaille, J. C. (1996) Axonal sprouting of CA1 pyramidal cells in hyperexcitable hippocampal slices of kainate treated rats. *Eur. J. Neurosci.* **8,** 736–748.

Persohn, E., Pollerberg, G. E. and Schachner, M. (1996) Immunoelectron-microscopic localization of the 180 kD component of the neural cell adhesion molecules N-CAM in postsynaptic membranes. *J. comp. Neurol.* **288,** 92–100.

Pfeiffer, F., Graham, D. and Betz, H. (1982) Purification by affinity chromatography of the glycine receptor of rat spinal cord. *J. biol. Chem.* **257,** 9389–9393.

Pfistermüller, D. M., Blaas, D. and Hodits, R. A. (1996) Preferential recognition of the very low-density lipoprotein receptor ligand binding site by antibodies from phage display libraries. *FEBS Lett.* **396,** 14–20.

Phelps, S. (1991) Ultrastructural changes in field CA1 of the kainic acid-lesioned hippocampus of the rat. Ph.D. Thesis University of Southampton, Southampton, U. K.

Phelps, S., Mitchell, J. and Wheal, H. V. (1991) Changes to synaptic ultrastructure in field CA1 of the rat hippocampus following intracerebroventricular injection of kainic acid. *Neuroscience* **40,** 687–699.

Pitas, R. E., Boyles, J. K., Lee, S. H., Foss, D. and Mahley, R. W. (1987) Astrocytes synthesize apolipoprotein E and metabolize apolipoprotein E containing lipoproteins. *Biochem. Biophys. Acta* **917,** 148–161.

Pollard, H., Khrestchatisky, M., Moreau, J. and Ben-Ari, Y. (1993) Transient expression of the NR2C subunit of the NMDA receptor in developing rat brain. *Neuroreport* **4,** 411.

Pollerberg, E. G., Schachner, M. and Davoust, J. (1986) Differentiation state-dependent surface mobilities of two forms of the neural cell adhesion molecule. *Nature* **324,** 462–465.

Prior, P., Schmitt, B., Grenningloh, G., Pribilla, I., Multhaup, G., Beyreuther, K., Maulet, Y., Werner, P., Langosch, D., Kirsch, J. and Betz, H. (1992) Primary structure and alternative splice variants of gephyrin, a putative glycine receptor-tubulin linker protein. *Neuron* **8,** 1161–1170.

Pyapali, G. K. and Turner, D. A. (1994) Denervation-induced dendritic alterations in CA1 pyramidal cells following kainic acid hippocampal lesions in rats. *Brain Res.* **652,** 279–290.

Radpour, S. and Thomson, A. M. (1990) Coactivation of local circuit synapses mediated by *N*-methyl-D-aspartate receptors in the CA1 region of the hippocampus may initiate longterm potentiation of Schaffer collateral input. *Neurosci. Lett.* **38**(Suppl.), S79.

Raisman, G. (1969) Neuronal plasticity in the septal nuclei of the adult rat. *Brain Res.* **14,** 25–48.

Rebeck, G. W., Reiter, J. S., Strickland, D. K. and Hyman, B. T. (1993) Apolipoprotein E in sporadic Alzheimer's Disease: allelic variation and receptor interactions. *Neuron* **11,** 575–580.

Rebeck, G. W., Harr, S. D., Strickland, D. K. and Hyman, B. T. (1995) Multiple, diverse senile plaque-associated proteins are ligands of an apolipoprotein E receptor, the alpha2-macroglobulin receptor/low-density-lipoprotein receptor related protein. *Ann. Neurol.* **37,** 211–217.

Represa, A., Le Gall La Salle, G. and Ben-Ari, Y. (1989) Hippocampal Plasticity in the kindling model of epilepsy in rats. *Neurosci. Lett.* **99,** 345–350.

Resink, A., Villa, M., Benke, D., Mohler, H. and Balazs, R. (1995) Regulation of the expression of NMDA receptor subunits in rat cerebellar granule cells: effect of chronic K + -induced depolarisation and NMDA exposure. *J. Neurochem.* **64,** 558–565.

Ronn, L. C., Bock, E., Linnemann, D. and Jahnsen, H. (1995) NCAM-antibodies modulate induction of long-term potentiation in rat hippocampal CA1. *Brain Res.* **677,** 145–151.

Rosenmund, C. and Westbrook, G. L. (1993) Calcium-induced actin depolymerization reduces NMDA channel activity. *Neuron* **10,** 805–814.

Rusakov, D. A., Davies, H. A., Krivko, I. M., Stewart, M. G. and Schachner, M. (1994) Training in chicks alters PSA–N-CAM distribution in forebrain cell membranes. *Neuroreport* **5,** 2469–2473.

Rutishauser, U. (1996) Polysialic acid and the regulation of cell interactions. *Cell Biol.* **8,** 679–684.

Saito, A., Pietromonaca, S., Kwor-chie Loo, A. and Farquhar, M. (1994) Complete cloning and sequencing of rat gp330/"megalin", a distinctive member of the low density lipoprotein receptor gene family. *Proc. natl Acad. Sci. U. S. A.* **91,** 9725–9729.

Sanan, D. A., Weisgraber, K. H., Russel, S. J., Mahley, R. W., Huang, D., Saunders, A., Schmechel, D., Wisniewski, T., Frangione, B., Roses, A. D. and Strittmatter, W. J. (1994) Apolipoprotein E associates with beta amyloid peptide of Alzheimer's disease to form novel monofibrils. Isoform apoE4 associates more efficiently than apoE3. *J. clin. Invest.* **94,** 860–869.

Sanson, B., White, P. and Vincent, J. P. (1996) Uncoupling cadherin-based adhesion from wingless signaling in Drosophila. *Nature* **383,** 627–630.

Sassoè-Pognetto, M., Kirsch, J., Grünert, U., Greferath, U., Fritschy, J. M., Möhler, H., Betz, H. and Wässle, H. (1995) Colocalization of gephyrin and GABAA-receptor subunits in the rat retina. *J. comp. Neurol.* **357,** 1–14.

Schmechel, D. E., Saunders, A. M., Strittmatter, W. J., Crain, B. J., Hulette, C. M., Joo, S. H., Pericak-Vance, M. A., Goldgaber, D. and Roses, A. D. (1993) Increased amyloid á-peptide deposition in cerebral cortex as a consequence of apolipoprotein E genotype in late-onset Alzheimer disease. *Proc. natl Acad. Sci. U. S. A.* **90,** 9649–9653.

Schmieden, V., Kuhse, J. and Betz, H. (1992) Agonist pharmacology of neonatal and adult glycine receptor a subunits: identification of amino acid residues involved in taurine activation. *EMBO J.* **11,** 2025–2032.

Schmitt, B., Knaus, P., Becker, C.-M. and Betz, H. (1987) The Mr 93,000 polypeptide of the postsynaptic glycine receptor is a peripheral membrane protein. *Biochemistry* **26,** 805–811.

Schneider, W. J., Kovanen, P. T., Brown, M. S., Goldstein, J. L., Utermann, G., Weber, W., Havel, R. J., Kotite, L., Kane, J. P., Innerarity, T. L. and Mahley, R. W. (1981) Familial dysbetalipoproteinemia: abnormal binding of mutant apolipoprotein E to low density lipoprotein receptors of human fibroblasts and membranes from liver and adrenals of rats, rabbits and cows. *J. clin. Invest.* **68,** 1075–1085.

Scholey, A. B., Rose, S. P. R., Zamani, M. R., Bock, E. and Schachner, M. (1993) A role for the neural cell adhesion molecule in a late, consolidating phase of glycoprotein synthesis 6 hours following passive avoidance training of the young chick. *Neuroscience* **55,** 499–509.

Scholey, A. B., Mileusnic, R. and Schachner, M. (1995) A role for a chicken homolog of the neural cell adhesion molecule L1 in consolidation of memory for a passive avoidance task in the chick. *Learning and Memory* **2,** 17.

Schuman, E. M. and Madison, D. V. (1994) Nitric oxide and synaptic function. *A. Rev. Neurosci.* **17,** 153–183.

Schuster, C. M., Davis, G. W., Fetter, R. D. and Goodman, C. S. (1996a) Genetic dissection of structural and functional components of synaptic plasticity. I. Fasciclin II controls synaptic stabilization and growth. *Neuron* **17,** 641–654.

Schuster, C. M., Davis, G. W., Fetter, R. D. and Goodman, C. S. (1996b) Genetic dissection of structural and functional components of synaptic plasticity. II. Fasciclin II controls presynaptic structural plasticity. *Neuron* **17,** 655–667.

Schuster, T., Krug, M. and Schachner, M. (submitted) Hippocampal long-term potentiation increases the proportion of spine synapses expressing the largest isoform of the neural cell adhesion molecule (NCAM180). Submitted.

Shakibaei, M. and Frevert, U. (1996) Dual interaction of the malaria circumsporozoite protein with the low density lipoprotein receptor related protein (LRP) and heparan sulfate proteoglycans. *J. exp. Med.* **184,** 1699–1711.

Simpson, L., Wheal, H. V. and Williamson, R. (1991) The contribution of non-NMDA and NMDA receptor to graded bursting activity in the CA1 region of the hippocampus in a chronic model of epilepsy. *Can. J. Physiol. Pharm.* **69,** 1091–1098.

Skibo, G. G., Davies, H. A., Rusakov, D. A., Stewart, M. G. and Schachner, M. (in press) Increased immunogold labelling of NCAM isoforms in synaptic active zones of the chick striatum 5–6 h after one-trial passive avoidance training. *Neuroscience* in press.

Sontheimer, H., Kettenmann, H., Schachner, M. and Trotter, J. (1990) The neural cell adhesion molecule (NCAM) modulates K^+ channels in cultured glial precursor cells. *Eur. J. Neurosci.* **3,** 230–236.30.

Sotelo, M. D. and Palay, S. L. (1971) Altered axons and axon terminals in the lateral vestibular nucleus of the rat. *Lab. Invest.* **25,** 653–671.

Stallmeyer, B., Nerlich, A., Schiemann, J., Brinkmann, H. and Mendel, R. R. (1995) Molybdenum co-factor biosynthesis: the Arabidopsis thaliana cDNA cnx1 encodes a multifunctional two-domain protein homologous to a mammalian neuroprotein, the insect protein Cinnamon and three *Escherichia coli* proteins. *Plant J.* **8,** 751–762.

Staubli, U., Vanderjkusgm, P. and Lynch, G. (1990) An inhibitor of integrin receptors blocks long-term potentiation. *Behav. Neural Biol.* **53,** 1–5.

Stefansson, S., Lawrence, D. A. and Argraves, W. S. (1996) Plasminogen activator inhibitor-1 and vitronectin promote cellular clearance of thrombin by low density lipoprotein receptor-related proteins 1 and 2. *J. biol. Chem.* **271,** 8215–8220.

Stern, P., Behe, P., Schoepfer, R. and Colquhoun, D. (1992) Single-channel conductances of NMDA receptors expressed from cloned cDNAs: comparison with native receptors. *Proc. R. Soc. Lond. (B)* **250,** 271–277.

Steward, O. (1986) Lesion-induced growth in the hippocampus: in search of cellular and molecular mechanisms. In: *The Hippocampus*, pp. 65–111. Eds. R. L. Isaacson and K. H. Pribham. Plenum, New York.

Stockley, E. W., Cole, H. M., Brown, A. D. and Wheal, H. V. (1993) A system for quantitative morphological measurement and electrotonic modelling of neurones: three-dimensional reconstruction. *J. Neurosci. Meth.* **47,** 39–51.

Stork, O., Welzl, H., Cremer, H. and Schachner, M. (1997) Increased intermale aggression and neuroendocrine response in mice deficient for the neural cell adhesion molecules (NCAM). *Eur. J. Neurosci.* **9,** 1117–1125.

Strickland, D. K., Ashcom, J. D., Williams, S., Battey, F., Behre, E., McTigue, K., Battey, J. F. and Argraves, W. S. (1991) Primary structure of a2-macroglobulin receptor-associated protein. Human homologue of a Heyman nephritis antigen. *J. biol. Chem.* **266,** 13364–13369.

Strittmatter, W. J., Saunders, A. M., Schmechel, D., Pericak-Vance, M., Enghild, J., Salvesan, G. S. and Roses, A. D. (1993a) Apolipoprotein E: high-avidity binding to beta-amyloid and increased frequency of type 4 allele in late-onset familial Alzheimer disease. *Proc. natl Acad. Sci. U. S. A.* **90,** 1977–1981.

Strittmatter, W. J., Weisgraber, K. H., Huang, D. Y., Dong, L-M., Salvesen, G. S., Pericak-Vance, M., Schmechel, D., Saunders, A. M., Goldgaber, D. and Roses, A. D. (1993b) Binding of human apolipoprotein E to synthetic amyloid á peptide: isoform-specific effects and implications for late-onset Alzheimer disease. *Proc. natl Acad. Sci. U. S. A.* **90,** 8098–8102.

Südhof, T. C., Goldstein, J. L., Brown, M. S. and Russel, D. W. (1985) The LDL receptor gene: a mosaic of exons shared with different proteins. *Science* **228,** 815–822.

Sundstrom, L. E., Mitchell, J. and Wheal, H. V. (1993) Bilateral reorganisation of mossy fibres in the rat hippocampus after unilateral intracerebroventricular kainic acid. *Brain Res.* **609,** 321–326.

Sutula, T., Xiao-Xian, H., C, Cavazos, J. and Scott, G. (1988) Synaptic reorganisation in the hippocampus induced by abnormal functional activity. *Science* **239,** 1147–1150.

Sutula, T., Cascino, G., Cavazos, J., Parada, I. and Ramirez, L. (1989) Mossy fibre synaptic reorganisation in the epileptic human temporal lobe. *Ann. Neurol.* **26,** 321–330.

Takahashi, S., Kawabayasi, Y., Nakai, T., Sakai, J. and Yamamoto, T. (1992) Rabbit very low density lipoprotein receptor; a low density lipoprotein receptor like protein with distinct ligand specificity. *Proc. natl Acad. Sci. U.S.A.* **89,** 9252–9256.

Takahashi, S., Oida, K., Ookubo, M., Suzuki, J., Kohno, M., Murase, T., Yamamoto, T. and Nakai, T. (1996) Very low density lipoprotein receptor binds apolipoprotein E2/2 as well as apolipoprotein E3/3. *FEBS Lett.* **386,** 197–200.

Takeuchi, M., Hata, Y., Hirao, K., Toyoda, A., Irie, M. and Takai, Y. (1997) SAPAPs a family of PSD-95/SAP90-associated proteins localized at postsynaptic density. *J. biol. Chem.* **272,** 11943–11951.

Taleb, O. and Betz, H. (1994) Expression of the human glycine receptortal subunit in Xenopus oocytes: apparent affinities of agonists increase at high receptor densities. *EMBO J.* **13,** 1318–1324.

Tauck, D. L. and Nadler, J. V. (1985) Evidence of functional mossy fibre sprouting in hippocampal formation of kainic acid treated rats. *J. Neurosci.* **5,** 1016–1022.

Thomson, A. M. and West, D. C. (1986) *N*-methylaspartate receptors mediate epileptiform activity evoked in some, but not all, conditions in rat neocortical slices. *Neuroscience* **19,** 1161–1177.

Todd, A. J., Spike, R. C., Chong, D. and Neilson, M. (1995) The relationship between glycine and gephyrin in synapses of the rat spinal cord. *Eur. J. Neurosci.* **7,** 1–11.

Todd, A. J., Watt, C., Spike, R. C. and Sieghart, W. (1996) Colocalization of GABA, glycine and their receptors at synapses in the rat spinal cord. *J. Neurosci.* **16,** 974–982.

Tooyama, I., Kawamata, T., Akiyama, H., Moestrup, S. K., Gliemann, J. and McGeer, P. L. (1993) Immunohistochemical study of alpha 2 macroglobulin receptor in Alzheimer and control postmortem human brain. *Molec. chem. Neuropathol.* **18,** 153–160.

Traub, R. D., Jefferys, J. G. R. and Whittington, M. A. (1994) Enhanced NMDA conductance can account for epileptiform activity induced by low Mg2+ in the rat hippocampus. *J. Physiol.* **478,** 379–393.

Triller, A., Cluzeaud, F., Pfeiffer, F., Betz, H. and Korn, H. (1985) Distribution of glycine receptors at central synapses: an immunoelectron microscopicy study. *J. Cell Biol.* **101,** 683–688.

Tsunoda, S., Sierralta, J., Sun, Y., Bodner, R., Suzuki, E., Becker, A., Socolich, M. and Zuker, C. S. (1997) A multivalent PDZ-domain protein assembles signalling complexes in a G-protein-coupled cascade. *Nature* **388,** 243–249.

Turner, D. A. and Wheal, H. V. (1991) Excitatory synaptic potentials in kainic acid-denervated rat CA1 pyramidal neurons. *J. Neurosci.* **11,** 2786–2794.

Turner, D. A., Wheal, H. V., Cole, H. M. and Stockley, E. W. (1991) Three-dimensional reconstructions and analysis of the cable properties of neurones. In: *Cellular Neurobiology: A Practical Approach*, pp. 225–246. Eds. J. Chad and H.V Wheal. IRL Oxford University Press, Oxford.

Uchida, N., Honjo, Y., Johnson, K. R., Wheelock, M. J. and Takeichi, M. (1996) The catenin/cadherin adhesion system is localized in synaptic junctions bordering transmitter release zones. *J. cell. Biol.* **135,** 767–779.

Walsh, F. S. and Dohert, P. (1996) Cell adhesion molecules and neuronal regeneration. *Curr. Opin. Cell. Biol.* **8,** 707–713.

Warshawsky, I., Herz, J., Broze, G. J. and Schwartz, A. L. (1996) The low density lipoprotein receptor-related protein can function independently from heparan sulfate proteoglycans in tissue factor pathway inhibitor endocytosis. *J. biol. Chem.* **271,** 25873–25879.

Webb, J. C., Patel, D. D., Jones, M. D., Knight, B. L. and Soutar, A. K. (1994) Characterization and tissue-specific expression of the human "very low density lipoprotein (VLDL) receptor" mRNA. *Hum. Molec. Genet.* **3,** 531–537.

Webb, D. J., Hussaini, I. M., Weaver, A. M., Atkins, T. L., Chu, C. T., Pizzo, S. V., Owens, G. K. and Gonias, S. L. (1995) Activated alpha 2-macroglobulin promotes mitogenesis in rat vascular smooth muscle cells by a mechanism that is independent of growth-factor-carrier activity. *Eur. J. Biochem.* **234,** 714–722.

Wheal, H., Lancaster, B. and Bliss, T. (1983) Long-term potentiation in Schaffer collateral and commissural systems of the hippocampus: in vitro study in rats pretreated with kainic acid. *Brain Res.* **272,** 247–253.

Williamson, R. and Wheal, H. V. (1992) The contribution of AMPA and NMDA receptors to graded bursting activity in the hippocampal CA1 region in an acute model of eilepsy. *Epilepsy Res.* **12,** 179–188.

Willnow, T. E. (1996) The low density lipoprotein receptor related protein is processed by furin in vivo and in vitro. *Biochem. J.* **313,** 71–76.

Willnow, T. E. and Herz, J. (1994) Genetic deficiency in low density lipoprotein receptor-related protein confers cellular resistance to Pseudomonas exotoxin A. Evidence that this protein is required for uptake and dgradation of multiple ligands. *J. Cell Sci.* **107,** 719–726.

Willnow, T. E., Armstrong, S. A., Hammer, R. E. and Herz, J. (1995) Functional expression of low density lipoprotein receptor-related protein is controlled by receptor-associated protein in vivo. *Proc. natl Acad. Sci. U. S.A.* **92,** 4537–4541.

Willnow, T. E., Hilpert, J., Armstrong, S. A., Rohlmann, A., Hammer, R. E., Burns, D. K. and Herz, J. (1996a) Defective forebrain development in mice lacking gp330/megalin. *Proc. natl Acad. Sci. U. S.A.* **93,** 8460–8464.

Willnow, T. E., Rohlmann, A., Horton, J., Otani, H., Braun, J. R., Hammer, R. E. and Herz, J. (1996b) RAP, a specialized chaperone, prevents ligand-induced ER retention and degradation of LDL receptor-related endocytotic receptors. *EMBO J.* **15,** 2632–2639.

Wisden, W., Laurie, D. J., Monyer, H. and Seeburg, P. H. (1992) The distribution of 13 GABAA receptor subunit mRNAs in the rat brain. I. Telencephalon, diencephalon, mesencephalon. *J. Neurosci.* **12,** 1040–1162.

Wisniewski, T., Castano, E. M., Golabek, A., Vogel, T. and Frangione, B. (1994) Acceleration of Alzheimer's fibril formation by apolipoprotein E in vitro. *Am. J. Pathol.* **145,** 1030–1035.

Wolf, B. B., Lopes, M. B. S., Vandenberg, S. R. and Gonias, S. L. (1992) Characterization and immunohistochemical localization of a2-macroglobulin receptor (low density lipoprotein receptor-related protein) in human brain. *Am. J. Pathol.* **141,** 37–42.

Wolfer, D. P., Mohajeri, H. M., Schachner, M. and Lipp, H-P. (in press) More selective searching and relearning in the Morris water maze in transgenic mice ectopically expressing the neural cell adhesion molecule L1 in astrocytes. *Eur. J. Neurosci.* in press.

Wong, E. V., Schaefer, A. W., Landreth, G. and Lemmon, V. (1996) Involvement of p90 (rsk) in neurite outgrowth mediated by the cell adhesion molecule L1. *J. biol. Chem.* **271,** 18217–18223.

Wu, S. M. and Pizzo, S. V. (1996) Low density lipoprotein receptor-related protein/alpha 2-macroglobulin receptor on murine peritoneal macrophages mediates the binding an catabolism of low density lipoprotein. *Arch. Biochem. Biophys.* **326,** 39–47.

Wüstenberg, F., Berlin, K., Scharnagl, H., März, W., Ohm, T. G. and Müller, W. (1997) Complexes of apo E isoforms and β-amyloid peptides elevate intracellular calcium levels differentially. In: *Alzheimer's Disease: Biology, Diagnosis and Therapeutics.* Eds. K. Iqbal, B. Winblad, T. Nishimura, M. Takeda and H. M. Wisniewski. Wiley, Chichester.

Wyne, K. L., Pathak, K., Seabra, M. C. and Hobbs, H. H. (1996) Expression of the VLDL receptor in endothelial cells. *Arterioscler. Thromb. Vasc. Biol.* **1996,** 407–415.

Wyszynski, M., Lin, J., Rao, A., Nigh, E., Beggs, A. H., Craig, A. M. and Sheng, M. (1997) Competitive binding of alpha-actinin and calmodulin to the NMDA receptor. *Nature* **385,** 439–442.

Yamazaki, H., Bujo, H., Kusonoki, J., Seimiya, K., Kanaki, T., Morisaki, N., Schneider, W. J. and Saito, Y. (1996) Elements of neural adhesion molecules and a yeast vacuolar protein sorting receptor are present in a novel mammalian low density lipoprotein receptor family member. *J. biol. Chem.* **271,** 25761–25768.

Yankner, B. A. (1996) Mechanisms of neuronal degeneration in Alzheimer's disease. *Neuron* **6,** 921–932.

Yokode, M., Pathak, R. K., Hammer, R. E., Brown, M. S., Goldstein, J. L. and Anderson, R. G. W. (1992) Cytoplasmic sequence required for basolateral targeting of LDL receptor in livers of transgenic mice. *J. Cell Biol.* **117,** 39–46.

Zheng, G., Bachinsky, D. R., Stamenkovic, I., Strickland, D. K., Brown, D., Andres, G. and McCluskey, R. T. (1994) Organ distribution in rats of two members of the low-density lipoprotein receptor gene family, gp330 and LRP/alpha2-MR, and the receptor-associated protein (RAP). *J. Histochem. Cytochem.* **42,** 531–542.

Enhanced long-term potentiation and impaired learning in mice with mutant postsynaptic density-95 protein

Martine Migaud*†, Paul Charlesworth*†, Maureen Dempster*†, Lorna C. Webster*†, Ayako M. Watabe‡, Michael Makhinson‡, Yong He§, Mark F. Ramsay†, Richard G. M. Morris†, John H. Morrison§, Thomas J. O'Dell‡ & Seth G. N. Grant*†

* Centre for Genome Research, and † Centre for Neuroscience, University of Edinburgh, Roger Land Building, West Mains Road, Edinburgh EH9 3JQ, UK
‡ Department of Physiology and The Brain Research Institute, School of Medicine, University of California at Los Angeles, Los Angeles, California 90095, USA
§ Fishberg Research Centre for Neurobiology, Mount Sinai School of Medicine, Box 1065, One Gustave Levy Place, New York, New York 10029-6574, USA

Specific patterns of neuronal firing induce changes in synaptic strength that may contribute to learning and memory. If the postsynaptic NMDA (*N*-methyl-D-aspartate) receptors are blocked, long-term potentiation (LTP) and long-term depression (LTD) of synaptic transmission and the learning of spatial information are prevented. The NMDA receptor can bind a protein known as postsynaptic density-95 (PSD-95), which may regulate the localization of and/or signalling by the receptor. In mutant mice lacking PSD-95, the frequency function of NMDA-dependent LTP and LTD is shifted to produce strikingly enhanced LTP at different frequencies of synaptic stimulation. In keeping with neural-network models that incorporate bidirectional learning rules, this frequency shift is accompanied by severely impaired spatial learning. Synaptic NMDA-receptor currents, subunit expression, localization and synaptic morphology are all unaffected in the mutant mice. PSD-95 thus appears to be important in coupling the NMDA receptor to pathways that control bidirectional synaptic plasticity and learning.

In the mammalian hippocampus and other brain structures involved with memory formation, certain patterns of synaptic activity result in long-lasting modifications of the efficiency of synaptic transmission. In the CA1 region of the hippocampus, a train of low-frequency stimulation produces a reduction in synaptic efficacy (LTD) and high-frequency stimulation produces an increase (LTP)[1,2]. Mechanisms proposed to underlie these modifications of synaptic strength include changes in the sensitivity of postsynaptic transmitter receptors, activation of previously silent receptors, generation of retrograde messengers to the presynaptic terminal, structural changes in dendritic spines, and activation of transcription in the nucleus[1,2]. Although activation of the NMDA receptor initiates these complex events, its interactions with postsynaptic proteins and the signalling pathways immediately downstream from it are poorly understood.

The NMDA receptor is formed by the assembly of a common NR1 subunit with one or more of four different NR2 subunits, NR2A–D (refs 3, 4). The NR2 subunits have long cytoplasmic carboxy-terminal domains which contain sites for phosphorylation[5] and interaction with cytoplasmic proteins. *In vitro*, the C terminus of NR2 subunits binds to PSD-95/SAP90, chapsyn-110/PSD-93, and other related members of the membrane-associated guanylate kinase (MAGUK) family[6–9]. PSD-95/SAP90 (refs 10, 11) is an abundant postsynaptic density protein and contains several domains that participate in protein–protein interactions, including three PDZ/DHR (for PSD-95, Dlg, ZO-1/Dlg-homologous region) domains, an SH3 (Src-homology-3) domain and a guanylate kinase (GK)-homology domain. The second PDZ domain (PDZ2) can bind to the C terminus of the NR2 subunits[6,9]. PSD-95 has no detectable enzymatic activity and acts as an adapter molecule through protein–protein interactions mediated by the discrete domains. Although the function of PSD-95 at the synapse is unknown, in fibroblasts it mediates the localization of the NMDA receptor to focal clusters, indicating that PSD-95 may be required for the localization of such receptors to synapses[7].

To determine the function of PSD-95 in the brain, we characterized mice carrying a targeted mutation in the PSD-95 gene. Our results provide evidence that PSD-95 is important in signal transduction. NMDA-receptor-mediated synaptic plasticity was dramatically altered, with synapses becoming inappropriately strengthened after stimulation by a wide range of frequencies. The learning of PSD-95-mutant mice was impaired, supporting predictions of neural-network models that depend on bidirectional synaptic plasticity to mediate learning and memory.

PSD-95-mutant mice

The first two PDZ domains of PSD-95 bind to the NMDA-receptor subunits 2A (NR2A) and 2B (NR2B)[6,9], to K^+ channels[12] and to neuronal nitric oxide synthase[13] *in vitro*. We generated mice carrying a targeted mutation in the PSD-95 gene that leaves the first two PDZ domains intact by introducing a stop codon into the PDZ3 domain and replacing downstream sequences with an internal ribosome entry site that drives a β-galactosidase reporter gene (Fig. 1a). The targeting construct was electroporated into embryonic stem (ES) cells and Southern blot analysis indicated that homologous recombination had occurred in 5 clones out of 75 analysed (6.7%) (Fig. 1b). Three ES cell lines were microinjected into C57BL/6 blastocysts and two clones generated germline chimaeras, which were crossed onto the MF1 genetic background. No biochemical, anatomical, electrophysiological or behavioural differences were found between mice generated from two independent targeted clones. Heterozygous mice were intercrossed and the genetic status of the mice was determined by genomic Southern blotting and polymerase chain reaction (PCR) (Fig. 1b). From 70 litters, 602 mice were genotyped at weaning: 191 (32%) were wild type, 316 (52%) were heterozygotes, and 95 (16%) were homozygotes, demonstrating a distortion of the expected mendelian ratio ($\chi^2 = 32.1$, $P < 0.0001$). Runting was evident in 42% of viable homozygotes, which then recovered and reached the size of their wild-type littermates at ~6 weeks of age. Runting seemed to result from inadequate competition for feeding with wild-type siblings, because homozygous pups fostered to wild-type mothers were of normal size. Homozygous males and females were fertile and showed

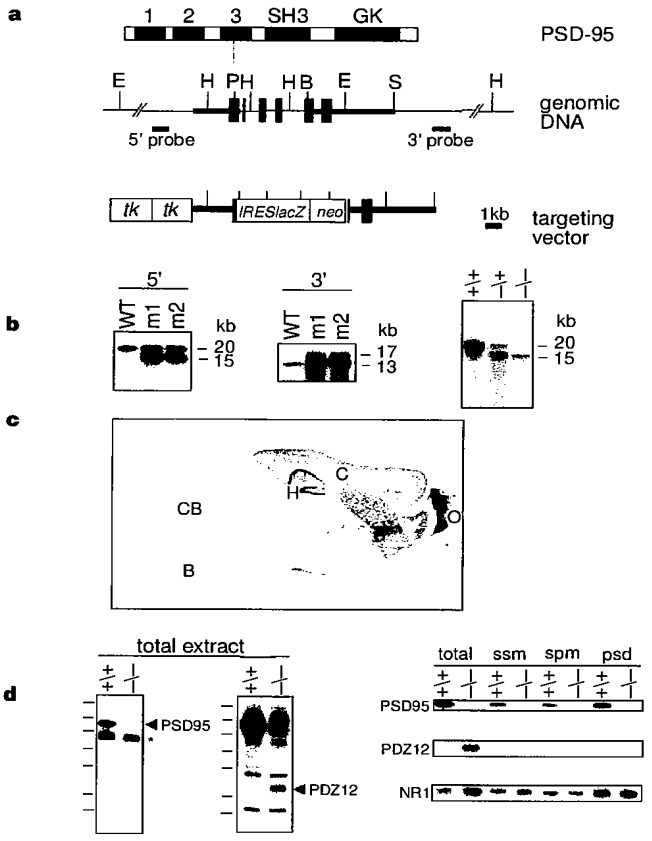

Figure 1 Targeted disruption of the PSD-95 gene. **a**, Top: PSD-95 protein with three PDZ domains (labelled 1, 2, 3), an Src homology 3 (SH3) domain and a guanylate kinase homology region (GK). Middle: PSD-95 gene with restriction-enzyme cutting sites (E, *Eco*RI; H, *Hin*dIII; P, *Pvu*II; B, *Bam*H1; S, *Sac*I); black boxes, exons, thick horizontal lines, homology regions used in the targeting vector; Southern blot probes are indicated. Bottom: targeting vector. *tk*, thymidine kinase gene; *IRES*, internal ribosome-entry sequence; *lacZ*, β-galactosidase gene; *neo*, neomycin-resistance gene. The dotted vertical line from the PDZ3 domain (upper) to the *Pvu*II site (middle) represents the position of the stop codon inserted into PDZ3. **b**, Left and centre, genomic Southern blot from ES cell clones (m1 and m2) digested with *Eco*RI and *Hin*dIII, hybridized with 5′ and 3′ probes, respectively. Right: genomic Southern blot of *Eco*RI-digested DNA from littermates of a heterozygote intercross and probed with the 5′ probe. Wild type (WT) (+/+), heterozygote (−/+) and homozygote (−/−) are indicated. **c**, Expression pattern of PSD-95 using X-gal-stained sagittal brain section. B, brainstem; H, hippocampus; C, cortex; CB, cerebellum; O, olfactory bulb. **d**, Immunoblots of PSD-95 protein in total forebrain extracts (left, middle panels) and in synaptosome subfractions (right panels) of wild-type mice (+/+) and PSD-95 mutants (−/−). Left: full-length PSD-95 in wild-type is indicated; asterisk, nonspecific band; size markers correspond to M_r 205K, 112K, 87K, 69K, 56K, 39K, 34K. Middle: the same blot was stripped and reprobed with an antibody recognizing PSD-95 N-terminal to the PDZ3 domain. The band labelled PDZ12 is found only in extracts of PSD-95 mutant mice and corresponds to the N-terminal domain expressed in the mutants. Right: extracts from synaptosome (ssm), synaptic plasma membrane (spm) and postsynaptic density (psd) fractions from wild-type and mutant mice immunoblotted with antibodies recognizing full-length PSD-95 (upper strip), N-terminal PDZ12 (middle strip) and NR1 (lower strip). The PSD-95^{PDZ12} (PDZ12) protein was not detected in spm or psd fractions even at very long exposures.

no sign of seizure, tremor or ataxia or of neurological abnormality. The expression of PSD-95 was shown by X-gal staining of brains of mutant mice (Fig. 1c) to be high in the forebrain, particularly in CA1 pyramidal neurons of the hippocampus and in granule cells in the dentate gyrus, in agreement with studies of messenger RNA *in situ*[6,13].

To determine the effects of mutating the PSD-95 protein we immunoblotted whole extracts from forebrain, synaptosomes, and synaptosome subfractions with antibodies raised against PSD-95 (Fig. 1d). Using three separate antibodies against PSD-95, a 95K band (corresponding to a relative molecular mass of 95,000) was detected for wild-type mice which was absent in homozygote mice. Immunoblotting with antibodies against the amino terminus of PSD-95 detected a 40K band in whole-brain extracts from homozygote mice, which corresponds to PDZ domains 1 and 2 and is now referred to as PSD-95^{PDZ12}. The PSD-95^{PDZ12} band was not detected in synaptosomes, in synaptic plasma membranes or in postsynaptic density fractions of homozygote mice, in contrast to full-length PSD-95 which was readily detectable in these fractions in wild-type mice (Fig. 1d). Control immunoblotting with antibodies specific for the NMDA R1 subunit (NR1) indicated that the distribution of NR1 in these fractions was the same as in wild-type mice. These results show that PSD-95^{PDZ12} does not localize to postsynaptic densities or to synaptic plasma membranes, but without a suitable antibody we cannot confirm this by immunohistochemistry. In PSD-95-mutant mice, no binding of PSD-95^{PDZ12} to the NMDA receptor could be detected by immunoprecipitation assay, although PSD-95 bound to the NMDA receptor from wild-type mice (data not shown). The amount of PSD-95^{PDZ12} found in PSD-95 mutants was ~10-fold less than full-length PSD-95 in wild-type, and as RNAse protection assays indicated that the level of mRNA in each was comparable (data not shown), the reason why we detected no interaction between PSD-95^{PDZ12} and the NMDA receptor is probably because PSD-95^{PDZ12} is not localized to synapses. This is consistent with data showing that the C-terminal domains of Dlg are required for membrane and subcellular localization[14].

Several other related neuronal MAGUK proteins have been described in addition to PSD-95, including chapsyn-110/PSD-93, SAP102 and SAP97 (refs 7, 8, 13, 15). The levels of these proteins were unaltered in our mutant mice (data not shown). We showed that chapsyn-110/PSD-93 could still interact with the NMDA receptor in PSD-95-mutant mice by immunoprecipitation and by immunoblotting the complex with antibodies against the NMDA receptor (data not shown). We conclude that the NMDA receptor in our PSD-95-mutant mice is bound by another MAGUK protein.

Synaptic localization of NMDA receptors

We next investigated the expression and localization of the NMDA receptor. The total amount of NR1, NR2A and NR2B proteins was the same in wild-type and mutant mice, and immunoprecipitation of each subunit and immunoblotting with the other subunits revealed no change in the composition of the receptor complexes (data not shown). These results indicate that PSD-95 is unlikely to play a role in regulating the stoichiometry of the NMDA-receptor subunit interaction *in vivo*. PSD-95 is highly expressed in the CA1 region of the hippocampus (Fig. 1c). Using light and electron microscopy, we found that the intensity of the Nissl staining pattern (data not shown) and the distribution of the dendritic marker MAP2 and of the synaptic-terminal marker synaptophysin were the same in the homozygous mutant and wild-type mice, indicating that the mutation does not affect cell density or cytoarchitectonic patterns (Fig. 2a–d). NR1 was widely distributed in soma and dendrites of CA1 in both mutant and wild-type mice and appeared similar in the light microscope (Fig. 2e, f). Electron microscopy revealed no changes in the morphology of these asymmetric synapses nor any difference in synapse density (Fig. 2i, j). Immunogold studies of NR1 in CA1 stratum radiatum detected no difference between the mutant and wild-type mice in the character-

istics or density of NR1 immunogold labelling of asymmetric synapses (Fig. 2g, h). In both sets of mice, NR1 was present primarily in the synaptic cleft and within the postsynaptic specialization, with minimal labelling in the neighbouring cytoplasm and no significant presynaptic labelling. Although these techniques are not quantitative, we found no major difference between mutant and wild-type mice in hippocampus CA1 synapse architecture or in NMDA-receptor localization. The localization of the NMDA receptor to the synapses of PSD-95 mutants by electron microscopy was confirmed by electrophysiological assay (see below).

NMDA-receptor function in mutant mice

We investigated the NMDA currents in primary cultured neurons derived from PSD-95-mutant and wild-type mice. Peak currents elicited by brief application of 250 μM NMDA/25 μM glycine in magnesium-free medium were not significantly different (3,907 ± 285 pA, $n = 36$ for PSD-95 mutant; 3,204 ± 328 pA, $n = 22$ for wild type; $t(56) = 1.578$, $P = 0.12$). Furthermore, the NMDA-receptor current–voltage relation did not change in PSD-95-mutant neurons in the presence and absence of magnesium (Fig. 3a, b). We investigated the synaptic expression of NMDA receptors in hippocampal slices using whole-cell voltage-clamp recordings to examine the NMDA-receptor-mediated component of excitatory postsynaptic currents (EPSCs) in CA1 pyramidal cells: we found no difference in the results from cells of wild-type and mutant animals (Fig. 3c). At a holding potential of −80 mV, where the NMDA-receptor ion channels are blocked by Mg^{2+}, EPSCs in CA1 pyramidal cells from wild-type animals ($n = 15$ cells from 4 animals) and PSD-95 mutants ($n = 18$ cells from 5 animals) have a similar ($t(7) = 0.49$; not significant), small NMDA-receptor-mediated component. The NMDA-receptor-mediated component of EPSCs from wild-type and PSD-95 mutant cells was also the same ($t(7) = 0.27$; not significant) at a holding potential of +40 mV, where the NMDA-receptor-mediated component of the EPSCs is larger owing to the relief of the Mg^{2+} block of the channel. These results show that NMDA-receptor channel properties are unaffected and that the receptors are normally localized to synapses in PSD-95-mutant mice. Moreover, field potential recordings showed that the maximal α-amino-3-hydroxy-5-methyl-4-isoxazole propionate (AMPA)-receptor-mediated field excitatory postsynaptic potential (fEPSP) amplitude evoked in wild-type and mutant slices was not significantly different (wild type: 8.6 ± 0.5 mV, $n = 69$ slices, 13 animals; PSD-95 mutant: 7.8 ± 0.4 mV, $n = 70$ slices, 15 animals), indicating that there is no gross disruption of synaptic transmission in our PSD-95-mutant mice.

We also compared paired-pulse facilitation, a short presynaptic form of synaptic plasticity, in the two sets of mice (Fig. 3d). We found that paired-pulse facilitation at inter-pulse intervals of 20, 50, 100 and 200 ms was significantly greater in slices from PSD-95-mutant mice ($P < 0.05$). As PSD-95 is thought to be a postsynaptic protein in forebrain synapses[16], this enhanced paired-pulse facilitation may be due to postsynaptic changes[17], or to retrograde signalling to the presynaptic terminal through PSD-95 interaction with neuroligin and neurexin[18] (as shown in Fig. 6a), or to some other effect such as an alteration in presynaptic K^+-channel function[19].

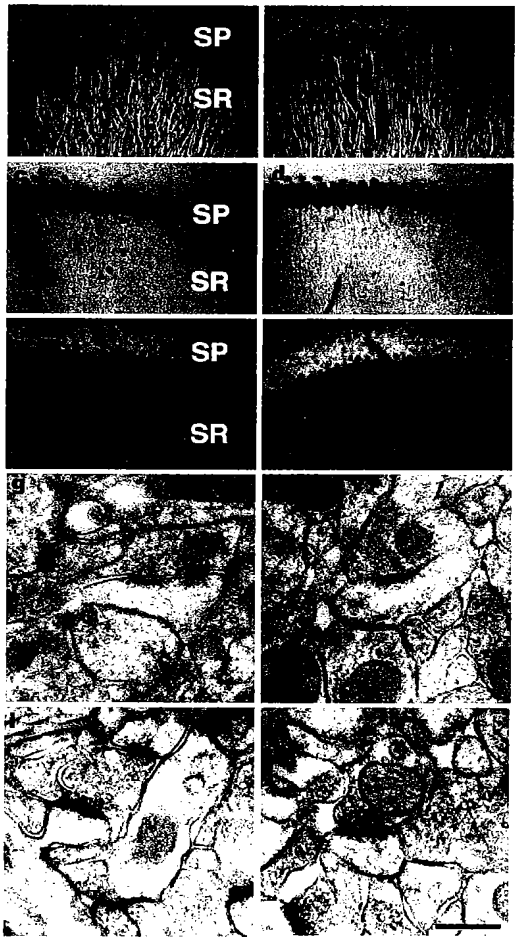

Figure 2 Anatomy and NR1 localization in hippocampus CA1 region of mice. **a**, **c**, **e**, **g**, **i**, Wild-type mice; **b**, **d**, **f**, **h**, **j**, PSD-95 mutant mice. **a**, **b**, MAP2 immunofluorescence; **c**, **d**, synaptophysin immunofluorescence; **e**, **f**, NR1 immunofluorescence; all photomicrographs are from a similar field of CA1, with the pyramidal cell layer (SP) at the top of the field, and the remaining two-thirds of the field occupied by the stratum radiatum (SR). **g**, **h**, Immunogold localization of NR1. Note that NR1 is localized at asymmetrical synapses in mutant and wild type mice. **i**, **j**, Standard morphology of the ultrastructure, with axospinous asymmetrical synapses shown in each case. Scale bar in **j** represents: for **a**–**f**, 70 μm; for **g**–**j**, 0.25 μm.

Synaptic plasticity in PSD-95 mutants

At many synapses in the brain, activation of postsynaptic NMDA receptors triggers complex multicomponent signalling pathways that can produce persistent changes in synaptic strength, such as LTP and LTD[1,2]. We therefore investigated whether PSD-95 might have a role in NMDA-receptor signalling by examining NMDA-receptor-dependent forms of synaptic plasticity in hippocampal slices from PSD-95-mutant mice. A conventional high-frequency stimulation protocol (100 Hz) that induces NMDA-receptor-dependent LTP produced a significantly larger potentiation of synaptic transmission in slices from PSD-95-mutant mice ($t(12) = 2.59$, $P < 0.025$; Fig. 4a). Immediately after high-frequency stimulation, the potentiation of synaptic transmission was similar in slices from wild-type and PSD-95-mutant mice; however, although synaptic strength remained at a steady-state potentiated level in wild-type slices (fEPSPs were potentiated to 193.6 ± 9.3% of baseline 60 min after high-frequency stimulation; $n = 7$), synaptic strength continued to grow over the next 30 min in slices from PSD-95-mutant mice (fEPSPs potentiated to 242.8 ± 17.5% of baseline; $n = 7$). To find the full extent of the enhanced LTP and the maximal LTP that could be generated in slices from PSD-95-mutant mice, we induced saturating levels of LTP with multiple trains of 100-Hz stimulation. As shown in Fig. 4b, LTP saturated at a much higher potentiated level in slices from mutant mice (298.4 ± 39.0% of baseline; $n = 5$) compared with wild-type slices (174.8 ± 14.0% of baseline; $n = 4$, $t(7) = 2.98$, $P < 0.05$).

We next quantified LTP induced by trains of low-frequency presynaptic stimulation. A 900-pulse train of 5-Hz stimulation, a near-threshold protocol for LTP induction[20], induced a small amount of LTP in slices from wild-type mice; fEPSPs were potentiated to

126.5 ± 7.3% of baseline after 45 min ($n = 7$) (Fig. 4c). In slices from PSD-95-mutant mice, synaptic transmission was potentiated to near saturation (fEPSPs were 278.4 ± 17.4% of baseline; $n = 6$) (Fig. 4c). The NMDA-receptor antagonist 2-amino-5-phosphonovaleric acid (AP5) blocked 5-Hz-stimulation-induced LTP in both wild-type and PSD-95-mutant mice (fEPSPs in slices from PSD-95-mutant mice were 110.2 ± 11.7% of baseline ($n = 5$) in 100 μM D,L-AP5 and 98.5 ± 3.4% of baseline in slices from wild-type mice ($n = 5$)), indicating that the enhanced LTP in slices from PSD-95-mutant mice is not due to upregulation of NMDA-receptor-independent

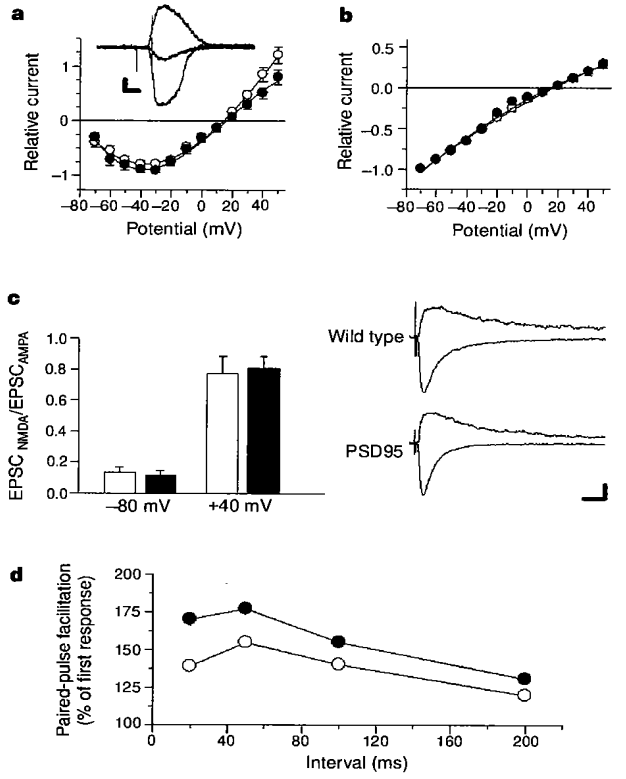

Figure 3 NMDA-receptor currents and synaptic physiology. **a**, Current–voltage relationship for NMDA (250 μM)-receptor-gated currents recorded in the presence of magnesium (1 mM) (white circles, wild type ($n = 10$); filled circles, PSD-95 mutant ($n = 16$)). Insert, currents recorded from a single PSD-95 mutant cell at –70 mV (middle trace), –20 mV (lower trace), and +50 mV (upper trace). Calibration bars are 50 ms and 100 pA. **b**, Current–voltage relationship for NMDA (250 μM)-receptor-gated currents recorded in magnesium-free solution (white circles, wild type ($n = 12$); filled circles, PSD-95 mutant ($n = 24$)). **c**, Synaptic NMDA-receptor currents. The bars show the magnitude of the NMDA-receptor-mediated component EPSCs (normalized to the magnitude of the AMPA-receptor-mediated component; see Methods). At postsynaptic holding potentials of both –80 mV and +40 mV, the NMDA-receptor-mediated component of the EPSCs in CA1 pyramidal cells from PSD-95 mutants (black bars) is indistinguishable from that seen in pyramidal cells from wild-type animals (white bars). Traces show representative EPSCs elicited in a wild-type cell (top) and a PSD-95-mutant cell (bottom) at +40 mV (outward-going currents) and –80 mV (inward-going currents). Each trace is the average of four EPSCs elicited at each holding potential. Calibration bars indicate 20 ms and 50 pA. **d**, Paired-pulse facilitation of fEPSPs was measured using pairs of presynaptic fibre stimulation pulses separated by 20, 50, 100 and 200 ms. Note the larger facilitation ($P < 0.05$) seen in slices from PSD-95-mutant animals (filled symbols) compared to wild type (open symbols). Each point is the mean ± s.e.m. (error bars are smaller than point used to plot the mean value).

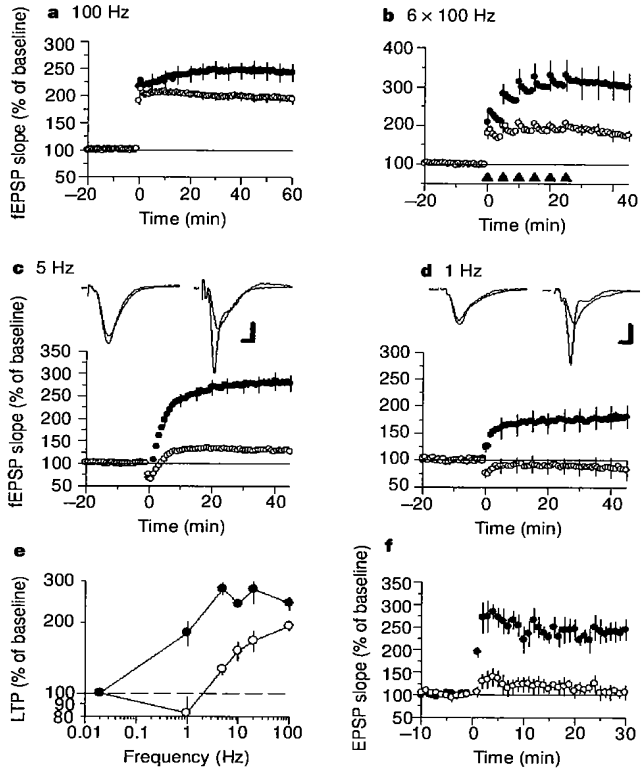

Figure 4 Frequency-dependent changes in synaptic strength. **a**, High-frequency stimulation-induced LTP was elicited using two trains of 100-Hz stimulation delivered at time zero. Note the larger potentiation seen 60 min after 100-Hz stimulation in slices from PSD-95 mutant animals (black symbols) compared with slices from wild-type animals (white symbols). **b**, Single 1-s trains of 100-Hz stimulation were delivered six times (at points indicated by black triangles) starting at time zero. Synaptic transmission in wild-type slices (white symbols) shows no further increase after the second train; transmission in slices for PSD-95 mutants continues to increase and saturates at a much higher level. **c**, **d**, 900 stimulation pulses were delivered at time zero at either 5 Hz (**c**) or 1 Hz (**d**). Although these stimulation protocols produce small amounts of either LTP (5 Hz) or LTD (1 Hz) in slices from wild-type animals (white symbols), both stimulation protocols induce large LTP in slices from PSD-95 mutant animals (black symbols). The fEPSPs in **c** were recorded during baseline and 45 min after 5-Hz stimulation in wild-type (left) and PSD-95 mutant animals (right). The fEPSPs in **d** were recorded before and 45 min after 1-Hz stimulation in slices from wild-type (left, smaller response is after 1-Hz stimulation) and PSD-95 mutant animals (right, larger response is after 1-Hz stimulation). Calibration bars in **c** and **d** indicate 2 mV and 2 ms. **e**, Summary of the ability of different frequencies of synaptic stimulation to induce persistent changes in synaptic strength in hippocampal slices from wild-type (white symbols) or PSD-95 mutant (black symbols) animals; 0.02 Hz, which corresponds to the stimulation frequency used to monitor synaptic transmission throughout the experiments, had no effect on synaptic transmission in slices from wild-type and PSD-95 mutant animals. The line at 100% of baseline corresponds to no lasting change in synaptic strength. **f**, EPSPs evoked once every 30 s were recorded intracellularly from individual CA1 pyramidal cells. Following 10 min of baseline recording, 30 EPSPs (evoked at 0.5 Hz) were each paired with a 150-ms, 1.0-nA depolarizing current pulse delivered through the recording electrode starting 10 ms after the start of an EPSP. Data are from 12 wild-type cells ($n = 4$ animals; white symbols) and 11 PSD-95 mutant cells ($n = 4$ animals; black symbols).

forms of LTP. A large enhancement of LTP in PSD-95-mutant slices was also stimulated by intermediate frequencies. In wild-type slices, 900 pulses of 10 and 20 Hz induced potentiations of 151.6 ± 14.8% ($n = 4$) and 167.4 ± 17.7% of baseline ($n = 6$), respectively, whereas fEPSPs from PSD-95-mutant mice were potentiated to 240.2 ± 4.6% ($n = 5$) and 277.3 ± 37.5% ($n = 6$) of baseline, respectively. Finally, we used a low-frequency protocol (1 Hz, 900 pulses) that induces LTD in hippocampal slices[21] from young wild-type mice and induces a small and nonsignificant depression of synaptic transmission in slices from adult wild-type mice (fEPSPs were 82.2 ± 19.6% of baseline ($n = 4$, $t(3) = 0.91$), compared with pre-1 Hz baseline) (Fig. 4d). In response to this stimulation protocol, slices from adult PSD-95-mutant mice showed a significant LTP (fEPSPs were 180.4 ± 21.8% of baseline; $n = 5$, $t(4) = 3.69$, $P < 0.025$) (Fig. 4d). As summarized in Fig. 4e, these results indicate that the frequency sensitivity of LTP induction in the CA1 region of the hippocampus is altered in PSD-95-mutant mice.

To determine whether the enhanced LTP was due to altered inhibitory synaptic transmission, we tested potentiation in the presence of GABA inhibitors. Although 50 pulses of stimulation at 2.5 Hz elicited little LTP in slices from wild-type mice (fEPSPs were potentiated to 126.5 ± 8.3% of baseline; $n = 7$), we found that synaptic transmission was potentiated to 232.76 ± 30.4% of baseline in slices from PSD-95-mutant mice ($n = 3$, $t(8) = 4.93$, $P < 0.005$, compared to wild-type). When inhibitory synaptic transmission was blocked by 50–100 μM picrotoxin, 50 pulses of 2.5 Hz still elicited a significantly ($t(4) = 2.99$, $P < 0.025$) larger LTP in slices from PSD-95-mutant mice (fEPSPs were potentiated to 271.9 ± 31.1% ($n = 3$) of baseline in slices from PSD-95 mutants, and 175.6 ± 8.3% ($n = 3$) of baseline in slices from wild-type mice). In addition, when inhibitory synaptic transmission was blocked by 100 μM picrotoxin and intracellular microelectrodes were used to record EPSPs, we found that pairing low-frequency presynaptic fibre stimulation (0.5 Hz) with postsynaptic depolarization induced significantly larger LTP in cells from PSD-95 mutants (30 min post-pairing EPSPs were 105 ± 11.8% of baseline in wild-type cells and 245 ± 25.1% of baseline in PSD-95 mutant cells; $t(6) = 4.64$, $P < 0.005$; Fig. 4f). Therefore, the enhanced induction of LTP in PSD-95 mutants does not seem to arise from alterations in inhibitory synaptic transmission. Moreover, the larger potentiation induced by pairing low-frequency presynaptic fibre stimulation with postsynaptic depolarization in PSD-95 mutants indicates that changes in paired-pulse facilitation or postsynaptic excitability are unlikely to underlie the LTP enhancement seen in PSD-95 mutants.

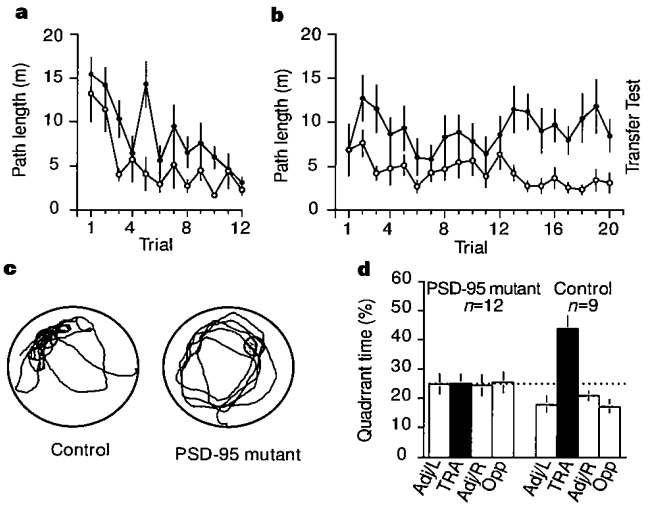

Figure 5 Behavioural data. **a**, Path length across 3 days of training to a visible cue (4 trials per day). By trial 12, the path lengths of both groups in the 2-m-diameter pool were equivalent and close to the minimum possible. Control, white symbols; PSD-95, filled symbols (mean ± 1 s.e.m.). **b**, Path length across 5 days of place-learning to a hidden platform. Wild-type controls learn to take relatively direct paths, whereas PSD-mutant mice persist in taking circuitous routes. **c**, **d**, Representative swim paths (**c**) and per cent time spent in each quadrant (**d**) during the 60-s transfer test in which the hidden platform (grey in **c**) is not present in the pool. Wild-type mice consistently search in the correct location but PSD-95 mutant mice swim all over the pool. Further training (for up to 32 trials) failed to reveal spatial learning in PSD-95 mutant mice (see text). The horizontal dotted line at 25% in **d** indicates chance performance. Training quadrant, TRA; adjacent left, Adj/L; adjacent right, Adj/R; opposite, Opp.

Learning and memory in PSD-95 mutants

Neural-network models of learning and memory incorporating bidirectional synaptic plasticity (LTP and LTD) predict that major alterations in the frequency function should be deleterious to learning. We therefore tested spatial learning in a watermaze, which is dependent on hippocampus NMDA-receptor function[22,23]. Adult littermate wild-type ($n = 9$) and homozygous ($n = 12$) mice swam in the pool and mounted the platform in the normal ways. With the experimenter blind with respect to genotype, we monitored the animals as they learned to approach a platform marked with a visible cue (Fig. 5a). Both wild-type and PSD-95 mutants reduced the length of their path across the training period (Fig. 5a). Although the mutant mice were initially slower, no difference between groups was seen over the last 6 trials ($P < 0.05$). We then tested spatial learning using the hidden platform version of the watermaze. The mutant mice had significantly longer swim paths than wild-type mice (controls, 4.32 ± 0.30 m; PSD-95 mutants, 9.04 ± 0.50 m; $F(1, 19) = 5.66$, $P < 0.05$; Fig. 5b). After 20 training trials, performance in a transfer test (with the platform removed) was used as an index of learning (Fig. 5c, d). Wild-type mice showed a spatial bias towards the training quadrant, spending significantly more time searching there than in the other three quadrants ($F(3, 24) = 13.84$; $P < 0.0001$), unlike the mutant mice ($F < 1$, $P < 0.9$; group by quadrant interaction, $F(3, 57) = 5.41$; $P < 0.005$). The mice were then given further training using a smaller platform until they reached a specified criterion, or until 32 trials had been completed. All controls (9/9) reached this criterion in 15.1 ± 2.4 trials whereas only 2/12 PSD-95 mutants were successful, giving a group mean of 29.3 ± 2.0 trials ($F(1, 9) = 20.51$; $P < 0.0005$). The PSD-95-mutant mice therefore had a marked inability to learn the position of the hidden platform, an effect also seen when NMDA receptors are blocked[22,23].

Discussion

PSD-95 has been suggested in *in vitro* studies[7] to localize NMDA receptors to the synapse and our results show that they are synaptically localized in PSD-95-mutant mice. This raises the possibility that other molecules may be more important in localizing NMDA-receptor subunits to the synapse. Receptor localization could be achieved by actin in dendritic spines[24]; actin may interact with NMDA-receptor subunits through α-actinin[25] and spectrin[26]. The NMDA receptor may experience two sets of interactions: one controlling receptor localization and turnover, which is independent of PSD-95, and a second operating through PSD-95 on signal-transduction pathways that control synaptic strength (Fig. 6a).

A wide range of frequencies and patterns of pre- and postsynaptic activity probably act through NMDA-receptor-dependent forms of synaptic plasticity to modulate dynamically the strength of excitatory synaptic transmission *in vivo*. In our PSD-95-mutant mice, the frequency-response function controlling the induction of persistent changes in synaptic efficacy[24] showed a dramatic leftward and upward shift so that all frequencies tested (1, 5, 10, 20, 100 Hz) induced LTP. This propensity towards potentiation was most marked at low frequencies, where for example 1-Hz stimulation produced no potentiation in wild-type mice but a large LTP in the PSD-95 mutants. This enhanced LTP requires the activation of NMDA receptors and reaches the enhanced level during the first

30 min after high-frequency stimulation (100 Hz). Postsynaptic kinases and phosphatases are known to regulate long-term plasticity during this time window[1,2], which suggests that a pathway downstream from the NMDA receptor has been modified in the PSD-95 mutants. Components of this pathway could include PSD-95-binding proteins such as SynGAP[28,29], neuroligin[18], GKAP/SAPAP[30,31], neuronal NO synthase[13] and postsynaptic phosphatases that participate in LTD. A model of the NMDA receptor, PSD-95 and associated proteins in a signal-transduction complex (Fig. 6a) in which the associated proteins participate in downstream signalling is in keeping with the 'transducisome' model described for *Drosophila*, where the Trp calcium channel binds PDZ-domain-containing proteins that mediate assembly of a signalling complex[32]. One function of this complex that is suggested by our paired-pulse facilitation data is to allow the postsynaptic NMDA receptor to regulate transmitter release as a result of PSD-95/neuroligan/neurexin interaction with the presynaptic terminal.

Mathematical models of synaptic plasticity that include bidirectional modifications of synaptic strength (potentiation and depression)[27,33] when incorporated into neural-network simulations have implications that bear on our PSD-95-mutant mice (Fig. 6b, c). Unlike networks composed of synapses exhibiting only potentiation of synaptic strength, bidirectionally modifiable synapses can increase storage capacity, reduce errors, and limit the number and strength of potentiated synapses to an optimum for memory storage[34,35]. Hippocampal neurons fire in the θ range of 4–12 Hz during exploratory behaviour[36], and in this range neurons in PSD-95 mutants show dramatic LTP, unlike neurons in wild-type mice which are near the threshold between LTP and LTD. Consequently, training of PSD-95-mutant mice in a spatial learning task might cause too many synapses within the network to become strongly potentiated and not enough to be depressed, resulting in a degradation of information storage and recall capacity, which manifests as a learning impairment. Genetic manipulation of PSD-95 will enable bidirectional regulation of synaptic strength to be controlled and provide further insight into synaptic plasticity and neural networks and their integrated function in learning and memory. □

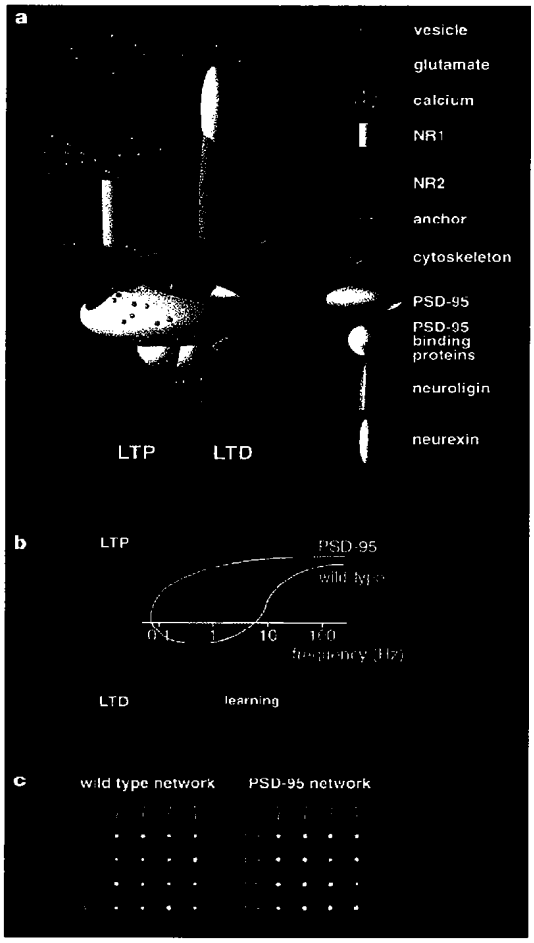

Figure 6 Model for PSD-95 function. **a**, The NMDA-receptor/PSD-95 complex at the synapse with presynaptic terminal with synaptic vesicles (top) and dendritic spine (bottom). NR2 subunits bind PSD-95, which binds neuronal NO synthase, SynGAP, GKAP/SAPAP proteins and neuroligin, which binds the presynaptic protein neurexin. Anchoring proteins tether the transduction complex through NMDA-receptor subunits to the postsynaptic cytoskeleton. Glutamate release from the presynaptic terminal leads to Ca^{2+} influx, which together with PSD-95 and associated proteins may regulate the balance between LTP and LTD (arrows). **b**, **c**, A model to explain the learning defects in PSD-95 mutant mice, based on learning rules using bidirectional synaptic plasticity. **b**, Postsynaptic activity (as a function of the frequency of trains of synaptic stimulation in Hz) is plotted against the corresponding degree of LTP (red) and LTD (blue). The green box (labelled learning) shows the firing frequency of hippocampal CA1 neurons during exploratory behaviour: in this range, synapses in wild-type mice may show either LTP or LTD, whereas PSD-95 mutant synapses are more likely to show LTP. **c**, This is indicated in a neural network in which PSD-95 mutants have an inappropriately higher number of synapses showing LTP (red) and too few showing LTD (blue). Grey triangles are cell bodies, and processes are lines that intersect as synapses; the colour (blue–red) indicates the strength of synaptic transmission.

Methods

Gene targeting and biochemistry. The targeting vector comprised 1.6-kb and 4.2-kb bands of, respectively, 5′ and 3′ genomic DNA flanking a cassette (TAG3IRES1acZpA-MC1neopA) containing the positive selectable marker MC1-neo (neomycin). The 5′ end of this cassette contained stop codons in all reading frames to terminate translation of PSD-95 at the *Pvu*II site in PDZ3, followed by an internal ribosome-entry site (IRES) which allows a β-galactosidase reporter gene to be expressed under the control of PSD-95. For negative selection, two copies of the thymidine kinase gene (MC1-tk) was ligated 5′ to the 5′ homology arm. The targeting construct was linearized and electroporated into ES cells (E14Tg2αIV clone). For Southern blot analysis, 5–15 μg DNA from ES cells or tail tips were digested with *Eco*RI or *Hin*dIII and probed with a 0.8-kb cDNA fragment (5′ probe) or a 1.2-kb genomic DNA (3′ probe) flanking the homology region. Genotyping using PCR required two independent reactions. The wild-type allele was amplified (220-bp product) using a forward primer upstream of the *Pvu*II site in the PDZ3 domain (AACCAAGGCGGATCGTGATCCA) and a reverse primer (TCTCTTTGGTGGGCAGTG). The mutant allele (2-kb product) was amplified using a forward primer in the *neo* gene (CATTCGACCACCAAGCG AAAGATC) and a reverse primer (CAGGGAGCGGGGACGGATGA) in PSD-95. Amplification was for 30 cycles of 30 s at 93 °C, 60 s at 55 °C, 60 s at 72 °C. Standard procedures were used for synaptosome preparation, protein extraction, immunoblotting and immunoprecipitation. Antibodies: against NR1, mAb 54.1 and pAb 1516 (Chemicon); against PSD-95, pAb138, raised against the N-terminal 438 residues of a mouse PSD-95 fusion protein, and mAb PSD-95 (Transduction Labs).

Neuroanatomy. All procedures relating to the care and treatment of mice conformed with institutional and NIH guidelines. Nine mice were anaesthetized with a lethal dose of chloral hydrate and perfused with aldehydes, dissected, post-fixed, and sectioned[37]. 50-μm vibratome sections were used for immunohistochemistry and 15-μm freshly frozen sections were used for X-gal (5-bromo-4-chloro-3-indolyl-β-galactoside) (Nova Biochem) staining. Primary antibodies were: anti-NR1 mAb 54.1 (1/100); anti-synaptophysin mAb SY38 (1/10; Boehringer); non-phosphorylated neurofilament mAb SMI32 (1/7,500; Steinburger Monoclonal); MAP2 mAb HM2 (1/800; Sigma Immuno Chemicals). Standard procedures were followed for immunofluorescent staining, mounting and coverslipping[37]. Sections were examined and photographed by experimenters blind to genotype. For post-embedding immunogold localization, six additional mice were perfused with a fixative composed of 2.5% glutaraldehyde, 1% paraformaldehyde and 0.1% picric acid in 0.1M PBS, pH

7.3. After fixation, vibratome sections of CA1 were collected, embedded in resin, thin-sectioned, prepared for post-embedding immunogold localization of NR1, and viewed at 60 kV on a Zeiss CH-10 electron microscope, as described[37]. Control experiments in which grids were incubated in buffer instead of the NR1 antibody showed no immunogold labelling.

Electrophysiology. 400-μm-thick slices of mouse hippocampus were maintained at 30 °C in an interface-type recording chamber perfused with a murine artificial cerebrospinal fluid (ACSF) containing 124 mM NaCl, 4.4 mM KCl, 25 mM Na_2HCO_3, 1 mM NaH_2PO_4, 1.2 $MgSO_4$, 2 mM $CaCl_2$ and 10 mM glucose. fEPSPs elicited by Schaffer collateral/commissural fibre stimulation were recorded in the CA1 region as described[20]. Glass microelectrodes filled with 2 M CsCl (resistance, 60–140 MOhms) were used to record EPSPs from individual CA1 pyramidal cells and current injected through the recording electrode was used to hyperpolarize cells to between −90 and −95 mV. There were no differences between mutant and wild-type cells in either resting membrane potential or input resistance. In these experiments, slices with the CA3 region removed were bathed in a modified, 100 μM picrotoxin-containing ACSF in which the concentrations of $CaCl_2$ and $MgSO_4$ were raised to 4.0 mM each and the concentration of KCl was reduced to 2.4 mM. High-frequency-stimulated LTP was induced using 2-s and 1-s trains of 100-Hz stimulation (intertrain interval was 10 s). Saturating levels of LTP were induced by six deliveries of single 1-s trains of 100-Hz stimulation every 5 min. To test synaptic responses mediated by NMDA receptors in mutant and wild-type mice, we used whole-cell voltage-clamp techniques to record EPSCs due to Schaffer collateral fibre stimulation in CA1 pyramidal cells held at membrane potentials between −80 and +40 mV. Low-resistance (3–5 MΩ; access resistances ranged from 12.5 to 27 MΩ) patch-clamp electrodes were filled with a solution containing 140 mM CsCl, 1 mM $MgCl_2$, 0.2 mM EGTA, 2 mM Mg-ATP, 0.3 mM GTP and 10 mM HEPES, pH 7.2. In some experiments, electrodes were filled with a solution containing 122.5 mM caesium gluconate, 15 mM CsCl, 2.5 mM TEA-Cl, 1.4 mM NaCl, 0.2 mM EGTA, 2 mM Mg-ATP, 0.3 mM GTP and 10 HEPES, pH 7.2. In these experiments, slices with the CA3 region removed were maintained at room temperature (20 to 22 °C) in a submerged recording chamber perfused (2–3 ml per min) with a modified ACSF containing 100 μM picrotoxin, 2.4 mM KCl, and double the normal concentrations of $CaCl_2$ and $MgSO_4$. The AMPA- and NMDA-receptor-mediated components of the EPSCs were estimated from the amplitude of the synaptic currents measured at 5 and 50 ms after the start of the EPSC, respectively. To compare across cells the size of the NMDA-receptor-mediated component of the EPSC, it was normalized to the size of the AMPA-receptor-mediated component. All values are reported as mean ± s.e.m., n being the number of mice. All experiments were performed blind, and after data collection the genotypes were revealed for analysis. Primary cultures of forebrain neurons were prepared from individual neonatal mice (P1) as described[38]. Whole-cell patch-clamp recordings were made from cells cultured for 12–20 days (wild type, mean age of 13.6 d; PSD-95 mutant, mean age of 16.3 d), which was after the age at which PSD-95 expression was observed by using X-gal staining. The composition of the recording electrode solution was (in mM): $CsMeSO_3$ 100, Cs-BAPTA 5, HEPES 15, Mg-ATP 4, Na-GTP 0.4, sucrose 40, adjusted to pH 7.2 with CsOH. The composition of the bathing medium was (in mM): NaCl 140, KCl 3, $CaCl_2$ 2.5, HEPES 15, glucose 10, $MgCl_2$ 0 or 1, adjusted to pH 7.4 with NaOH. Currents were evoked by brief (50-ms) application of 250 μM NMDA + 25 μM glycine. The calculated junction potential of +15 mV was not corrected for in the data shown here. Student t-tests were used to assess statistical significance.

Behavioural testing. We used an open-field watermaze (2 m in diameter, opaque water, 25 ± 1 °C, automated swim-path monitoring). Visible platform training: mice were trained to a randomly located platform with a striped flag protruding above it (4 trials per day for 3 days; 30-cm-diameter platform; curtains drawn around the pool to occlude extra-maze cues; maximum trial duration was 90 s; intertrial interval (ITI), 10 min). Hidden platform training: we used a hidden platform with the extra-maze cues visible (4 trials per day, 5 days, 30-cm platform; platform area/pool area was 1/44; 30 s was spent on the platform at the end of each trial; ITI, 10 min). Transfer test: 10 min after the previous training trial, mice were placed in the pool for 60 s (platform absent; the start position was opposite to whatever training quadrant had bene used for an individual animal). Training to criterion: extended hidden-platform training, using a smaller hidden platform (20 cm diameter; platform area/pool area was 1/100) until the animals completed 2 consecutive days with each trial of <20 s, or until 32 trials had been done.

Received 9 June; accepted 13 October 1998.

1. Bear, M. F. & Malenka, R. C. Synaptic plasticity: LTP and LTD. *Curr. Opin. Neurobiol.* **4,** 389–399 (1994).
2. Bliss, T. V. P. & Collingridge, G. L. A synaptic model of memory: long-term potentiation in the hippocampus. *Nature* **361,** 31–39 (1993).
3. Hollman, M. & Heinemann, S. Cloned glutamate receptors. *Annu. Rev. Neurosci.* **17,** 31–108 (1994).
4. Nakanishi, S. & Masu, M. Molecular diversity and functions of glutamate receptors. *Annu. Rev. Biophys. Biomolec. Struct.* **23,** 314–348 (1994).
5. Smart, T. G. Regulation of excitatory and inhibitory neurotransmitter-gated ion channels by protein phosphorylation. *Curr. Opin. Neurobiol.* **7,** 358–367 (1997).
6. Kornau, H.-C., Schenker, L. T., Kennedy, M. B. & Seeburg, P. H. Domain interaction between NMDA receptor subunits and the postsynaptic density protein PSD-95. *Science* **269,** 1737–1740 (1995).
7. Kim, E., Cho, K.-O., Rothschild, A. & Sheng, M. Heteromultimeriozation and NMDA receptor-clustering activity of chapsyn-110, a member of the PSD-95 family of proteins. *Neuron* **17,** 103–113 (1996).
8. Müller, B. M. *et al.* SAP102, a novel postsynaptic protein that interacts with NMDA receptor complexes *in vivo*. *Neuron* **17,** 255–265 (1996).
9. Niethammer, M., Kim, E. & Sheng, M. Interaction between the C terminus of NMDA receptor subunits and mutliple members of the PSD-95 family of membrane-associated guanylate kinases. *J. Neurosci.* **16,** 2157–2163 (1996).
10. Cho, K. O., Hunt, C. A. & Kennedy, M. B. The rat brain postsynaptic density fraction contains a homolog of the *Drosophila* discs-large tumor suppressor protein. *Neuron* **9,** 929–942 (1992).
11. Kistner, U. *et al.* SAP90, a rat presynaptic protein related to the product of the *Drosophila* tumor suppressor gene *dlg-A*. *J. Biol. Chem.* **268,** 4580–4583 (1993).
12. Kim, E., Niethammer, M., Rothschild, A., Jan, Y. N. & Sheng, M. Clustering of shaker-type K^+ channels by interaction with a family of membrane-associated guanylate kinases. *Nature* **378,** 85–88 (1995).
13. Brenman, J. E. *et al.* Interaction of nitric oxide synthase with the postsynaptic density protein PSD–95 and alpha1-syntrophin mediated by PDZ domains. *Cell* **84,** 757–767 (1996).
14. Hough, C. D., Woods, D. F., Park, S. & Bryant, P. J. Organizing a functional junctional complex requires specific domains of the *Drosophila* MAGUK discs-large. *Genes Dev.* **11,** 3242–3252 (1997).
15. Müller, B. M. *et al.* Molecular characterization and spatial distribution of SAP97, a novel presynaptic protein homologous to SAP90 and the *Drosophila* discs-large tumor suppressor protein. *J. Neurosci.* **15,** 2354–2366 (1995).
16. Hunt, C. A., Schenker, L. J. & Kennedy, M. B. PSD-95 is associated with the postsynaptic density and not with the presynaptic membrane in forebrain synapses. *J. Neurosci.* **16,** 1380–1388 (1996).
17. Wang, J. H. & Kelly, P. A. T. Attenuation of paired-pulse facilitation associated with synaptic potentiation mediated by postsynaptic mechanisms. *J. Neurophysiol.* **78,** 2707–2716 (1997).
18. Irie, M. *et al.* Binding of neuroligins to PSD-95. *Science* **277,** 1511–1515 (1997).
19. Tejedor, F. J. *et al.* Essential role for dlg in synaptic clustering of shaker K^+ channels *in vivo*. *J. Neurosci.* **17,** 152–159 (1997).
20. Mayford, M., Wang, J., Kandel, E. R. & O'Dell, T. J. CaMKII regulates the frequency-response function of hipocampal synapses for the production of both LTD and LTP. *Cell* **81,** 891–904 (1995).
21. Dudek, S. M. & Bear, M. F. Bidirectional long-term modification of synaptic effectiveness in the adult and immature hippocampus. *J. Neurosci.* **13,** 2910–2918 (1993).
22. Morris, R. G. M., Anderson, E., Lynch, G. S. & Baudry, M. Selective impairment of learning and blockade of long-term potentiation by an *N*-methyl-D-aspartate receptor antagonist, AP5. *Nature* **319,** 774–776 (1986).
23. Tsien, J. Z., Huerta, P. T. & Tonegawa, S. The essential role of hippocampal CA1 NMDA receptor-dependent synaptic plasticity in spatial memory. *Cell* **87,** 1327–1338 (1996).
24. Allison, D. W., Gelfand, V. I., Spector, I. & Craig, A. M. Role of actin in anchoring postsynaptic receptors in cultured hippocampal neurons: Differential attachment of NMDA versus AMPA receptors. *J. Neurosci.* **18,** 2423–2436 (1998).
25. Wyszynski, M. *et al.* Competitive binding of α-actinin and calmodulin to the NMDA receptor. *Nature* **385,** 439–442 (1997).
26. Wechsler, A. & Teichberg, V. I. Brain spectrin binding to the NMDA receptor is regulated by phosphorylation, calcium and calmodulin. *EMBO J.* **17,** 3931–3939 (1998).
27. Bienenstock, E., Cooper, L. & Munro, P. Theory for the development of neuron selectivity: orientation specificity and binocular interaction in visual cortex. *J. Neurosci.* **2,** 32–48 (1982).
28. Kim, J. H., Liao, D., Lau, L.-F. & Huganir, R. SynGAP: a synaptic RasGAP that associates with the PSD-95/SAP90 protein family. *Neuron* **20,** 683–691 (1998).
29. Chen, H.-J., Rojas-Soto, M., Oguni, A. & Kennedy, M. B. A synaptic Ras GTPase-activating protein (p135 SynGAP) inhibited by CaM kinase II. *Neuron* **20,** 895–904 (1998).
30. Naisbitt, S. *et al.* Characterization of guanylate kinase-associated protein, a postsynaptic density protein at excitatory synapses that interacts directly with postsynaptic density-95/synapse-associated protein 90. *J. Neurosci.* **17,** 5687–5696 (1997).
31. Takeuchi, M. *et al.* SAPAPs: A family of PSD-95/SAP90-associated proteins localized at postsynaptic density. *J. Biol. Chem.* **272,** 11943–11951 (1997).
32. Tsunoda, S. *et al.* A multivalent PDZ-domain protein assembles signalling complexes in a G-protein-coupled cascade. *Nature* **388,** 243–249 (1997).
33. Sejnowski, T. J. Statistical constraints on synaptic plasticity. *J. Theor. Biol.* **69,** 387–389 (1977).
34. Willshaw, D. & Dayan, P. Optimal plasticity from matrix memories: what goes up must come down. *Neural Comp.* **2,** 85–93 (1990).
35. Hancock, P. J. B., Smith, L. S. & Phillips, W. A. A biologically supported error-correcting learning rule. *Neural Comp.* **3,** 201–212 (1991).
36. Otto, T., Eichenbaum, H., Wiener, S. I. & Wible, C. G. Learning-related patterns of CA1 spike trains parallel stimulation parameters optimal for inducing hippocampal long-term potentiation. *Hippocampus* **1,** 181–192 (1991).
37. Morrison, B. M., Janssen, W. G. M., Gordon, J. W. & Morrison, J. H. Light and electron microscopic distribution of the AMPA receptor subunit, GluR2, in the spinal cord of control and G86R mutant superoxide dismutase transgenic mice. *J. Comp. Neurol.* **395,** 523–534 (1998).
38. Rayport, S. *et al.* Identified postnatal mesolimbic dopamine neurons in culture: morphology and electrophysiology. *J. Neurosci.* **12,** 4264–4280 (1992).

Acknowledgements. We thank A. J. H. Smith for advice and for the 129 genomic library, J. Ure for embryo injection, L. Anderson and J. Young for mouse care, W. Janssen for technical assistance, F. Johnston and G. Brown for photography, and R. Ellaway for illustrations. This work was supported by the Fyssen Foundation (M.M.) and the BBSRC (M.M., M.D. and P.C.), by grants from the NIH and the Charles A. Dana Foundation (J.H.M. and Y.H.), the Esther A. and Joseph Klingenstein Fund and the Pew Charitable Trusts (T.J.O.), a grant from the National Institute of Mental Health (T.J.O.), and the Wellcome Trust (L.C.W. and S.G.N.G.).

Correspondence and requests for materials should be addressed to S.G.N.G. (e-mail: seth.grant@ed.ac.uk).

NMDA receptor pathways as drug targets

John. A. Kemp[1] and Ruth M. McKernan[2]

[1] EVOTEC Neurosciences GmbH, Schackenburgallee 114, D-22525 Hamburg, Germany

[2] Neuroscience Research Centre, Merck Research Laboratories, Terlings Park, Eastwick Road, Harlow, Essex CM20 2QR, UK

Correspondence should be addressed to R.M.M. (ruth_mckernan@merck.com)

Published online 28 October 2002; doi:10.1038/nn936

Since the mid 1980s, there has been a great deal of enthusiasm within both academia and industry about the therapeutic potential of drugs targeting the NMDA subtype of glutamate receptors. That early promise is just beginning to translate into approvable drugs. Here we review the reasons for this slow progress and critically assess the future prospects for drugs that act on NMDA receptor pathways, including potential treatments for some major disorders such as stroke and Alzheimer's disease, for which effective therapies are still lacking.

Glutamate is the main excitatory neurotransmitter in the mammalian CNS and mediates neurotransmission across most excitatory synapses. Three classes of glutamate-gated ion channels (AMPA, kainate and NMDA receptors) transduce the postsynaptic signal. NMDA receptors are abundant, ubiquitously distributed throughout the brain, fundamental to excitatory neurotransmission and critical for normal CNS function. Activation of the NMDA receptor is complex; both glutamate and glycine binding are required to open the ion channel and permit calcium entry. Glutamate has the neurotransmitter role, as it is released from presynaptic terminals in an activity-dependent manner, whereas glycine acts as a modulator, which is present in the extracellular fluid at more constant levels. The ion-channel integral to the NMDA receptor is voltage-dependently blocked by magnesium, and depolarization removes this block. Thus the NMDA receptor acts as a coincidence detector, linking neurotransmitter activation with the electrical state of the neuron. Sustained NMDA receptor activation promotes signaling to the nucleus that culminates in CREB phosphorylation, multiple gene activation and long-term synaptic plasticity (the mechanism underlying learning and memory). However, excess glutamate chronically overstimulates NMDA receptors, and excess intracellular calcium causes excitotoxicity (the glutamate-dependent mechanism by which neurons die in various CNS disorders). Too much is as harmful as too little. The NMDA receptor's role in excitotoxicity has driven the search for antagonists as neuroprotective agents. Its role in synaptic plasticity, on the other hand, has inspired research into receptor potentiators to treat cognitive dysfunction.

Fortunately, the NMDA receptor complex is bristling with modulatory sites, and the late 1970s and 1980s saw the development of agonists, antagonists and modulators acting at different binding sites[1] (**Fig. 1**). In the last decade, the molecular biology of the NMDA receptor family has been defined, and we now know that these receptors are composed of an NR1 subunit in combination with one or more NR2 subunits[2] and, less commonly, an NR3 subunit[3,4].

The NR2 subunits, of which there are four (A–D), determine the pharmacology and other properties of NMDA receptors, with further contributions from alternative splicing of NR1, particularly in exon 5 (ref. 5). There are differences in subunit expression. Whereas NR1 and NR2A are ubiquitous, NR2B is restricted to the forebrain, 2C to the cerebellum, and NR2D is much rarer than other subtypes. Differential assembly of receptor subunits allows for subtype- selective compounds, such as the prototypical NR2B selective blocker ifenprodil[6]. Detailed studies with selective compounds will be necessary to understand the distribution of different structural subtypes with greater clarity than is currently provided by mRNA distribution or currently available radioligands.

NMDA receptor antagonists

In theory, any CNS disorder in which neuronal loss is caused by glutamate-induced excitotoxicity has the potential to be treated by blocking NMDA receptors. The list includes cerebral ischemia, which occurs after stroke or brain trauma—dying neurons at the damaged core release glutamate to overactivate those in the penumbra. The NMDA receptor blocking approach may also be applied to neurodegenerative disorders in which excess glutamate is not the primary problem, but compromised neurons become sensitized to excitotoxic damage (for example, Parkinson's and Huntington's diseases). Finally, disorders such as epilepsy and neuropathic pain, in which there is overactivity of excitatory pathways, would also be candidates for NMDA receptor antagonist treatment.

Among these disorders, the preclinical rationale for the acute treatment of brain ischemia is strongest[7], and nonselective NMDA antagonists are the most consistently neuroprotective agents in animal models of stroke. Nevertheless, clinical trials in stroke and traumatic brain injury with NMDA antagonists have so far failed[7–9]. Is it time to conclude that NMDA receptor antagonists do not work in humans? Perhaps not. Although brain levels of drugs cannot routinely be measured in patients, the plasma levels achieved in recent studies were consistently below those needed for maximal neuroprotection in animal models[7]. NMDA antagonists have a number of adverse CNS effects, including hallucinations, a centrally mediated increase in blood pressure and, at high doses, catatonia and anesthesia (for which the NMDA ion-

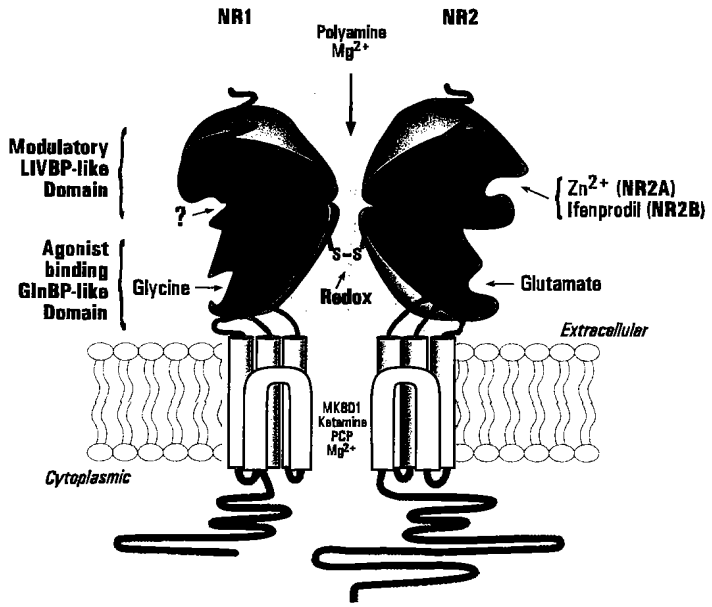

Fig. 1. NMDA receptor model showing potential sites for drug action. The extracellular part, made up of the N-terminal region and the extracellular loop between TM3 and TM4, contains two clam shell-like domains per subunit that for the agonist binding sites and modulatory binding sites[37]. The endogenous ligand for the modulatory domain on NR2A appears to be zinc. Although an endogenous ligand remains to be determined for NR2B, it is the site of action of ifenprodil-like compounds on NR2B. In addition to its critical channel blocking action, Mg^{2+} also appears to be the endogenous ligand for the polyamine modulatory site. Possible drug targets are highlighted in yellow.

channel blockers phencyclidine and ketamine were initially developed). These mechanism-based side effects have limited the doses used clinically[7]. Furthermore, the difficulty of conducting clinical trials in disorders with hugely variable outcomes such as stroke is considerable, so improved patient selection and trial methodology may help. It is premature to give up. The key issue is whether drugs that reduce NMDA activity can be developed without these dose-limiting side effects while still retaining some benefit.

Subtype-selective compounds or those with improved biochemical mechanisms may provide a step forward. The NR2B selective antagonist ifenprodil is neuroprotective in animal models of stroke without the severe side-effects of earlier drugs[10]. Subtype selectivity and a unique activity-dependent mechanism contribute to its superiority. Ifenprodil preferentially targets persistently activated receptors, but with a different mechanism of action from the open ion channel blockers (PCP and MK-801). Unlike these latter compounds, which become trapped within the closed receptor channel, leading to an accumulation of block, ifenprodil-like inhibitors have a reduced affinity and unbind from unactivated receptors leaving transiently activated receptors relatively unaffected[11] (**Fig. 1**).

A number of more potent and selective NR2B subunit antagonists have since been described, most of which are neuroprotective in animal models and produce minimal side effects at maximally neuroprotective doses (for example, CP-101606, Ro 25-6981 and Ro 63-1908)[7,12]. Encouragingly, in humans, CP-101606 (traxoprodil) did not induce the usual side-effects seen with nonselective NMDA antagonists. However, enthusiasm for this approach has been tempered by its reported failure in a clinical trial of traumatic brain injury (press release from Pfizer, October 2001). It is to be hoped that further trials with different compounds, assisted by improved measures of how much drug reaches the receptor (for example, by positron emission tomography) and the closer tracking of CNS damage will enable the potential of these drugs to be more fully tested.

The adverse effects of nonselective compounds has prevented widespread testing, particularly in disorders where they would need to be given chronically (unlike the acute treatment of stroke). However, the improved side effect profile of NR2B-selective compounds in humans has encouraged the initiation of clinical trials for other disorders. Animal studies indicate an important physiological role for NMDA receptors in both the induction and maintenance of neuropathic pain states, and nonselective NMDA receptor antagonists have consistent antinociceptive properties in both animals and humans[14]. In animal studies, NR2B-selective antagonists are antinociceptive at doses below those that impair motor coordination and elicit stimulant activity[15,16]. We wait with interest to see whether a similar margin occurs in humans as NR2B-selective compounds approach clinical trials.

An alternative approach to avoid unwanted side effects is to ensure that NMDA receptors are only partially blocked. So far, this has been most effectively achieved through the glycine site on the receptor, for which partial agonists exist. Pathological activation should be less likely because without full agonism at the glycine site, even at high glutamate concentrations, the receptor cannot be fully active. Preclinical studies suggest that glycine-site antagonists do indeed possess better side-effect profiles than high-affinity channel blockers, although chemically it has proved challenging to develop potent glycine-site antagonists that mimic the small amino acid with the right drug-like qualities for chronic dosing[17,18].

NMDA antagonists have been known for several years to have beneficial effects in animal models of Parkinson's disease (PD). When nigrostriatal dopamine is depleted, glutamatergic pathways to the striatum and basal ganglia output nuclei become overactive. In preclinical dopaminergic lesion models, NMDA antagonists act in a synergistic way with levodopa and dopamine agonists[19]. Consistently, the development of nonselective NMDA antagonists for PD has been hampered by their side effects. However, amantadine, a low-affinity NMDA receptor channel blocker, is used to treat Parkinson's disease in some countries and has also been shown to improve levadopa-induced dyskinesias in humans[20]. NR2B-selective antagonists have also been effective in rodent and primate PD models and may have therapeutic potential either as stand-alone therapies or in combination with dopamine agonists.

For certain disorders, low-affinity channel blockers have a better therapeutic window than high-affinity blockers, such as MK-801 and PCP, possibly due to their more transient block of activated receptor channels. Interestingly, in this regard, a low-affinity channel blocker, Memantine, has recently received approval for the treatment of moderately severe to severe Alzheimer's disease. Merz will launch Memantine (Axura) later this year. Given the critical role of NMDA receptor activation in

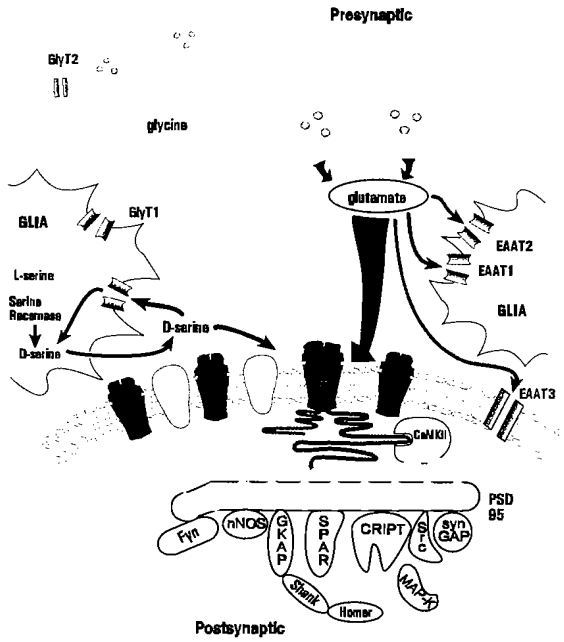

Fig. 2. A prototypic glutamatergic synapse depicting factors influencing NMDA receptor–mediated neurotransmission. Additional possible drug targets are highlighted in yellow.

learning and memory, it seems counter-intuitive that an NMDA antagonist would improve the symptomatology of Alzheimer's disease. However, there is support from preclinical studies that low levels of NMDA antagonism can improve learning in certain tasks[21,22], although the precise mechanism underlying this remains unclear.

It is interesting to speculate which mechanism, among low-affinity channel blockers (for example, memantine), glycine site antagonists, glutamate antagonists or allosteric antagonists, would be most beneficial. Glycine or glutamate antagonists have to compete with high levels of endogenous transmitter, and therefore high doses would need to be given. The more consistent glycine levels may be easier to block partially but may not be so well tolerated because glycine acts at all subtypes. Ifenprodil-like compounds are more likely to be well tolerated because of their subtype selectivity and activity-dependent mechanism of action, but these attributes could result in a reduced efficacy compared to nonselective compounds. Only clinical testing will tell.

NMDA receptor enhancers

The balance of evidence indicates that potentiating NMDA receptors should be beneficial for treating cognitive disorders and schizophrenia. There is possibly some utility in anxiety disorders[23]. Nonselective NMDA receptor channel blockers (such as PCP or ketamine) disrupt memory formation and cause a schizophrenic-like syndrome in humans, recapitulating both the positive and negative symptoms[24,25]. Transgenic mice in which the expression of NR1 subunits is reduced show a schizophrenic-like phenotype. Indeed, hypofunction of the glutamate system may be central not only to the treatment of schizophrenia but also to its etiology. Fortunately, there are multiple ways of enhancing NMDA receptor function, some of which have already been tried clinically. Direct activation of the receptor by glutamate site agonists has not been explored because of obvious concerns over excitotoxicity. Of the known modulatory sites on the ion-channel complex, activation of the glycine site has shown some clinical benefit. Glycine or other glycine site agonists, D-serine and D-cycloserine, given in addition to standard antipsychotic therapy, have both been reported to show efficacy in treating schizophrenia including the cognitive deficits[26,27]. Whether a glycine site agonist can generate the same level of therapeutic benefit in the absence of other neuroleptic agents remains to be determined, and glycine enhancement has so far failed to treat all aspects of the disorder. Furthermore, selective, drug-like glycine site agonists have proven even harder to develop than antagonists.

Some companies have taken the approach of trying to increase extracellular levels of glycine by blocking glycine re-uptake into neurons through the glyT-1 transporter (using drugs such as ALX 5407 and ORG 24598). This assumes that CNS levels of glycine are insufficient to saturate the glycine site, for which there is some evidence[28]. Blocking neurotransmitter transporters is a seemingly tractable target because other highly effective drugs work through this mechanism (for instance, SSRIs). An analogous approach is to increase extracellular levels of D-serine, another endogenous ligand for the glycine site[29], by inhibiting re-uptake into glia. Similarly, preventing synthesis of D-serine by inhibiting serine racemase[30] could theoretically have utility as an indirect inhibitor of NMDA activity.

Reduction of NMDA receptor function with drugs or genetic manipulation clearly disrupts learning and memory in animals. Similarly overexpression of the NR2B subunit improves learning and memory in mice[31]. Perhaps it will be possible to find small molecules that potentiate NMDA receptors in the way that benzodiazepines (such as Valium) enhance activation of $GABA_A$ receptors. The principle has been proven for another class of glutamate receptors, the AMPA receptors, for which aniracetam, CX516 and LY-404187 potentiate the receptor, mainly through suppression of desensitization (see review by Lynch in this volume). If AMPA receptor potentiators can be beneficial in cognitive disorders, then those acting through the NMDA receptor have equal, if not greater, merit. Small molecules that potentiate NMDA receptors have been identified[32], at least in principle.

Future prospects

Work in the NMDA receptor field indicates that developing compounds safe enough to pass the highest hurdles is not easy. Realistically, compounds with more subtle profiles (subtype-selective or activity-dependent blockers) are more likely to make the grade, as are those that affect the availability of agonists upstream of the receptor. The domain on NR2B to which ifenprodil binds also exists on all other ionotropic glutamate receptor subunits and is the site to which zinc binds to block NR2A receptors. Thus, by targeting this site there is the potential to develop compounds selective for other subtypes.

The recent explosion in genomics, proteomics[33] and in understanding the structure of the excitatory synapse[34] has identified a plethora of proteins that might modify glutamate neurotransmission downstream of receptor activation. The NMDA receptor is part of a postsynaptic signaling complex known as the postsynaptic density, composed of PSD-95 and many other PDZ domain–interacting proteins, including kinases, and other signaling and scaffolding proteins (Fig. 2). Some of these represent potential drug targets. Although protein–protein interactions

have been notoriously difficult to disrupt using small molecules of the type that readily penetrate the brain, many regulatory enzymes interact with NMDA receptors, some in a subunit-selective manner (for example, CaMKII interactions with NR2B), offering further subtlety of action. The magnitude and specificity of modulating NMDA function by blocking receptor-specific kinases is as-yet uncharacterized. Recent intriguing data suggest that synaptic and extrasynaptic NMDA receptors serve different functions[35,36]. If confirmed, this offers yet another route to physiological specificity once the subtypes and/or post-receptor mechanisms are better understood.

Given the many, varied opportunities to modify NMDA receptor activity, the potential for finding therapeutically valuable drugs is high. However, the balance between blocking NMDA neurotransmission and potentiating it is a critical one. Will we be able to find effective drugs for schizophrenia without increasing the propensity to damage from stroke? Will subtle blockade of NMDA receptors relieve pain without disrupting learning? If we are fortunate and/or skilled enough, it may be possible to correct an over- or under-active glutamate system with the appropriate drug. It is worth bearing in mind, however, that the brain has had the whole of evolution to generate that balance. What are the chances that the pharmaceutical industry can improve on it in a decade or two?

RECEIVED 25 JUNE; ACCEPTED 13 AUGUST 2002

1. Watkins, J. C. in *The NMDA Receptor* (eds. Collingridge, G. L. & Watkins, J. C.) 1–30 (Oxford Univ. Press, New York, 1994).
2. McBain, C. J. & Mayer, M. L. N-methyl-D-aspartic acid receptor structure and function. *Physiol. Rev.* 74, 723–760 (1994).
3. Das, S. *et al.* Increased NMDA current and spine density in mice lacking the NMDA receptor subunit NR3A. *Nature* 393, 377–381 (1998).
4. Chatterton, J. E. *et al.* Excitatory glycine receptors containing the NR3 family of NMDA receptor subunits. *Nature* 415, 793–798 (2002).
5. Kemp, J. A. & Kew, J. N. C. in *Drugs And The Pharmaceutical Sciences* Vol. 89 (ed. Leff, P.) 297–321(Marcel Dekker, New York, 1998).
6. Williams, K. Ifenprodil discriminates subtypes of the N-methyl-D-aspartate receptor: selectivity and mechanisms at recombinant heteromeric receptors. *Mol. Pharmacol.* 44, 851–859 (1993).
7. Kemp, J. A., Kew, J. N. C. & Gill, R. *Handbook of Experimental Pharmacology* Vol. 141 (eds. Jonas, P. & Monyer, H.) 495–527 (Springer, Berlin, 1999).
8. Lees, K. R. *et al.* Glycine antagonist (gavestinel) in neuroprotection (GAIN International) in patients with acute stroke: a randomised controlled trial. GAIN International Investigators. *Lancet* 355, 1949–1954 (2000).
9. Sacco, R. L. *et al.* Glycine antagonist in neuroprotection for patients with acute stroke: GAIN Americas: a randomized controlled trial. *JAMA* 285, 1719–1728 (2001)
10. Gotti, B. *et al.* Ifenprodil and SL 82.0715 as cerebral anti-ischemic agents. I. Evidence for efficacy in models of focal cerebral ischemia. *J. Pharmacol. Exp. Ther.* 247, 1211–1221 (1988).
11. Kew, J. N. C., Trube, G. & Kemp, J. A. A novel mechanism of activity-dependent NMDA receptor antagonism describes the effect of ifenprodil in rat cultured cortical neurones. *J. Physiol. (Lond.)* 497, 761–772 (1996).
12. Gill, R. *et al.* Pharmacological characterization of Ro63-1908 (1-[2-(4-hydroxy-phenoxy)-ethyl]-4-(4-methyl-benzyl)-piperidin-4-01), a novel sinotype-selective N-methyl-D-aspartate antagonist. *J. Pharmacol. Exp. Ther.* 302, 940–948 (2002)
13. Schwarcz, R. J. Glutamate 2000: old dog, new tricks. *Pharmacol. Exp. Ther.* 296, 659–662 (2001).
14. Parsons, C. G. NMDA receptors as targets for drug action in neuropathic pain. *Eur. J. Pharmacol.* 429, 71–78 (2001).
15. Boyce, S. *et al.* Selective NMDA NR2B antagonists induce antinociception without motor dysfunction: correlation with restricted localisation of NR2B subunit in dorsal horn. *Neuropharmacology* 38, 611–623 (1999).
16. Chizh, B.A., Headley, P.M. & Tzschentke, T.M. NMDA receptor antagonists as analgesics: focus on the NR2B subtype. *Trends Pharmacol. Sci.* 22, 636–642 (2001).
17. Tranquillini, M. E. & Reggiani, A. Glycine-site antagonists and stroke. *Expert Opin. Investig. Drugs* 8, 1837–1848 (1999).
18. Leeson, P. D. & Iversen, L. L. The glycine site on the NMDA receptor: structure-activity relationships and therapeutic potential. *J. Med. Chem.* 37, 4053–4067 (1994).
19. Chase, T. N., Oh, J. D. & Konitsiotis, S. Antiparkinsonian and antidyskinetic activity of drugs targeting central glutamatergic mechanisms. *J. Neurol.* 247 (Suppl. 2), 36–42 (2000).
20. Del Dotto, P. *et al.* Intravenous amantadine improves levadopa-induced dyskinesias: an acute double-blind placebo-controlled study. *Mov. Disord.* 16, 515–520 (2001)
21. Lederer R., Radeke E. & Mondadori, C. Facilitation of social learning by treatment with an NMDA receptor antagonist. *Behav. Neural Biol.* 60, 220–224 (1993).
22. Mondadori, C., Weiskrantz, L., Buerki, H., Petschke, F. & Fagg, G. E. NMDA receptor antagonists can enhance or impair learning performance in animals. *Exp. Brain Res.* 75, 449–456 (1989).
23. Davis, M. The rde of NMDA receptors and MAP kinase in the amygdala in extinction of fear: clinical implications for exposure therapy. *Eur. J. Neurosci* 16, 395–398 (2002).
24. Krystal, J. H. *et al.* NMDA agonists and antagonists as probes of glutamatergic dysfunction and pharmacotherapies in neuropsychiatric disorders. *Harv. Rev. Psychiatry* 7, 125–143 (1999).
25. Tsai, G. & Coyle, J. T. Glutamatergic mechanisms in schizophrenia. *Annu. Rev. Pharmacol. Toxicol.* 42, 165–179 (2002).
26. Tamminga, C. Schizophrenia and glutamatergic transmission. *Crit. Rev. Neurobiol.* 12, 21–36 (1998).
27. Heresco-Levy, U. *et al.* Placebo-controlled trial of D-cycloserine added to conventional neuroleptics, olanzapine or risperidone in schizophrenia. *Am J. Psychiatry* 159, 480–482 (2002).
28. Tsai,G., Yang, P., Chung L. C., Lange, N. & Coyle, J. T. D-serine added to antipsychotics for the treatment of schizophrenia. *Biol. Psychiatry* 44, 1081–1089 (1998).
29. Mothet, J. P. *et al.* D-serine is an endogenous ligand for the glycine site of the N-methyl-D-aspartate receptor. *Proc. Natl. Acad. Sci. USA* 97, 4926–4931 (2000).
30. Wolosker, H., Blackshaw, S. & Snyder, S. H. Serine racemase: a glial enzyme synthesizing D-serine to regulate glutamate-N-methyl-D-aspartate neurotransmission. *Proc. Natl. Acad. Sci. USA* 96, 13409–13414 (1999).
31. Tang, Y. P. *et al.* Genetic enhancement of learning and memory in mice. *Nature* 401, 63–69 (1999).
32. Malayev, A., Gibbs, T. T. & Farb, D. H. Inhibition of the NMDA response by pregnenolone sulphate reveals subtype selective modulation of NMDA receptors by sulphated steroids. *Br. J. Pharmacol.* 135, 901–909 (2002).
33. Husi, H., Ward, M. A., Choudhary, J. S., Blackstock, W. P. & Grant, S. G. Proteomic analysis of NMDA receptor-adhesion protein signaling complexes. *Nat. Neurosci.* 3, 661–669 (2000).
34. Sheng, M. The postsynaptic NMDA-receptor–PSD-95 signaling complex in excitatory synapses of the brain. *J. Cell. Sci.* 114, 1251 (2001).
35. Hardingham, G. E., Fukunaga, Y. & Bading, H. Extrasynaptic NMDARs oppose synaptic NMDARs by triggering CREB shut-off and cell death pathways. *Nat. Neurosci.* 5, 405–414 (2002).
36. Lu, W. *et al.* Activation of synaptic NMDA receptors induces membrane insertion of new AMPA receptors and LTP in cultured hippocampal neurons. *Neuron* 29, 243–254 (2001).
37. Perin-Dureau, F., Rachline, J., Neyton, J. & Paoletti, P. Mapping the binding site of the neuroprotectant ifenprodil on NMDA receptors. *J. Neurosci.* 15, 5955–5965 (2002).